Interacting Gold Nanoparticles and Proteins in Diagnostics and Catalyses

A Thesis Submitted in Partial Fulfillment of the Requirements for the award of the degree of

DOCTOR OF PHILOSOPHY

By

Jashmini Deka
Roll No. 05612212

Department of Chemistry
Indian Institute of Technology Guwahati
Assam – 781 039
INDIA

December 2010

Contents

Page No.

Declaration i

Certificate ii

Acknowledgements iii

Chapter 1 Introduction

1.1 Nanotechnology 1
1.2 Nanotechnology in medicine 2
1.3 Nanoparticles 5
1.4 Gold Nanoparticles (Au NPs) 9
1.5 Proteins: The biological working horses 14
1.6 Motivation behind the thesis 15
1.7 Layout of the thesis 17
References

Chapter 2 Retention of Enzymatic activity of α-Amylase in the Reductive Synthesis of Gold Nanoparticles

2.1 Introduction 27
2.2 Materials and Methods 29
2.3 Results and Discussions 31
2.4 Summary 40
References

Chapter 3 Probing Au Nanoparticle Uptake by Enzyme Following Digestion of Starch-Au-Nanoparticle Composite

3.1 Introduction 45
3.2 Materials and Methods 46
3.3 Results and Discussions 49
3.4 Summary 63
References

Chapter 4 **Sensitive Protein Assay with Distinction of Conformations Based on Visible Absorption Changes of Citrate-Stabilized Au Nanoparticles**

4.1 Introduction 67
4.2 Materials and Methods 70
4.3 Results and Discussions 72
4.4 Summary 98
References

Chapter 5 **Estimating Conformation Content of a Protein Using Citrate-Stabilized Gold Nanoparticles**

5.1 Introduction 103
5.2 Materials and Methods 105
5.3 Results and Discussions 108
5.4 Summary 124
References

Chapter 6 **Modulating Enzymatic Activity in the Presence of Gold Nanoparticles**

6.1 Introduction 129
6.2 Materials and Methods 131
6.3 Results and Discussions 134
6.4 Summary 146
References

Chapter 7 **Overview of the thesis and future prospects**

7.1 Overview of the work done 149
7.2 Materials and Methods 151
References

Appendix 157

Publications and Presentations 171

Declaration

I hereby declare that the matter embodied in this thesis is the result of investigations carried out by me in the Department of Chemistry, Indian Institute of Technology Guwahati, India under the guidance of Dr. Anumita Paul, Associate Professor, Department of Chemistry.

In keeping with the general practice of reporting observations, due acknowledgements have been made wherever the work described is based on the findings of other investigators.

I. I. T. Guwahati **Jashmini Deka**

December, 2010

Certificate

It is certified that the work described in this thesis, entitled "***Interacting Gold Nanoparticles and Proteins in Diagnostics and Catalyses***", done by Ms. **Jashmini Deka** for the award of degree of Doctor of Philosophy is an authentic record of the results obtained from the research work carried out under my supervision in the Department of Chemistry, Indian Institute of Technology Guwahati, India, and this work has not been submitted elsewhere for a degree.

I. I. T. Guwahati
December, 2010

Dr. Anumita Paul
Associate Professor
(Thesis Supervisor)

Acknowledgements

The period of past 5.5 years of my life has been a great learning experience for me, both in professional as well as personal front. I could have never imagined of completing my thesis work without the love and support of a few people to whom I would remain indebted for rest of my life. I consider this space of my thesis as important as any other chapter, since it gives me an opportunity to pay my deepest gratitude to them.

I feel fortunate to get an opportunity to pay my heartfelt acknowledgement to my thesis supervisor, Dr. Anumita Paul for her constant support, encouragement and help throughout my research work. Her deep knowledge and critical analysis of a topic always helped me to fight out through odd problems and improve the quality of the work. She has been a wonderful teacher to me.

I was blessed to be associated with Prof. Arun Chattopadhyay through out my thesis work. He has been the dynamic source of constant motivation which ignited and kept the zeal to work harder and harder, alive in me. He inspires his students by his own dedication, sincerity and enthusiasm. His down to earth personality made discussions with him much easier, which was the propellant behind my work. He taught me the bottom-line of good work, "just understand what you are doing, enjoy your work, have faith in yourself and good papers will come to you."

I shall forever remain indebted to you Madam and Sir, for your kindness, for giving me all the freedom to think, work and write at my own pace, giving me your valuable time whenever required and the best possible environment to work in. As you always wished Sir, for your students, the time spent at IITG in your lab would remain as the most cherish able time in their lives.

While working in the field of Nanoscience I realized the gravity of collaborative work. I am highly grateful to Dr. Atul Kumar Singh for his great help during our collaboration. My work between the Department of Chemistry, Department of Biotechnology and Center for Nanotechnology became much easier due to the friendly behavior and sincere support as and when required by my friends like Archana, Manab, Gopi, Pallab, Rama, Dilip, Kaustav, Paran da, Mano da, Pranjoli, Shilpa, Amaresh, Madhuchanda di and

Upashi. My special acknowledgements to Tridip da and Abhijit who started the work on α-amylase, with which my thesis work started and continued.

I take this opportunity to thank Dr. A. Ramesh who has been a strong stimulation behind my work. I am grateful to him for his constant encouragement and fruitful discussions. I am also thankful to Dr. S. S Ghosh for his support and encouragement.

I would like to thank Prof. A. T Khan, Chairman of my doctoral committee for his valuable suggestions and advice. I also thank all other faculty and staff members of Department of Chemistry for their cooperation whenever required. I am thankful to the staff members of Academic Section, Central Library, Students' Affair, R & D Section and Accounts Section of IITG for their timely help. I shall also like to thank the CIF at IITG for providing the instrumental facility. Special thanks to Indrajeet, Kula da, Chandan da and Madhurjya for their help with the instruments. I thank MHRD and CSIR for fellowships. Thanks are due to the staff of Bani Mandir, Core 3 tea stall and my hostel mess staff for their great service.

I take this opportunity to pay my humble thanks to my lab seniors (Gitanjali ba, Biswa Bhaiya and Sonit) who helped me in learning the basics of research through various softwares, instruments, and other lab techniques. Thanks are due to my old lab mates (Debajyoti, Ali and Muruga) who were besides me while I was struggling to get familiar and settle down with my lab works. I would always remember Indrani, Jhumur, Partha and Pankaj for their nice company.

I feel privileged to have a very fine combination of present lab mates who always made me feel comfortable by extending their love, care and a conducive environment to work in, which is just apt for mutual growth and development. We believed in finding reasons to smile amidst all hardships. Thanks Sadhu, Subhojit, Raihana, Rumi, Palash, Rama, Saty and Shankar da for being the world's best juniors/ lab mates.

I am thankful to all my friends at IITG who made my stay here an enjoyable one. Thanks Shiva, Chaitanya, Subhash, Amardeep for your constant encouragement. I shall always cherish my friendship with Prasanta, Ballav, Gunin da, Pranjal da, Bolin da, Sahid da, Francis, Anusuya, Rosi, Rupam, Deepjyoti, Bimlesh, Moushumi, Atul, Sarala di, Ramesh and all other seniors, friends and juniors in Department of Chemistry. My

sincere thanks to Krishna for his friendship, help and valuable suggestions from time to time.

It's my great pleasure to thank all my teachers who have taught me till now and helped me stand where I am today. I shall always remain thankful to all my friends at school and college for their love and support. Special thanks to Priyanka, Anurag, Utpal, Shruti and Khaleda. Thanks Sumana and Bani for your inspiration.

Following friends made the framing of my thesis (my PhD work) a smooth process: Moni (thanks for waking me up every morning for the last 5 years!), Purabi ba, Rumi, Raihana, Porinita, Cosmika, Tapashi, Sumitra, Meenaxi, Maya di, Seema, Anupa, Anamika with whom I shared all my raw feelings. These people made my stay in hostel a great experience. Thanks to all my orkut/ FB friends too. Thanks all.

I would pay special thanks to a few of my school friends whom I met again after a long gap, who gave me great strength by showing their unshakeable faith in me. Thanks Abhishek, Jayanti and Mukesh for your incomparable friendship.

Finally I would like to express my gratitude to my parents who gave me a fantastic childhood, great love and much freedom to develop my individuality. My heartfelt thanks to my beloved sister and brother-in-law for their incomparable love, support and patience. I have been thanking to God everyday to have blessed me with such a family. They always insisted 'finish your PhD nicely' rather than 'finish your PhD fast'. And that gives a great stimulation to chase my dreams. Thanks once again for being with me all the time. I was comforted everyday by those few minutes of phone calls with my niece and nephew who sparked new energy in me with their love. Thanks sweethearts.

Jashmini Deka

Chapter 1

Introduction

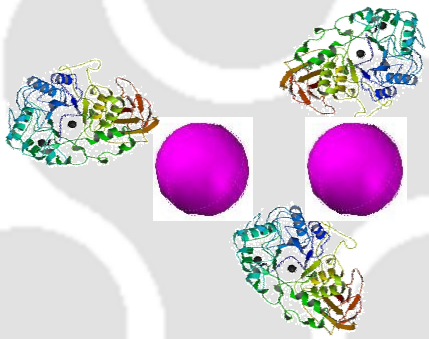

1.1 Nanotechnology:

The idea of nanotechnology was introduced in 1959 in the revolutionary talk called "There's Plenty of Room at the Bottom" by Richard Feynman, a physicist at Caltech. Though the term 'nanotechnology' was not mentioned explicitly, Feynman suggested that it will eventually be possible to precisely manipulate atoms and molecules. The talk reflected the vast possibilities in the field of research known as 'nanoscience and nanotechnology' today.

The term nanotechnology [from the Latin *nanus*, Greek *nanos* dwarf] is defined in the literature in a variety of ways, all of which have their advantages and limitations. In general, nanotechnology is concerned with dimensions and tolerance limits of 1–100 nm (1 nm=10^{-9} m), as well as with the manipulation of single atoms and molecules. Despite this size restriction, nanotechnology commonly refers to structures that are up to several hundred nanometers in size and those are developed by top down or bottom-up engineering of individual components. A more specific definition was given in 2000 by the US National Nanotechnology Initiative: "Nanotechnology is concerned with materials and systems whose structures and components exhibit novel and significantly improved physical, chemical and biological properties, phenomena and processes due to their nanoscale size."

The ample potential in the field of nanotechnology could be dreamt of and realized, inspired by the fact that many life sustaining activities in the cellular level are based primarily on the input and reactivity of small molecules which necessitate nanoscale operations and transformations to specifically facilitate gathering, processing, and transmission of chemical information.[1] The nanometer scale (1–100 nm) incorporates collections of atoms or molecules, whose properties are neither those of the individual constituents nor those of the bulk. On this scale, many of the atoms are still located on the surface, or one layer removed from the surface, as opposed to the interior. This scale is attractive in biological systems.[2–4] Indeed the elementary functional units of biological systems- enzymes, motors, membranes, nucleic acids, etc.- all comprise nanoscale components. Many proteins are ~10's of nm in size. Since structures can be accurately designed on the nanometer scale they can be incorporated into biological systems, due to the similar size scales. The ability to rationally design structures on the same size as

biological molecules generates the ability to probe and modify biological systems. Furthermore, biological systems can be used to build up nanomaterials of specific shape and function. Biological systems are complex, with synthesis, structure, and function all poorly understood in detail. The living cell can be considered as an integrated self-regulating complex chemical system which runs principally by nanoscale miniaturization, and this specific level of dimensional constraint is critical for the materialization and sustainability of cellular life in its minimal form. Thus the complex yet wonderfully working cells and many more such examples from nature (such as the hydrophobicity of lotus leaves, strength of the spider web) which are based on nanoscale attributes have sparked new enthusiasm among scientists to explore and harness the unique opportunities extended by this new class of nanomaterials.

1.2 Nanotechnology in medicine

The application of nanotechnology to drug delivery is widely expected to change the present scenario of pharmaceutical and biotechnology industries.[5-11] The pharmaceutical companies are believed to be drying up in many cases, and it is considered that a number of blockbuster drugs will come off patent in the near-term.[12] The development of nanotechnology products may play an important role in adding a new series of therapeutics to the present pharmaceutical companies. For example, using nanotechnology, it is expected to achieve **(1)** improved delivery of poorly water-soluble drugs; **(2)** targeted delivery of drugs; **(3)** transcytosis of drugs across tight epithelial and endothelial barriers; **(4)** delivery of large macromolecule drugs to intracellular sites of action; **(5)** co-delivery of two or more drugs or therapeutic modality for combination therapy; **(6)** visualization of sites of drug delivery by combining therapeutic agents with imaging techniques;[13] and **(7)** real-time monitoring of the *in vivo* efficacy of a therapeutic agent.[7] Lipid vesicles, which were described in the 1960s and later became known as liposomes were among the first nanotechnology drug delivery systems.[14] Subsequently, a variety of other organic and inorganic biomaterials for drug delivery were developed. The first controlled release polymer system for delivery of macromolecules was described in 1976.[15] More complex drug delivery systems capable of responding to changes in pH to trigger drug release,[16] as well as the first example of cell specific targeting of liposomes,[17,18] were first described in 1980. There are over two dozen

nanotechnology therapeutic products that have been already approved for clinical use to date.[19] Among these products, liposomal drugs and polymer-drug conjugates are two dominant classes. The majority of these therapeutic products improve the pharmaceutical efficacy which in some cases also provides life-cycle extension of drugs after patent expiration.

Even after 30 years of the reported use of targeted liposomes, nanotechnology it still far from its direct application and significant clinical impact on human health. To extract better dividends from this technology there is a high need to address the following points: **(1)** *Delivery vehicle*-whether the combination of biomaterials and the processes to develop targeted drug delivery system is optimal for product development? **(2)** *Drugs*-whether the properties of the therapeutics as well as their site and mode of action is suited for targeting to confer an advantage? **(3)** *Diseases and diagnosis*- whether the newer materials provide more sensitive and simple diagnostic tools for diseases?

1.2.1 *Delivery Vehicle:*

There are a number of parameters that are important for the successful development and manufacturing of targeted drug delivery vehicles.[20] These include **(a)** the use of biocompatible materials with simple robust processes for biomaterial assembly, conjugation chemistry, and purification steps; **(b)** the ability to optimize various related biophysiochemical parameters ; and **(c)** developing strategies so as to manufacture large quantities of targeted drug delivery systems needed for clinical rendition. The physical properties of the vehicle, such as size, charge, surface hydrophilicity, and the nature and density of the ligands on their surface, can all impact the biodistribution of the drug particles.[20,21] The presence of targeting ligands can increase the interaction of the drug delivery system with a subset of cells in the target tissue, which can potentially enhance cellular uptake by receptor-mediated endocytosis. Thus an intelligent selection or design of the drug carrier would be a great step towards efficient drug delivery.

1.2.2 *Drugs:*

The choice of therapeutic for targeted delivery is another key issue which needs careful consideration. The delivery of therapeutics with intracellular sites of action for which cellular uptake is inefficient may be best achieved with targeted delivery vehicles.[22] In

some cases, it is believed that targeting may decrease the efficiency of diffusion and uniform tissue distribution. The optimization of the ligand density on the drug delivery surface can facilitate the balance between tissue penetration and cellular uptake, resulting in optimal therapeutic efficacy. The targeting of cell surface receptors that participate in membrane recycling pathways facilitates the uptake of targeted drug delivery systems through receptor-mediated endocytosis. A proper understanding of endosomal trafficking pathways, which are complex and can vary among receptors, can also facilitate the engineering of suitable targeted delivery systems.

1.2.3 *Diseases and detection:*

There has been an increasing effort to develop new disease biomarkers and associated ligands for use in targeted drug delivery applications. While targeted drug delivery systems have been developed for a numerous of important diseases, the current focus of research is solid tumors, cardiovascular diseases, and immunological diseases. The currently approved nanotechnology therapeutic products for cancer therapy, function by accumulating in tumor tissue through the enhanced permeability and retention (EPR) effect[23] and releasing their payload in the extravascular tumor tissue for antitumor efficacy. Tumor tissue accumulation is a passive process which is largely mediated by the biophysicochemical properties of the nanoparticles (NPs) and not by active targeting.[24] Active targeting is significant only after the release of the drug particles. Hence the accumulation of the NPs and mode of drug release would be an interesting field to be studied and better techniques for diagnosing the advancement of a disease would be always desirable to follow the effectiveness of the drug delivery system used.

With recent scientific advances, it will be increasingly feasible to engineer targeted or multifunctional nanotechnology products for therapeutic applications. While both organic and inorganic technologies are under development, controlled-release polymer technologies and liposomes will likely continue to have the greatest clinical impact in the future. It is widely accepted that with continued resources, medicine and the field of drug delivery will be largely affected by the advances in nanotechnology in the years to come.

1.3 Nanoparticles:

NPs of noble metals belong to the most extensively studied colloidal systems in the field of nanoscience and nanotechnology. In addition to an exceptionally ***large surface to volume*** ratio, certain types of NPs demonstrate fascinating size-dependent optical, electrical, magnetic and catalytic properties that are of potential interest for a large number of applications ranging from optoelectronics to biodetection. Physicists predicted that NPs in the diameter range 1-10 nm (intermediate between the size of small molecules and that of bulk metal) would display electronic structures, reflecting the electronic band structure of the NPs, owing to quantum-mechanical rules.[25] The resulting physical properties strongly depend on the particle size, interparticle distance, nature of the protecting organic shell, and shape of the NPs.[26]

1.3.1 *Surface Plasmon Resonance*

The interesting optical properties in the NPs arise due to a phenomenon called surface plasmon resonance (SPR). The excitation of surface plasmons by light is denoted as a SPR for planar surfaces or localized surface plasmon resonance (LSPR) for nanometer-sized metallic structures. Electromagnetic surface waves can propagate along the interface between conducting materials and a dielectric[27] over a broad range of frequencies, ranging from dc and radio frequencies up to the visible. The free electrons in the metal (d electrons in silver and gold) are free to travel through the material. For example, the mean free path in gold (Au) and silver is ~50 nm, therefore in particles smaller than this, no scattering is expected from the bulk. Thus, all interactions are expected to be with the surface. When the wavelength of light is much larger than the NP size it can set up standing resonance conditions. Surface plasmons are characterized by strong field enhancement at the interface, while the electric field vector decays exponentially away from the surface (in the nm range).[28-30] When the dimensions of the conductor are reduced, boundary and surface effects become very important, and for this reason, the optical properties of small metal NPs are dominated by such a collective oscillation of conduction electrons in resonance with incident electromagnetic radiation.[31] For many metals such as Pb, In, Hg, Sn, and Cd, the plasma frequency lies in the UV part of the spectrum and NPs do not display strong color effects. Such small metal particles are also readily oxidized making surface plasmon experiments difficult.

The coinage elements are exceptional. First they are more noble and form air-stable colloids. Second due to d-d band transitions, the plasma frequency is pushed into the visible part of the spectrum. Hence, surface plasmon experiments are most commonly carried out with Cu, Ag, and Au. Although most interest has focused on size effects, the resonance frequency depends on quite a few additional factors, including particle shape and the nature of the surrounding medium, among others, and their influence is in general larger than that of size. The optical features of the LSPR (e.g., peak absorption, linewidth) depend on the size, shape, composition of the metal NPs, its surface charge, surface-adsorbed species, interparticle interactions, and the refractive index of the surrounding medium.[31]

For nonspherical NPs, such as rods, disks, and triangular prisms, the LSPRs are typically split into distinctive dipole and quadrupole plasmon modes.[32-34] For nanorods, the resonance wavelength depends on the orientation of the electric field relative to the particle, and thus, oscillations either along (longitudinal) or across (transversal) the rod are possible. Because of the dimensionality of anisotropic shapes, the frequencies associated with the various resonance modes can be quite different, and thus the optical properties can be largely affected. Since these resonances arise from the particular dielectric properties of the metals, they can be easily modeled using the equations derived by Mie for the resolution of Maxwell equations for the absorption and scattering of electromagnetic radiation by small spheres[35] and their modification by Gans for ellipsoids.[36]

1.3.2 *Nanoparticles in biodetection*

Other than the application in optical and electronic devices, inorganic NPs has been successfully used as biological labels and drug delivery systems.[37] Due to the wide horizon of their possible size, shape, composition and ability to bind various molecules they have been an attractive tool for detecting biomolecules (such as DNA, RNA, nucleic acis, proteins/ enzymes etc.) and interactions between various molecules, which is the basis of sensor designing.[38-40] Diagnosis of certain diseases, such as cancer, requires detection of very low levels of proteins that serve as markers for that particular disease. Developing more sensitive assays for these proteins is of critical importance since early diagnosis can greatly increase the efficacy of treatment. For example, the

oligonucleotide-mediated NP aggregation process has been extensively used for the development of simple and highly sensitive colorimetric biosensors for oligonucleotides by Mirkin[41,42] and others.[43-45] The exceptional quenching ability of metallic NPs makes them excellent materials for Forster resonance energy transfer (FRET)-based biosensors,[46] for example, for the fabrication of molecular beacons for sensing DNA.[47] There are reports on NP-based enzyme sensing approaches,[48-53] which show distinct advantages over traditional methods and immunological detection strategies in terms of their potential rapidity and sensitivity.

The most widely used NPs in applications intended for diagnostics are plasmonic noble metal NPs, magnetic NPs and quantum dots (QDs). These three groups of NPs are also in many aspects complementary to each other as they offer different means of detection, enabling a large number of applications in various chemical environments, both *in vivo* and *in vitro*.[54] Of all available NPs, gold nanoparticles (Au NPs) have been most extensively studied for bioassay applications. This is mainly because of their interesting optical properties (high extinction coefficient) in addition to the well established methods for synthesis of Au NPs with various sizes and geometries in addition to other properties (discussed in detail later in this chapter).[55]

1.3.3 *What makes Nanoparticles so desirable in biodetection?*

Following intriguing properties of NPs makes them a promising candidate in biodetection:

- Biomacromolecule surface recognition by NPs as artificial receptors.
- Their ability to respond to any changes in the surrounding medium which is reflected through changes in optical or magnetic behavior.
- The unique physicochemical properties of NPs coupled with the inherent increase in signal-to-noise ratio provided by miniaturization[56] makes these systems promising candidates for sensing applications.[55]
- Their ability to bind wide range of metal and semiconductor core materials which imparts properties such as fluorescence and magnetic behavior.[7]

- The size of NP cores can be tuned from 1.5 nm to more than 10 nm depending on the core material, providing a suitable platform for the interaction of NPs with proteins and other biomolecule.[57]
- Metallic NPs also possess superb quenching ability[46] and photoluminescence.[58-60]
- NP-based materials are attractive alternatives to the fluorescence- or radiolabeled enzyme substrates of traditional enzymatic assays, owing to their photostability, ease of synthesis, and ability to conjugate to biological molecules.

A sensor generally consists of two components: a recognition element for target binding and a transduction element for signaling the binding event. The SPR band is sensitive to the surrounding environment, signaling changes in solvent and binding. A particularly useful output is the red-shift (to ca. 650 nm) and broadening of the plasmon band due to the interparticle plasmon coupling.[61] This phenomenon leads to the popular and widely applicable colorimetric sensing.

1.3.4 *Basic principles involved in molecule detection*

Changing the dielectric constant of the surrounding material affects the oscillation frequency due to the varying ability of the surface to accommodate electron charge density from the NPs. Since the SPR signals are dependent on the dielectric constant, any change in the dielectric constant would shift the SPR signals. Changing the solvent changes the dielectric constant, but the capping material is most important in determining the shift of the plasmon resonance due to the local nature of its effect on the surface of the NP. Thus, chemically bonded molecules can be detected by the observed change they induce in the electron density on the surface, which results in a shift in the surface plasmon absorption maximum. This is the basis for the use of noble metal NPs as sensitive sensors.

Colloidal particles tend to have a limited stability with regards to aggregation, and most NP suspensions are not thermodynamically stable. The adsorption or immobilisation of a chemical species on the particle surface can drastically alter the properties of the solid–liquid interface, which has a profound effect on the stability of the particles. Dispersed NPs are always subject to Brownian motion and frequently undergo collisions and the fate of the particles after collision depends on the sum of the attractive

and repulsive forces acting between them. van der Waals forces, electrostatic interactions, solvation forces, and osmotic and entropic interactions related to macromolecular adsorption are the four most important forces that govern the NP stability.[62] ***Factors such as solution pH, ionic strength and type of buffer might disturb the delicate balance in these forces and lead to particle aggregation which brings changes in the dielectric constant of the medium***. Thus, the ability of metal NPs to respond to subtle physicochemical changes in the local environment can be utilized to translate molecular interactions into detectable signals that can be recorded using standard laboratory equipment and sometimes even by the naked eye.

For example, if we consider the NP enzyme sensors, they consist of a biological substrate molecule immobilized onto the NP surface. The activity of an enzyme results in some form of modification of the substrate and a subsequent change in the NPs' local environment, leading to the generation of a user-readable signal, for example, optical or electronic. This forms the basis of detection/ enzyme assay for many enzymes by NPs. Similarly, the aggregation of NPs due to presence of some foreign matters leads to the shift in SPR because of changes induced in the dielectric constant (either due to displacement of coating material of the NP or due to the change in the local environment or both), which can be easily read and can be used to detect/ estimate molecules interacting with the NPs.

1.4 Gold Nanoparticles (Au NPs)

Michael Faraday, in 1857, was the first person to report the preparation of Au colloids, by reduction of an aqueous solution of chloroaurate ($AuCl_4^-$) using phosphorus in CS_2 (a two-phase system). The term "colloid" (from the French, *colle*) was coined shortly thereafter by Graham, in 1861.[55] The major use of Au colloids in medicine in the Middle Ages was perhaps for the diagnosis of syphilis, a method which remained in use until the 20th century[63] including its curative powers in diseases such as heart problems, arthritis, dysentery, epilepsy and tumors. Colloidal Au was used to make ruby glass and for coloring ceramics, and these applications are still continuing now. Perhaps the most famous example is the Lycurgus Cup that was manufactured in the 5th to 4th century B.C. The ultrafine size of the Au particles was later on found to be the reason behind such astonishing properties of Au.

1.4.1 *Synthesis of Au NPs*

In the 20th century, various methods for the preparation of Au colloids were reported and reviewed. Among the conventional methods of synthesis of Au NPs by reduction of Au (III) derivatives, the most popular one till date has been that using citrate reduction of $HAuCl_4$ in water, which was introduced by Turkevitch in 1951.[64] It leads to Au NPs of ca. 20 nm. In an early effort, reported in 1973 by Frens,[65] the effect of changing the ratio of reducing/ stabilizing agents on the size of resulting NPs was discussed. This method is very often used even now when a rather loose shell of ligands is required around the Au core in order to prepare a precursor to valuable Au NP-based materials.

Generally, chemical methods of synthesis usually involve the chemical reduction of the parent metal salts by reagents such as sodium borohydride, hydroxylamine, polyvinyl pyrrolidone. The synthesized Au NPs can then be stabilized by some other ligands. The stabilization of Au NPs with alkanethiols was first reported in 1993 by Mulvaney and Giersig, who showed the possibility of using thiols of different chain lengths and their analysis.[66] Other methods include, Brust-Schiffrin method, which uses the thiol ligands that strongly bind Au due to the soft character of both Au and S atoms.[67] Other than thiols, ligands such as phosphine, phosphine oxide, amine, carboxylates have been successfully used as capping agent for stabilizing synthesized Au NPs.[55] Physical methods such as photochemistry (UV, near-IR), sonochemistry, radiolysis and thermolysis have also been used to synthesize Au NPs.[55] Although these methods may successfully produce pure and well-defined NPs, the stringent reaction conditions used in the syntheses may not be suitable for biological and biochemical applications. In this regard, biological systems have been helpful in the synthesis and assembly of nanoscale materials, forming sophisticated macroscopic systems with striking structural features. A host of biological methods for Au NP synthesis have been reported. The details have been discussed in Chapter 2.

1.4.2 *Shape dependent advantages*

Anisotropic features in nonspherical NPs make them ideal candidates for enhanced chemical, catalytic, and local field related applications. Nonspherical plasmon resonant NPs offer favorable properties for their use as analytical tools, or as diagnostic and therapeutic agents.[68] Nonspherical particles provide ample corners, vertices, defects,

kinks, and steps.[69] Exposure of different crystallographic facets, together with the increased number of edges, corners, and faces, is of critical importance in controlling the catalytic activity and selectivity of metal NPs. In the case of spherical NPs, the LSPR can be tuned by increasing the particle size. However, the dipolar LSPR band becomes significantly broadened due to radiation damping.[70] The LSPR can be tuned more elegantly without sacrificing the linewidth of the resonance through changing the nanoparticle geometry.

A proportion of the incident light falling on the NPs is scattered, but the absorbed light causes heating in the particles resulting in a highly localized increase in temperature, which can be exploited in the various proposed photo-thermal therapeutic uses of Au NPs. This effect is more pronounced in nanorods and nanoshells. Au nanorods are elongated NPs with a defined aspect ratio, whereas core–shell NPs typically are comprised of a thin Au film that covers a dielectric core. Due to the presence of both a transverse and a longitudinal plasmon mode nanorods display two plasmon bands in the extinction spectrum. These bands can be shifted by altering the aspect ratio of the particles. In core–shell particles, the appearance of the plasmon band depends on the thickness of the shell and the size and geometry of the core. It is convenient to shift the wavelength of maximum absorption into the near infrared because the body is more transparent at those wavelengths. This can be achieved with Au nanoshells[71] by enhancing the dipole–dipole interaction between aggregated Au nanospheres[72,73] or by decreasing the symmetry of the particles, for example, through the formation of nanorods.[74] All these types of particles have been shown to effectively convert light into thermal energy, a process that is of large interest for e.g. thermal ablation of cancer cells and photo-triggered drug release. Recently, the efficiency of popcorn shaped Au NPs in targeted diagnosis, nanotherapy treatment and *in situ* monitoring of photothermal therapy for prostate cancer has been reported.[75]

1.4.3 *SPR of Au NPs*

As discussed in section 1.3.1 for metal NPs, the surface plasmon band (SPB) is due to the collective oscillations of the electron gas at the surface of NPs (6s electrons of the conduction band for Au NPs) that is correlated with the electromagnetic field of the incoming light, i.e., the excitation of the coherent oscillation of the conduction band. The

ligand shell alters the refractive index and causes either a red or blue shift, which is reflected in the spectroscopic data obtained. This principle has been widely used towards the development of various strategies of biomolecule detection using Au NPs (details are discussed in Chapter 4 and Chapter 5).

1.4.4 *Fluorescence of chromophores in close vicinity to Au NPs surface*

Metal NPs are known to affect the optical properties of a molecule in its close vicinity. The effect on the fluorescence of a chromophore which is close to the surface of metal NPs is due to the strong electromagnetic field generated at the surface of NPs.[76] However the fluorescence can either be quenched or enhanced depending on various parameters such as the chemical nature of the metal, the particle shape and size, the position and orientation of the chromophore with respect to the particle and the environment in which the fluorescence process takes place. For example, it has been found that fluorescence brightness can be switched between quenching or enhancement by just varying the metal-chromophore distance.[77] Chromophores within 5 nm of the surface interact electronically with the surface to donate the excited electrons to the metal, thus quenching the fluorescence by non-radiative pathways available in the metal NP. However, as the distance is increased the electric field is still strong enough to enhance the fluorescence probability, but the NP is not able to interact directly with the electrons of the metal. In this regard, a comprehensive study has been carried out by Mennucci *et al*[78] that discusses the various conditions that give rise to fluorescence quenching or enhancement. Thus, the change in the intrinsic fluorescence of fluorophores can be an important tool while studying their interaction with NPs. We have used this principle to establish interaction between Au NPs and proteins by measuring the intrinsic fluorescence of the tryptophan group of the protein in the presence of the Au NPs in the reaction conditions. The details are discussed in Chapter 5 and Chapter 6 of the thesis.

1.4.5 *Surface Enhanced Raman Scattering (SERS)*

In a metallic NP, incident light can couple to the plasmon excitation of the metal, which involves the light induced motion of all the valence electrons.[31] This can increase the cross section for interaction with light to many folds. For example, the cross-section for elastic light scattering from a 50-nm Au nanocrystal can be a million-fold larger than the cross section for absorption or emission of electromagnetic radiation from any

molecule or even quantum dot chromophore. The large field enhancement in the vicinity of Au nanocrystals is well known to lead to the surface enhanced Raman scattering (SERS) effect, and developments in this area may well change the picture. Mirkin and colleagues[79] have shown that it is possible to detect a wide range of biological macromolecules through binding events involving Au nanocrystals that have been coated with specific molecules that offer a distinct Raman signature. Ray *et al* report the use of Au-nano-popcorn based SERS assay for targeted sensing, nanotherapy treatment and *in situ* monitoring of photothermal nanotherapy response during the therapy process for prostate cancer.[75] An enhancement of the Raman signal intensity by several orders of magnitude (2.5×10^9) was observed by the group.

Thus it is evident that Au NPs have enormous power as a diagnostic tool. Not only can changes in the SPR absorbance be detected to detect the adsorbed species in chemical, biochemical, sensing, and medical fields, but also the scattering signal can be used in imaging techniques to observe different binding with functionalized NPs.

1.4.6 *Biocompatibility of Au NPs*

The Au solution, whose curative properties were explored long back, has been termed as 'drinkable' since then. As evident from literature the 'drinkable Au' was a pink colored solution containing Au in neutral form, was present under extreme sub-division which was not visible to human eye which definitely pointed towards the nanoform of the Au particles.[80-84] These descriptions of Au colloids point towards its biocompatibility and non toxicity and thus its safe use in biological purposes.

1.4.7 *Au NPs in nanomedicine*

Colloidal Au NPs have become an important alternative as imaging agents due to their potential noncytotoxic, facile immunotargeting[4] as well as due to their non susceptibility to photobleaching or chemical/thermal denaturation, a problem commonly associated with dyes.[85] Recently, strongly absorbing Au NPs have been shown to offer excellent promise for cell and tissue imaging by using techniques such as multiphoton plasmon resonance microscopy[86] and photoacoustic tomography.[87] Similarly, the ***strong light scattering of Au NPs*** has been exploited for real-time optical imaging of precancer by using confocal reflectance microscopy.[88] El-Sayed *et al*. have demonstrated

differentiation of cancerous cells from noncancerous cells by dark field light-scattering imaging and absorption spectroscopy of solid ~40 nm Au nanospheres immunotargeted to EGFR overexpressed on cancer cells.[89] Along with cancer imaging and diagnostic applications, the ability of Au NPs to efficiently convert absorbed light into localized heat can be readily employed for therapy based on photothermal destruction of cancerous cells.[90-92] For example, Hirsch et al[90] employed NIR absorbing silica- Au core-shell particles for photothermal destruction of human breast carcinoma cells *in vitro* as well as solid tumors *in vivo*. Thus from imaging to treatment Au NPs finds huge application in the field of nanomedicine.

1.5 Proteins: The biological working horses

Proteins are rightly being termed as 'the biological working horses', since they carry out vital functions in every cell. Based on their pool of functions they have been categorized as enzymes, structural proteins, transport proteins, motor proteins, storage proteins, signal proteins, receptor proteins etc. Almost all biological functions inside our cells are carried out by one or more than one such protein. To carry out their task, proteins must fold into a complex three-dimensional structure. Hence, a slightest disturbance in their level in our body or defect in their functional structure may lead to their malfunctioning and thus give rise to several ailments which can be the root cause of various diseases such as cancers, Parkinson, Alzheimers' etc. The sequencing of the human genome and that of numerous pathogens has opened the door for proteomics by providing a sequence-based framework for mining proteomes. As a result, there is intense interest in applying proteomics to foster a better understanding of disease processes, develop new biomarkers for diagnosis and early detection of disease, and accelerate drug development. The growing interest in proteomics creates numerous opportunities as well as challenges to meet the needs for high sensitivity and high throughput required for disease-related investigations. Relevant to nanotechnology, it has been established that, enzymes can serve as a set of structurally diverse biological tools assembling unique nanostructures. An additional attraction is that enzymes are commercially available in pure form and they have diverse chemical, biochemical, and biological functions as such or on supported surfaces. The details regarding various roles of enzymes in nanotechnology has been included in Chapter 2.

Protein detection methods have largely been dominated by enzyme-linked immunological assays (i.e., ELISA), where specific antibody binding to a target analyte is amplified by a secondary colorimetric enzyme reaction. Although this is a well-established procedure found in many clinical settings, the technique, in its traditional sense, is limited by the requirement of producing high-quality antibodies, multiple washing steps, and low capacity for multiplexed analyte detection. Many of these limitations are now being addressed by the development of novel detection strategies that incorporate the magnetic, optical, and electronic properties associated with metallic NPs into high-sensitivity sensing devices for a broad range of target analytes. For instance, the amenability of antibody-conjugated magnetic particles to physical separation, coupled with the enormous amplification potential of enzymatic DNA replication (polymerase chain reaction) can be used to detect ultralow concentrations of disease-related proteins in serum.[93,94] Furthermore, protein detection using optical methods can be carried out by homogeneous NP assays, including whole blood, without the need for additional separation and purification.[95] For example, antibody-functionalized Au nanoshells have been tailored to specifically detect target analytes in a protein-rich background using the principles of a sandwich-immunoassay, where analyte-driven aggregation of the nanoshells results in a red-shift in their absorption spectra.[94]

1.6 Motivation behind the thesis

As discussed so far, nanomaterials hold great promises in the field of medicine and hence its final application calls for immediate attention towards the issues related to the compatibility of the nanoscale materials to be used with the various biological components involved. Understanding the interactions between biomolecules and nanomaterials is of fundamental interest for the development of responsive NPs and for facilitating the design of robust surface chemistries and sensing strategies that enable specific detection even in complex environments. The bio–nano interface is also of considerable interest for understanding any potential risk involved in using nanomaterials, especially for *in vivo* applications. [96] The field of targeted drug delivery calls for immediate attention towards the understanding of the NP-biomolecule interaction (as discussed in section 1.2).

For example, any changes induced in the structure of a biomolecule such as protein/enzyme due to the presence of NPs may lead to positive or negative effects on the activity/ properties of the later. Since the function of a protein is much dependent on its tertiary structure, a deep understanding of the interaction of the concerned NPs with the proteins is quite essential for judicious use of the NPs towards nanomedicine. The effect of the presence of NPs on the activity of enzymes has been an important concern and being studied by various groups. Even though there are literature on the study of effect of metal NPs on the structure and function of enzymes, [97-100] still not much attention has been paid on understanding the intricacies involved in the final application of the technology in medicine. NP–protein interactions can regulate multiple biological processes such as protein–protein interactions, protein–nucleic acid interactions and enzyme activity. Reports that some nanomaterials catalyze the formation of protein fibrils provided evidence that interactions between proteins and nanophase materials can induce modifications in protein structure, leading to the growth of extended assemblies. The various studies concerning the NP-protein interaction [101-105] suggest that the diversity of protein structure gives rise to complexity of interaction behavior between the two.

Thus, inspired by the enormous potential uses of metal NPs (especially Au NPs) in the field of nanotechnology (more so in nanomedicine) and the need of a deeper knowledge on the subject involving the interactions of the NPs with the biomolecules, the focus of the present thesis has been to develop a better understanding of the interaction of Au NPs with biomolecules (proteins in the present case). Mainly α-amylase, amyloglucosidase (AMG), bovine serum albumin (BSA) and green fluorescent protein (GFP) have been used for the study. α-amylase has been used as a role model for most of the studies. A few questions such as how would an enzyme behaves in the presence of Au NPs (whether covalently attached to the NPs or not) or how would a drug vehicle carrying Au NPs for targeted delivery or diagnosis might open up in the presence of an enzyme have been attempted to be solved. As an interesting outcome of the study, there has been development of simple, sensitive and efficient methods based on the optical properties of citrate-stabilized Au NPs for estimation of amount of protein in a given solution as well as of the conformation content of a protein in a mixture of its native and denatured forms. The methods are based on the optical response of Au NPs

towards the proteins which brings changes in its SPR signals which can be detected and quantified based on the principles discussed in detail in section 1.3.1.

1.7 Layout of the thesis:

In the following, the thesis chapters, starting with the Chapter 2, are described in short, consisting of essential aim and findings.

Chapter 2:

Chapter 2 deals with the reductive synthesis of Au NPs by the enzyme α-amylase. It was found that the presence of free thiol groups led to the reduction of the Au precursor used and further stabilization of the NPs formed. This provided us with an opportunity to carry out experiments leading to understanding of the mechanism involved in the NP synthesis by an enzyme, which was not pursued previously by researches working on this field; although several groups had earlier taken recourse to the use of biomolecules (including enzymes) in the eventual syntheses of metal NPs. It was for the first time that a pure protein was used as the reducing agent in the synthesis of metal NPs such as those of Au. It's worthwhile to mention here that α-amylase was found to retain its biological activity in the enzyme- Au NP composite thus formed.

Chapter 3:

The first work provoked us to investigate digestion of Au NP encapsulated starch by α-amylase. Starch is a well-known drug delivery vehicle and understanding digestion of the encapsulated NPs might bring new information related to nanoscale drug delivery especially using the optical properties of the NPs. There are indeed requirements of detailed knowledge of delivery, fate and functioning at the target, and finally release from the body of the nanomaterials being proposed to be used in nanomedicine. And that's an area where a lot of unanswered questions remain. In particular, the question of what happens when the drug-containing NPs reach their intended target is a pertinent one. One can ask: how do the drug molecules get released from the delivery vehicle? In other words, how does the 'envelope' get opened? What is the fate of the NPs post opening? In **Chapter 3** starch-Au NP composite has been synthesized and the digestion of starch monitored spectroscopically in the presence of its digestive enzyme α-amylase. The study gave rise to new knowledge about the fate of the Au NPs when the composite

came in contact with α-amylase. It also led to the development of a method of following starch digestion (in the form of a composite) by UV-vis spectroscopy that monitored the change in the surface plasmon resonance (SPR) peak of the Au NPs in the composite. Our findings suggested that the specificity of release of encapsulated NPs could be achieved with an appropriate combination of encapsulating materials and the choice of an appropriate enzyme that would cleave the encapsulation to release the NPs.

Chapter 4:

Chapter 4 discusses the use of unique optical properties of the citrate-stabilized Au NPs in estimating the amount of protein (with distinction of its conformation) present in a medium. Proteins are well known for their vital roles in various life sustaining processes and hence are considered of high importance. A slight change in their level or their conformation in our body may lead to various disorders. Hence a proper knowledge about their structure and concentration is highly desirable. The method developed herein was based on the non-covalent and non-specific electrostatic interactions of protein(s) with the Au NPs. The interaction of various amino groups present on the surface of the protein with the citrate-stabilized Au NPs possibly led to the agglomeration of the NPs, which formed the basis of the method. The change in area under the SPR peak of the Au NPs were correlated to the amount of protein (and their conformation) and thus used to estimate the amount in an unknown sample.

Chapter 5:

Based on principles similar to the third work, the fourth work was designed so as to develop a method to quantitatively estimate the conformational content (purity) of a protein in a mixture of its native and denatured forms, which is discussed in **Chapter 5**. It was based on the fact that the two forms of the same protein interacted differently with the citrate-stabilized Au NPs and thus leading to different levels of agglomeration. The content could be quantified by measuring the change in area under the SPR peaks.

Chapter 6:

Finally, we were interested in knowing how the interaction between a protein, like α-amylase and citrate-stabilized Au NPs could alter/ affect its biological activity. This has been discussed in ***Chapter 6***. The substrate (starch) dependent activity of α-amylase was

measured by following the product (maltose) formation. It was found that the specific activity of the enzyme in presence of Au NPs was as high as 8-fold as compared to that in the presence of the same amount of free protein and also the activity could be modulated by changing the concentration of the enzyme. The increase in the extent of agglomeration of the Au NPs in presence of increasing amount of enzyme was found to be the reason behind the decrease in the specific activity with increasing enzyme concentration.

Chapter 7:

The final chapter presents an overview of the work done for the present thesis, the essential outcome and the future prospective works that can be framed from the questions that arises after the work.

References

1. Niemeyer, C. M. *Angew. Chem. Int. Ed*. **2001**, *40*, 4128.
2. Rosi. N. L.; Mirkin, C. A. *Chem. Rev*. **2005**, *105*, 1547.
3. Shenhar, R.; Rotello, V. M. *Acc. Chem. Res*. **2003**, *36*, 549.
4. Katz, E. Willner, I. *Angew. Chem., Int. Ed*. **2004**, *43*, 6042.
5. Whitesides, G. M. *Nat. Biotechnol*. **2003**, *21*, 1161.
6. LaVan, D. A.; McGuire, T.; Langer, R. *Nat. Biotechnol*. **2003**, *21*, 1184.
7. Ferrari, M. *Nat. Rev*. *Cancer,* **2005**, *5*, 161.
8. Farokhzad, O. C.; Karp, J. M.; Langer, R. *Exp. Opin. Drug Delivery* **2006**, *3*, 311.
9. Zhang, L.; Gu, F. X.; Chan, J. M.; Wang, A. Z.; Langer, R. S.; Farokhzad, O. C. *Clin. Pharmacol. Ther*. **2008**, 83, 761.
10. Langer, R. *Nature* **1998**, *392*, 5.
11. Langer, R. *Science* **1990**, *249*, 1527.
12. Glass, G. *Nat. Rev. Drug Discovery* **2004**, 3, 1057.
13. Liong, M.; Lu, J.; Kovochich, M.; Xia, T.; Ruehm, S. G.; Nel, A. E.; Tamanoi, F.; Zink, J. I. *ACS Nano* **2008**, *2*, 889.
14. Bangham, A. D.; Standish, M. M.; Watkins, J. C. *J. Mol. Biol*. **1965**, *13*, 238.
15. Langer, R.; Folkman, J. *Nature* **1976**, *263*, 797.
16. Yatvin, M. B.; Kreutz, W.; Horwitz, B. A.; Shinitzky, M. *Science* **1980**, *210*, 1253.
17. Leserman, L. D.; Barbet, J.; Kourilsky, F.; Weinstein, J. N. *Nature* **1980**, *288*, 602.
18. Heath, T. D.; Fraley, R. T.; Papahdjopoulos, D. *Science* **1980**, *210*, 539.
19. Wagner, V.; Dullaart, A.; Bock, A.-K.; Zweck, A. *Nat. Biotechnol*. **2006**, *24*, 1211.
20. Gu, F.; Zhang, L.; Teply, B. A.; Mann, N.; Wang, A.; Radovic-Moreno, A. F.; Langer, R.; Farokhzad, O. C. *Proc. Natl. Acad. Sci. U.S.A*. **2008**, *105*, 2586.
21. Decuzzi, P.; Pasqualini, R.; Arap, W.; Ferrari, M. *Pharm. Res*. **2009**, *1*, 235.

22. Dreher, M. R.; Liu, W.; Michelich, C. R.; Dewhirst, M. W.; Yuan, F.; Chilkoti, A. J. *Natl. Cancer Inst*. **2006**, *98*, 335.

23. Matsumura, Y.; Maeda, H. *Cancer Res*. **1986**, *46*, 6387.

24. Jain, R. K. *Adv. Drug Delivery Rev*. **2001**, *46*, 149.

25. Alivisatos, A. P. *Science* **1996**, *271*, 933.

26. Brust, M.; Kiely, C. J. *Colloids Surf. A: Physicochem. Eng. Asp*. **2002**, *202*, 175.

27. Collin, R. *Field Theory of Guided Waves*, 2nd ed.; Wiley: New York, **1990**.

28. Ritchie, R. H. *Phys. Rev*. **1957**, *106*, 874.

29. Raether, H. *Surface Plasmons*; Springer-Verlag: Berlin, **1988**.

30. Barnes, W. L.; Dereux, A.; Ebbesen, T. W. *Nature* **2003**, *424*, 824.

31. Kreibig, U.; Vollmer, M. *Optical Properties of Metal Clusters*; Springer-Verlag: Berlin, **1996**.

32. Nelayah, J.; Kociak, M.; Stephan, O.; Garcia de Abajo, F. J.; Tence, M.; Henrard, L.; Taverna, D.; Pastoriza-Santos, I.; Liz-Marzan, L. M.; Colliex, C. *Nat. Phys*. **2007**, *3*, 348.

33. Hao, E.; Schatz, G. C. *J. Chem. Phys*. **2004**, *120*, 357.

34. Gans, R. *Ann. Phys*. **1925**, *76*, 29.

35. Mie, G. *Ann. Phys*. **1908**, *25*, 377.

36. Gans, R. *Ann. Phys*. **1912**, *37*, 881.

37. Roco, M. C. *Curr. Opin. Biotechnol*. **2003**, *14*, 337.

38. Wilson, R. *Chem. Soc. Rev*. **2008**, *37*, 2028.

39. Rosi, N. L.; Mirkin, C. A. *Chem. Rev*. **2005**, *105*, 1547.

40. Ghadiali, J. E.; Stevens, M. M. *Adv. Mater*. **2008**, *20*, 4359.

41. Elghanian, R.; Storhoff, J. J.; Mucic, R. C.; Letsinger, R. L.; Mirkin, C. A. *Science* **1997**, *277*, 1078.

42. Reynolds, R. A.; Mirkin, C. A.; Letsinger, R. L. *J. Am. Chem. Soc*. **2000**, *122*, 3795.

43. Li, H. X.; Rothberg, L. J. *J. Am. Chem. Soc*. **2004**, *126*, 10958.

44. Chakrabarti, R.; Klibanov, A. M. *J. Am. Chem. Soc*. **2003**, *125*, 12531.

45. Storhoff, J. J.; Lucas, A. D.; Garimella, V.; Bao, Y. P.; Muller, U. R. *Nat. Biotechnol*. **2004**, *22*, 883.

46. Sapsford, K. E.; Berti, L.; Medintz, I. L. *Angew. Chem. Int. Ed*. **2006**, *45*, 4562.

47. Dubertret, B.; Calame, M.; Libchaber, A. J. *Nat. Biotechnol*. **2001**, *19*, 365.

48. Xiao, Y.; Pavlov, V.; Levine, S.; Niazov, T.; Markovitch, G.; Willner, I. *Angew. Chem.*, *Int. Ed*., **2004**, *43*, 4519.

49. Pavlov, V.; Xiao, Y.; Willner, I. *Nano Lett*., **2005**, *5*, 649.

50. Baron, R.; Zayats, M.; Willner, I. *Anal. Chem*., **2005,** *77*, 1566.

51. Wang, Z.; Lee, J.; Cossins, A. R.; Brust, M. *Anal. Chem*., **2005**, *77*, 5770.

52. Wang, Z.; Levy, R.; Fernig, D. G.; Brust, M. *J. Am. Chem. Soc*., **2006**, *128,* 2214.

53. Bornscheuer, U. T. *Nat. Biotech*. **2004**, *22*, 1098.

54. De, M.; Ghosh P. S.; Rotello, V. M. *Adv. Mater*. **2008**, *20*, 4225.

55. Daniel, M. C.; Astruc, D. *Chem. Rev*. **2004**, *104*, 293.

56. Sheehan, P. E.; Whitman, L. J.; *Nano Lett*. **2005**, *5*, 803.

57. Hostetler, M. J.; Wingate, J. E.; Zhong, C. J.; Harris, J. E.; Vachet, R. W.; Clark, M. R.; Londono, J. D.; Green, S. J.; Stokes, J. J.; Wignall, G. D.; Glish, G. L.; Porter, M. D.; Evans, N. D.; Murray, R. W. *Langmuir* **1998**, *14*, 17.

58. Zheng, J.; Zhang, C.; Dickson, R. M. *Phys. Rev. Lett*. **2004**, *93*, 77402.

59. van Dijk, M. A.; Lippitz, M.; Orrit, M. *Acc. Chem. Res*. **2005**, *38*, 594.

60. Lakowicz, J. R. *Anal. Biochem*. **2005**, *337*, 171.

61. Su, K. H.; Wei, Q. H.; Zhang, X.; Mock, J. J.; Smith, D. R.; Schultz, S.; *Nano Lett*. **2003**, *3*, 1087.

62. Stuart, M. A. C.; Fleer, G. J.; Lyklema, J.; Norde, W.; Scheutjens, J. M. H. M. *Adv. Colloid Interface Sci*., **1991**, *34*, 477.

63. Brown, D. H.; Smith, W. E. *Chem. Soc. Rev*. **1980**, *9*, 217.

64. Turkevitch, J.; Stevenson, P. C.; Hillier, J. *Faraday Soc*. **1951**, *11*, 55.

65. Frens, G. *Nature: Phys. Sci*. **1973**, *241*, 20.

66. Giersig, M.; Mulvaney, P. *Langmuir* **1993**, *9*, 3408.

67. Brust, M.; Fink, J.; Bethell, D.; Schiffrin, D. J.; Kiely, C. J. *J. Chem. Soc., Chem. Commun*. **1995**, 1655.

68. Sau, T. K.; Rogach, A. L.; Ja¨ckel, F.; Klar, T. A.; Feldmann. J. *Adv. Mater*. **2010**, *22*, 1805.

69. Herron, N.; Thorn, D. L. *Adv. Mater*. **1998**, *10*, 1173.

70. Yguerabide, J.; Yguerabide, E. E. *Anal. Biochem*. **1998**, *262*, 137.

71. Sershen, S. R.; Westcott, S. L.; Halas, N. J.; West, J. L. *J. Biomed. Mater. Res*. **2000**, *51*, 293.

72. Peceros, K.E.; Xu, X.; Bulcock, S. R.; Cortie, M. B. *J. Phys. Chem. B.* **2005**, *109*, 21516.

73. Norman, Jr., T. J., Grant, C. D.; Magana, D.; Cao, D.; Bridges, F.; Liu, J.; van Buuren, T.; Zhang, J. Z. *J. Phys. Chem. B.* **2002**, *106*, 7005.

74. Pérez-Juste, J.; Pastoriza-Santos, I.; Liz-Marzán, L. M.; Mulvaney. P. *Coord. Chem. Rev*. **2005**, *249*, 1870.

75. Lu, W.; Singh, A. K.; Khan, S. A. Senapati, D.; Yu, H.; Ray, P. C. *J Am Chem Soc*. **2010** *Article ASAP* (DOI: 10.1021/ja104924b)

76. J. Lakowicz, C. Geddes, I. Gryczynski, J. Malicka, Z. Gryczynski, Aslan, K.; Lukomska, J.; Matveeva, E.; Zhang, J.; Badugu, R.; Huang, J. *J. Fluoresc*., **2004**, *14*, 425.

77. Kuhn, S.; Hakanson, U.; Rogobete, L.; Sandoghdar, V. *Phys. Rev. Lett*. **2006**, *97*, 017402.

78. Vukovic, S.; Corni, S.; Mennucci, B. *J. Phys. Chem. C* **2009**, *113*, 121.

79. Cao, Y. W. C.; Jin, R. C.; Mirkin, C. A. *Science* **2002**, *297*, 1536.

80. Kunckels, J. *Nuetliche Observationes oder Anmerkungen von Auro und Argento Potabili*; Schutzens: Hamburg, **1676**.

81. Savage, G. *Glass and Glassware; Octopus Book*: London, **1975**.

82. Helcher, H. H. *Aurum Potabile oder Gold Tinstur*; J. Herbord Klossen: Breslau and Leipzig, **1718**.

83. *Dictionnaire de Chymie*; Lacombe: Paris, **1769**.

84. Ostwald, W. *Zur Geschichte des Colloiden Goldes*. *Kolloid Z.* **1909**, *4*, 5.

85. Landsman, M. L. J.; Kwant, G.; Mook, G. A.; Zijlstra, W. G. J. *Appl. Physiol*. **1976**, *40*, 575.

86. Yelin, D.; Oron, D.; Thiberge, S.; Moses, E.; Silberberg, Y. *Opt. Express* **2003**, *11*, 1385.

87. Wang, Y.; Xie, X.; Wang, X.; Ku, G.; Gill, K. L.; O'Neal, D. P.; Stoics, G.; Wang, L. V. *Nano Lett*. **2004**, *4*, 1689.

88. Sokolov, K.; Follen, M.; Aaron, J.; Pavlova, I.; Malpica, A.; Lotan, R.; Richards-Kortum, R. *Cancer Res*. **2003**, *63*, 1999.

89. El-Sayed, I. H.; Huang, X., El-Sayed, M. A. *Nano Lett*. **2005**, *5*, 829.

90. Hirsch, L. R.; Stafford, R. J.; Bankson, J. A.; Sershen, S. R.; Rivera, B.; Price, R. E.; Hazle, J. D.; Halas, N. J.; West, J. L. *Proc. Natl. Acad. Sci. U.S.A*. **2003**, *100*, 13549.

91. Loo, C.; Lowery, A.; Halas, N.; West, J.; Drezek, R. *Nano Lett*. **2005**, *5*, 709.

92. Huang, X.; El-Sayed, I. H.; Qian, W.; El-Sayed, M. A. J. Am. Chem. Soc. 2006, 128, 2115.

93. Wacker, R.; Ceyham, B.; Alhorn, P.; Schueler, D.; Lang, C.; Niemeyer, C. M. *Biochem. Biophys*. *Res. Commun*. **2007**, 357, 391.

94. Nam, J.; Thaxton, C. S.; Mirkin, C. A. *Science* **2003**, *301*, 1884.

95. Hirsch, L. R.; Jackson, J. B.; Lee, A.; Halas, N. J.; West, J. L. *Anal. Chem*. **2003**, *75*, 2377.

96. Nel, A.; Xia, T.; Madler, L.; Li, N. *Science*, **2006**, *311*, 622.

97. You, C. C.; Agasti, S. S.; De, M.; Knapp, M. J.; V. M. Rotello. *J. Am. Chem. Soc*. **2006**, *128*, 14612.

98. Dyal, A.; Loos, K.; Noto, M.; Chang, S. W.; Spagnoli, C.; Shafi, K. V. P. M. Ulman, A.; Cowman, M.; Gross, R. A. *J. Am. Chem. Soc*. **2003**, *125*, 1684.

99. Wu, C. S.; Wu, C. T.; Yang, Y. S.; Ko, F. H. *Chem. Commun*., **2008**, *42*, 5327.

100. Brennan, J. L.; Kanaras, A. G.; Nativo, P.; Tshikhudo, T. R.; Rees, C.; Fernandez, L. C.; Dirvianskyte, N.; Razumas, V.; Skjot, M.; Svendsen, A.; Jørgensen, C. I.; Schweins, R.; Zackrisson, M.; Nylander, T.; Brust, M.; Barauskas, J. *Langmuir* **2010**, *26*, 13590.

101. Lacerda, S. H. D. P.; Park, J. J.; Meuse, C.; Pristinski, D.; Becker, M. L.; Karim, A.; Douglas, J. F. *ACS Nano*, **2010**, *4*, 365.

102. Calzolai, L.; Franchini, F.; Gilliland, D.; Rossi, F. *Nano Letter*, **2010**, *10*, 3101.

103. Lynch, I.; Dawson, K. A. *Nanotoday* **2008**, *3*, 40.

104. Zhang, D.; Neumann, O.; Wang, H.; Yuwono, V. M.; Barhoumi, A.; Perham, M.; Hartgerink, J. D.; Wittung-Stafshede, P.; Halas, N. J. *Nano Letters* **2009**, *9*, 666.

105. Wu, X.; Narsimhan, G. *Langmuir* **2008**, *24*, 4989.

Chapter 2

Retention of Enzymatic activity of α-Amylase in the Reductive Synthesis of Gold Nanoparticles

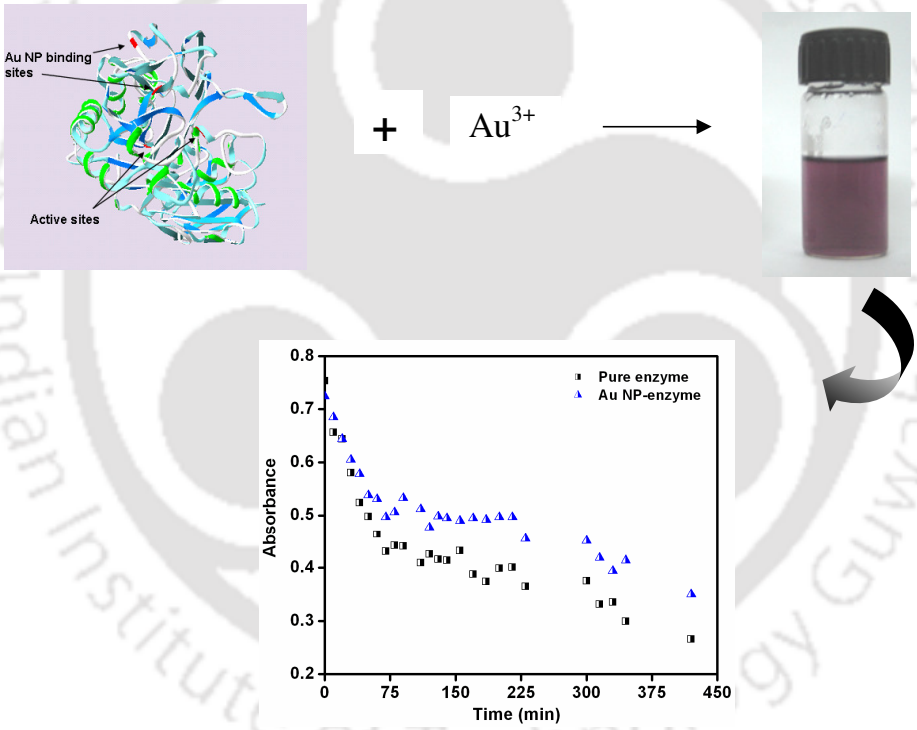

* Rangnekar, A.; Sarma, T. K.; Singh, A. K.; Deka, J.; Ramesh, A.; Chattopadhyay, A. *Langmuir* **2007**, *23*, 5700-5706.

Outline:

The growing interest in nanomaterials ever since the discovery of their unique properties and applications is concomitant with the development of newer and better methods of their synthesis. For medical applications this also means that utmost care has to be taken in their synthesis so as to minimize any potential risks to a living entity. Since the final aim in medical applications would be to inject such NPs in vivo, hence use of biological methods would always be preferable over other existing methods. This chapter discusses the mechanism of synthesis of gold nanoparticles (Au NPs) by an enzyme α-amylase. In this work we have also tried to check for any changes in the biological activity of the enzyme after NP synthesis. The observations suggest that the presence of free and exposed S-H groups is essential in the reduction of $AuCl_4^-$ to Au NPs and the enzyme retains its biological activity after NP synthesis. Fortuitously, the enzymatic functional group of α-amylase is positioned opposite to that of the free and exposed S-H group, which makes it ideal for the production of Au NPs; binding of the enzyme to Au NPs via Au-S bond and also retention of the biological activity of the enzyme.

2.1 Introduction:

Development of protocols for the synthesis of metal nanoparticles (NPs) has been an important aspect of research activities toward fabrication of miniaturized sensors, electronic components, spectroscopic enhancers, functional nanostructures and microimaging probes.[1] In this regard, aqueous and other organic solution-phase synthetic routes have enabled the synthesis of a variety of functional inorganic quantum dots or nanoparticles.[2,3] These nanoscale functional building blocks are expected to be useful for the bottom-up approaches to materials assembly and have therefore received attention owing to their intrinsic size-dependent properties and consequent application potentials.[4] An important case in point here is the synthesis and functionalization of Au NPs for appropriate chemical and biological applications, taking advantage of its Surface Plasmon Resonance and other noble metal properties. Presently, there are a host of chemical and biological (including the use of microorganisms) routes available for the synthesis of Au NPs with subsequent functionalization for the development of appropriate devices. The chemical methods of synthesis usually involve the chemical reduction of the parent metal salts by reagents such as sodium borohydride, hydroxylamine, polyvinyl pyrrolidone. Au NPs can also be readily formed by reduction of tetrachloroauric acid in the presence of thiol capping agents.[5] Although these methods may successfully produce pure and well-defined NPs, the stringent reaction conditions

used in the syntheses may not be suitable for biological and biochemical applications. On the other hand, biological systems have been helpful in the synthesis and assembly of nanoscale materials, forming sophisticated macroscopic systems with striking structural features.[6] Biosynthesis acquires special importance owing to its specificity and environment friendly nature and is conceivably amicable to functionalization. Microbial synthesis of NPs has been reported earlier.[7-9] In this regard, enzymes can possibly serve as a set of structurally diverse biological tools assembling unique nanostructures. An additional attraction is that enzymes are commercially available in pure form and they have diverse chemical, biochemical, and biological functions as such or on supported surfaces. It has been reported that a lipase enzyme immobilized on magnetic NPs could be reused over a longer period than the free enzyme.[10] Au NPs when functionalized with a redox enzyme, apo-glucose oxidase, can act as an electron relay between the biocatalyst and the electrode.[11] Further, there have been several reports in using enzyme as mediator or catalyst in synthesizing Au NPs.[12]

The primary challenge in developing NP-based enzymatic devices is to be able to chemically immobilize an enzyme, which will retain its activity or improve its function while being attached to the NP. This would be of even greater significance if the whole process could be performed under physiological condition without having to resort to functionalization of key molecules at various steps. In the present investigation, we report for the first time the reductive synthesis of Au NPs by a pure enzyme (α-amylase) and concomitant surface functionalization of the NPs in the same reaction. The Au NP- α-amylase complex was purified, characterized, and tested for the functional activity of the enzyme attached to the NP. It must be mentioned here that the synthesis of the Au NP- α-amylase complex was carried out based on the experiments done by Rangnekar *et al.*[13] Interestingly, the enzymatic activity of the Au NP- α-amylase complex was found to be retained in the complex. Structural analysis shows that the native form of the enzyme could support the formation of Au NPs by the enzyme, immobilization as well as retention of the activity of the enzyme. A mechanism of NP formation deciphering the role of exposed functional groups of enzyme in the reductive synthesis and binding of the enzyme molecule is suggested. The primary conclusion is that the presence of free and exposed thiol groups in α-amylase, and the catalytic site being away from the active site, supports such complementary functions, while several other enzymes which lack free and exposed thiol groups do not even produce the NPs.

2.2. Materials and Methods

2.2.1 *Enzymes and Reagents*

Commercially available pure enzymes and bovine serum albumin (BSA) were purchased from Sigma-Aldrich and Fluka. $HAuCl_4$ solution (17% w/v in dilute HCl) was purchased from Aldrich, and diluted subsequently for use. Water soluble starch powder was purchased from E-Merck (India) and Gram's iodine solution was purchased from Himedia Private limited, Mumbai. For all the experiments, ultrafiltered milliQ water (Millipore, USA) was used.

2.2.2 *Synthesis of Gold Nanoparticle*[13]

Hog pancreatic α-amylase, was used to study the synthesis of Au NPs. Reactions was carried out in a total volume of 5.0 mL at 37 °C for a period of 48 h and consisted of enzymes solution prepared in phosphate buffer of pH 7.0 reaction buffer (recommended by manufacturer), and $HAuCl_4$ (4.5×10^{-4} M). The concentration of enzymes was 1.0 mg mL^{-1} for the experiments. Sample was taken at regular intervals, and Au NP formation was monitored by recording UV-visible spectra in the range of 300-800 nm in a Cary 50 UV-visible spectrophotometer (Varian Inc.). A control sample consisting of buffer and $HAuCl_4$, without enzyme was also maintained. A parallel set of experiment was performed with heat-denatured enzyme for the NP synthesis. The denaturation was achieved by heating the enzyme solution at 80 °C for 30 min.

2.2.3 *Isolation and Purification of Au NP- α-Amylase Complex*

Au NPs were synthesized by incubating α-amylase and $HAuCl_4$ solution at 37 °C for 48 h as mentioned before. The NP-α-amylase complex was harvested by centrifugation at 20,000 rpm and 25 °C for 20 min. The supernatant was discarded and the pellet of NP-enzyme complex was resuspended in 10 mM phosphate buffer (pH 7.0). The NP-enzyme complex was recovered again by centrifugation at 20,000 rpm and 25 °C for 20 min, and the buffer was discarded. The buffer wash was repeated twice.

2.2.4 *Spectroscopy and Microscopy Studies*

The UV-vis spectroscopy studies were performed in PerkinElmer Lambda25 UV/Vis Spectrometer. TEM images of the NP complex were recorded in a JEOL microscope

(JEMCX 100) at 80 kV accelerating voltage. The images were recorded immediately after the synthesis of the NPs, and also after studying the kinetics of starch degradation by Au NP-enzyme complex.

2.2.5 *Functional Characterization of Au NP-α-Amylase Complex*

The protein content in the Au NP-enzyme complex was estimated by using the standard Bradford method.[14] This was carried out by separating the whole of the complex from the solution using centrifugation as mentioned before and then resuspending into a buffer solution. Also, the estimation was ascertained by measuring the unreacted enzyme (α-amylase) in the supernatant by the same method. The results were consistent with each other. Starch agar solution (3%) was prepared in double distilled water, autoclaved, and poured into a petri plate. After solidification of agar, three distinct wells were punctured into the agar plate and filled with 200.0 µL of 10 mM potassium phosphate buffer, 1.0 mg mL^{-1} α-amylase solution, and Au-NP- α-amylase complex resuspended in phosphate buffer, respectively. The plate was incubated at 37 °C overnight, and α-amylase activity was tested by flooding the plate with iodine solution and observing zone of clearance. For time dependent starch digestion activity, 280.0 µL of 1.0 mg/mL of α-amylase was added to 34.32 mL of 3.0 mg mL^{-1} of starch solution and the mixture diluted to 60.0 mL with buffer which was then incubated at 37^0C. The starch degradation kinetics was then tested by taking out aliquots from the reaction mixture at regular intervals and adding 50.0 µL of iodine solution measuring absorbance values at 620 nm at regular intervals. We have also performed the digestion of starch in absence of iodine by enzyme only and also by the Au-NP-enzyme complex. Aliquots were taken from the reaction mixture from time to time and iodine was added to monitor the formation of starch-iodine complex by absorption at 620 nm. It must be mentioned here that the kinetics experiments were performed using equal amount of protein in both the composite and free enzyme during hydrolysis of starch.

2.2.6 *Modification of Free Thiol Groups of a-Amylase*

In order to modify the free cysteine thiol groups of α-amylase, 187.0 µL of 6.0 mM 2,2′-dithiobis (5-nitropyridine) (DTNP) in dimethyl sulfoxide (DMSO) was added to 1.5 mL of 2.0 mg/mL enzyme solution, and the final reaction volume was made up to 9.4 mL with 100 mM phosphate buffer. The reaction mixture was stirred overnight, which

resulted in a pale yellow colored solution. The UV-vis spectrum of the sample was measured to ascertain modification of the free cysteine thiol groups of α-amylase. The solution was then treated with 245.0 µL of $HAuCl_4$ so that the final concentration was 4.5×10^{-4} M and kept for 48 h in an incubator set at 37 °C. The control experiment was performed with buffered enzyme and $HAuCl_4$ only in the presence of DMSO. The UV-vis spectrum of the initial mixture consisted of peaks at 280 and 319 nm corresponding to the enzyme and DTNP, while that at 12 h (overnight incubation) consisted of a single peak at 387 nm characteristic of the formation of 5-nitropyridine-2-thione. This indicates the modification of the free thiol groups of the enzyme as established before.[15] It may be mentioned here that dialysis of the mixture did not reduce the color (as well as intensity of the peak at 387 nm). Also, dialyzed mixture and non-dialyzed mixture produced the same results.

2.3 Results and Discussions

2.3.1 *Enzymatic Synthesis of Au Nanoparticles*

When native α-amylase was added to a buffered solution (pH 7.0) of $AuCl_4^-$, the solution turned light pink in 6 h and was dark purple in 48 h. The visible spectrum of the solution (Figure 1A) recorded at different time period consisted of an increasingly intense absorption at ca. 530 nm, characteristic of the surface plasmon resonance (SPR) of Au NPs. Control sample did not show any color and consequently did not have any peak in the visible region indicating that α-amylase is responsible for the synthesis of Au NPs. Further, when denatured α-amylase was used an intense peak around 550 nm appeared within 24 h (Figure 1B), indicating that denatured protein also produced Au NPs. The difference in peak positions between Au NPs synthesized by native and denatured α-amylase could be due to different particle size produced in the media. However, it is interesting to note that when the same reaction was carried out in the presence of other enzymes, except for the α-amylase (Figure 2A) and EcoRI, neither BSA, nor any of the other enzymes tested, namely ribonuclease A (RNase A), lysozyme, alkaline phosphatase, horse radish peroxidase (HRP), Taq DNA polymerase, *PvuII*, could produce any color in the solution that is characteristic of the formation of Au NPs (Figure 2B). The tests with enzymes other than α-amylase were performed by Rangnekar

et al.[13] In addition, the reaction mixtures, which were colorless, did not show any absorption peak in the UV-vis spectra (not shown here).

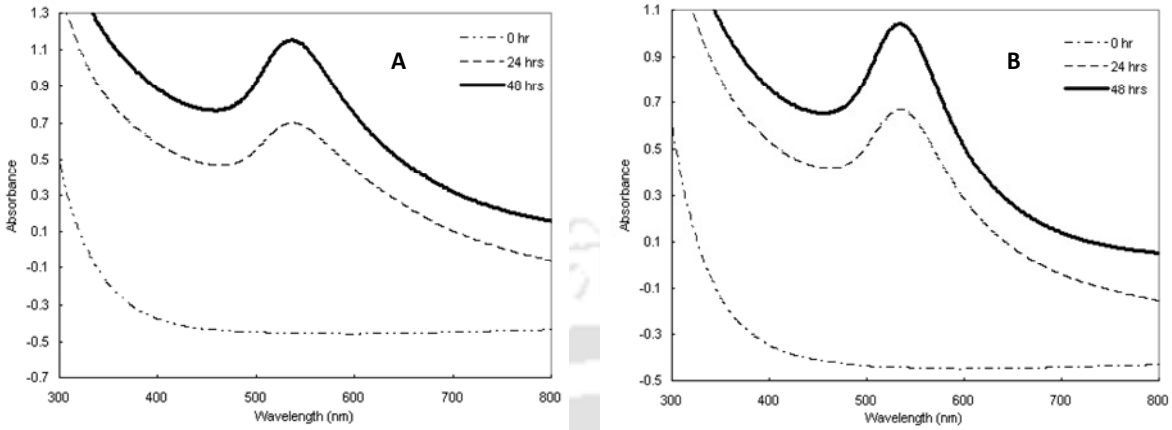

Figure 1. *UV-Vis spectra of Au NP solution synthesized by* ***(A)*** *native and* ***(B)*** *denatured α-amylase solution (taken from Abhijit Rangnekar BTP thesis 2006*[13]*).*

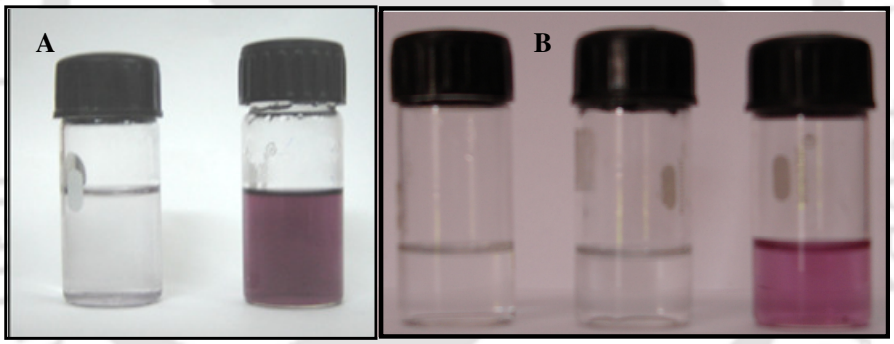

Figure 2. ***(A)*** *Synthesis of gold nanoparticle (Au NP) by α-amylase. Photographs of control sample (left) and Au NP solution synthesized by α-amylase (right).* ***(B)*** *Photographs of samples of Taq DNA polymerase, PvuII and EcoRI (left-right) treated with buffered* $AuCl_4^-$. *The color of Au NP formed could only be seen in the sample containing EcoRI (photographs in 2B are taken from Abhijit Rangnekar BTP thesis 2006*[13]*).*

2.3.2 *Characterization of Au NP – α-amylase complex*

Au NP–α-amylase complex was purified by a simple centrifugation process as described below. A dark purple pellet was obtained upon centrifugation of the α-amylase synthesized Au NP solution for 20 min at 20,000 rpm. The supernatant was clear indicating complete recovery of NPs in the pellet. Sedimentation of soluble proteins is

possible only by ultra-centrifugation. Hence, at the speed employed, free enzyme remained in the solution. The procedure was repeated three times after which the pellet could be easily resuspended in buffer, indicating lack of agglomeration. The estimation of protein content in the complex using the Bradford method revealed that the composite contained 40% of original protein and the remaining 60% was left in the supernatant as unreacted enzyme. A transmission electron micrograph (TEM) obtained from a drop-coated film of as –prepared Au-NPs exhibited well-dispersed, individual particles of size range 5-20 nm without the presence of noticeable agglomeration (Figure 3A). We also pursued TEM measurements of the complex NPs after starch digestion (details are discussed later) and a typical micrograph is shown in Figure 3B, which showed that the digestion of the starch by the complex did not change the sizes of the particle or neither lead to any discernible agglomeration.

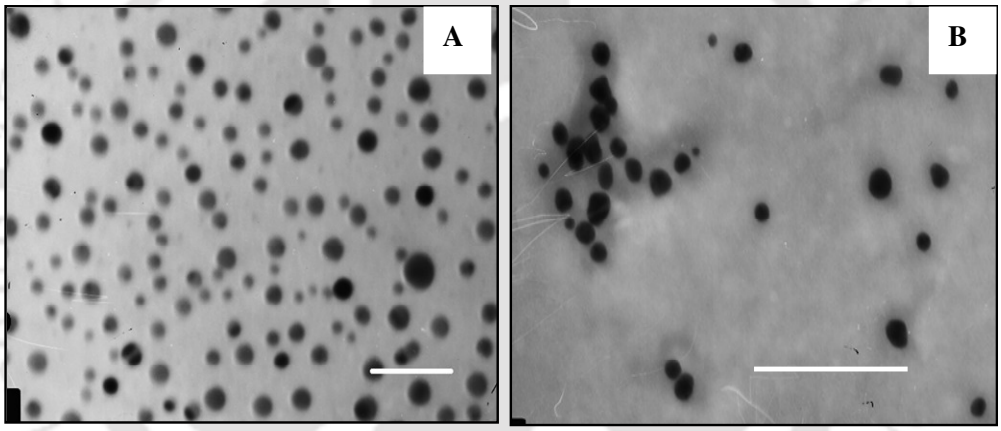

Figure 3. *Transmission electron micrograph of* ***(A)*** *Au NPs synthesized by α-amylase cast on copper grid. Scale bar is 50 nm.* ***(B)*** *Au NPs coated with α-amylase after treatment with starch-iodine solution. Scale bar is 100 nm (taken from Abhijit Rangnekar BTP thesis 2006[13]).*

2.3.3 *Enzymatic activity of Au NP – α-amylase complex*

We pursued the starch agar plate test for enzymatic activities of the complex vis-à-vis the pure enzyme. The clear zone obtained around the wells in starch agar plate indicates the α-amylase activity. The results of such tests are shown in Figure 4A, where the largest zone is due to α-amylase only, the medium one is due to Au-NP-α-amylase complex and the control (with no α-amylase) failed to produce any zone. As clear from the figure, the zone of activity associated with the Au NP – α-amylase complex was

smaller than that of pure enzyme. This could be due to limited diffusion of Au NP – α-amylase complex in the solid medium compared to that of the free enzyme. Besides, the amount of α-amylase present in the complex is less compared to that of the added free enzymes and hence difference in size of the zones. Further, the digestion of starch was pursued by following UV-vis absorption of starch-iodine solution in the presence of enzyme only and also in the presence of complex studied separately. Figure 4B represents the decrease in absorbance of the starch–iodine complex in the presence of pure enzyme and in the presence of the Au NP–α-amylase complex. It is evident that hydrolysis was nearly complete in 400 min for both the cases. However, since products are not removed from the reaction mixtures it is plausible that the time for completion would be much longer as the products are likely to inhibit the enzymatic activity. Also, clear from the graph is that at a qualitative level the rate of starch digestion by both the composite as well as free enzyme are similar. Hence, it can be concluded that the activity of the enzyme was retained in the composite.

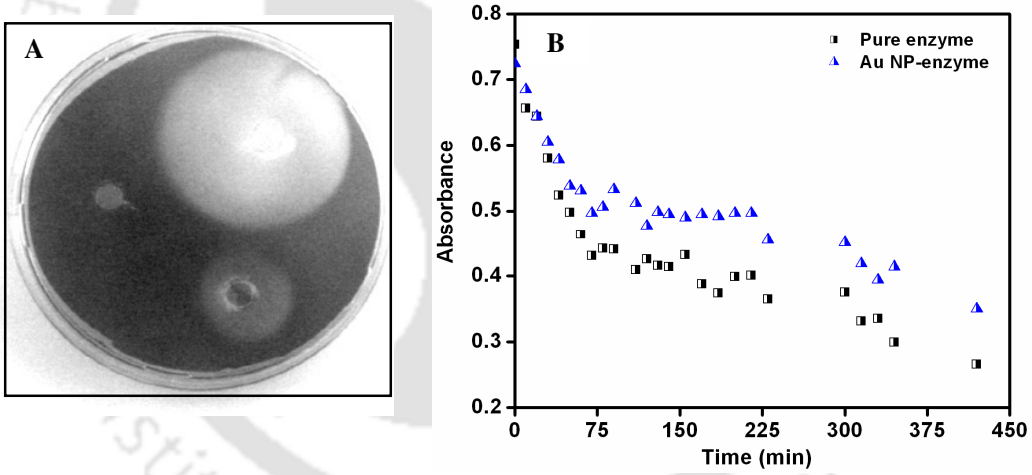

Figure 4. ***(A)*** *Starch agar plate assay for enzymatic activity of pure α-amylase (larger zone), Au NP- α-amylase complex (medium sized zone) and control.* ***(B)*** *Kinetics of starch digestion, with pure α-amylase and Au NP- α-amylase complex as followed by the absorbance at 620 nm.*

It is possible that the α-amylase molecules immobilized on to the surface of Au NPs are aligned in such a way that the catalytic sites of a large number of enzyme molecules are exposed directly to the medium (and thus to starch molecules), while the non catalytic sites are attached to Au NPs surface.Whereas the free enzymes have both the sites exposed to starch. Burt and co-workers[16] reported similar augmentation of surface interaction for Au NP-BSA conjugate. However, the details of the mechanism of

enzymatic activity need to be further studied under different experimental conditions such as concentration of starch, enzyme as well as starch-iodine complex to ascertain the exact nature of the kinetics.

2.3.4 *Proposed Mechanism of Au NP-α-Amylase Complex Formation and Associated Enzyme Activity*

Enzymes are known for their catalytic activity that is highly specific and efficient. But they have rarely been exploited as a reactant or as an agent to perform functions other than catalysis. The numerous functional groups, present in the side chains of the constituent amino acids, account for their three-dimensional structures with desired functionality. One of the functional groups that could be of important consequence in the present set of studies is the thiol group (-SH), which is present in the side chain of cysteine. It is known that the -SH group reacts with Au to form Au-S bonds. However, the -SH group could also be used for the reduction of metal cations (especiallyAu^{3+}) to form corresponding metal atoms. Consequently, the enzyme containing a free and exposed thiol group could be used as a reducing agent. α-amylase, which has two free and exposed thiol groups[17,18] could have reacted with $AuCl_4$-, and form Au NPs, which is probably the case herein. The ability of the heat-denatured α-amylase to synthesize Au NPs indicated that only the native three-dimensional structure of α-amylase was not essential in the process. The increased rate of production of NPs by denatured enzyme vis-a-vis native (Figure 1) indicated rapid reduction of Au^{3+} to Au^0 by exposed functional groups.

Table 1. *Functional Groups of Enzymes and BSA*[17]

Enzyme/Protein	Number of cysteines	Number of disulfide linkages	Number of free thiol group
α-amylase	12	5	2 (exposed)
Bovine Serum Albumin	35	17	1 (buried)
Ribonuclease A	8	4	-
Lysozyme	8	4	-
Alkaline Phosphatase	4	2	-
Horse Radish Peroxidase	8	4	-
Taq DNA polymerase	3	-	-
*Pvu*II	-	-	-
*Eco*RI	1	-	1 (exposed)

The reducing amino acids present in any enzyme (or protein) are cysteine (thiol group) and histidine (tertiary amine group). But tertiary amine is known to act as reducing agent only in organic environment.[19] So, in the present case of enzymatic synthesis of Au NPs, it is essentially the free thiol groups that are responsible for the reduction of Au^{3+} to Au^{0}. This is further supported by studies with other enzymes, which are described below. We have used other enzymes (and proteins), some of which have free and exposed thiol groups while the other do not have free thiol groups at all. Table 1 indicates number of cysteine and number of free thiol groups present in the enzymes and protein used in the present study.

It is evident that there are two free thiol groups present in α-amylase, one each in BSA and *EcoR*I, whereas no free thiol group exists in any of the other enzymes. This fact possibly explains the inability of enzymes other than α-amylase and *EcoR*I to perform reduction of Au^{3+} to Au^{0} and synthesize NPs. Considering the structures of α-amylase and BSA, it can be proposed that the thiol groups present in α-amylase are exposed on the surface of the enzyme, in the vicinity of each other. On the other hand, in BSA, the single thiol group is surrounded by other atoms (buried in the three-dimensional structure), and hence not exposed to the solvent, whereas in *EcoR*I, the free thiol group is on the surface. The structural analyses of the above enzymes leads to the conclusion that the proteins and enzymes which have free and exposed thiol groups in their native forms (α-amylase, *EcoR*I) can produce Au NPs by the reduction of the Au^{3+}. On the other hand, proteins (BSA) or enzymes which do not have free and exposed -SH groups do not produce Au NPs in their native conformation. This explains the observation that native α-amylase and *EcoR*I could reduce Au^{3+} to Au^{0}, whereas native BSA failed to do so. Further, those proteins and enzymes that do not have thiol group at all do not produce Au NPs either in their native or denatured state.

We also observed that the synthesis of Au NP by α-amylase led to the decrease in the pH of the medium. This implies that the reduction of Au^{3+} to Au^{0} involves release of H^{+} ions in the solution. The free thiol group of cysteine presumably provided the proton and electron (to Au^{3+}) and the sulfur atoms contributed to the formation of disulfide bonds. The reaction, balanced stoichiometrically, could be

$$2Au^{3+} + 3HS\text{-}R\text{-}SH \longrightarrow 2\,Au^{0} + 6\,H^{+} + 3\,{}^{\cdot}S\text{-}R\text{-}S^{\cdot} \qquad [1]$$

Since each α-amylase molecule has two free and exposed thiol group juxtaposed with each other, one of the possibilities of steps leading to the formation of products (Au NPs) is that for two Au^{3+} ions three α-amylase molecules would be present in the vicinity. Thus, in all, three α-amylase molecules associate and react with two Au^{3+} ions for the synthesis of Au NPs and six thiol groups from three molecules of α-amylase form three disulfide bonds. The involvement of multiple molecules accounted for the slow rate of Au NPs synthesis owing to slow diffusion rate, steric hindrance, and a low collision frequency (even in case of formation of reaction intermediates), justifying the minimum time of 6 h required for the observable product formation.

On the basis of all the characterization studies, it could well be inferred that α-amylase gets attached to the NPs following synthesis. NPs are generally unstable due to their inherent high surface free energy and need to be stabilized against aggregation by suitable surface modifications. In the present study, we observed that the NPs formed by α-amylase were stable in the medium and could be kept for weeks without any precipitation. On the other hand, as discussed above, α-amylase contains free and exposed-SH groups, which are known to have high affinity for Au. Thus Au NPs formed in the medium could react with the -SH groups of α-amylase and form Au-S-bond as per the following known reaction:

$$R\text{-}SH + Au \longrightarrow R\text{-}S\text{-}Au + \tfrac{1}{2} H_2 \qquad [2]$$

Hence, α-amylase molecule having cysteine SH functional groups exposed on the surface readily binds and confers stability to the NPs. Stability of cysteine capped NPs has been reported earlier.[20] Since the two free thiol groups (Cys 103, Cys 119) present on the surface of α-amylase are spatially close to each other,[17] attachment of a NP to one thiol group would facilitate binding with the neighboring -SH group. Since the sizes of the Au NPs (typically about 10 nm in diameters) are larger than those of α-amylase, it is possible that many α-amylase molecules could bind with the same Au NP thus forming a shell around the NP. It is important to mention here that according to the mechanism proposed for the synthesis of Au NPs, there would not be any free thiol groups in α-amylase molecule, which has already taken part in the Au NP synthesis. It could well be that the enzyme molecule that binds to the NP is different from the one that has taken part in the synthesis. Hence, NP synthesis and binding of α-amylase to NP could be

delineated events. The presence of excess enzyme ensures both the synthesis and stability of Au NPs by forming Au-NP-enzyme complex.

In order to have further evidence of the involvement of the free thiol groups of the enzyme in the reduction of $HAuCl_4$ to Au NPs, we pursued the following experiments. The free thiol groups of the enzyme were modified by reaction with DTNP. This was followed by treatment with $HAuCl_4$, which did not result in the production of Au NPs, while the control with enzyme only produced NPs under identical conditions. The results are shown in Figure 5. As clear from Figure 5A1, the characteristic color of Au NPs was absent in case of the modified enzyme, while that was clearly present in the pure enzyme (Figure 5A2). It may be mentioned here that the enzyme upon treatment with DTNP exhibited a peak at 387 nm (shown in Figure 5B), which is the characteristic of the product of the reaction of DTNP and thiols.[15] This peak, however, disappeared upon treatment with $HAuCl_4$ (Figure 5B) indicating the effect of $HAuCl_4$ on the spectrum of the product (5-nitropyridine-2-thione). The inhibition of the production of Au NPs by the modified enzyme was further evidenced in the corresponding UV-visible spectra shown in Figure 6A. As clear from the figure the spectrum of the mixture consisting of the modified enzyme and $HAuCl_4$ after 24 h consisted of no peaks corresponding to Au NPs (at 540 nm). On the other hand, the untreated enzyme produced peak that is characteristic of Au NPs present in the solution. We also observed that when the concentration of DTNP added to the enzyme was low, followed by addition of $HAuCl_4$, formation of Au NPs could be observed. This means that the product of the reaction of enzyme with DTNP (5-nitropyridine-2-thione) does not interfere with the formation of Au NPs by enzyme. We also observed that DTNP treated enzyme retained its activity in starch agar plate. This is shown in Figure 6B. These experiments clearly establish that free thiols of the enzyme were indeed involved in the reduction of $HAuCl_4$, which supports the mechanism as proposed.

Proteins could undergo conformational changes when linked to NPs, which would evidently alter their function. However, in the present study, enzymatic activity of the Au NP-α-amylase complex was retained. This is possibly because the site on the surface of the enzyme for binding to the NP is diametrically opposite to the active (catalytic) site of the enzyme (Figure 7). Such site-specific association of NP to proteins reiterates the importance of conjugation that does not obstruct key sites such as the active site of the enzyme. Additionally, even if there was marginal surface modification upon binding of

α-amylase to Au NP, it would have occurred only locally, near the binding site, and it might not affect the overall conformation of the enzyme. Hence, the complex exhibited enzymatic activity.

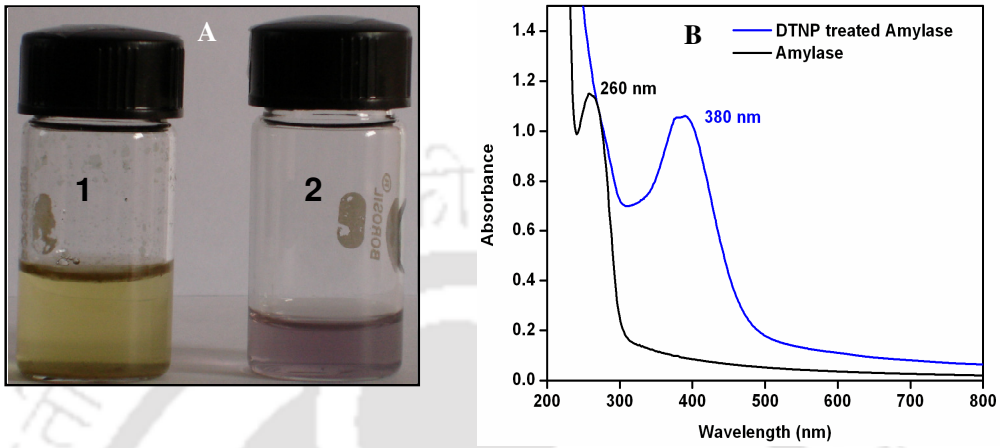

Figure 5. ***(A)*** *Photographs of* ***(1)*** *DTNP-treated enzyme plus $HAuCl_4$ after 24 h and* ***(2)*** *control experiment with enzyme plus $HAuCl_4$ after 24 h. DMSO solvent was present in both the samples.* ***(B)*** *UV-vis spectra of enzyme-only and Enzyme treated with DTNP.*

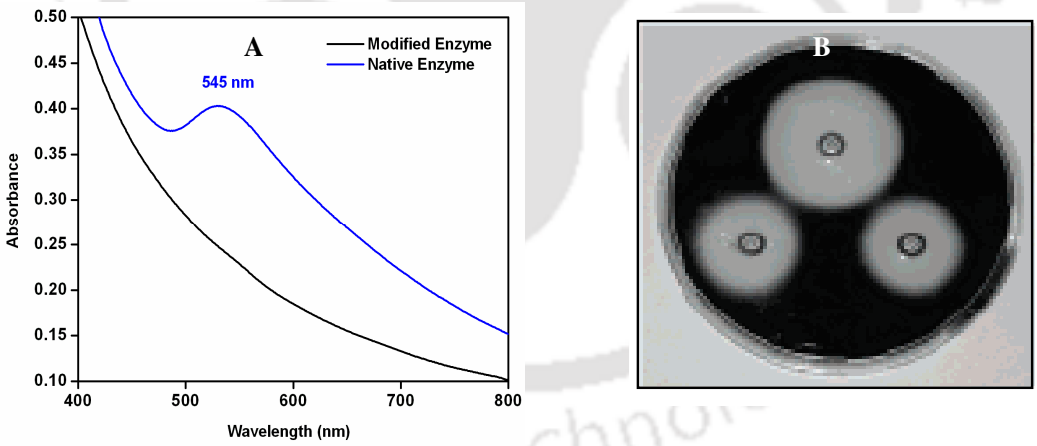

Figure 6. ***(A)*** *UV-vis spectra of samples in Figure 5A (1 and 2).* ***(B)*** *Starch-agar plate assays of enzyme-only (large spot), enzyme-DTNP in DMSO (bottom left), and enzyme in DMSO (bottom right).*

Further, the starch degradation kinetics (Figure 4B) for pure enzyme and Au NP-α-amylase complex highlighted interesting results. The rate of starch degradation in case of the complex was comparable to that of pure enzyme. This indicates that the enzyme attached to the NP was biologically active. This observation could be explained by

speculating the mechanism of enzyme action. In case of soluble (free) enzyme, the activity of the enzyme is purely based on the collision frequency between the enzyme and the substrate molecule and their steric orientations. In case of immobilized enzyme, this limitation is overcome by immobilizing the enzyme on a solid surface as the active sites of the enzymes are exposed and are away from Au surface. This means a significant number of enzyme molecule are preferentially oriented toward the medium and away from Au NPs thus facilitating the reaction between starch and the enzyme molecules. However, further works are needed to establish the exact nature of attachment and reaction kinetics.

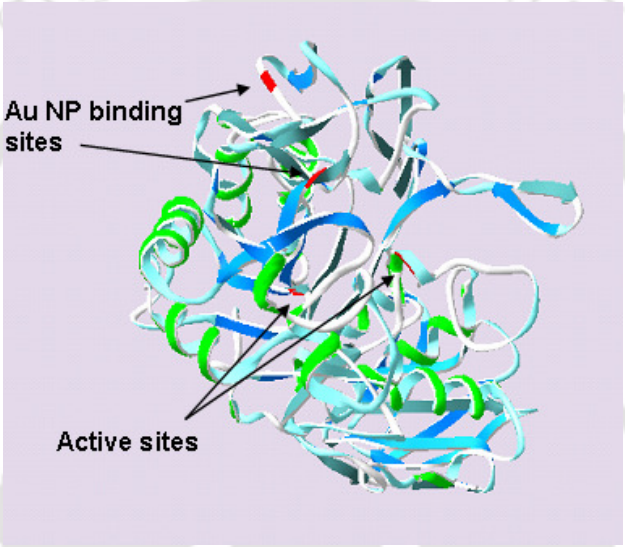

Figure 7. *The three-dimensional structure of α-amylase showing the respective locations of* ***(A)*** *Au NP binding site containing free thiol groups and* ***(B)*** *the active site (catalytic site) for the starch degradation. RASMOL was used for viewing the three-dimensional structure. The protein data base (PDB) number is 1DHK.*

2.4 Summary

To the best of our knowledge, this is the first report on the detailed mechanistic study of reductive synthesis of Au NP by exposed functional groups of a pure enzyme with concurrent display of enzymatic activity of the NP-enzyme complex. That specific functional groups of an enzyme synthesizes Au NPs from its parent cationic salt, with retention of the activity of the enzyme, without the need of several steps involving synthesis of NPs and subsequent functionalization assumes significance in the wake of efforts of creating nanobiofunctional devices. This is all the more important when properties of both the NPs and the enzyme can be retained while carrying out the

synthesis and functionalization of the biomolecules under physiological conditions. The understanding achieved herein in terms of mechanism of synthesis and retention of activity would be of significance for the in situ generation of nanobiomaterials and their use in targeted drug delivery, probes or even for simple enhancement of biological activity of the parent molecule.

References:

1. Fan, H.; Yang, K.; Boye, D. M.; Sigmon, T.; Malloy, K. J.; Xu, H.; Lopez, G. P.; Brinker, C. J. *Science* **2004**, *304*, 567-571.

2. Murray, C. B.; Norris, D. J.; Bawendi, M. G. *J. Am. Chem. Soc*. **1993**, *115*, 8706-8715.

3. Sun, S. H.; Murray, C. B.; Weller, D.; Folks, L.; Moser, A. *Science* **2000**, *287*, 1989-1992.

4. Jovin, T. M. *Nat. Biotechnol*. **2003,** 21, 32-33.

5. Brust, M.; Bethell, D.; Schiffrin, D. J; Kiely, C. J. *Adv. Mater*. **1995**, *7*, 795-797.

6. Whitesides, G. M.; Grzybowski, B. *Science* **2002**, *295*, 2418-2421.

7. Nair, B; Pradeep, T. *Cryst. Growth. Des*. **2002**, *2*, 293-298.

8. Ahmad, A.; Senapati, S.; Khan, M. I.; Kumar, R.; Ramani, R.; Srinivas, V.; Sastry, M. *Nanotechnology* **2003**, *14*, 824-828.

9. Sastry, M.; Ahmad, A.; Khan, M. I.; Kumar, R. *Curr. Sci*. **2003**, *85 (2)*, 162-170.

10. Dyal, A.; Loos, K.; Noto, M.; Chang, S. W.; Spagnoli, C.; Shafi, K. V. P. M.; Ulman, A.; Cowman, M.; Gross, R. A. *J. Am. Chem. Soc*. **2003**, *125*, 1684-1685.

11. Xiao, Y.; Patolsky, F.; Katz, E.; Hainfeld, J. F.; Willner, I. *Science* **2003**, *299*, 1877-1881.

12. Willner, I.; Baron, R.; Willner, B. *Adv. Mater*. **2006**, *18*, 1109-20.

13. Rangnekar, A. *B. Tech Project Thesis* **2006**.

14. Bradford, M. M. *Anal. Biochem*. **1976**, *72*, 248-254.

15. Sharma, P.; Sathyanarayana, S.; Kumar, P.; Gupta, K. C. *Anal. Biochem.* **1990**, *189*, 173-177.

16. Burt, J. L.; Gutierrez-Wing, C.; Miki-Yoshida, M.; Jose-Yacaman, M. *Langmuir* **2004**, *20*, 11778-11783.

17. Buisson, G.; Duee, E.; Haser, R.; Payan, F. *EMBO J.* **1987**, *6*, 3909-3916.

18. Berman, H. M.; Westbrook, J.; Feng, Z.; Gilliland, G.; Bhat, T. N.; Weissig, H.; Shindyalov, I. N.; Bourne, P. E. *Nucleic Acids Res*. **2000**, *28*, 235-242.

19. Aslam, M.; Fu, L.; Su, M.; Vijayamohanan, K.; Dravid, V. P. *J. Mater. Chem.* **2004**, *14*, 1795-1797.

20. Santosh, A.; Remant, B. K. C.; Dharmaraj, N.; Bhattarai, N.; Kim, C. H.; Kim, H. Y. *Spectrochim. Acta, Part A* **2006**, *63*, 160-163.

Chapter 3

Probing Au Nanoparticle Uptake by Enzyme Following Digestion of Starch-Au-Nanoparticle Composite

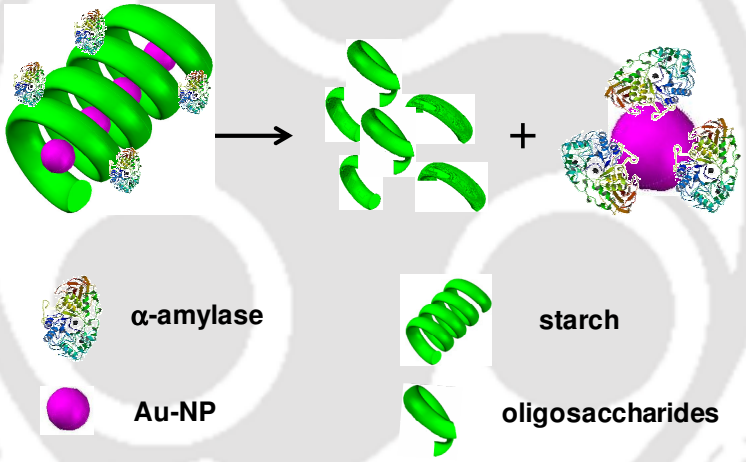

* Deka, J.; Paul, A.; Ramesh, A.; Chattopadhyay, A. *Langmuir (Letter)* **2008**, *24(18)*, 9945-9951.

Outline:

Gold nanoparticles (Au NPs) holds huge potential in the field of nanomedicine owing to its unique properties such as optical properties, biocompatibility, ease of surface modification, high extinction coefficient and is thus being widely used in targeted drug delivery and diagnostics. In our laboratory starch-stabilized Au NPs were prepared previously, which can be a promising candidate in nanomedicine. Our previous work with α-amylase (discussed in chapter 2), which is the digestive enzyme for starch, prompted us to carry out detailed study on the effect of this enzyme on starch when present as a stabilizer for Au NPs. This is significant since final application of such a drug carrier demands a deep understanding of various probable complicacies that may arise while administering the drug in vivo since an efficacious delivery of drug demands a deep prior knowledge of the mechanism of drug release. However not many studies has been done in this regard. Hence the study was undertaken to establish a mechanism of behavior of a drug carrier (starch in present case) in presence of an enzyme (α-amylase in present case).

3.1 Introduction

The advent of nanotechnology has bestowed new enthusiasm in the fields of targeted drug delivery, controlled drug release, imaging and therapeutics, owing primarily to the size-dependent properties of nanoparticles (NPs) that are not available with the conventional materials. In particular, Au NPs with their high optical extinction coefficients have been successfully used in nanomedicine because of their low cytotoxicity,[1] capability to undergo easy surface modification with thiol containing molecules[2] and immobilization of wide range of biomolecules such as amino acids,[3] proteins/enzymes[4,5] and DNA.[6] Functionalized Au NPs have been used to complex gadolinium ions (Gd^{3+}) to achieve higher efficiency in magnetic resonance imaging (MRI) as compared to gadolinium chelates that are normally used for clinical diagnosis.[7]

In targeted therapeutics the delivery vehicles are as much important as the drug itself. Naturally, the delivery systems, such as soluble polymers, microcapsules, lipoproteins, liposomes and micelles that are currently in use tend to maximize biocompatibility, bioavailability and site-specific delivery and also to minimize drug degradation. In this respect, starch-based polymers have received considerable attention in their use for pulsatile release of drugs, peptides and other bioactive agents[8,9] and in the generation of biodegradable hydrogels.[10] Further, starch-encapsulated superparamagnetic iron oxide

nanoparticles (SPIONs) have been used as superior magnetic resonance contrast agents.[11] Interestingly, use of starch for aqueous dispersions of carbon nanotubes,[12] metal and semiconductor NPs,[13-18] polyaniline and its nanocomposite[19] increases the application potentials of these nanomaterials in biological systems. However, advanced applications also require better understanding of the implications of the starch-encapsulated NPs in physiological environments. A case in point is following the mechanism of enzymatic digestion of a starch-NP composite vis-à-vis that of starch alone and the fate of the NPs subsequent to digestion. Surprisingly, notwithstanding the volumes of work on the use of starch as the encapsulating materials, there is no report on the release of the NPs from starch following delivery.

Herein we report results of the studies on the enzymatic release of Au NPs encapsulated in starch. In particular, we observed that the digestion of Au NP-starch composite by α-amylase not only lead to the degradation of starch into its lower analogues, but also resulted in the release of encapsulated Au NPs and their subsequent uptake by the enzyme. In addition to conventional biochemical and microscopy probes, the surface plasmon resonance (SPR) of Au NPs provided a convenient way of following the reaction and to establish the mechanism. Our observations indicated that the rate of digestion of starch-Au NP composite by α-amylase was similar to that of pure starch and the free thiol groups of the enzyme possibly facilitated the uptake of Au NPs by the enzyme in comparison to other carbohydrate degrading enzymes like amyloglucosidase (AMG).

3.2 Materials and Methods

3.2.1 *Preparation of Starch-Au NP complex*

A 5.0 mg/mL stock solution of starch (Soluble Starch Extrapure; SRL) was prepared by dissolving 800.0 mg of starch in 160.0 mL boiling water. NP synthesis was carried out by adding 160.0 μL of 1.73 X 10^{-2} M $HAuCl_4$ and 800.0 μL of H_2O_2 to the starch solution followed by ultrasonication for 20 min. The solution was left overnight and then centrifuged for 20 min at 20,000 rpm and at 25^0C. The supernatant was discarded and the pellet was resuspended in 10.0 mM phosphate buffer (pH 7.0). The cycle of centrifugation and buffer wash was performed twice more. Finally, the pellet was

suspended in 20.0 mL of buffer. The presence of Au NPs and starch in the solution was tested by UV-vis spectroscopy (using a Perkin Elmer Lambda25 spectrophotometer) and iodine test, respectively. Transmission electron microscopy (TEM) was performed using a Jeol 2100 machine (operating at 200 kV). The images were recorded after drop-coating solutions on carbon coated copper grids. All the subsequent experiments were performed with this solution only.

3.2.2 *Estimation of starch in the composite using GOD-POD Method*

150.0 mL of starch-Au NP solution (prepared as discussed in the above section) was centrifuged and redispersed in 20.0 mL buffer (pH 7.0). To 10.0 mL of this solution 100.0 μL of α-amylase (1.0 mg/mL) was added and incubated overnight at 37^0C, followed by centrifugation at 20,000 rpm to remove the Au NPs from it. The pH of the supernatant obtained was adjusted to 4.5, using dilute HCl, to which 30.0 μL of 3.0 mg / mL solution of amyloglucosidase (from *Aspergillus niger*, Fluka) was added and the solution was incubated at 55^0C for 8 h. The resultant mixture was tested for glucose using the glucose test kit based on GOD-POD method (GOD-POD Kit, Span Diagnostics, India). The amount of starch in the starch-Au NP composite was estimated by measuring the amount of glucose produced and comparing the same as obtained from known concentrations of starch solutions (0.03 mg/mL, 0.05 mg/mL and 0.5 mg/mL) under the same reaction conditions.

3.2.3 *Enzymatic Starch Digestion Studies*

For the starch digestion kinetics studies, 17.0 μL of 1.0 mg / mL α-amylase (from hog pancreas; Fluka), prepared in 10.0 mM phosphate buffer, was added to 26.0 mL of the starch-Au NP composite solution having a starch concentration of 0.05 mg / mL (as determined using GOD-POD method). An equivalent concentration of free starch solution was also taken for comparing kinetics of digestion of free starch vis-à-vis starch-Au NP composite. 2.0 mL aliquots from each of the reaction mixtures were withdrawn at regular time intervals; to each of which 100.0 μL of iodine solution (Gram's Iodine, HiMedia) was added and the UV-vis spectra of the solutions were subsequently recorded (using a Perkin Elmer Lambda25 UV/Vis Spectrometer or Varian Cary 50 Bio UV-vis Spectrophotometer). For kinetics data the areas of the curves were plotted as a function of time.

3.2.4 *Analysis of the enzyme digested starch-Au NP composite*

a) Analysis of the presence of starch digested product(s): 60.0 μL of 1.0 mg / mL α-amylase solution was added to 10.0 mL of the starch-Au NP composite (so that the final concentration of protein is 0.14 μg / mL) and incubated overnight at 37°C. The solution was then centrifuged at 20,000 rpm for 20 min, followed by buffer wash of the precipitate. The precipitate was dispersed in 10.0 mL acetate buffer (pH 4.5) and the pH of the supernatant was adjusted to 4.5 using dilute HCl. Both the dispersed solution (from the precipitate) and the supernatant were then treated with 30.0 μL of 3.0 mg / mL solution of amyloglucosidase (from *Aspergillus niger*, Fluka), prepared in acetate buffer of pH 4.5, followed by incubation at 55^0C for 8 h. The solutions were then tested for the presence of glucose using the glucose test kit (GOD-POD Method, Span Diagnostics, India).

b) Analysis of the presence of enzyme: 1.4 mL of 1.0 mg/mL α-amylase solution was added to 13.6 mL of the starch-Au NP solution and centrifuged at 20,000 rpm for 20 min; the precipitate was then washed with buffer and the supernatant collected. The precipitate was resuspended in 1.5 mL buffer. Both the precipitate and the supernatant were tested for the presence of enzyme by the standard Bradford test for protein.[20]

3.2.5 *Quantitative analysis for protein content after digestion of starch-Au NP composite*

For this purpose, 1.0 mL each of the three enzyme (native α-amylase, native AMG and denatured α-amylase) solutions was added to 6.0 mL of starch-Au NP composite (separately) and all the reaction mixtures were kept at room temperature for 5 h. The solutions were then centrifuged at 20,000 rpm for 20 min, followed by the buffer wash of the precipitate obtained. The precipitate was redispersed in 1.5 mL buffer and the supernatant was also collected for analysis. Standard Bradford test for protein was conducted for the supernatant as well as the original stock solution of the enzyme used in the experiment. The amount of protein in the precipitate was calculated by the following equation.

Amount of protein in precipitate (Pp) = Amount of protein in 1 mL of the parent enzyme (PEnz) – Amount of protein in supernatant (Ps)

Also, iodine tests were performed with the precipitate and the supernatant for the presence of undigested starch, if any.

3.2.6 *Electrophoretic detection of α-amylase-Au NP composite following digestion of starch-Au NP composite.*

The digestion of starch-Au NP composite by α-amylase and subsequent recovery of the precipitate following digestion was accomplished as mentioned before. The presence of α-amylase in the pellet was ascertained by agarose (1.2%) gel electrophoresis.[21] The samples analyzed were: starch-Au NP composite, α-amylase, α-amylase-Au NP composite obtained after digestion and Au NPs only. The samples were mixed in a ratio of 5:1 (v/v) with 30% glycerol and loaded on the gel. The conventional sample loading dye consisting of 30% glycerol and the tracking dyes bromophenol blue and xylene cyanol was loaded in one of the wells to monitor the electrophoretic run. Following electrophoresis, the gel was photographed and subsequently stained overnight with 0.1% Coomasie Brilliant Blue R-250 prepared in a mixture of methanol and acetic acid (25:10 v/v). The gel was extensively destained in a solution of methanol and acetic acid (25:10 v/v) and the protein bands obtained were photographed appropriately.

3.2.7 *Experiment for SPR based kinetics study*

UV-vis spectra of the enzyme treated starch-Au NP composite were recorded at various time intervals. The areas under the curves were calculated and then plotted as functions of time. The iodine test for the digestion of starch in the composite was followed as before.

3.3 Results and Discussions

As mentioned above, starch stabilized Au NPs were prepared following reduction of $HAuCl_4$ by H_2O_2 in the presence of starch, a method developed in our laboratory.[13] The UV-vis spectrum of the starch-Au NP composite shows a maximum at 531 nm which is characteristic of the SPR of Au NPs (Figure 1A). Transmission electron microscopy (TEM) of the composite (Figure 1B) revealed the presence of well-dispersed spherical NPs with diameters in the range of 10-30 nm. The concentration of starch in the composite was estimated from the visible absorption spectrum of starch-iodine complex

(and confirmed by using GOD-POD method) and was determined to be 0.05 mg/mL. Interestingly, the presence of Au NPs in the starch-Au NP composite did not inhibit the formation of starch-iodine complex.

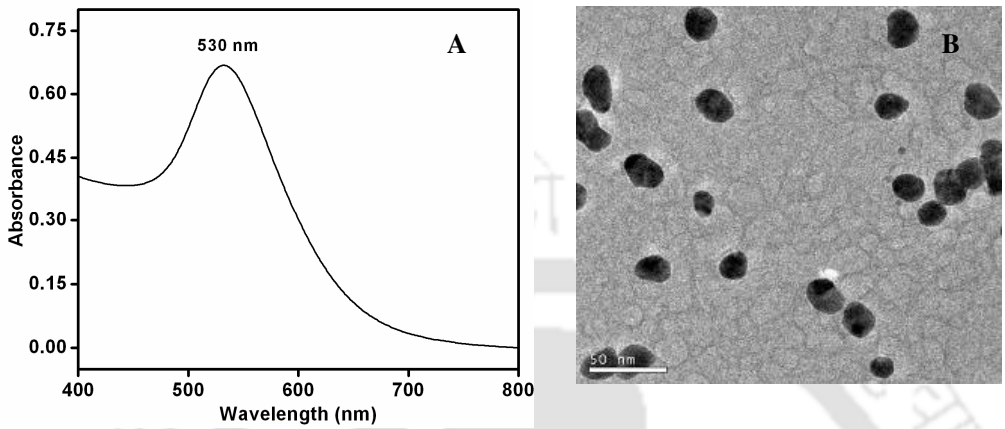

Figure 1. ***(A)*** *UV-vis spectrum of starch-Au NP composite and* ***(B)*** *TEM image of the composite (Scale bar is 50 nm).*

For example, when iodine was added gradually to the composite to achieve a final iodine concentration of 2.65 mg/mL, the peak due to Au NPs at 531 nm shifted gradually to 565 nm, which is the characteristic of the starch-iodine complex. It was also observed that after addition of a copious amount of iodine, i.e. in excess of 2.65 mg/mL, the peak position as well as intensity did not change.

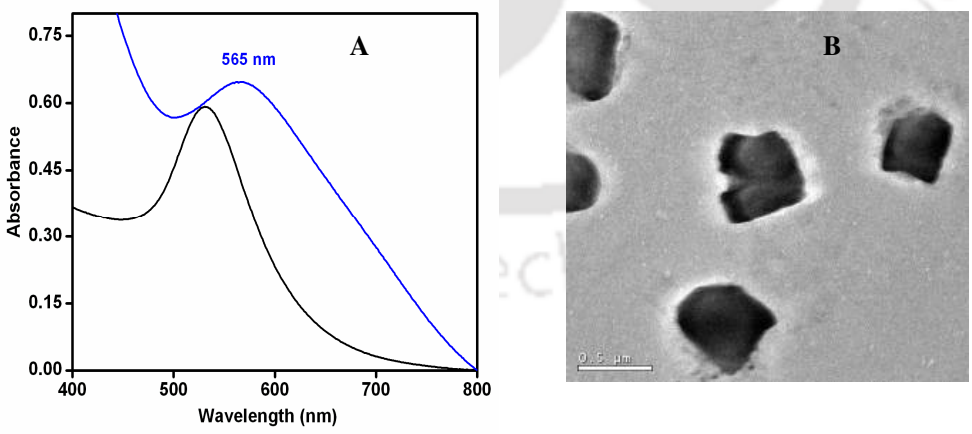

Figure 2. ***(A)*** *UV-vis spectra of starch-Au NP composite (black line) as compared to that of starch-Au NP in presence of iodine (blue line)* ***(B)*** *TEM image of the mixture of the composite and iodine (Scale bar is 0.5 µm).*

The absorption spectra of starch-Au NP composite and that of the same after addition of excess iodine are shown in Figure 2A. The details of changes in the absorption spectra of the composite upon addition of various amounts of iodine are shown in Figure 3-1 of Appendix. Further, this concentration (2.65 mg/mL) of iodine was used to estimate starch for all the subsequent experiments. TEM measurements indicated agglomeration of Au NPs into primarily cubic in shape (Figure 2B), which possibly is the reason for loss of SPR absorption. The presence of crystalline Au in the cubic structures was apparent from the selected area diffraction pattern as shown in Figure 3A. Further, a higher resolution picture of the agglomerate could not be obtained due to melting of the same at higher electron energy. The sample became opaque and hence no clear image could be obtained (Figure 3B).

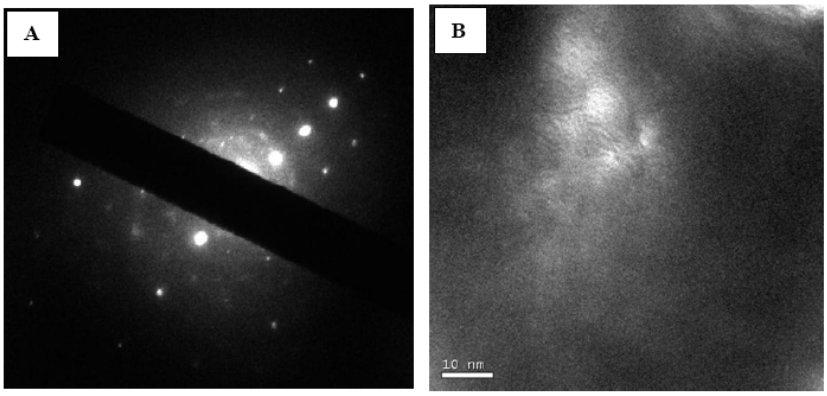

Figure 3. ***(A)*** *Selected area electron diffraction (SAED) pattern of starch-Au NP–iodine agglomerates. The pattern corresponds to the TEM image in Figure 2B.* ***(B)*** *High resolution TEM image of iodine treated starch-Au NPs, which shows melting of the cubes.*

Also, the presence of Au NPs in the iodine treated composite was confirmed by X-ray diffraction (XRD; Figure 4). It has been reported earlier that in the presence of iodine, Au NPs agglomerate due to the chemisorption of iodine on the NPs leading to increase in van der Waals attractive forces between the iodine-coated Au NPs, which may well be the case here too.[22] Thus addition of iodine to the composite leads to the formation of agglomerated Au NPs as well as starch-iodine complex. This indicates that Au NPs possibly occupied the hydrophobic core of starch leading to the formation of a helical assembly akin to starch-iodine complex. When excess iodine was added, the Au NPs in

the composite formed agglomerated large crystals with iodine, while starch-iodine complex was formed subsequently.

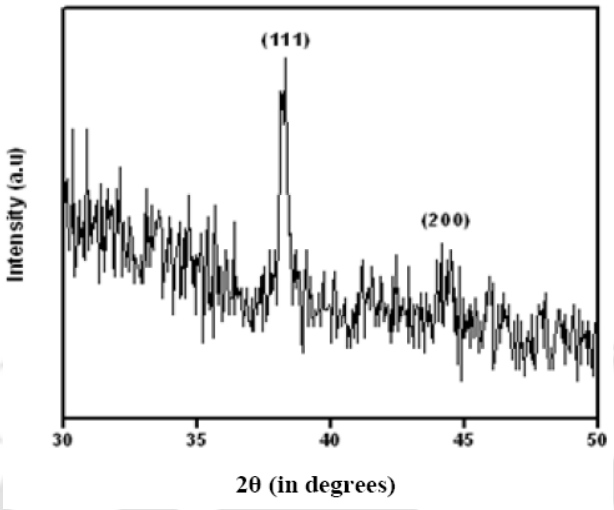

Figure 4. *X-ray diffraction (XRD) pattern of iodine treated starch-Au NP composite. The principal Braggs reflections (corresponding to Au) are identified.*

This is evidenced by the gradual change in the UV-vis absorption upon addition of iodine. Otherwise at lower concentrations of iodine, starch-iodine complex would be formed in addition to the presence of individual Au NPs. Thus two separate peaks should be observable, which is not the case here (refer to Figure 3-1, Appendix). In other words, if Au NPs were located at a different site then starch-iodine complex would be formed independently and preferentially. This also supports earlier speculation that hydrogen bonded amylopectin rings in starch are capable of folding around Au NPs providing stability to the NPs.[23] It may be pointed here that in the control experiment, when bare Au NPs were treated with iodine the characteristic absorption spectrum due to the NPs vanished and a subsequently a strong background due to iodine could be observed in the spectrum (refer to Figure 3-2, Appendix). TEM measurements indicated that the Au NPs agglomerated in the presence of iodine much in the same way as the NPs stabilized by starch. In fact, the agglomerated particles were primarily cubic in shape, which is similar to that observed for starch stabilized NPs in the presence of iodine (Figure 5). The cubic crystal formation was also apparent from the SAED patterns of the crystal (Figure 5C).

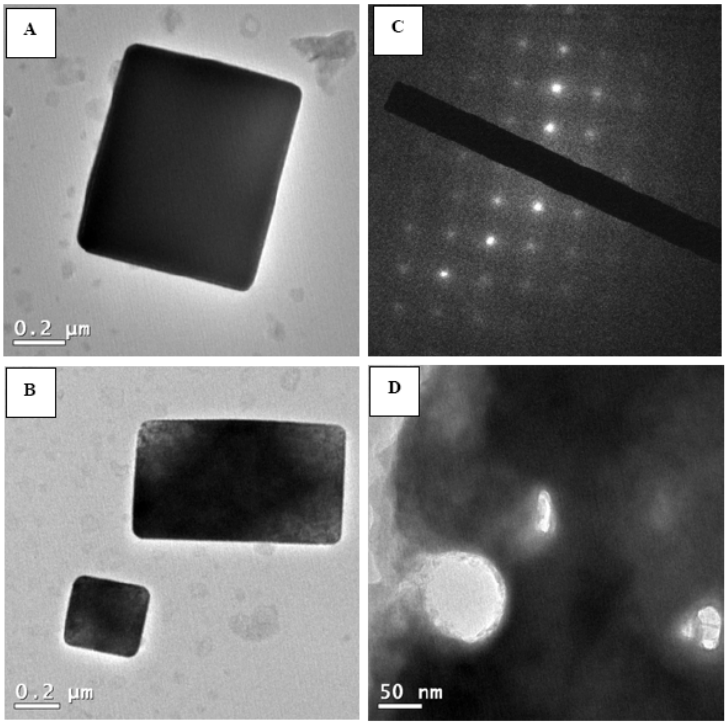

Figure 5. ***(A)*** *and* ***(B)*** *are TEM images of Au NP only (in absence of starch) treated with iodine.* ***(C)****. SAED pattern corresponding to the crystal in 'A'.* ***(D)****. High resolution TEM image of the crystal in 'A' (which shows the melting of the cube).*

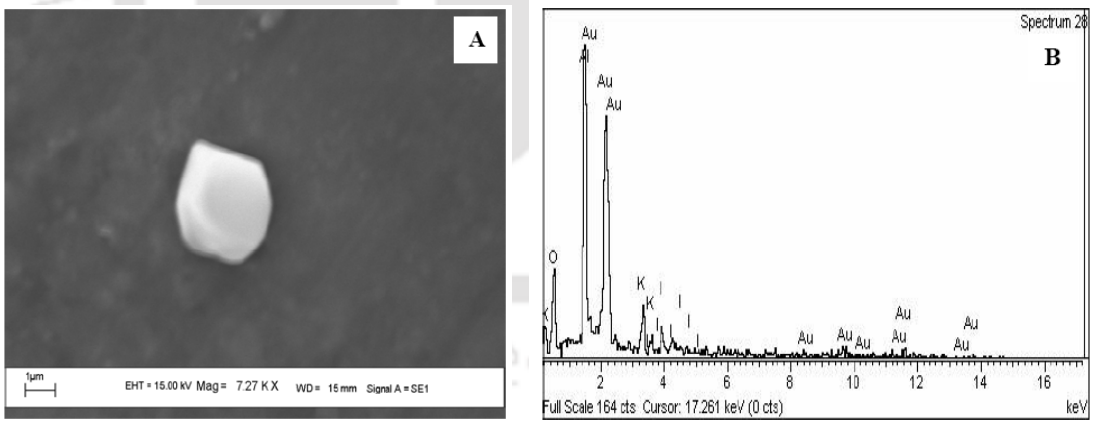

Figure 6. ***(A)*** *Scanning electron microscope image of Au NP treated with iodine and* ***(B)*** *its energy dispersive X-ray analysis (EDX). The Al peak is due to the sample holder.*

Additionally, energy dispersive X-ray (EDX) spectroscopy along with scanning electron microscopy measurements revealed the presence of iodine and gold in the crystals

(Figure 6). It may also be mentioned here that literature reports suggest that iodine may also be responsible for partially or fully leeching the Au NPs leading to the formation of AuI.[24,25] However, since XRD measurement (Figure 4) indicates the presence of Au crystals in the treated sample, the NPs may not be completely leeched in the present case, and if at all AuI was formed it may be present primarily as a thin shell of the Au NP. Since the time of iodine treatment in the present set of experiments was short, it is in the media. An important point to be addressed is whether estimation of starch (in the composite) could be pursued using standard iodine method. The UV-vis spectroscopic results clearly demonstrate the usefulness of the present method of following starch digestion kinetics using iodine even in the composite. For example, as shown in Figure 7A, the Au NP peak at the end of complete digestion is very weak, indicating that the background spectrum due to Au NPs is of negligible consequence. In other words, addition of iodine completely removes Au NPs from starch (agglomeration of Au by iodine led to loss of the peak) and the peak that is observed is due to starch-iodine complex and thus provided a quantitative estimate of the starch concentration. The results are comparable to those of digestion of starch (alone) by enzyme (i.e. in absence of Au NPs) as shown in Figure 7B.

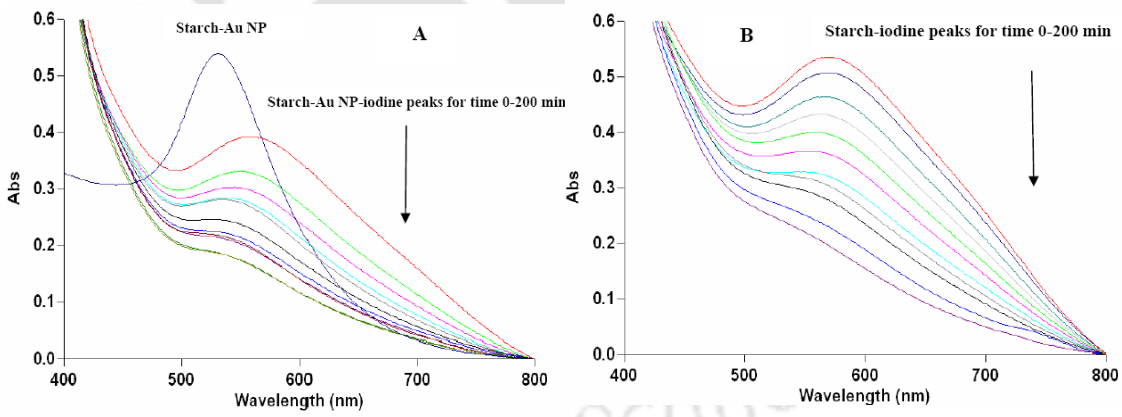

Figure 7. ***(A)***. *UV-vis spectra of iodine treated starch-Au NP composite at different time intervals of starch digestion in the composite (0.05 mg/mL). Also shown separately is the peak due to Au NP –starch composite.* ***(B)***. *UV-vis spectra of starch-iodine complex at different time intervals of digestion of bare starch (0.05 mg/mL).*

Additionally, the quantity of starch present in starch-Au NP composite solution was estimated by first converting starch into glucose using α-amylase and AMG enzymes.

This was followed by estimation of glucose produced by standard GOD-POD method (Figure 8). The starch concentration (0.03 mg/mL) estimated this way was found to be comparable with the estimation of starch using iodine method. Essentially, the above results support the validity of the present method of estimation of starch by iodine in the presence of Au NPs. That starch-iodine complex was formed even in the presence of Au NPs provided an opportunity for spectroscopic monitoring of kinetics of digestion of starch (in the composite) by α-amylase. The results of the kinetics studies, shown in Figure 9, indicate that the rate of digestion of starch was comparable for both free starch as well as that in the composite.

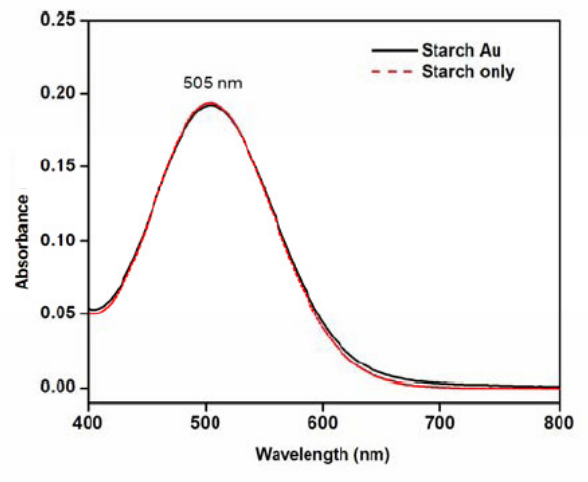

Figure 8. *Glucose test for the estimation of starch present in the starch-Au NP composite (solid black line) and 0.03 mg/mL starch (serrated red line) solution. The production of glucose was estimated by the GODPOD method. H_2O_2 produced from glucose was estimated from the absorption of quinoneimine dye with a peak at 505 nm, which was equivalent to the amount of glucose present in the medium.*

For example, while it took 50 min for 50% decay in both the cases, the digestion was complete for both the samples in 200 min. This indicates that the presence of Au NPs did not affect the structure of starch and impede the enzyme-substrate complex formation. Also, it could be possible that Au NPs present in the composite were spatially distant from the 1, 4 glycosidic bonds of starch which were thus accessible for cleavage by the enzyme. It is interesting to observe that kinetics of the starch digestions in both the cases could be fitted with single exponentials indicating that the order of both the reactions is one.

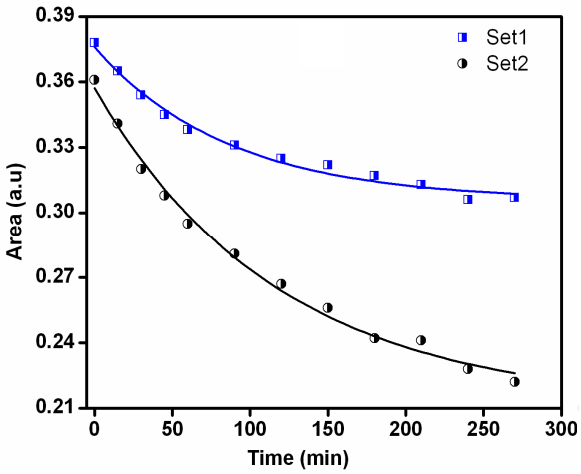

Figure 9. *Comparative kinetics study of starch digestion in starch-Au NP composite and bare starch (the Y-axis represents area under the graph at that particular time).*

Our next aim was to probe the Au NPs following digestion of the composite by the enzyme. In other words, it would be important to know whether the sizes of the Au NPs would be retained or altered as a result of digestion. Also, it would be interesting to know whether the NPs would be attached to the fragments of starch after the digestion or would be stabilized by the enzyme itself. For this purpose, 0.4 μg/mL α-amylase solution (actual protein concentration) was added to the starch-Au NP composite. Following incubation, the mixture was centrifuged at high speed to separate the Au NPs, which was further redispersed in buffer solution. The UV-vis spectra of both the supernatant and the redispersed solution were then recorded. It was observed that the spectrum of the redispersed solution consisted of a peak at 532 nm, indicating the presence of Au NP, while the supernatant was devoid of such spectrum (Figure 10A). TEM picture of the redispersed solution (Figure 10B) showed homogenous distribution of spherical Au NPs with sizes in the range of 10-30 nm, which were same as the original NPs present in the composite. Thus the process of enzymatic digestion did not lead to any change of particle size of the NPs. Further, both the redispersed solution (obtained from the precipitate) and the supernatant showed negative starch-iodine test (results not shown) indicating that starch digestion was complete in the process. The redispersed solution and the supernatant were then treated with amyloglucosidase to convert the oligosaccharides, which might have been produced in the process of starch digestion, into glucose.

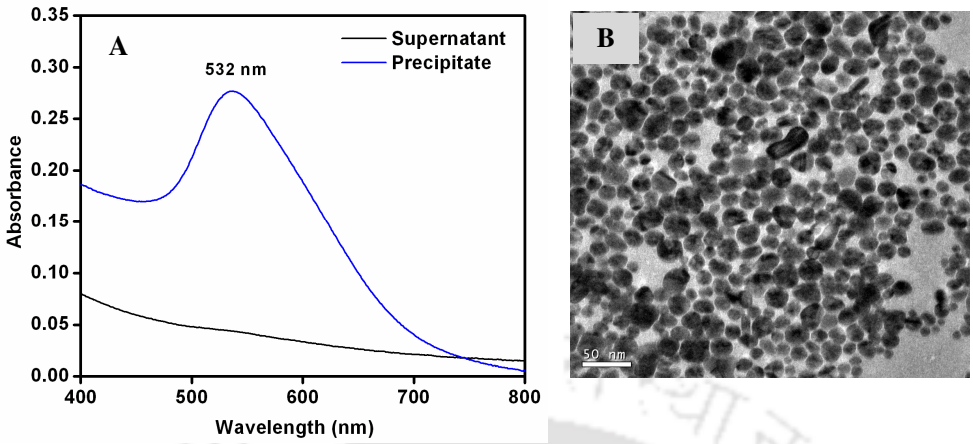

Figure 10. ***(A)*** *UV-vis spectra of the supernatant and the precipitate redispersed in buffer after centrifugation.* ***(B)*** *TEM image of the precipitate (Scale bar is 50 nm).*

The production of glucose was estimated by the GOD-POD method. H_2O_2 produced from glucose was estimated from the absorption of quinoneimine dye with a peak at 505 nm, which was equivalent to the amount of glucose present in the medium. It is interesting to observe from the UV-vis spectra shown in Figure 11A that the redispersed solution showed no trace of glucose whereas supernatant showed positive test for glucose with the characteristic peak present at 505 nm.

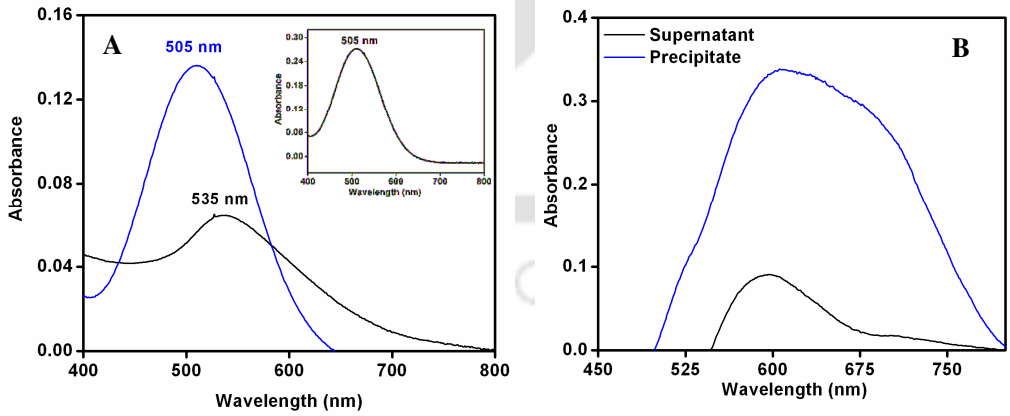

Figure 11. ***(A)*** *Glucose test with the precipitate (redispersed in buffer) (black line) and supernatant (blue line). The inset shows the positive test shown by the precipitate on addition of standard glucose.* ***(B)*** *Bradford test for protein in precipitate and supernatant obtained from α-amylase treated starch-Au NP composite.*

That the presence of the peak due to Au NPs in the redispersed solution did not interfere with the glucose test was confirmed by adding glucose to the same followed by the GOD-POD test. As shown in the inset of Figure 11A, the glucose, if present in the medium, could be tested even in the presence of Au NPs. The above results clearly demonstrate that Au NPs were not attached to the oligosaccharides that were produced following digestion of the composite by α-amylase. Hence the question arises whether the NPs were attached to the enzyme following digestion. The presence of protein in the redispersed solution as well as in the supernatant was tested by the standard Bradford test. The corresponding UV-vis spectra with a characteristic peak at 595 nm, shown in Figure 11B, revealed the presence of protein in both the samples. However, the intensity of the measured absorbance evidently pointed out an overwhelming presence of the protein in the redispersed solution (obtained from the precipitate) compared to that in the supernatant. Quantitative analysis (refer to Figure 3-3, Appendix) indicated the protein content in the redispersed solution to be 73% (approximately 0.3 μg/mL), while the rest was in the supernatant.

Thus the enzyme not only released NPs from starch following digestion into oligomers but also had stabilized the NPs following their release. Under the conditions of the present set of experiments the majority of proteins were attached to the NPs and no products of starch were associated with them. Importantly, the release of NPs from starch and subsequent stabilization by enzyme did not lead to agglomeration of the NPs. Dynamic light scattering (DLS) based particle size analyses of the starch-Au NP composite and the enzyme-Au NP composite obtained after digestion indicated reduction in average sizes following digestion (Figure 12). The average particle sizes for the starch-Au NP composite was found to be 92.5 $\pm$ 9.2 nm, whereas that of enzyme-NP composite was 40.0 $\pm$ 4.0 nm. The larger size in the starch composite is due to large size of undigested starch molecules. The reduction in particle size following digestion is commensurate with the release of Au NPs from starch (larger size) followed by stabilization by enzyme (smaller size). Also, these results are consistent with the total size of particles composing of Au NPs (average 10 - 30 nm) covered by a monolayer of enzyme (twice that of 6 nm, which is the diameter of α-amylase). Further, it is important to mention here that the Au NP stabilized enzyme (obtained after digestion) retained its

catalytic activity as evidenced from the results of the catalytic activity test in a starch-agar plate. The results are shown in Figure 13.

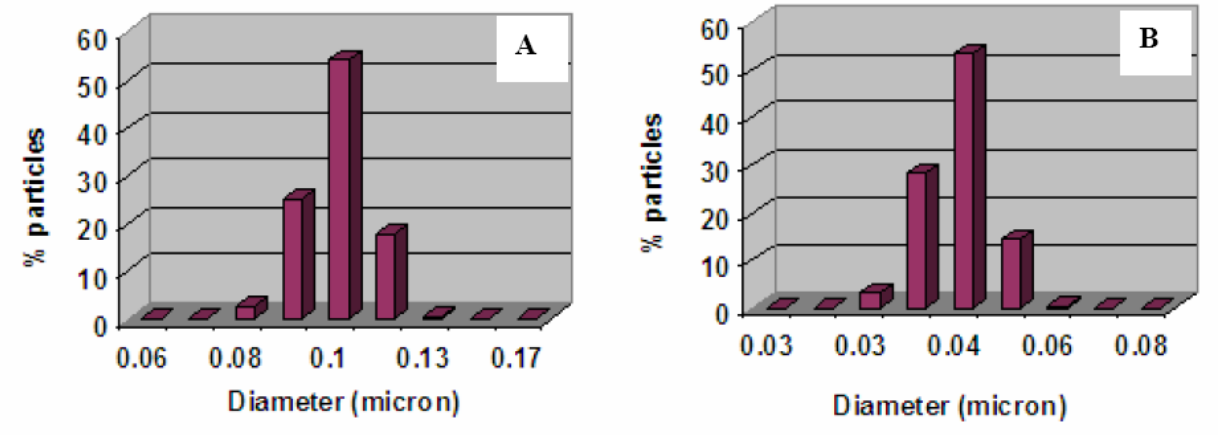

Figure 12. *Dynamic light scattering (DLS) based particle size analysis of* ***(A)*** *starch-Au NP composite and* ***(B)*** *enzyme sequestered Au NPs.*

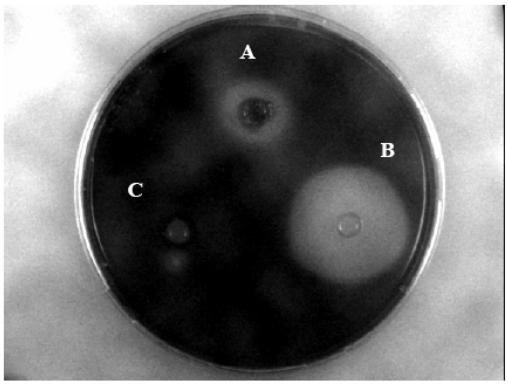

Figure 13. *Test for enzymatic activity of Au NP- enzyme complex obtained after digestion of starch- Au NP composite by α-amylase. The picture was recorded from starch-agar plate treated with iodine solution following incubation with* ***(A)*** *α-amylase-Au NP composite obtained from digested starch-Au NP composite,* ***(B)*** *α-amylase alone, and* ***(C)*** *10.0 mM phosphate buffer (pH 7.0).*

The electrophoretic analysis of α-amylase-Au NP composite is depicted in Figure 14. The image of the unstained gel in Figure 14A clearly revealed the characteristic purple color of Au NP in the samples loaded in lanes 1, 5 and 7, which correspond to starch-Au

NP, α-amylase-Au NP (obtained as pellet following starch-Au NP digestion) and Au NP alone. The α-amylase-Au NP sample was overloaded to compensate for the sensitivity problems associated with Coomassie Brilliant Blue staining and easy visualization of protein bands. Further, the samples were loaded in alternate wells to avoid any bleed from adjacent wells.

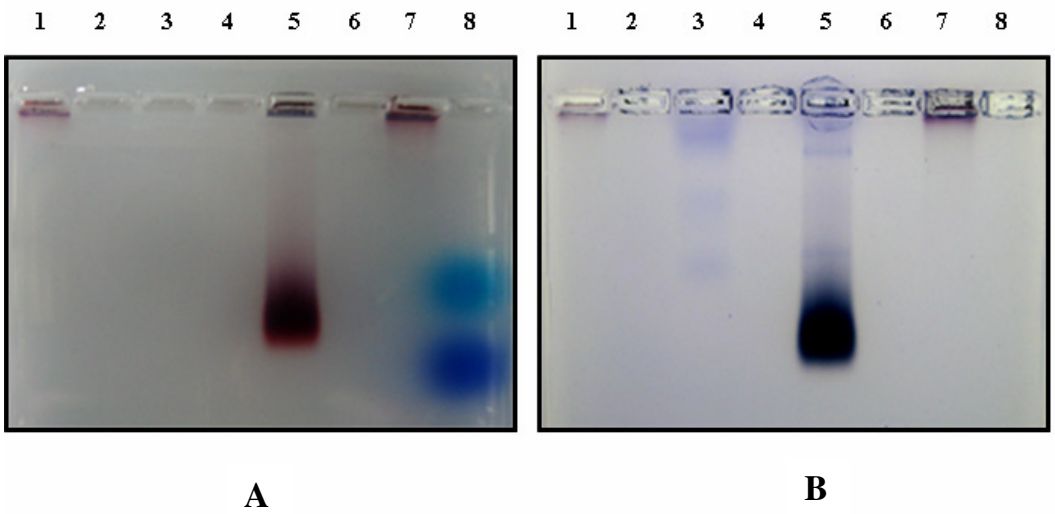

Figure 14. *(A) Unstained agarose gel;* ***(B)*** *Gel A stained with Coomassie Brilliant Blue R-250. Lanes: 1. Starch-Au NP composite; 3.α-amylase; 5.α-amylase-Au NP composite recovered after starch digestion; 7.Au NP alone; 8.Gel loading dye.*

It is also evident from the image that starch-Au NP and Au NP alone (lanes 1 and 7) are retained in the well as they fail to migrate in the gel. However, the sample in lane 5 consisting of α-amylase-Au NP migrated appreciably and was observed to possess a dark purple front, indicating the presence of Au NPs. A portion of the sample was also retained in the well (Lane 5) which could probably be due to overloading of the sample. Coomasie Brilliant Blue staining of the gel revealed the presence of protein bands as shown in Figure 14B**.** In case of native α-amylase loaded as a control sample, three distinct protein bands were observed, which probably indicate multimeric forms of the enzyme (lane 3). These forms are expected to appear as the electrophoresis was performed under non-denaturing and non-reducing conditions. Interestingly, the protein bands corresponding to control α-amylase sample were also detected in the α-amylase-Au NP sample (lane 5, Figure 14B) but with retarded mobility. This can be attributed to the adsorption of α-amylase molecules onto Au NP surface leading to the formation of

α-amylase-Au NP composite, whose mobility differs from the native enzyme molecule. Further, the observation that the mobility of the α-amylase-Au NP composite (Lane 5, Figure 14B) differed from the parent enzyme molecule (Lane 3, Figure 14B) probably indicates that the enzyme molecules did not dissociate from the NP during the course of electrophoresis. Retardation of mobility due to adsorption of the protein onto the NP surface has also been reported earlier for Au NP-cytochrome c complex.[21] Further, that the intense purple front observed for the α-amylase-Au NP composite in Figure 14A appeared blue following Coomassie Brilliant Blue staining (lane 5, Figure 14B) indicates the presence of protein along with the NPs. The characteristic purple color of the Au NPs for samples in lane 1 and 7 were retained even after Coomasie Brilliant Blue staining indicating the lack of protein in these samples. Collectively the results obtained from α-amylase activity test on starch-agar plate and the electrophoretic detection of α-amylase-Au NP composite clearly indicate the association of the enzyme molecule with the Au NPs. The process of digestion of the starch-Au NP composite leading to release of the NPs and their subsequent stabilization by the enzyme is shown schematically in Figure 15.

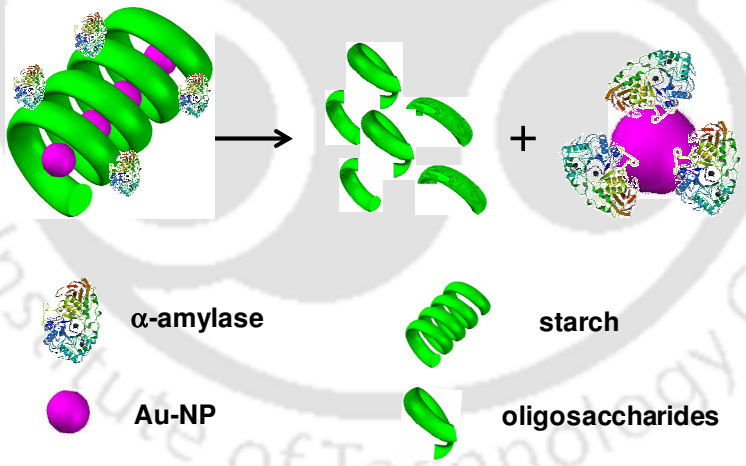

Figure 15. *Schematic representation of the proposed mechanism of Au NP transfer from the starch-AuNP composite to the enzyme. The 3D structure of α-amylase is retrieved from Protein Data Base (PDB) entry 1DHK.*

The enzyme α-amylase in its native conformation has two free and exposed thiol groups that are known to facilitate the synthesis of Au NPs from its parent salt ($AuCl_4^-$) and also stabilizes the NPs, while retaining its enzymatic activity.[5] In the present set of

investigations, another central question that remains to be answered is whether the NPs were attached to the enzyme prior to the digestion of starch. In other words, whether the digestion of starch in the composite is a prerequisite for the release of NPs. The answer came from the results of treatment of the composite with denatured α-amylase enzyme and also separately with the enzyme AMG, which does not have any free thiol group and which cleaves the 1, 6 glycosidic bonds in starch. When heat denatured α-amylase was incubated with the composite solution for 2 h followed by centrifugation and then tests for starch and enzyme were performed, it was observed that all the NPs were still associated with starch (which co-precipitated during centrifugation), while the enzyme remained free in solution without any NP attached to them. On the other hand, treatment of AMG resulted in the complete exchange of NPs with the enzyme (refer to Figure 3-3, Appendix). However, interestingly 63% of the total AMG were attached to the NPs, which was much less than that of α-amylase. Thus essentially the enzymatic digestion is necessary for the release of the NPs and the released NPs are subsequently stabilized by the enzymes. It is interesting to note that higher concentration of the free and exposed thiol group containing enzyme could be attached to the released NPs in comparison to that not having any thiol group. This possibly indicates that in the case of α-amylase the enzymes are attached to the NPs in a more organized fashion, with the formation of S-Au bonds, in comparison to AMG, which might have been attached to the NPs in a more random fashion stabilizing the NPs electrostatically.

Finally, we were interested in the possibility of using the SPR absorption of Au NPs as a probe for the enzymatic digestion of starch. It was observed that the SPR peak of Au NPs decreased in magnitude consequent to the digestion of starch by α-amylase, while there was little change in the absorption maximum (wavelength) (refer to Figure 3-4 in Appendix for the UV-Vis spectra). The change in the absorption could be due to change in the environment and hence the dielectric constant of the medium surrounding the NPs. In the present case Au NPs that were originally dispersed in starch were subsequently stabilized by the enzyme. This represents a significant change in the environment and hence it is not surprising that the absorption changed. The results of time-dependent change of peak area due to Au NPs and that due to starch-iodine composite prepared by adding iodine to the solution (containing starch - Au NP composite), taken from the same stock, are shown in Figure 16A (set 1) and Figure 16B. It is interesting to observe that

both the results are similar i.e exponential decay with respect to the kinetics of digestion of starch encapsulating Au NPs. The graphs could be fitted with single exponentials and the exponential constants were found to be the same.

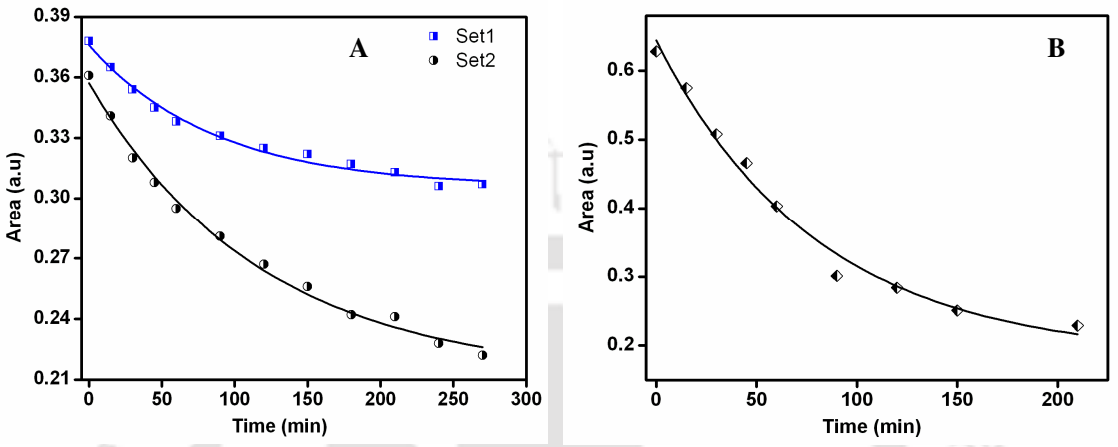

Figure 16. ***(A)*** *Au NP SPR probes of the digestion of the starch-Au NP composite by α-amylase. Set1 represents digestion studies with enzyme concentration being the same as in Figure 9. Set 2 was pursued with ten times the enzyme concentration of that in Set 1.* ***(B)*** *Digestion kinetics as followed by iodine test using the same reaction condition as in (A)-set 1.*

Further, as shown in Figure 16A (set 2), when the same digestion was performed with higher concentration of enzyme (i.e. ten times as that in set 1) the rate was faster and decayed exponentially. At still higher concentrations of the enzyme precipitation was observed and thus was not pursued. However, the results clearly show that the enzymatic digestion of the composite could also be followed by the SPR absorption of Au NPs.

3.4 Summary

In a nutshell, the present set of experimental results suggest that specificity of release of encapsulated NPs could be achieved with appropriate combination of encapsulating materials and choice of appropriate enzyme that would cleave the encapsulation in order to release the NPs. In particular, the release of Au NPs from starch by α-amylase followed by stabilization by Au-S bonds or electrostatically points to different options for the availability of the NPs after release. In other words, the electrostatically

stabilized NPs may be more amenable to interaction with other substrates than the chemically stabilized (through S-Au bonds) ones. Further, it is important to note that the present studies open the possibility of following release of NP-based drugs by observing the changes in SPR of the NPs. Interestingly, the studies revealed that the rate of digestion of free starch and the composite followed the same kinetics. The release of NPs encapsulated in biofriendly starch by specific enzymes demonstrated in our investigation can serve as a prototype model to study digestion of biofunctionalized NPs and may open newer research avenues where stabilization and release of NPs could be achieved using well known therapeutic biomolecules This would particularly be useful for nanoscale drug delivery and imaging studies *in vitro*.

References:

1. Connor, E. E.; Mwamuka, J.; Gole, A.; Murphy, C. J.; Wyatt M. D. *Small* **2005**, *1 (3)*, 325-327.

2. Daniel, M. C.; Astruc, D. *Chem Rev.* **2004**, *104(1)*, 293-346.

3. a) Selvakannan, P. R.; Mandal, S.; Phadtre, S.; Gole, A.; Pasricha, R.; Adhyanthaya, S.; Sastry, M. *J. Colloid Interface Sci.* **2004**, *269*, 97-102; b) Selvakannan, P. R.; Mandal, S.; Phadtre, S.; Pasricha, R.; Sastry, M. *Langmuir* **2003**, *19*, 3545-3549.

4. a) Niemeyer, C. M.; Ceyhan, B. *Angew. Chem. Int. Ed.* **2001**, *40*, 3685-3688; b) Gole, A.; Dash, C.; Ramakrishnan, V.; Savikar, S. R.; Mandle, A. B.; Rao, M.; Sastry, M. *Langmuir* **2001**, *17*, 1674-1679.

5. Rangnekar, A.; Sarma, T. K.; Singh, A. K.; Deka, J.; Ramesh, A.; Chattopadhyay, A. *Langmuir* **200**7, *23*, 5700-5706.

6. a) Alivisators, A. P.; Peng, X.; Wilson, T. E.; Loweth, C. L.; Bruchez, M. P. Jr.; Schultz, P. G. *Nature* **1996**, *382*, 609-611; b) Kanaras, A. G.; Wang, Z.; Bates, A. D.; Cosstick, R.; Brust, M. *Angew. Chem. Int. Ed.* **2003**, *42*, 191-194.

7. Debouttiere, P. J.; Roux, S.; Vocanson, F.; Billotey, C.; Beuf, O.; Regiullon, A. F.; Lin, Y.; Rostaing, S. P.; Lamartine, R.; Perriat, P.; Tillement, O. *Adv. Funct. Mater.* **2006**, *16*, 2330-2339.

8. Bjork, E.; Isaksson, U.; Edman, P.; Artursson, P. *J. Drug Target* **1995**, *2(6)*, 501-507.

9. Malafaya, P. B.; Elvira, C.; Gallardo, A.; Roman, J. S.; Reis, R. L. *Journal of Biomaterial Science* **2001**, *12(11)*, 1227-1241.

10. Elvira, C.; Mano, J. F.; San, R. J.; Reis, R. L. *Biomaterials* **2002**, *23(9)*, 1955-66.

11. Kim, D. K.; Mikhaylova, M.; Wang, F. H.; Kehr, J.; Bjelke, B.; Zhang, Y.; Tsakalakos, T.; Muhammed, M. *Chem. Mater.* **2003**, *15(23)*, 4343-4351.

12. Star, A.; Steuerman, D. W.; Heath, J. R.; Stoddart, J. F. *Angew. Chem. Int. Ed.* **2002**, *41*, 2508-2512.

13. Sarma, T. K.; Chattopadhyay A. *Langmuir* **2004**, *20(9)*, 3520-3524.

14. Raveendran, P., R.; Fu, J.; Wallen, S. L. *Green Chem.* **2006**, *8*, 34-38.

15. Raveendran, P., R.; Fu, J.; Wallen, S. L. *J. Am. Chem. Soc.* **2003**, *125*, 13940-13941.

16. Niu, S. F.; Liu, Y.; Xu, X. H.; Lou, Z. H.; Zhejiang, J. *Univ. Sci .B* **2005**, *6(10)*, 1022-1027.

17. He, F.; Zhao, D. *Environ. Sci and Technol.* **2005**, *39*, 3314-3320.

18. Vigneshwaran, N.; Kumar, S.; Kathe, A. A.; Varadarajan, P. V.; Prasad, V. *Nanotechnology* **2006**, *17*, 5087-5095.

19. Sarma, T. K.; Chattopadhyay, A. *Langmuir* **2004**, *20(11)*, 4733-4737.

20. Bradford, M. M. *Anal. Biochem.* **1976**, *72*, 248-254.

21. Aubin-Tam, M.E.; Hamad-Schifferli, K. *Langmuir* **2005**, *21(26)*, 12080-12084.

22. Cheng, W.; Dong, S.; Wang, E. *Angew. Chem. Int. Ed.* **2003**, *42(4)*, 449-452.

23. Kannan, R.; Rahing, V.; Culter, C.; Pandrapragada, R.; Katti, K. K.; Kattumuri, V.; Robertson, J. D.; Casteel, S. J.; Jurisson, S.; Smith, C.; Boote, E.; Katti, K. V.; *J. Am. Chem. Soc.* **2006**, *128*, 11342-11343.

24. Singh, S.; Pasricha, R.; Bhatta, U. M.; Satyam, P. V.; Sastry, M.; Prasad, B. L. V. *J. Mater. Chem.* **2007,** *17,* 1614–1619.

25. Huang, Y.; Li, D.; He, P.; Sun, C.; Wang, M; Li, J. *J. Electroanal. Chem.* **2005**, *579*, 277–282.

Chapter 4

Sensitive Protein Assay with Distinction of Conformations Based on Visible Absorption Changes of Citrate-Stabilized Au Nanoparticles

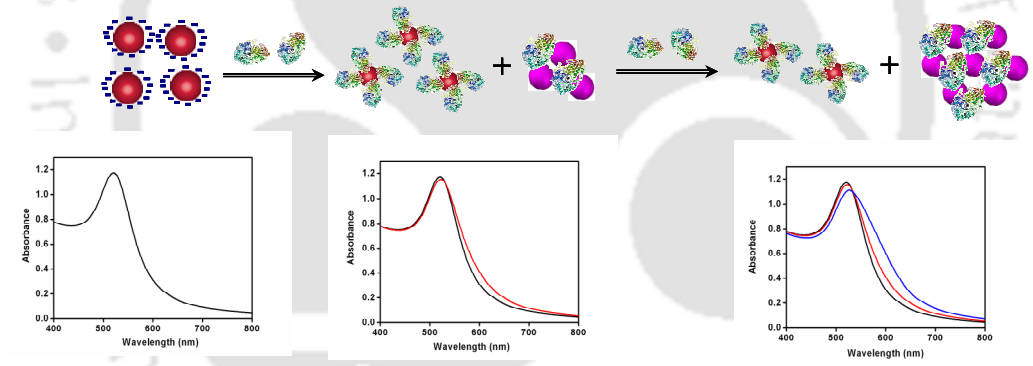

* Deka, J.; Paul, A.; Chattopadhyay, A. *J. Phys. Chem. C*. **2009**, *113*, 6936–6947.

Outline:

Proteins perform many vital roles in various life sustaining processes. Hence slightest variation in their amount or their activity may lead to the onset of different kinds of diseases. Development of simple and sensitive methods for estimating the amount of protein in a solution would therefore be quite desirable, which can contribute towards enhancing the efficiency of existing detection techniques and treatment process. In this chapter we introduce a new and potentially general method of assay of proteins in solution using gold nanoparticles (Au NPs). In addition, the method could distinguish conformations of protein (native and denatured forms). The method is based on the changes in visible absorption spectra of citrate-stabilized Au NPs upon addition of a measured amount of protein. The behavior of four proteins, namely α-amylase, green fluorescent protein (GFP), amyloglucosidase (AMG) and bovine serum albumin (BSA) have been found to be different with respect to changes in the spectra of Au NPs. The spectral behaviors were also different between the native and denatured forms of the same protein. Interestingly, spectral changes in the presence of thiol-containing proteins (α-amylase and GFP) were different from those that either did not contain thiol at all or contained thiol that was not exposed to the solution (AMG and BSA).

4.1 Introduction:

Proteins are one of the most important classes of biomolecules essential for life that are involved in virtually all functions of cell. Proteins also hold a special place in biomimetic systems where it can be used for biochemical synthesis, assembly or other functions pertaining to their catalytic activities.[1-3] Understanding and appropriate use of their broad spectrum of functions require knowledge about the structures in native and denatured forms and the concentrations *in vivo* as well as *in vitro*. For example, proteomics play a central role in understanding and monitoring of various diseases such as Alzheimer, heart diseases and cancers.[4-7] This calls for development of highly sensitive methods for early detection of protein related diseases and acquirement of extensive knowledge about the protein of interest. Fortunately, crystal structures of a large number of useful proteins are known.[8] In solution, not only is the knowledge of structure of the protein specific to its function important but also rapid quantification of its concentration is vital to its use in a medium. Conventional colorimetric methods for protein estimation such as Biuret, Bicinchonic Acid (BCA), Lowry and Bradford tests use a sequence of steps involving reactions with optically sensitive molecules, followed by generation of calibration curves using bovine serum albumin (BSA) as a reference protein, which render them

cumbersome. These methods although useful are not highly sensitive; the sensitivity range lying between 0.01 and 8.0 mg/mL, depending on the nature of the protein and the method used. On the other hand, modern experiments with ultra low quantities of biomaterials require development of newer methods – preferably using spectroscopic techniques – involving minimum number of chemicals and steps, for estimation of proteins in various reaction conditions, with possibly high sensitivity and specificity.

The advent of nanoscale science and associated technology brings newer opportunities in practicing biosciences that are unmatched by conventional means. For example, chemical and optical properties of inorganic nanoparticles (NPs) have been successfully employed in the field of biomedicine through sensing, drug delivery, and diagnostics.[9-13] The NPs have also been used in developing methods for identification and estimation of biomolecules,[14-16] and hence could be assumed to be potentially useful in proteomics as well. In this regard, surface plasmon resonance (SPR) of biocompatible Au NPs, with high optical extinction coefficient, has been found to be useful in developing NP-based diagnostics. For example, biofunctionalized Au NPs have been used for detection and quantification of proteins,[17-21] protein-protein[22-23] and protein-membrane interaction studies,[24] and separation of proteins.[25] On the other hand, SPR of bulk Au film and self-assembled Au NPs have been employed in the quantification of denaturation of biomolecules,[26] and study of conformational changes of proteins.[27-28] Further, there are reports on the use of colloidal gold in the assay of proteins using the color change in a spot.[29-30] There is also a report of using colloidal gold to estimate bovine serum albumin (BSA) by measuring change in absorbance.[31] Further, binding of BSA to Au NPs has been studied by quartz crystal microbalance.[32] In addition, latex agglutination[33] and sol-gel aggregation[34] of functionalized latex as well as Au NPs have earlier been used for protein assay, although with moderate levels of sensitivity. Interestingly, notwithstanding the aforementioned developments in the field, quantification of protein in a solution, taking advantage of the optical properties of non-functionalized Au NPs, remains largely unaddressed. The cited reports generally depend either on the conjugation of NPs with biomolecule for the recognition of antigen/protein of interest or modification of the biomolecule itself or use of low pH or polymer in increasing the sensitivity of the assay and are time consuming. Thus the development of a simple technique based on ordinary Au NPs (such as citrate stabilized Au NPs) in aqueous medium would be useful in quantitative and rapid estimation of proteins. The method would be even more versatile

if identification of proteins as well as differentiation of their native versus denatured conformations could simultaneously be established.

Herein we report the development of a new method for rapid and efficient quantification of proteins in aqueous solution based on changes in the SPR absorption of citrate-capped Au NPs in the medium. Addition of proteins to the medium containing citrate stabilized Au NPs led to broadening of the absorption spectrum, the area of which varied linearly over a range of concentration. That provided an easy way of estimation of concentration of a protein in the medium. However, beyond a critical concentration of the protein there was no change in the spectral behavior. Interestingly, the changes in spectral characteristics depended on the nature of the protein as well as its state. For example, α-amylase and green fluorescence protein (GFP), which contain free and exposed thiol groups in their native forms, led to changes in the spectra which were fundamentally different from those due to addition of amyloglucosidase (AMG) or bovine serum albumin (BSA) neither of which has any free and exposed thiol group in their native forms. Also, changes in the spectral characteristics of Au NPs were different for the native and denatured states for all the proteins; thus providing an opportunity to distinguish between the two states in the medium. For example, while the native form of α-amylase led to significant change in the spectral behavior of Au NPs, the denatured form had little effect on the same. Transmission electron microscopic (TEM) measurements indicated that agglomeration of NPs in the presence of proteins was the primary reason for the optical behaviors; the larger was the extent of agglomeration the larger was the change in the absorption spectra of Au NPs. Also the extent of agglomeration was dependent on the concentration and nature of proteins. The results were further substantiated by dynamic light scattering (DLS) based measurement of particle sizes. In order to account for the changes in the absorption spectra, we have proposed a model based on the agglomeration of Au NPs in the presence of proteins. In the analyses, deconvolutions of the spectra clearly indicated the appearance and subsequent increase of absorption due to agglomerated state at the expense of the unagglomerated one. Overall the method provided a new way of estimation of proteins in solution with the ability to distinguish between the nature of proteins and the state of the proteins, where the sensitivity is similar to other NP-based estimation. Also, the

method allowed estimation of protein with as low concentration as 2.0 ng/mL, thus providing a quick and easy assay of proteins with high sensitivity.

4.2 Materials and Methods

4.2.1 *Preparation of citrate stabilized Au NPs*

Au NPs were prepared by a known method of citrate reduction of $HAuCl_4$.[35-36] 250.0 µL of 1.73 X 10^{-2} M $HAuCl_4$ (Sigma- Aldrich Chemical Co.) was added to 10.0 mL of MilliQ grade water and then heated to boiling. Then 400.0 µL of 0.2 M tri-sodium citrate 2-hydrate (Merck) was added to the boiling solution (all at once) and the boiling (or refluxing) was continued for another 15 min to ensure complete reduction of $HAuCl_4$. The solution turned deep red indicating the synthesis of Au NPs. The red solution so obtained was cooled to room temperature; volume adjusted to 10.0 mL and finally was diluted to four times with phosphate buffer of pH 7.0 for further use.

4.2.2 *Preparation of enzyme/protein solution*

1.0 mg/mL of enzyme/protein solution was prepared by dissolving the solid protein in appropriate buffer - phosphate buffer of pH 7.0 for α-amylase (from *hog pancreas*, Fluka), GFP and BSA (SRL) and acetate buffer of pH 5.0 for AMG (from *Aspergillus Niger*, Fluka) was used. This was further diluted to ten times to obtain 0.1 mg/mL protein solution. It was observed that α-amylase was sparingly soluble in buffer solution (pH 7.0). Hence the 1 mg/mL α-amylase solution was stirred for 20 min for better mixing. This was followed by centrifugation at 5000 rpm for 20 min. The supernatant was collected and used for further analysis. It was also observed that the amount of protein present in the final solution thus prepared was much less than 1 mg/mL (as discussed later). GFP (wild type) was isolated and subsequently purified from overnight grown culture of GFP expressing *E. coli*[37]. This is followed by lyophilization and the dried protein was weighed for further sample preparation.

4.2.3 *Preparation of denatured enzyme/protein solution*

3.0 mL of the 0.1 mg/mL of enzyme/protein solution, prepared as discussed above, was kept in a water bath at 80 ^{0}C for 30 min. The volume was made up for the loss due to evaporation and the solution was then used for further analysis.

4.2.4 *Estimation of protein content in the 1.0 mg/mL enzyme/protein solution*

The actual protein content was calculated using the standard Bradford test[38] for protein for 1.0 mg/mL enzyme/protein solution. It was observed that the tests were carried out within the linear region of estimation using Bradford method.[39] This was used as a reference for calculating the amount of protein in the volume of enzyme solution used in further analyses. However, since BSA was the standard protein taken as reference in Bradford test and GFP was obtained as pure, the absolute amount of both the enzymes taken was considered as it is for further calculations. It is important to mention here that in the Experimental section the concentrations of enzyme/protein refer to are as prepared concentrations, whereas in the Results and Discussion (as well as Appendix) section the exact concentrations of them as estimated by Bradford test are mentioned. Further, since the enzyme/protein (especially sparingly soluble α-amylase) may contain stabilizers which might interfere with the Bradford test, it is best to carry out the estimation of concentrations where serial dilutions would result in linear behavior with respect to the test. Sample test for the linear change in absorbance of the probe dye (λ_{max} = 595 nm) as a function of α-amylase concentration is shown in Figure 4-1 (refer to Appendix). The calibration of the concentration of α-amylase measured using the present method has been performed using Bradford test in the linear region of absorbance change.

4.2.5 *Successive addition of enzyme/protein solution to citrate-capped Au NPs*

3.0 mL of the Au NP solution was taken in a cuvette and the UV-vis spectrum was recorded (using a Hitachi U-2800 spectrophotometer). 20.0 µL of 0.1 mg/mL solution of the enzyme/protein (α-amylase) was added to it, shaken well and again the UV-Vis spectrum was recorded. This was followed by the addition of 30.0 µL of protein solution followed by recording of UV-vis spectrum. Protein addition was continued (by adding 30.0 µL solution each time) followed by recording of UV-vis spectrum, till a saturation was achieved in the spectra. However in the case of AMG, BSA and GFP, enzyme/protein solution was added in an increment of 10.0 µL. All the UV-vis spectra were recorded immediately after addition of protein. All the peak areas were then calculated (after performing proper volume correction) and plotted against the concentration of the protein in the solution.

4.2.6 *Calculation of the area under the UV-vis spectrum*

This was performed automatically by the software associated with the data acquisition of the spectrophotometer. The area was calculated by joining a line between two points in the absorption spectrum encompassing the area above the line and the absorption spectrum (graph). For α-amylase the extreme wavelengths were set at 405 nm and 650 nm, while that for GFP and AMG were set at 405 and 750 nm and for BSA they were at 425 nm and 750 nm. A typical view of such area is shown in the Appendix (Figure 4-2). All the spectra were normalized to incorporate the dilution factor in the calculation of area. There was thus no need for additional baseline subtraction.

4.2.7 *Sample preparation for TEM analysis*

Solution containing Au NPs (before enzyme addition) and those of Au NPs in the presence of 0.03 mL and 0.06 mL α-amylase solution (each containing 0.1 mg/mL) were drop cast on Cu grids (right after enzyme addition and UV-vis analyses) and then left for air drying overnight. These grids were further analyzed by a Jeol 2100 TEM machine (operated at a maximum voltage of 200 kV). Similarly for the preparation of TEM samples with BSA (native and denatured) 0.03 mL and 0.16 mL of protein solution (each containing 0.1 mg/mL) were added to 3 mL of Au NP solution followed by drop-casting on the grid.

4.2.8 *Particle size analysis by DLS method*

18.0 mL of the Au NP solution was taken in a cell for which particle size distribution was measured using a Horiba LB-550 instrument. To this, 0.120 mL of 0.1 mg/mL α-amylase solution was added and shaken well before recording the particle size distribution again. The analysis was continued up to an addition of total of 1.38 mL α-amylase solution in the same cell. And the particle size distribution was recorded after each addition. The ratios of enzyme: Au NPs were kept the same as in the other experiments.

4.3 Results and Discussion

Upon addition of microgram quantity of any of the four proteins, namely α-amylase, AMG, GFP and BSA in their native forms, into ruby red colored citrate-capped Au NP solution, the color changed to purple. The intensity of the color increased upon addition

of further quantities of protein. However, there was no change observed after a certain concentration of the protein was added. Also, the distinction between changes in color due to different proteins could not be made with naked eye. Similar observations were made with the denatured proteins. UV-vis spectra of Au NPs upon addition of any of the proteins broadened, accompanied by small red-shifts in the maxima. However, for the sake of clarity, spectral characteristics due to addition of each protein would be presented separately in the following sections.

When 0.02 mL of 3.3 μg/mL solution of native α-amylase was added to 3.0 mL of the citrate-stabilized Au NP solution, the absorption maximum shifted from 522 nm to 524 nm (Figure 1A). There was also significant broadening of the peak, which is clear from the figure. The change in the spectral characteristics continued to occur upon further addition of the protein. However, at a concentration of 0.134 μg/mL of protein and above there was no change in the spectra indicating saturation in the observed effect. Interestingly, when similar experiments were carried out with denatured α-amylase, the changes in the spectra of the Au NPs were rather small (Figure 1B). Although the intensity of absorption changed discernibly, broadening of the spectra was rather small. A plot of the total area under the spectrum (details of calculation provided in the experimental section), shown in Figure 1C, was found to vary linearly with the concentration of native protein up to 0.106 μg/mL. At above that concentration, the change in area was small and gradually reached saturation at 0.134 μg/mL. On the other hand, the change in the area versus concentration of the denatured protein was less significant in comparison to that of native form of the protein. Although, there was a linear increase in the area with concentration the slope was significantly smaller than that of the native form (Figure 1D). Interestingly, the changes – albeit small- continued to occur at higher values of protein concentrations in comparison to that of the native form. For example, while the linearity was maintained till a concentration of 0.106 μg/mL of the native protein, the same could be observed for the denatured form at a concentration up to 0.337 μg/mL. The above results indicate that interactions of α-amylase with citrate stabilized Au NPs is dependent not only on the concentration of the protein but also on its (native versus denatured) tertiary structures. Thus changes in the absorption characteristics of citrate-stabilized Au NPs have the kernel of a method for simultaneous

estimation of protein concentration as well as obtaining knowledge of its tertiary structure in solution.

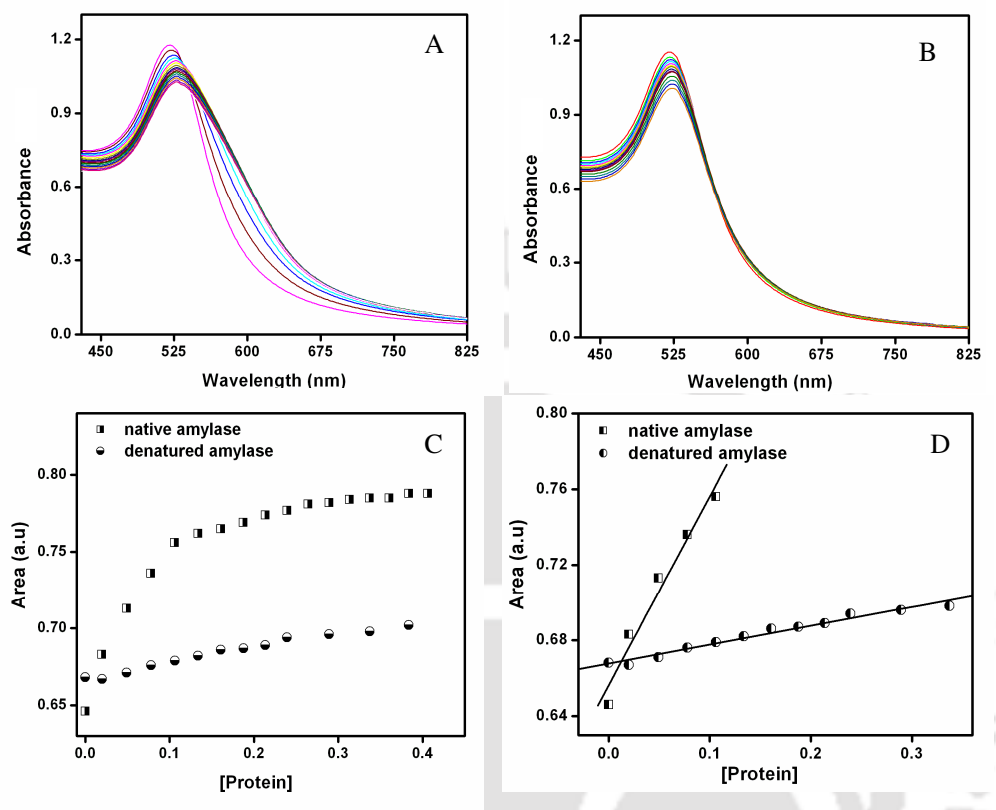

Figure 1. ***(A)*** *UV-vis spectra of Au NPs with various amounts of native α-amylase added successively (0.02 µg/mL to 0.41µg/mL of final protein concentration).* ***(B)*** *UV-vis spectra of Au NPs with various amounts of denatured α-amylase added successively (the successive concentrations were the same as in A).* ***(C)*** *Area under the curve versus the corresponding protein concentration (in µg/mL) for native and denatured α-amylase.* ***(D)*** *The linear region of the graphs in '**C**'.*

Further investigations by TEM measurements indicated agglomeration of Au NPs in the presence of native form of the protein. The results are shown in Figure 2. Figure 2A shows the image of citrate-stabilized Au NPs produced in the present method and in the absence of any protein. The particles produced were monodispersed in size and spherical in shapes. Also, the average particle size was calculated to be 7.4 nm $\pm$ 1.1 nm. Addition of 0.03 mL of 3.3 µg/mL α-amylase solution to 3.0 mL Au NP solution led to apparent aggregation of the NPs without affecting their size (Figure 2B). However, there were significant number of particles that were not aggregated as is clear from the figure. On further addition of the protein (0.06 µg/mL protein) the network of Au NP assembly

grew further which is clear from Figure 2C. In other words, at higher concentration of protein the size of the assembly as well as the percentage of particles involved in the assembly formation increased. It is also interesting to note that addition of denatured proteins did not lead to significant agglomeration even at higher concentrations of proteins.

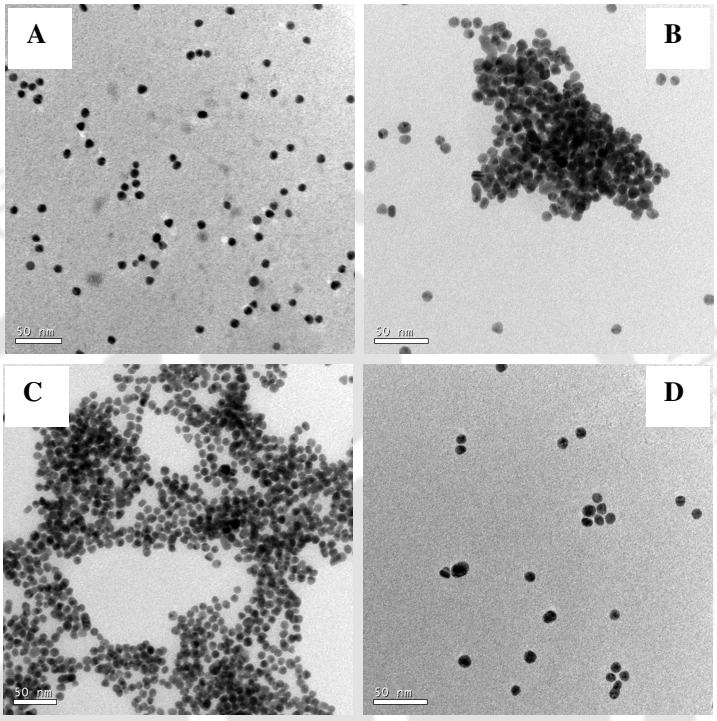

Figure 2. *TEM images of* ***(A)*** *citrate stabilized Au NPs,* ***(B)*** *Au NPs in the presence of 0.03 μg/mL of native α-amylase,* ***(C)*** *Au NPs in the presence of 0.06 μg/mL of native α-amylase and* ***(D)*** *Au NPs in the presence of 0.06 μg/mL of heat denatured α-amylase. Scale bar is 50 nm in all.*

A typical image is shown in Figure 2D, which clearly shows that almost all the particles remained largely separated even at a concentration of 0.06 μg/mL. The agglomeration induced by the native proteins of the same concentration was substantial (Figure 2C). Particle size distribution analysis recorded by DLS method also indicated agglomeration of NPs in the presence of native protein. For example, the average particle size of citrate stabilized Au NPs was found to be 33.9 $\pm$ 3.4 nm. Upon addition of 0.02 μg/mL of the native protein there was no significant change in the hydrodynamic diameter. On the other hand, the average size was 1.56 $\pm$ 0.15 μm upon addition of 0.05 μg/mL of the protein, which changed to 1.77 $\pm$ 0.17 μm when the concentration was 0.11 μg/mL. The sizes did not change significantly upon further addition of proteins.

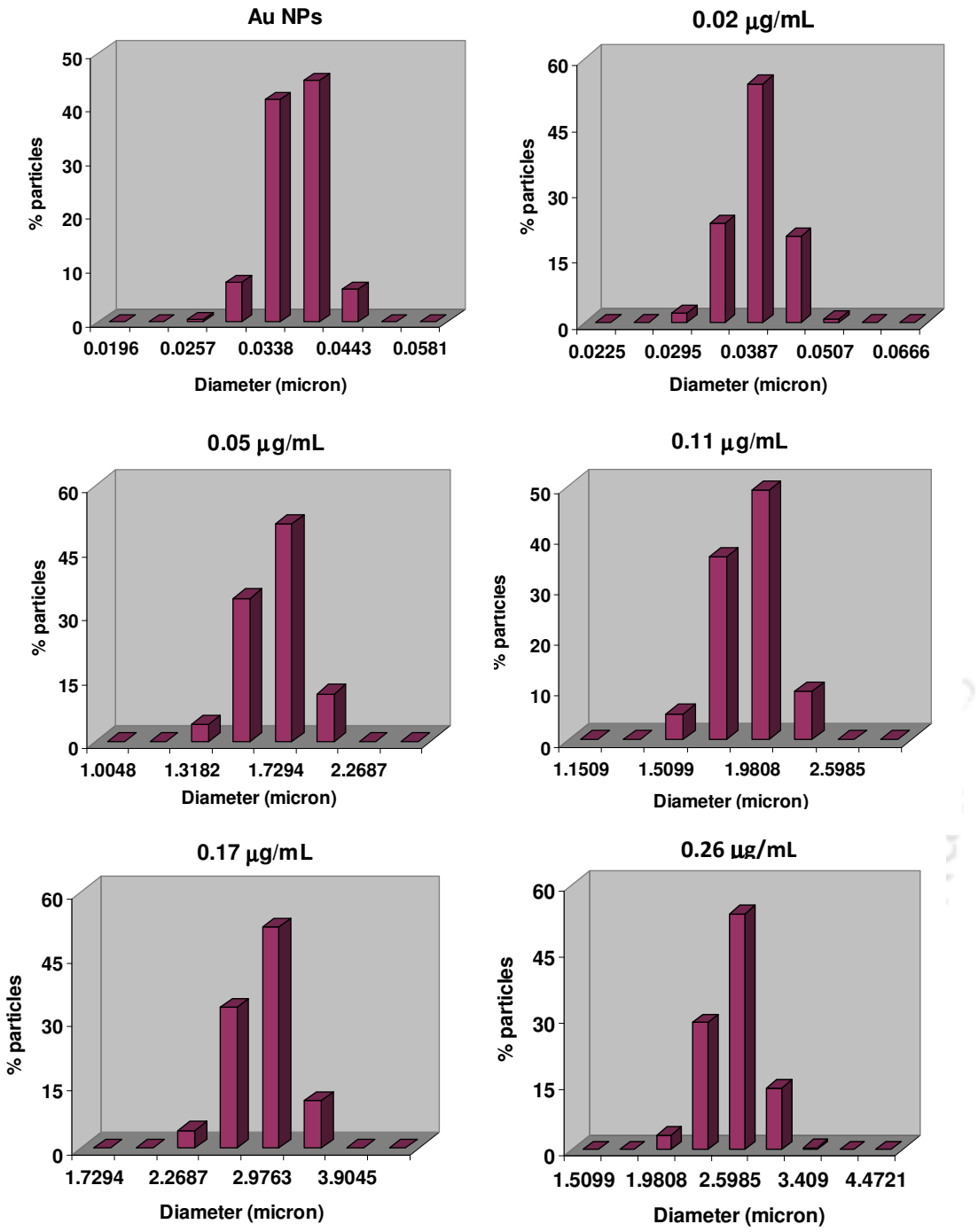

Figure 3. *Particle size distribution of citrate capped Au NPs on addition of various amounts of α-amylase (protein concentration mentioned as the legend on each graph), obtained by dynamic light scattering method (DLS).*

The details of the results of DLS measurements are shown in Figure 3. Further, dilution experiments suggest that agglomeration of the NPs in the presence of native protein was irreversible. For example, when the Au NP solution containing 0.08 µg/mL of native

protein was diluted to 1.5 times the original volume there was no change in the shape of the absorption spectrum (Figure 4). In other words, dilution of the protein containing Au NP dispersion did not lead to systematic changes in the absorption spectra. Also, the agglomerated composite of protein and NPs was quite stable with respect to volume dilution.

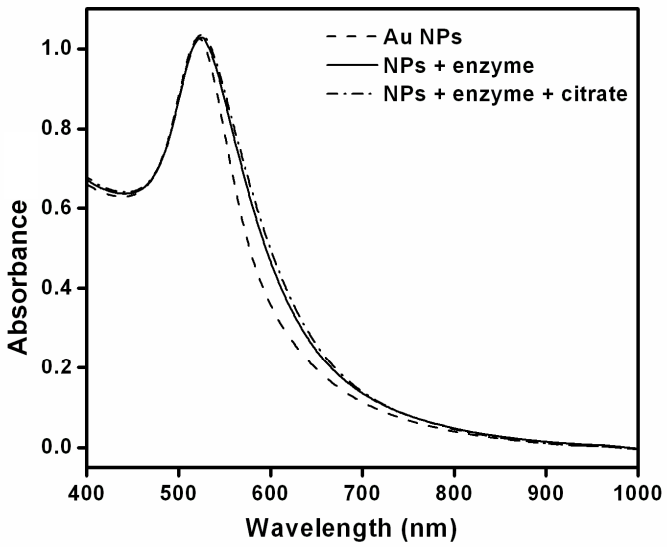

Figure 4. *UV-vis spectral analysis to check the reversibility of enzyme attachment to the NPs. Amount of α-amylase (0.1 mg/mL) added to 3 mL of Au NP solution is 0.08 mL and total sodium citrate solution (0.2 M, in buffer) added to this mixture is 1.2 mL.*

In order to understand whether agglomeration of Au NPs by native α-amylase was consequential due to addition of successive amounts of proteins or not, the following experiment was carried out. Ten 3.0 mL Au NP solutions were taken from the same stock solution and kept separately in test tubes. To each of the test tubes different amount of α-amylase was added and the final concentrations of proteins were the same as those corresponding to the graphs in Figure 1A (0.02 µg/mL, 0.04 µg/mL, 0.06 µg/mL etc.). However, the final concentrations were adjusted with addition of even smaller amount of proteins in several portions (in multiples of 0.002 µg/mL) and UV-vis spectra of all the solutions were recorded. The UV-vis spectra and the corresponding area versus protein concentration plot are shown in Figure 5 and Figure 7A respectively. As is clear from the graphs, the results are identical to those obtained using sequential addition (Figures 1A and 1C). Also, it is important to mention here that the lowest concentration

of protein that induced changes in the absorption spectrum of Au NPs was found to be 0.002 μg/mL. The above results led to three essential conclusions. First is that the effect of native α-amylase on the spectrum of Au NP solution is dependent on the concentration of protein and not on the mode of addition (sequential addition versus addition at once).

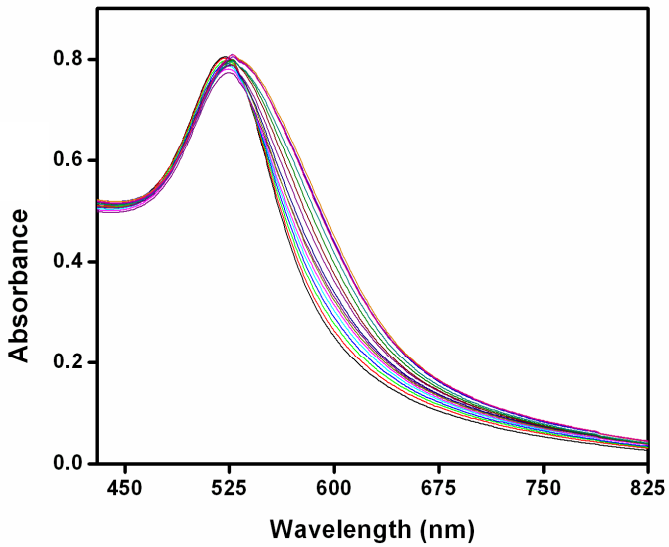

Figure 5. *UV-vis spectra of Au NPs on addition of various amount of α-amylase on small increments (0.002 μg/mL to 0.300 μg/mL of final protein concentration).*

Secondly, the spectroscopic absorption changes of Au NPs can be the basis of quantitative estimation of native α-amylase in solution. Thirdly, the lowest concentration of α-amylase that can be estimated is 40 picomolar (2 ng/mL), which is much less than obtained from the methods commonly used for the estimation of proteins in solution. Thus the method is not only simpler and easy to execute but also more sensitive than the conventional ones. Of course, the ability to differentiate between the native and denatured form of the protein is an additional advantage of the present method over others.

For a colloidal solution with N particles per unit volume the extinction of light could be written as,[40]

$$A = \log_{10}\frac{I_o}{I} = \frac{NQ_{ext}l}{2.303} \qquad (1)$$

Here, I_0 and I are the intensities of incident and transmitted light, l is the path length and Q_{ext} is the extinction coefficient of a single particle.

For very small metal particles, the absorption of light could be explained based on Mie scattering theory and the extinction coefficient can be written as,[40]

$$Q_{ext}(\lambda) = \frac{24\pi R^2 \varepsilon_m^{3/2}}{\lambda} \frac{\varepsilon''}{(\varepsilon' + 2\varepsilon_m)^2 + \varepsilon''^2} \qquad (2)$$

Here, R is the radius of the spherical NP, λ is the wavelength of the light, ε_m is the dielectric function of the medium, ε' and ε'' are the real and imaginary parts of frequency dependent dielectric function (ε) of the NP ($\varepsilon = \varepsilon' + i\varepsilon''$).

On the other hand, when the particle is coated by a layer of organic or inorganic material with different dielectric constant, the extinction coefficient of the particle can then be written as,[27]

$$Q_{ext}(\lambda) = \frac{8R\pi(\varepsilon_m)^{1/2}}{\lambda} \mathrm{Im}\left\{ \frac{(\varepsilon_2 - \varepsilon_m)(\varepsilon_1 + 2\varepsilon_2) + (1-g)(\varepsilon_1 - \varepsilon_2)(\varepsilon_m + 2\varepsilon_2)}{(\varepsilon_2 + 2\varepsilon_m)(\varepsilon_1 + 2\varepsilon_2) + (1-g)(\varepsilon_1 - \varepsilon_2)(2\varepsilon_2 - 2\varepsilon_m)} \right\} \qquad (3)$$

Here, ε_1 and ε_2 are the complex dielectric functions of the particle core and the surface coating; g is the volume fraction occupied by the surface coating. Thus the extinction of light not only depends on the dielectric property of NPs but also of the surface coating and the medium. When the protein is added to citrate stabilized Au NPs in aqueous medium, it might get attached to the NPs replacing the citrates completely or partially. At lower concentrations of the protein, the broadening that is observed could be due to change in dielectric constant of the coating owing to attachment of the protein. However, at higher concentrations, agglomeration of the proteins attached to the Au NPs as well as the excess ones occur. This leads to significant change in the dielectric constant of the coating as well as the immediate vicinity of the medium. Thus broadening becomes much pronounced. In addition, interaction between the NPs in close proximity in the agglomerated state would lead to broadening and red-shifting of the peak. This could be accounted for by the change in value of R in equation (3). We propose the following model in order to account for the changes in the spectra and to calculate the protein concentration-dependent absorbance of the Au NPs. The agglomeration of NP and protein could be written in the following way.

$$nAu_{NP} + mEnz \longrightarrow (Au_{NP})_n(Enz)_m \quad (4)$$

Here n is the number of NP and m is the number of enzyme molecules involved in the agglomerated composite formation. At lower concentrations of enzyme, when agglomeration is not significant then there would be two kinds of species that would lead to extinction of light – the unagglomerated Au NPs and agglomerated Au NP – enzyme composite. Thus the total extinction of light could be rewritten as,

$$A(\upsilon) = Q_{ext_{NP}}(\upsilon)C_{NP}l + Q_{ext_{comp}}(\upsilon)C_{comp}l \quad (5)$$

Here, the subscripts represent the species and C represents concentration of a particular species and *l* is the length of the cuvette (cell). Equation (5) could be written in terms of absorption as

$$A(\upsilon) = A_{NP}(\upsilon) + A_{comp}(\upsilon) \quad (6)$$

Here A(ν) is the frequency dependent total absorption and $A_{NP}(\nu)$ is that due to unagglomerated NP and $A_{comp}(\nu)$ is that due to composite. While there are reports of change in intensity of absorption and shift in peak position as measures of changes due to agglomeration of NP, a better and more comprehensive one would be related to oscillator strength, which is related to total area under the absorption spectrum. One can then write equation (6) as,

$$\int A(\upsilon)d\upsilon = \int A_{NP}(\upsilon)d\upsilon + \int A_{comp}(\upsilon)d\upsilon \quad (7)$$

One can also express equation (7) in terms of integration over wavelengths (λ),

$$\int A(\lambda)d\lambda = \int A_{NP}(\lambda)d\lambda + \int A_{comp}(\lambda)d\lambda \quad (8)$$

Thus the total area under the experimental absorption spectrum could be interpreted as superposition of spectra due to unagglomerated Au NPs and agglomerated NPs. The changes in the area would reflect changes in the concentration of both the species. In the present set of experiments, the changes were observed in terms of primarily spectral broadening, while in some instances accompanying red-shift in peak could be observed - albeit small. This made the comparison of absorption spectra of unaffected Au NPs and agglomerated Au NPs as such not possible. However, appropriate deconvolution of the spectra could be performed to discern the effect of agglomeration of the protein and NPs, in a more quantitative manner. In order to account for broadening of peak, each UV-vis

spectrum was deconvoluted using Lorentzian peak fitting routines available in standard commercial graphics software packages. Also, the Lorentzian fit after several iterations matched well with the absorption spectra with R^2 values better than 0.99. We have used commercially available software (Microcal Origin 7.0) for the analyses. The experimental spectra were deconvoluted and fitted by the non-linear curve fitting method using software in-built Lorentzian function. Multiple (two to five) peaks were used to get good fit by iterative methods. It was observed that the area of the peaks obtained after deconvolution were affected little by the choice of the number of baselines chosen to fit the curves. For example in the case of GFP the areas of peak 1 and peak 2 remained nearly the same when the data was fitted to one baseline and two peaks instead two baselines and two peaks (Figure 6). However, regression factors of curve fitting with lesser number of baselines were little poorer in the region outside the peak due to Au NPs i.e. below 450 nm and above 650 nm, which consist of background extinction.

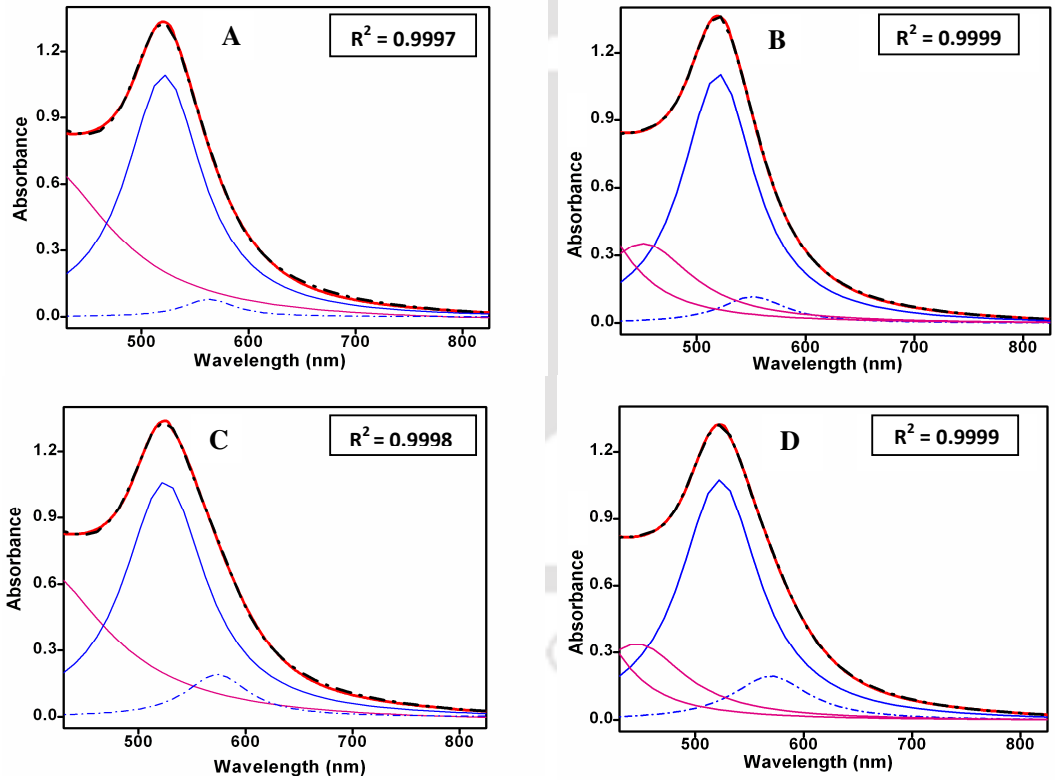

Figure 6. *Deconvoluted SPR peaks for Au NPs in the presence of denatured GFP.* ***(A)*** *The spectrum was recorded in the presence of 0.662 µg/mL of protein and the fitting was done with one baseline and two peaks,* ***(B)*** *the same spectrum being fitted with two baselines and two peaks.* ***(C)*** *The spectrum was recorded in the presence of 1.961 µg/mL of protein and the fitting was done with one baseline and two peaks,* ***(D)*** *the same spectrum being fitted with two baselines and two peaks. The regression factors (R^2) are shown in the legends.*

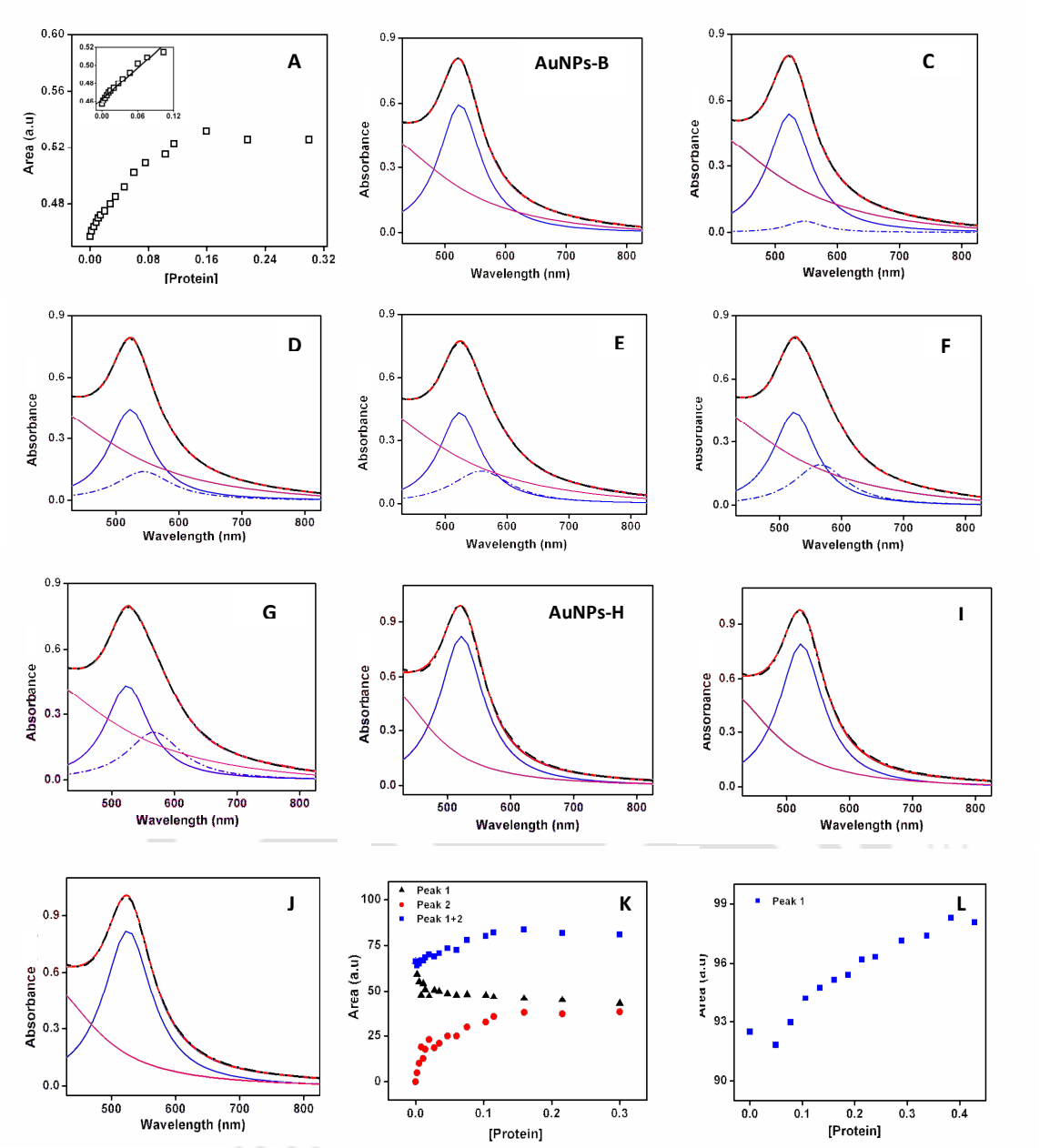

Figure 7. ***(A)*** *Area (under the curve) versus protein concentration (in μg/mL) plot for (native) α-amylase addition to Au NPs in small increments (inset shows the linear region).* ***(B)*** *Deconvoluted curves of Au NPs only used for native amylase.* ***(C-G)*** *Deconvoluted curves of Au NPs in presence of 0.002 μg/mL, 0.005 μg/mL, 0.075 μg/mL, 0.16 μg/mL and 0.3 μg/mL respectively of protein (native enzyme).* ***(H)*** *Deconvoluted curves of Au NPs only used for denatured enzyme.* ***(I-J)*** *Deconvoluted curves of Au NPs in presence of 0.02 μg/mL and 0.43 μg/mL of protein (denatured enzyme). Area (under the curve) versus protein concentration (in μg/mL) plot for the same set for all the peaks obtained after deconvolution of the UV-vis curves of* ***(K)*** *native α-amylase and* ***(L)*** *denatured α-amylase. The red curves shown in graphs* ***B-J*** *are the experimental curves and the dotted black lines show the Lorentzian fit achieved after deconvolution. The solid blue curves represent the 1st peak and the dotted blue ones are the 2nd peak. The curves in pink are baselines.*

Four examples are shown in Figure 6. Hence, it is probably reasonable to conclude that the present method of peak analyses works well for the observed spectra and can be used in general. The results corresponding to addition of native α-amylase are shown in Figure 7. As is clear from Figure 7B, the initial solution consisted of a single peak at 522 nm (along with a background) corresponding to that of Au NPs in citrate solution. When 0.002 μg/mL of protein was added to the solution, the intensity of the peak at 522 nm decreased significantly, while a second peak at 542 nm appeared (Figure 7C). Further addition of proteins decreased the intensity of the peak at 522 nm. On the other hand, the peak at higher wavelength not only increased in intensity but also the wavelength maximum red-shifted increasingly with concentration (Figures 7D to 7G).

These results indicate that with addition of the protein the agglomeration takes place and continue to increase with the concentration of protein. However, even in the agglomerated state the peak due to original Au NPs does not completely vanish, indicating that isolated Au NPs were present in significant numbers even in the agglomeration. In other words, addition of protein might not have removed the citrate cover to the NPs completely. On the other hand, proteins may lead to agglomeration of citrate stabilized NPs. Aggregation of the Au NPs is also known to be induced by London / van der Waals attractive forces between the nanoparticles.[41,42] Proteins contain various amino acid residues on their surface which can lead to charge neutralization by interacting with citrate and thus leading to agglomeration of the NPs. Amino groups, such as lysine and histidine, are known to show strong electrostatic interaction with citrate capped Au NPs. Further, it is plausible that even in the agglomerated composite there could be individual NPs that do not interact with each other electrostatically to give rise to a second peak and hence contributes to the intensity of the peak at 522 nm (i.e. unagglomerated Au NP). Interestingly, when denatured protein (α- amylase) was added to the Au NP solution there was no appearance of the second peak (Figures 7H to 7J), indicating lack of agglomeration. This is consistent with the observation of TEM measurements. Plot of area of the component peaks versus concentration of protein (Figure 7K) indicates that for the addition of native protein the area of the peak at 522 nm decreased linearly up to a protein concentration of 0.106 μg/mL, while the area of the peak at higher wavelength increased linearly up to the same concentration. Both the areas leveled off at above this concentration of protein. Also, the summation of the two

areas at different protein concentration increased linearly up to the protein concentration of 0.106 μg/mL and then leveled off, similar to the experimental observations (Figure 7L). On the other hand, in the case with denatured protein the area of the peak at 522 nm hardly changed, indicating that the denatured protein did not lead to significant changes in the spectral characteristics of Au NPs. Thus from both the experimentally observed spectra and their deconvolutions it is clear that changes in the absorption characteristics of Au NPs could be used to estimate the concentration of native α-amylase (up to an upper limit of 0.106 μg/mL), where the area of the absorption increases linearly with the concentration of the protein. On the other hand, the same experiments could be used to distinguish between the native and denatured form of the protein in solution.

Interestingly, addition of GFP to the citrate stabilized Au NP solution also led to observations of optical behavior similar to those with α-amylase. For example, broadening of the absorption spectrum was observed upon addition of the native protein (Figures 8A and 8B). However, the effect was pronounced at higher concentrations of the protein in comparison to that of α-amylase. For example, the linear region of spectral broadening of area was observed up to a protein concentration of 1.639 μg/mL (Figures 8C and 8D), which was much higher than that of α-amylase. Also, the broadening of spectra was less pronounced in the denatured protein (Figure 8A and 8B). In other words, the changes were much sharper with the native form than the denatured form of the protein. This is also similar to those observed in case of α-amylase. However, the changes in the case of denatured GFP were more significant than that due to the presence of denatured α-amylase. Interestingly, there is an isobestic point in the absorption spectra associated with both the native as well as denatured protein, occurring at 535 nm and 540 nm respectively. This possibly indicates conversion of individual Au NPs into agglomerated form in the presence of protein, while the shift in peak due to agglomeration is more prominent than those involved with α-amylase. Further, the lowest concentration of the native as well as denatured form of GFP that induced changes was 0.332 μg/mL. Deconvolutions of the spectra of Au NPs associated with both the native and denatured form of the protein indicate behavior similar to those of α-amylase (Figure 9). The original peak due to unagglomerated protein decreased gradually, while the peak due to agglomeration increased gradually up to a concentration of 1.639 μg/mL for the native protein.

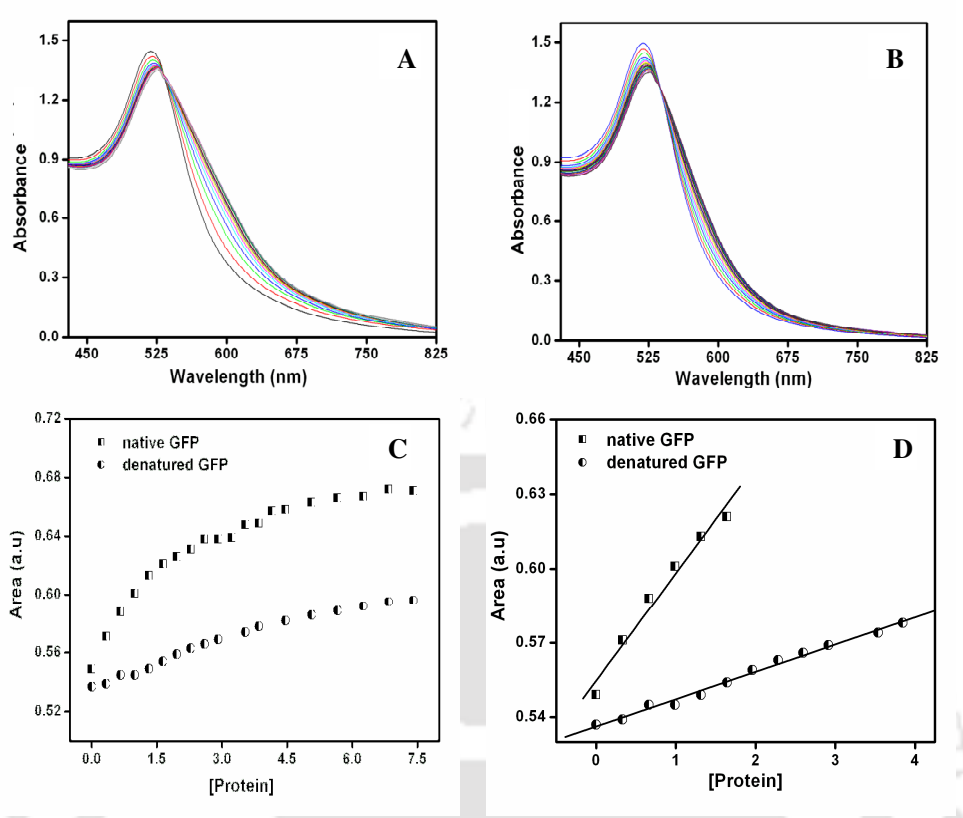

Figure 8. *UV-vis spectra Au NPs on successive addition of* ***(A)*** *native GFP and* ***(B)*** *denatured GFP (0.332 µg/mL to 7.407 µg/mL of final protein concentration).* ***(C)*** *Area under the graph versus the corresponding protein concentration (in µg/mL) for native and denatured GFP.* ***(D)*** *The linear region of the graphs in '****C****'.*

Similar results were observed for the denatured one; however, the changes were less dramatic as can be seen from the figure. The combination of decrease in the area of the graph due to unagglomerated Au NPs only and increase in the area of the agglomerated Au NPs spectra could account for the observed changes in the experimental spectra (Figures 10A and 10B).

The three-dimensional native structure of α-amylase in solution consists of two cysteine thiol groups that are exposed to the medium, which are known to covalently bind to Au NPs.[43, 44] On the other hand, native GFP in solution consists of a tertiary structure that has one cysteine thiol group that is exposed to the medium. Since Au NP is known to have strong affinity for thiol group that forms Au-S- bond on the surface of the NP, it is plausible that for both the proteins - in their native forms - thiol groups are

involved in the formation of agglomeration. One cannot, though, exclude the role of other amino acids that could interact with the NPs electrostatically.

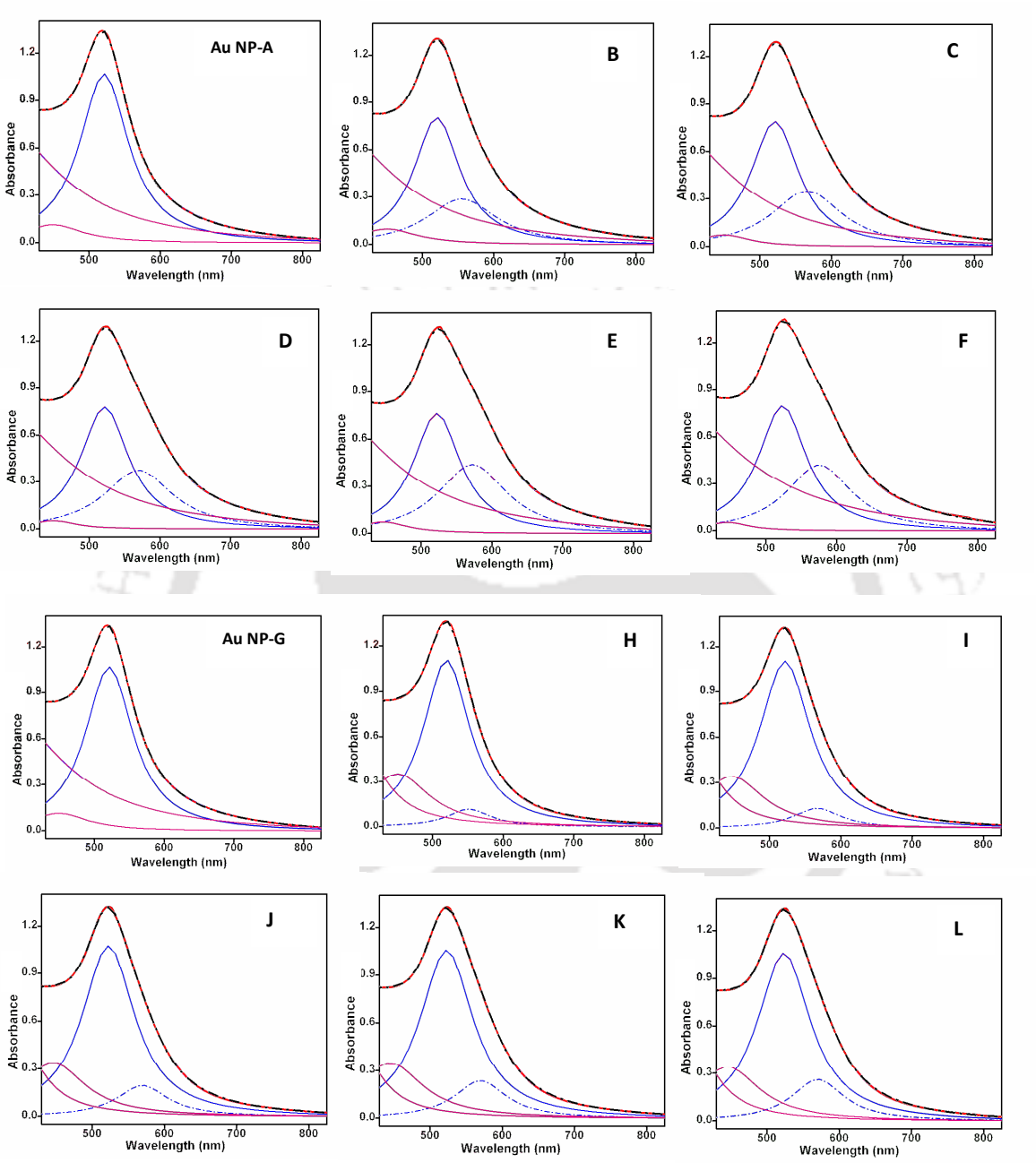

Figure 9. *Deconvoluted SPR peaks for* ***(A & G)*** *Au NPs used for native and denatured GFP,* ***(B-F)*** *Au NPs in presence of 0.662 µg/mL, 1.316 µg/mL, 1.961 µg/mL, 3.846 µg/mL and 5.063 µg/mL respectively of protein (native GFP),* ***(H-L)*** *Au NPs in presence of 0.662 µg/mL, 1.316 µg/mL, 1.961 µg/mL, 3.846 µg/mL and 5.063 µg/mL respectively of protein (denatured GFP). Red curve is the experimental curve, black dotted is the Lorentzian fit, solid blue is the 1st peak, dotted blue is the 2nd peak and pink ones are the baselines.*

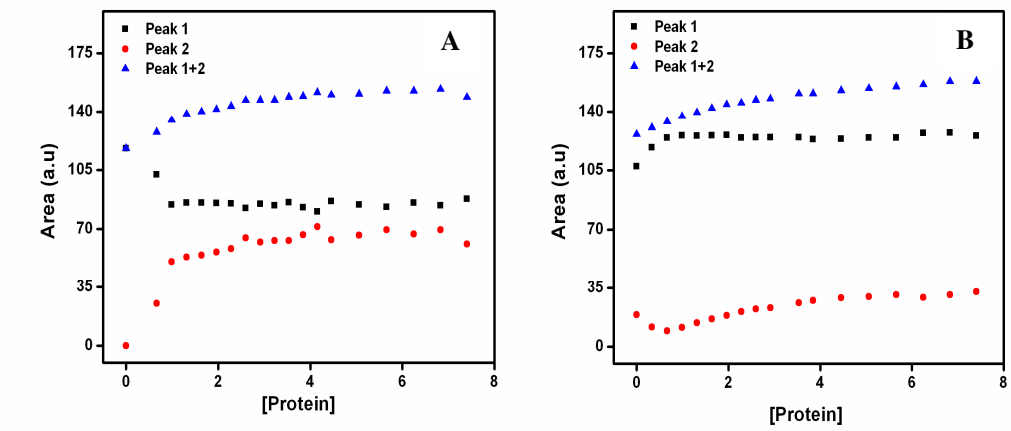

Figure 10. *The peak areas of all the component peaks and their summation against the protein concentration (in µg/mL) obtained by deconvolution for* ***(A)*** *native GFP and* ***(B)*** *denatured GFP.*

Overall, the interactions of the NPs with the proteins might be similar and that could involve changes in the tertiary structure of the protein, leading to agglomeration. On the other hand, the proteins in the denatured form need not have the thiol group exposed to the medium; it might be buried in the structure and may not be available for bonding with the NPs. This would mean that the interaction would primarily be electrostatic that might not necessarily lead to significant agglomeration of the protein and Au NPs. This could be the reason for the differences that has been observed with respect to interactions of the native and denatured forms of the proteins with Au NPs. On the other hand, the role of hydrophobic forces in the denatured conformations of the proteins may play a significant role in determining the interactions with the citrate stabilized NPs and consequently the changes in the spectra.

Further experiments with AMG showed significant broadening of spectra of Au NPs in the presence of both native and denatured proteins (Figure 11A and 11B). There were also significant decreases in intensity of absorption maxima for both the samples. However, shift in absorption maximum was more prominent in the samples consisting of denatured proteins than those containing native forms. The areas under the absorption spectra increased linearly up to limited concentrations for both the samples (about 1.0 µg/mL), as shown in Figure 11C. Above that concentration, further addition of protein did not result in further increase of area in the UV-vis spectra in either of the cases. However, for the samples consisting of denatured protein significant precipitation could be observed at above the concentration of 1.07 µg/mL, leading to loss of absorption

intensity. Interestingly, the trends in the slopes of the areas corresponding to AMG were different from those of samples with α-amylase and GFP. For example, the slope of the area versus concentration plot of the NPs in the presence of denatured protein is much steeper and closer to the slope of the native form (Figure 11D).

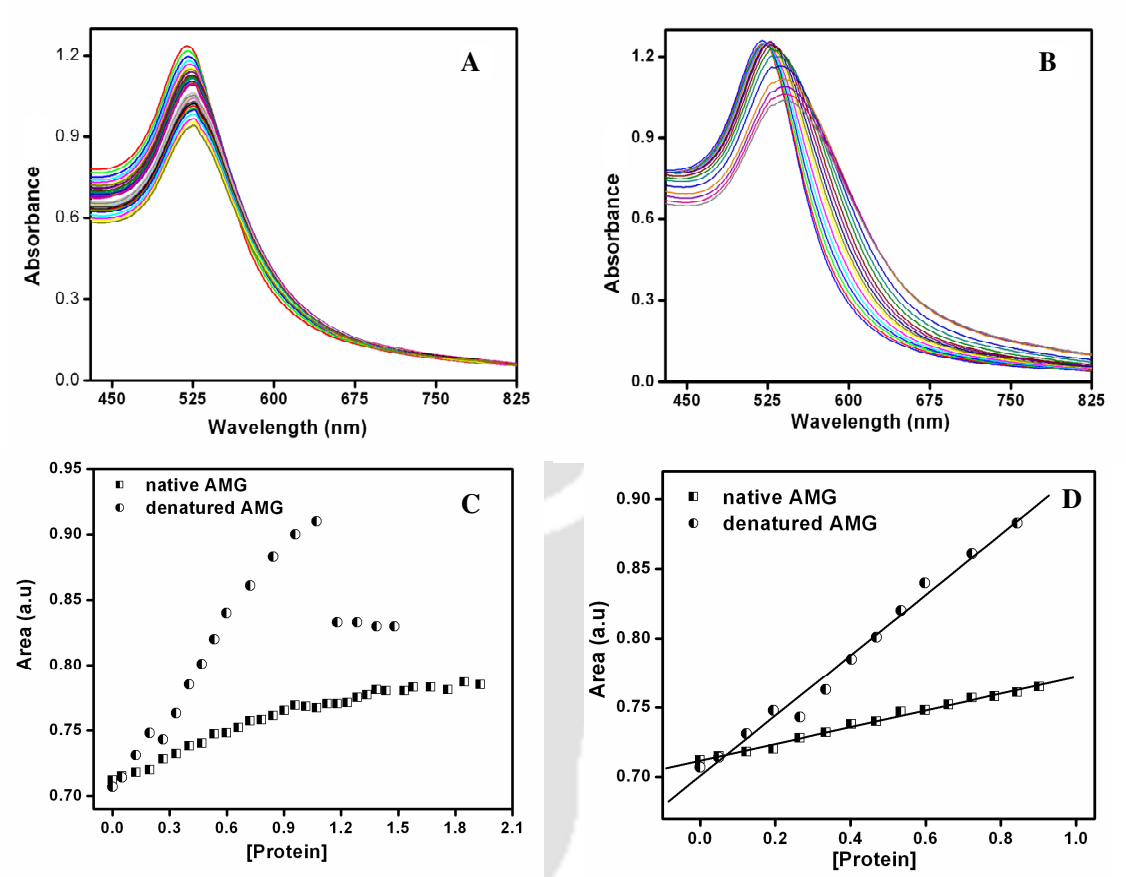

Figure 11. *UV-vis spectra Au NPs on successive addition of* ***(A)*** *native AMG (0.050 μg/mL to 1.931 μg/mL of final protein concentration) and* ***(B)*** *denatured AMG (0.050 μg/mL to 1.480 μg/mL of final protein concentration).* ***(C)*** *Area under the graph versus the corresponding protein concentration (in μg/mL) for native and denatured AMG.* ***(D)*** *The linear region of the graphs in '****C****'.*

Also, changes in the area of the graphs were more significant than those with the denatured forms of α-amylase and GFP. The concentrations of the protein at which values the saturations were reached were also much higher in comparison to other two proteins. The results indicate that interactions of protein with Au NPs depend strongly on its three dimensional conformation as well as the groups that are exposed to the medium. Experimental observations suggest that the interactions of Au NPs with proteins having

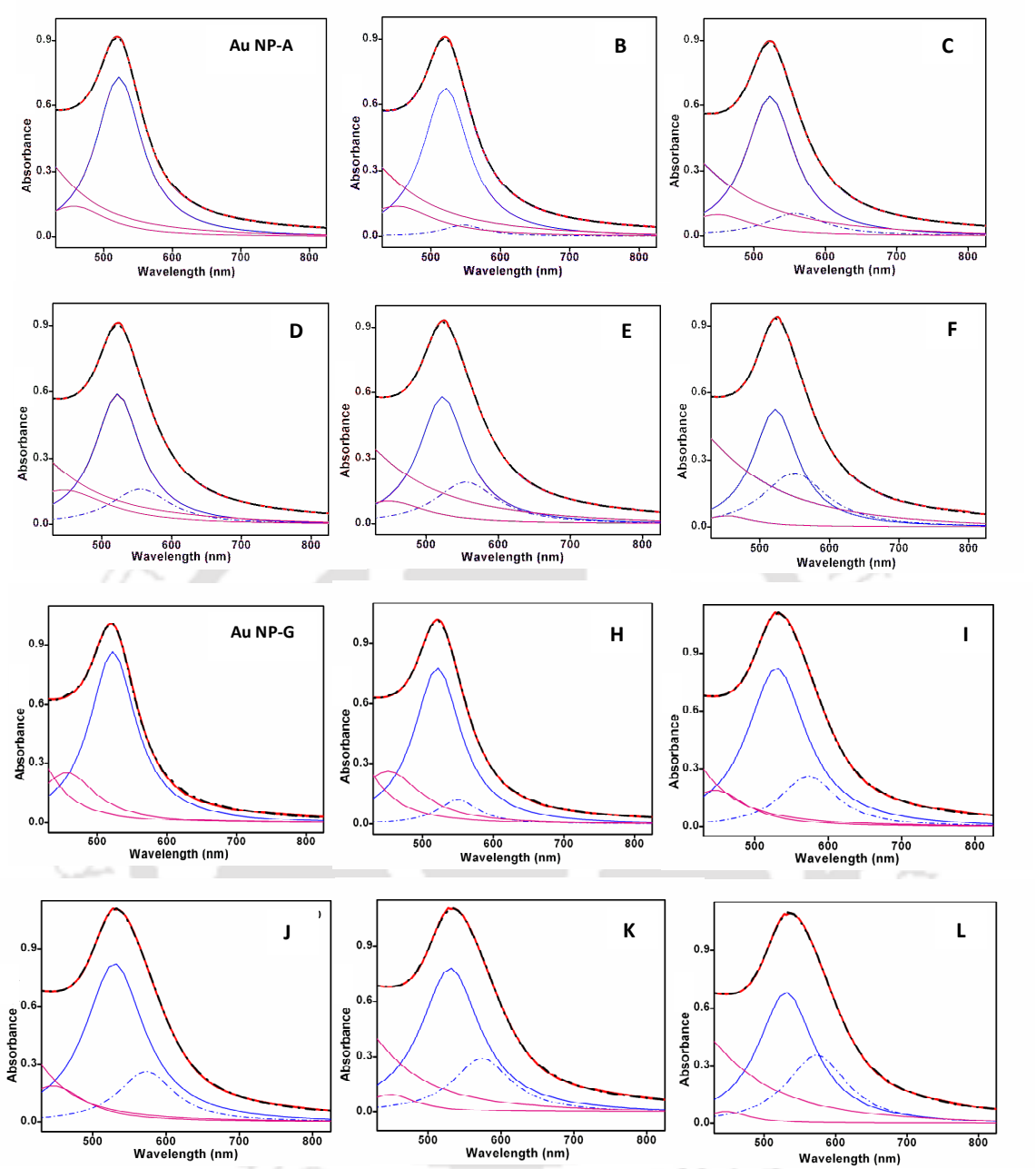

Figure 12. *Deconvoluted SPR peaks for* ***(A & G)*** *Au NPs for used for native and denatured AMG,* ***(B-F)*** *Au NPs in presence of 0.05 µg/mL, 0.334 µg/mL, 0.661 µg/mL, 1.016 µg/mL and 1.847 µg/mL respectively of protein (native AMG),* ***(H-L)*** *Au NPs in presence of 0.123 µg/mL, 0.469 µg/mL, 0.661 µg/mL, 0.722 µg/mL and 0.784 µg/mL respectively of protein (denatured AMG). Red curve is the experimental curve, black dotted is the Lorentzian fit, solid blue is the 1st peak, dotted blue is the 2nd peak and pink ones are the baselines.*

exposed thiol groups are different from those of non-thiol containing proteins. Further, Lorentzian fit of the absorption spectra of Au NPs in the presence of different

concentrations of native and denatured protein indicate that in addition to the peak due to unagglomerated NPs a second peak appeared, intensity of which increased with increasing concentrations of both forms of protein (Figure 12). Also, the original peak due to unagglomerated Au NPs decreased gradually in area with the amount of protein. Plots of the area of both types of peak indicate clearly the agglomeration of the NPs in the presence proteins – both in native and denatured forms (Figure 13A and 13B). Further, the trends in changes in the area of the deconvoluted absorption spectra - i.e. summation of the areas of the two graphs - matched well with the experimental observations. Overall, the observations indicated that for AMG the denatured form of the protein led to agglomeration of NPs much more than that due to the denatured form of other two proteins (α-amylase and GFP). Interestingly the denatured form led to more agglomeration than its native form, in comparison to the other two proteins.

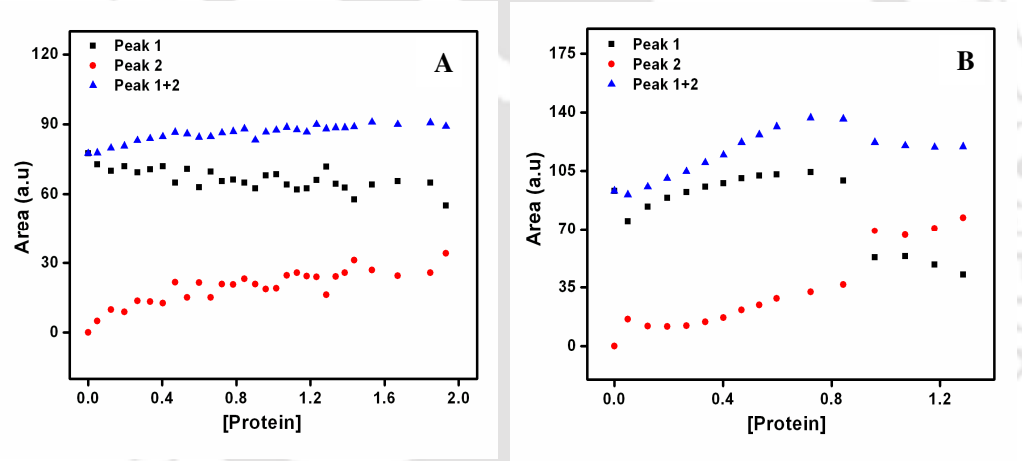

Figure 13. *The peak areas of all the component peaks and their summation against the protein concentration (in μg/mL) obtained by deconvolution for* ***(A)*** *native AMG and* ***(B)*** *denatured AMG.*

Further, addition of BSA to Au NPs exhibited results although apparently similar to the above enzymes but there were also fundamental differences from the others. For example, addition of both the native and denatured form of proteins led to broadening of the spectra. However, broadening and shifts of the peaks due to addition of denatured form were much more prominent than the native form of the protein (Figure 14A and 14B). These results are similar to those of AMG but very different from the other two proteins (α-amylase and GFP) used herein. Plots of area versus concentration of native as well as denatured protein (Figures 14C and 14D) showed that the changes associated

with addition of both forms of the protein were prominent; however, the slope of the graphs for the denatured one was much more steep than that with the native protein - in the linear region of the graphs. The linearity was valid up to a concentration of 1.639 µg/mL for both forms of the protein.

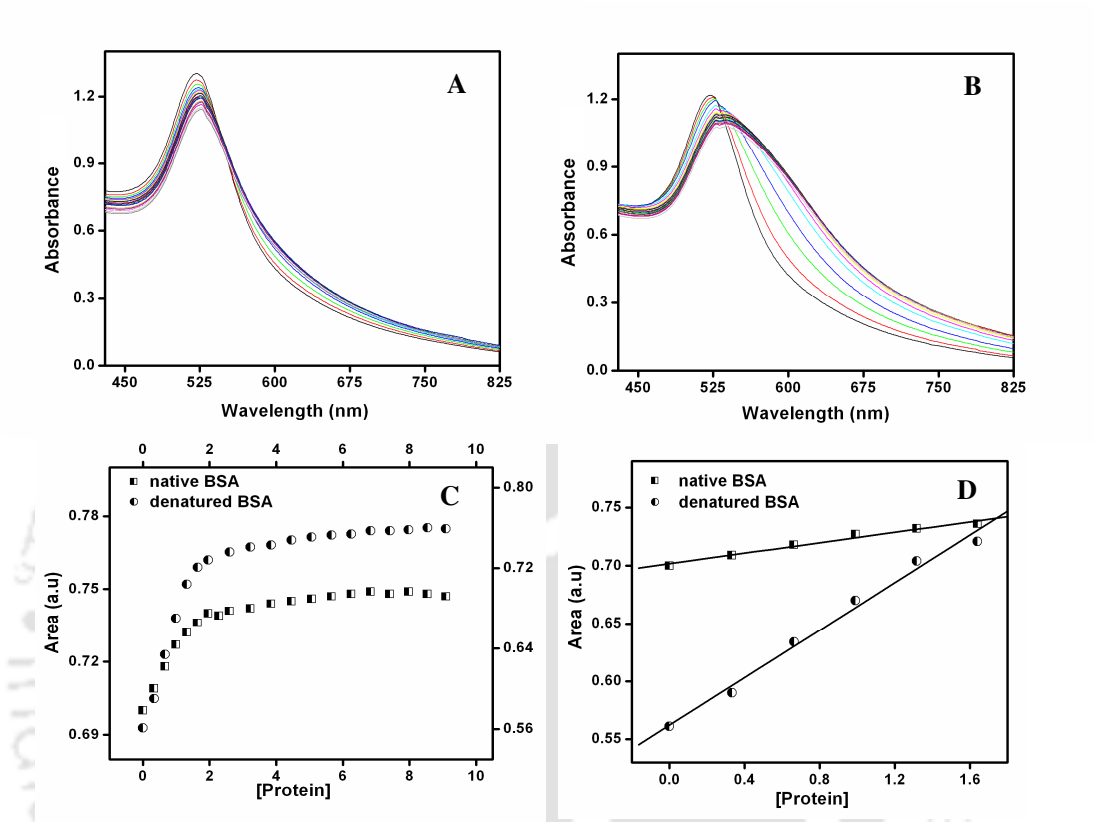

Figure 14. *UV-vis spectra Au NPs on successive addition of* ***(A)*** *native BSA and* ***(B)*** *denatured BSA (0.332 µg/mL to 9.091 µg/mL of actual protein concentration).* ***(C)*** *Area under the graph versus the corresponding protein concentration for native and denatured BSA (the left Y-axis is for native BSA and right Y-axis for denatured BSA)* ***(D)*** *The linear region of the graphs in '****C****'.*

Further, agglomeration of the NPs in the presence of both native and denatured forms of the protein was substantiated by TEM measurements (Figure 15). Deconvolutions of the absorption spectra (Figure 16) indicated that the best fits were obtained with three curves (in addition to the background) – one for the peak due to unagglomerated Au NPs, while the other two are due to agglomerated composites. The intensity of the peak due to Au NPs (unagglomerated) decreased with the addition of proteins, whereas two more peaks appeared simultaneously.

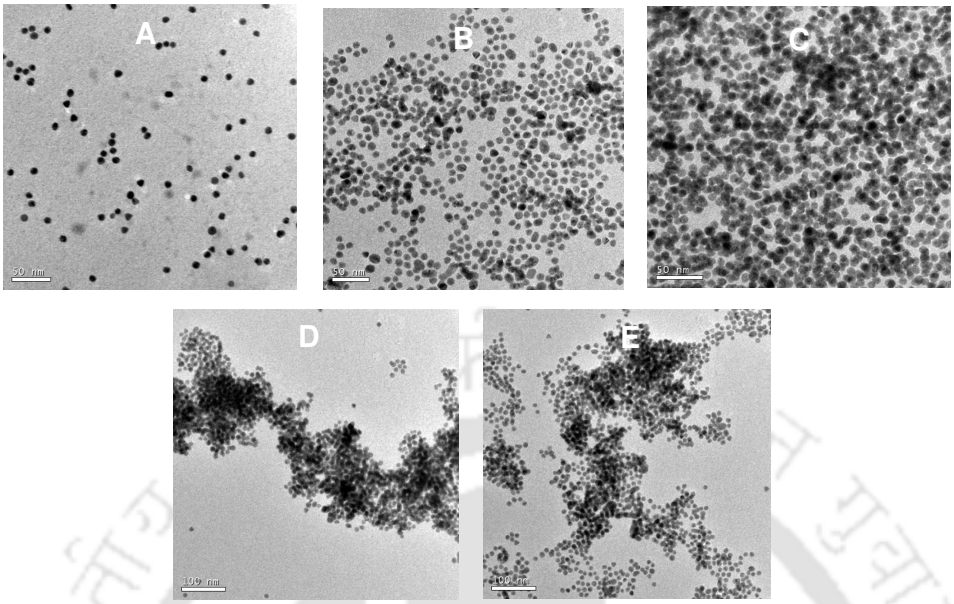

Figure 15. *TEM images of* ***(A)*** *Au NPs only* ***(B)*** *Au NPs in presence of 0.99 μg/mL of protein (native BSA)* ***(C)*** *Au NPs in presence of 5.06 μg/mL of protein (native BSA)* ***(D)*** *Au NPs in presence of 0.99 μg/mL of protein (denatured BSA) and* ***(E)*** *Au NPs in presence of 5.06 μg/mL of protein (denatured BSA). Scale bar in A-C is 50 nm and D-E is 100 nm.*

The total area due to three peaks matched well with the experimentally observed area versus protein concentration plot (Figure 17A and 17 B). This was valid for both forms of the protein. It is plausible that agglomeration of Au NPs in the presence of BSA follows a different path from the other three enzymes. It might also be true that there are two kinds of agglomeration; one where the peak shift is less and the change may be due to the change of dielectric constants and agglomeration similar to the other proteins. On the other hand, the peak at the higher wavelength could be due to strong inter-plasmon resonance coupling between the NPs and thus occur at higher wavelengths. This peak represents the agglomeration of Au NPs in the presence of the protein, which is specific to BSA. However, fundamentally, the results indicate different level of agglomeration in the presence of different proteins and their conformational states. Thus the present method not only provides a new way of estimating the protein concentration in a medium but also brings out evidences of specific to its nature and conformation in solution.

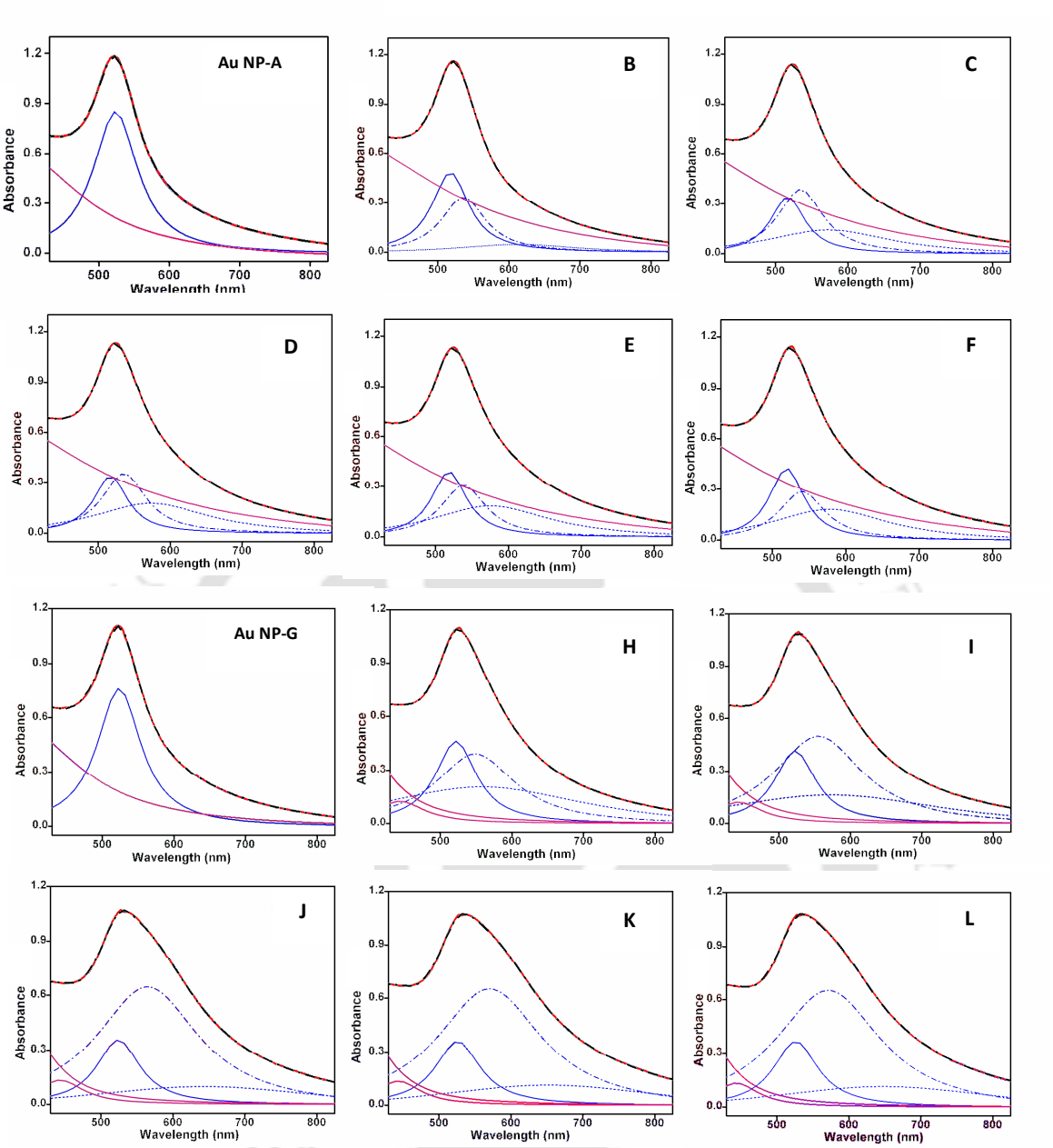

Figure 16. *Deconvoluted SPR peaks for* ***(A & G)*** *Au NPs for used for native and denatured BSA,* ***(B-F)*** *Au NPs in presence of 0.332 µg/mL, 0.990 µg/mL, 1.961 µg/mL, 3.846 µg/mL and 6.25 µg/mL respectively of protein (native BSA),* ***(H-L)*** *Au NPs in presence of 0.662 µg/mL, 0.990 µg/mL, 1.639 µg/mL, 2.597 µg/mL and 7.976 µg/mL respectively of protein (denatured BSA). Red curve is the experimental curve, black dotted is the Lorentzian fit, solid blue is the 1st peak, dotted blue is the 2nd peak, small dotted blue is the 3rd peak and pink ones are the baselines.*

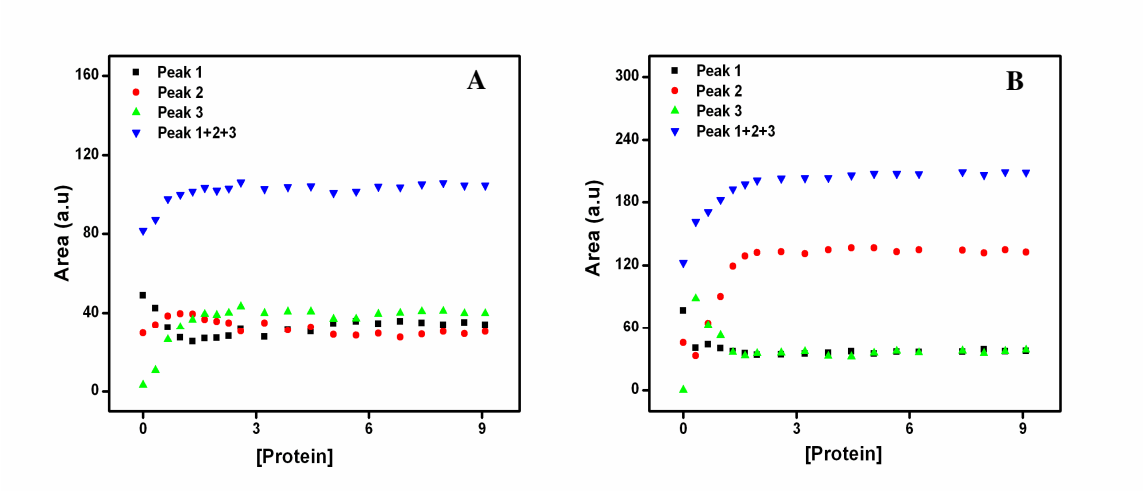

Figure 17. *The peak areas of all the component peaks and their summation against the protein concentration (in μg/mL) obtained by deconvolution for* ***(A)*** *native BSA and* ***(B)*** *denatured BSA.*

The results obtained with respect to the effect of four proteins on the UV-vis spectra of Au NPs are summarized in Table 1 and Table 2. Table 1 indicates the detection limit achieved using the present method of finding protein concentrations and absolute amount in solution, for all four of them in both their native and denatured forms. Similarly, the results of the deconvolution analyses of the UV-vis spectra of Au NPs in the presence of all four proteins are shown in Table 2. The results essentially show that the detection limit of protein concentration is dependent on the nature of the protein with its three-dimensional conformation.

The method is most sensitive to the detection of native α-amylase as the lowest concentration that can be detected is 2.0 ng/mL, the absolute amount used here being 6 ng. Interestingly, the denatured form leads to detection of the lowest concentration at 20 ng/mL, which is higher than that of the native form. The next lowest limit is for AMG (both in native and denatured forms) with a value of 50 ng/mL. The lowest limits for GFP and BSA were identical and the value was 330 ng/mL for both the native and denatured forms. On the other hand, the highest concentrations of the proteins that can be detected using the present method followed the same trend as those of the lowest limits. This is reasonable considering that the detection limits fall in the linear regimes of variation of absorbance with concentration of protein.

TABLE 1: *Experimental results of the sensitivity range of protein detection.*

S.No.	Enzyme/Protein	Sensitivity range of protein detection	
		µg/mL of protein (lower -upper limit)	µg of protein (lower--upper limit)
1.	Amylase - Native	0.002 – 0.100	0.006-0.330
2.	Amylase - Denatured	0.02 – 0.34	0.06-1.14
3.	GFP - Native	0.33 – 1.64	1.00-5.00
4.	GFP - Denatured	0.33 – 3.85	1.00-12.00
5.	AMG - Native	0.05 – 0.96	0.15-3.30
6.	AMG –Denatured	0.05 – 0.90	0.15-3.07
7.	BSA - Native	0.33 – 1.64	1.00-5.00
8.	BSA - Denatured	0.33 – 1.64	1.00-5.00

TABLE 2: *Details of component peaks for all sets of enzyme/protein used and as obtained from deconvolution of the SPR peaks.*

Sl. No.	Enzyme/Protein	No. of peaks	Peak shift (in nm)		
			Peak 1 (nm)	Peak 2 (nm)	Peak 3 (nm)
1.	Amylase - Native	02	Const. at 522	542-572	Nil
2.	Amylase-Denatured	01	Const. at 522	Nil	Nil
3.	GFP – Native	02	Const. at 522	542-572	Nil
4.	GFP – Denatured	02	Const. at 522	542-572	Nil
5.	AMG – Native	02	Const. at 522	542-562	Nil
6.	AMG – Denatured	02	Const. at 522	542-572	Nil
7.	BSA – Native	03	Const. at 522	542-572	572-583
8.	BSA - Denatured	03	Const. at 522	542-572	562-644

Further, as is clear from Table 2, the Lorentzian fit of the absorption spectra for different proteins revealed that typically, appearance of an additional peak (-other than the original absorption due to unagglomerated Au NPs-) is sufficient to account for the change in spectral characteristic of the spectra upon addition of proteins of different concentration. The second peak position appears at 542 nm and continuously changes till 572 nm in the linear regimes. This could possibly indicate the level of agglomerations of proteins with Au NPs which increases with protein concentration, giving rise to continuous change in dielectric constant and hence peak positions. The above results were found to be true for α-amylase (native form only), GFP and AMG. On the other hand, the denatured α-amylase form did not have a second peak indicating that there was no agglomeration; the change in intensity could be accounted for by the change in dielectric constant upon addition of the protein. Interestingly, in order to fit the absorption spectra due to BSA two additional peaks were required. The appearance and behavior of the first one was similar to those of the other proteins. The third peak appeared at a higher wavelength in the region of 572-584 nm for the native form and 562-644 nm for the denatured form. This clearly indicates a second process of agglomeration for both the forms of the protein and effect of the native form is different from that due to denatured form.

It is clear from the above results that the way a particular enzyme/protein interacts with citrate-capped Au NP is specific to its nature as well its three dimensional conformation. The protein specific interaction gives rise to different broadening in the absorption spectra, which depends on the nature and level of agglomeration of the composite of protein and citrate-capped NPs. Also, since the protein detection range differs from protein to protein, hence the way a protein interacts must be specific to its 3D conformation with the presence (and absence) of various amino acid residues which could interact with Au NPs leading to different consequent structures (agglomeration). The observation that the detection limit for native state of α-amylase being the lowest clearly indicates the role of free and exposed thiol groups present in the native structures of the proteins. However since the results with GFP are different it can be concluded that free and exposed thiol group alone does not play the key role in the change of absorbance characteristics of Au NPs. In other words, the amino acid residues other than those containing free and exposed thiols also play critical roles in the agglomeration of Au NPs in the presence of protein and subsequent effect on the spectra behavior of Au

NPs. This is all the more clear from the detection limits of AMG (both forms of the protein) being much lower than those of GFP. Also, the proteins attached to the NPs may facilitate agglomeration, which could be different for different proteins, leading to variation of the point of saturation in the absorption spectra. On the other hand, when the thiol groups in the denatured proteins may not be exposed to the solution, the affinity for binding to the NPs may be different and hence the changes in the absorption spectra would occur at protein concentration different from that of the native form; which may be driven primarily by electrostatic interactions involving other amino acid residues. For example, AMG and BSA, both of which lack free thiol groups on their surfaces in their native state, may interact with the Au NPs via the amino acid residues electrostatically only. This possibly occurs at higher concentrations of proteins and thus the higher detection limit. Interestingly, on being denatured, the buried free thiol group of the BSA might not necessarily be available to bring any change in the detection range of protein as has been observed experimentally. However, the detection limits for BSA and AMG being significantly different indicates that the nature of interactions between proteins and citrate-stabilized Au NPs may be more complex that to be explained based on simple electrostatic interactions between the amino acid residues. For example, the proteins upon being adsorbed on the NP surface may interact with other protein (present in other NP) very differently than that between two free proteins in solution and may give rise to more complicated interactions.

Finally, it may be mentioned here that the changes in the spectral characteristics of Au NPs may not be absolute with respect to addition of proteins. In other words, the exact changes in the spectra may vary depending on the sizes of the NPs and their distribution. However, in general NPs can be produced with reproducible sizes and their distribution with unique spectra, especially in the presence of stabilizers. We have observed that under the same reaction conditions the UV-vis absorption spectra of Au NPs produced from different batch could be superimposed. Thus the present method should provide reproducible results. On the other hand, in the event of NPs not being produced with predictable sizes and the UV-vis spectra of protein free Au NPs vary from sample to sample, a calibration curve could be obtained (with the protein and its concentration), which should be sufficient for identification and estimation of samples of unknown concentration and nature of protein following the above method. Further, it is important to mention here that in order for the method to be robust there should be no time-

dependence of the UV-vis spectra of the Au NPs upon addition of various amounts of proteins. As any such dependence would indicate secondary interactions and subsequent calculations of the concentrations from the changes in the area of the graph would then be erroneous. In order to probe this, we have recorded the time-dependent UV-vis spectra of Au NPs after addition of native amylase, native and denatured BSA. The results indicate that there is hardly any time-dependence in the peak of the Au NPs after addition of various amounts of proteins. Also, there is no substantial change in the area versus concentration plots with time for the above proteins. The corresponding time-dependent UV-vis spectra and area versus protein concentration plots are shown in the Appendix (Figures 4-3 to 4-5).

4.4 Summary

In conclusion, the series of experiments performed with four different enzymes/proteins have demonstrated a versatile, simple and rapid method of protein assay in solution- using optical absorption changes of citrate-stabilized Au NPs, which can be performed at room temperature and in both the native and denatured conformations of the proteins. The additional advantage of the method lies in its ability to distinguish between the native and denatured conformation of a particular enzyme/protein, in conjunction with the estimation of the amount of protein. The method relies on the interaction of the protein with citrate stabilized Au NPs leading to the changes in the absorption spectra due to the NPs. At low concentrations replacement of the citrate capping by the proteins led to broadening of the spectrum. On the other hand, at higher concentrations a second peak due to agglomeration of the NPs in the presence of protein appears which leads to further broadening of the spectrum. The method at present is applicable to pure proteins as the presence of interfering agents may lead to different results. The method is superior in comparison to conventional methods in terms of its ability to not only estimate low concentrations of protein rapidly but also distinguish the native conformations from the denatured one. The present work could lead to further understanding about the interactions between a protein and Au NPs and activity of the enzyme in the presence of the NPs, which we are currently pursuing. Finally, this simple and possibly general method may pave the way for the development of more versatile methods of protein and other biomolecule assays even *in vivo*.

References:

1. Sarikaya, M. *Proc. Natl Acad Sci. USA* **1999**, *96*, 14183.

2. Seeman, N. C.; Belcher, A. M. *Proc. Natl Acad Sci. USA* **2002**, *99*, 6452.

3. Ball, P. *Nature* **2001**, *409*, 413.

4. Hye, A.; Lynham, S.; Thambisetty, M.; Causevic, M.; Campbell, J.; Byers, H.L.; Hooper, C.; Rijsdijk, F.; Tabrizi, S. J.; Banner, S.; Shaw, C. E.; Foy, C.; Poppe, M.; Archer, N.; Hamilton, G.; Powell, J.; Brown, R. G.; Sham, P.; Ward, M.; Lovestone, S. *Brain* **2006**, *129*, 3042.

5. Hanash, S. *Nature* **2003**, *422*, 226.

6. Srinivas, P. R.; Srivastava, S.; Hanash, S.; Wright, G. L. Jr. *Clinical Chemistry* **2001**, *47(10)*, 1901.

7. Dunn, M. J. *Therapeutic Focus* **2000**, *5(2)*, 76.

8. http://www.rcsb.org

9. Shipway, A. N.; Katz, E.; Willner, I. *ChemPhysChem* **2000**, *1*, 18.

10. Portney, N. G.; Ozkan, M. *Anal Bioanal Chem*. **2006**, *384*, 620.

11. West, J. L.; Halas, N. J. *Annual Review of Biomedical Engineering* **2003**, *5*, 285.

12. Li, C. Z.; Liu, Y.; Luong, J. H. T. *Anal. Chem.* **2005**, *77(2)*, 478.

13. Jain, K. K. *Expert Rev Mol Diagn*. **2003**, *3(2)*, 153.

14. Storhoff, J. J.; Elghanian, R.; Mucic, R. C.; Mirkin, C. A.; Letsinger, R. L. *J. Am. Chem. Soc*. **1998**, *120 (9)*, 1959.

15. Hone, D. C.; Haines, A. H.; Russell, D. A. *Langmuir* **2003**, *19*, 7141.

16. Mayer, K. M.; Lee, S.; Liao, H.; Rostro, B. C.; Fuentes, A.; Scully, P. T.; Nehl, C. L.; Hafner, J. H. *ACS Nano* **2008**, *2(4)*, 687.

17. Chen, Y. M.; Yu, C. J.; Tseng, W. L. *Langmuir* **2008**, *24(7)*, 3654.

18. Casanova, D.; Giaume, D.; Moreau, M.; Martin, J. L.; Gacoin, T.; Boilot, J. P.; Alexandrou, A. *J. Am. Chem. Soc*. **2007**, *129(42)*, 12592.

19. Hirsch, L. R.; Jackson, J. B.; Lee, A.; Halas, N. J.; West, J. L. *Anal. Chem. 2003*, *7 (10)*, 2377.

20. Soman, C. P.; Giorgio, T. D. *Langmuir* **2008**, *24(8)*, 4399.

21. Mahmoud, K. A.; Hrapovic, S.; Luong, J. H. T. *ACS Nano* **2008**, *2(5)*, 1051.

22. Tsai, C. S.; Yu, T. B.; Chen, C.T. *Chem. Commun*. **2005**, 4273.

23. Bayraktar, H.; Ghosh, P. S.; Rotello, V. M.; Knapp, M. J. *Chem. Commun*. **2006**, 1390.

24. Baciu, C. L.; Becker, J.; Janshoff, A.; Sonnichsen, C. *Nano lett.* **2008**, *8(6)*, 1724.

25. Bao, J.; Chen, W.; Liu, T.; Zhu, Y.; Jin, P.; Wang, L.; Liu, J.; Wei, Y.; Li, Y. *ACS Nano* **2007**, *1(4)*, 293.

26. Chah, S.; Kumar, C. V.; Hammond, M. R.; Zare, R. N. *Anal. Chem*. **2004**, *76(7)*, 2112.

27. Chah, S.; Hammond, M. R.; Zare, R. N. *Chem. & Bio.* **2005**, *12*, 323.

28. Shang, L.; Wang, Y.; Jiang, J.; Dong, S. *Langmuir* **2007**, *23*, 2714.

29. Harrison, G.; Haffey, P.; Golub, E. E. *Anal. Biochem.* **2008**, *380(1)*, 1.

30. Moeremans, M.; Daneels, G.; Mey, J. D. *Anal. Biochem* **1985**, *145*, 315.

31. Stoscheck, C. M. *Anal. Biochem* **1987**, *160*, 301.

32. Brewer, S. H.; Glomm, W. R.; Johnson, M. C.; Knag, M. K.; Franzen, S. *Langmuir* **2005**, *21*, 9303.

33. Winkles, J.; Lunec, J.; Deverill, I. *Clinical Chemistry* **1987**, *33(5)*, 685-689.

34. Dykman, L.A.; Bogatyrev, V.A.; Khlebtsov, B.N.; Khlebtsov, N.G. *Anal. Biochem*. **2005**, *341*, 16-21.

35. Grabar, K.C.; Freeman, R.G.; Hommer, M.B.; Natan, M. J. *Anal. Chem*. **1995**, *67*, 735.

36. Frens, G. *Nat. Phys. Sci*. **1973**, *241*, 20.

37. Sanpui, P.; Pandey, S. B. ; Ghosh, S. S.; Chattopadhyay, A. *J. Colloid. Int. Sci*. **2008**, *326(1)*, 129.

38. Bradford, M. M. *Anal. Biochem*. **1976,** *72*, 248.

39. Zor, T. ; Selinger, Z. *Anal. Biochem*. **1996**, *236*, 302.

40. Mulvaney, P. *Langmuir* **1996**, *12*, 788.

41. Sato, K.; Hosokawa, K.; Maeda, M. *J. Am. Chem. Soc*. **2003**, *125*, 8102.

42. Zhao, W.; Chiuman, W.; Lam, J. C. F.; Brook, M. A.; Li, Y. *Chem. Commun*. **2007**, 3729.

43. Rangnekar, A.; Sarma, T. K.; Singh, A. K.; Deka, J.; Ramesh, A.; Chattopadhyay, A. *Langmuir* **2007**, *23(10)*, 5700.

44. Deka, J.; Paul, A.; Ramesh, A.; Chattopadhyay, A. *Langmuir*, **2008**, *24(18)*, 9945.

Chapter 5

Estimating Conformation Content of a Protein Using Citrate-Stabilized Gold Nanoparticles

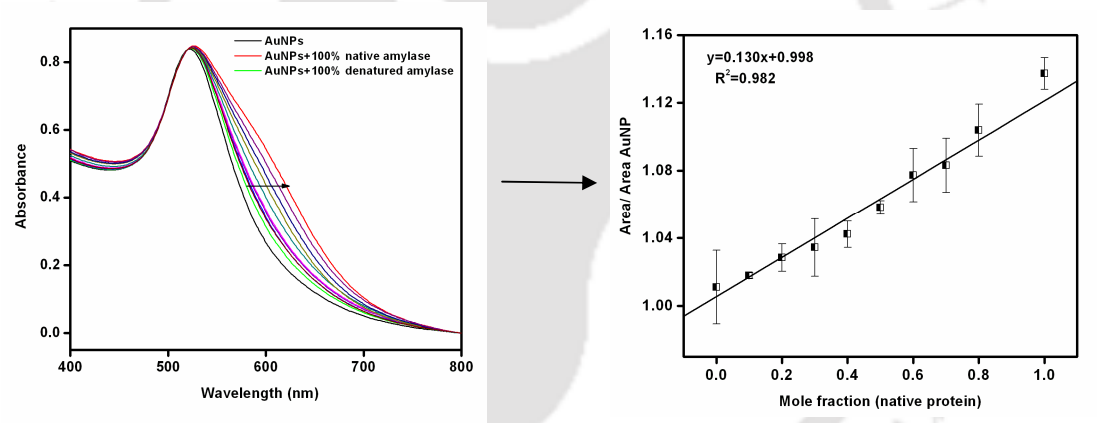

* Deka, J.; Paul, A.; Chattopadhyay, A. *Nanoscale (Communication)* **2010**, *2*, 1405–1412.

Outline:

Since the native state of a protein is crucial to its activity, a knowledge of its state (conformation) in a solution is of utmost importance in deciding the fate of its total activity, which in turn serves to keep a track of certain diseases and therefore their timely diagnosis and fast recovery. We have developed a method of estimating the amount of a protein in a solution along with the distinction of conformation based on the optical properties of citrate-stabilized gold nanoparticles (Au NPs) as discussed in chapter 4. This encouraged us to look for scope of Au NPs in developing methods which can provide the conformational content of a protein. As realized in chapter 4 the citrate-stabilized Au NPs respond differently to the presence of the two forms (native and denatured) of a same protein, it should, in principle be able to detect the amount of the conformational content (i.e. the quantity of one form, native or denatured) in a mixture of the two forms of the same protein provided the interaction of the two forms with Au NPs is independent and there is no association among them. In this chapter we discuss yet another method of estimating the conformational content of a protein in a solution, which is based on similar principles of Au NPs agglomeration in the presence of a protein as discussed in chapter 4.

5.1 Introduction:

Proteins, being ubiquitous in biological systems, have drawn considerable research attention in terms of understanding of their structures and functions. This has special relevance to diseases caused by misfolding or unfolding and consequent agglomeration of proteins. Further, use of proteins in catalyses makes the understanding of structure-function relationship crucial to chemical and biochemical industries. Fortunately, availability of a large number of crystal structures has made structure-function correlation easier.[1] However; knowledge of solution structure of the protein holds the key to the understanding of function of the molecules in solution. And it would be worthwhile if one could follow the evolution of conformation content of a protein – as it degrades, folds or unfolds in solution - in addition to understanding the folding and unfolding processes. It is interesting to observe that although there are several methods, based on nuclear magnetic resonance,[2,3] infrared spectroscopy,[4-6] differential scanning calorimetry,[7,8] near-UV circular dichroism,[3,4,9,10] fluorescence[4,11] and surface plasmon resonance[12-16] - among others - that are currently available for following the conformational changes in a protein, the estimation of conformation content in solution has somehow eluded appropriate attention.

On the other hand, there is a growing body of literature on the use of nanoscale materials for bioassays and diagnostics. For example, metal nanoparticles (NPs) especially those of gold (Au) and quantum dots have been of great use in the assay of protein[17-21] and DNA[22-26] and for observing denaturation of protein[12-16]. The general approach in probing biomolecules such as proteins and DNA using NPs has been to functionalize the NPs with specific groups that would attach specifically to target molecules, although use of unmodified Au NPs for probing DNA sequences is known.[24] The approach provides an easy way of identification and estimation of biomolecules using optical properties of the NPs. Interestingly, specificity of interactions between the probe and biomolecules has been deemed such important that non-specific interactions are considered as non-informative or of little significance. However, biomolecules such as proteins provide an opportunity to study the interaction between 'non-functionalized' citrate-stabilized Au NPs and the protein with some degree of specificity, as the (protein) molecules consist of both hydrophobic and hydrophilic groups in abundance. In addition, the conformational state of a protein could provide the required specificity in the interaction with citrate-stabilized Au NPs. In this regard, we have recently shown that optical properties of citrate-stabilized Au NPs could be used to probe concentration of protein with the distinction of its native and denatured states.[27] In other words; interactions between native and denatured states of a protein with citrate-stabilized Au NPs are of sufficient difference to be able to distinguish them in aqueous solution. Herein we had observed that interaction of proteins with citrate-stabilized Au NPs could lead to significant changes in the extinction spectrum of citrate-stabilized Au NPs, which is dependent on both the concentration of the protein and its conformation. For example, the change in the area under the UV-vis extinction spectrum of citrate-stabilized Au NPs as a result of addition of a protein solution varied linearly with the concentration of the protein. Moreover, the extent of change depended on the conformation of the protein thus providing a way of distinguishing the conformations.

Herein we report the use of citrate-stabilized Au NPs in the estimation of native and denatured fractions in a mixture of a protein. We have used α-amylase, bovine serum albumin (BSA) and amyloglucosidase (AMG) as the model proteins for the present study. For all the proteins, the changes in the area under the absorption spectrum due to citrate-stabilized Au NPs varied linearly with the mole fraction of the native (and thus

denatured) conformation. However, slopes of the graphs not only were different in magnitude but also in sign, indicating specificity of interactions not only based on conformational states but also on the nature of the protein. In addition, time-dependence of denaturation of a protein at various temperatures could be followed in terms of fraction of native (or denatured) conformations. The rate constants for denaturation indicated faster conformational changes in comparison to known rate of denaturation. The results have been explained by Mie scattering theory based on the changes in the dielectric constant of the stabilizer as a result of interaction of citrate-stabilized Au NPs with protein. In addition, significant change in the spectrum was associated with agglomeration of NPs in the presence of proteins. The observations have been exploited to develop a method for quick and easy assay of the purity of a protein in terms of its conformation content. This may be useful at least in routine laboratory analyses of known proteins using a UV-vis spectrophotometer. Our investigations also suggest that in a mixture of native and denatured proteins there may not be any associative interaction between the native protein-stabilized Au NPs and the denatured protein-stabilized Au NPs.

5.2 Materials and Methods

5.2.1 *Preparation of citrate stabilized Au NPs*

1.0 mL of 1.7262 x 10^{-2} M $HAuCl_4$ (Sigma- Aldrich Chemical Co.) was added to 40.0 mL of MilliQ grade water and then heated to boiling. Then, 1.0 mL of 0.5 M trisodium citrate 2-hydrate (E.Merck India Limited, Mumbai) solution was added to the boiling solution (all at once) and refluxed for another 30 min to ensure complete reduction of $HAuCl_4$. The solution turned deep red, indicating the formation of Au NPs.

5.2.2 *Preparation of native/denatured protein solution*

1.0 mg mL^{-1} solution of each protein, namely α-amylase (from hog pancreas, Fluka), BSA (Merck specialties private limited, Mumbai) and AMG (from Aspergillus niger, Fluka) was prepared by dissolving the respective solid proteins in phosphate buffer (of pH 7.0). However since α-amylase was only sparingly soluble, the solution obtained was further stirred for 15 min followed by centrifugation at 5000 rpm. The supernatant obtained was the 1.0 mg mL^{-1} solution. This was further diluted 10X to obtain 0.1 mg

mL^{-1} protein solution. For denaturation, a 3.0 mL portion of the 0.1 mg mL^{-1} of enzyme/protein solution, prepared as discussed above, was kept in a water bath at 70 ^{0}C for α-amylase and BSA and at 80 ^{0}C for AMG for 15 min. The solution was brought to room temperature and the volume was made up for the loss due to evaporation. The actual protein content in the as-prepared 1.0 mg mL^{-1} solution was calculated based on the standard Bradford test, which was reported in earlier studies[27] from the laboratory and the obtained values were used in the present study. The concentration of each protein expressed throughout the chapter is thus the actual protein content.

5.2.3 *Preparation of TGA-stabilized Au NPs*

600.0 mL of 1.7262 x 10^{-2} M $HAuCl_4$ (Sigma- Aldrich Chemical Co.) was added to 50.0mL of MilliQ grade water and was kept in ice water bath with constant magnetic stirring. To this solution 1.2 mL of 20.0 mM freshly prepared $NaBH_4$ (Merck specialties private limited, Mumbai) was added drop wise and with continued stirring for 2 h, after which the solution turned red, indicating formation of Au NPs. To the above solution 4.0 mL of 14.0 mM NaOH containing 120.0 mL of thioglycolic acid (Fluka) was added and stirred for another 1 h, which led to the formation of purple precipitates. The solution along with the precipitate thus formed was centrifuged at 10,000 rpm for 20 min and washed twice with ethanol (followed by centrifugation) to remove excess TGA. The pellet was then redispersed in 8.0 mL of phosphate buffer (pH = 7.0) for further experiments.

5.2.4 *UV-vis extinction spectra of citrate-stabilized Au NPs in the presence of proteins*

The citrate stabilized Au NPs solution as prepared was diluted (in phosphate buffer of pH 7.0) 2X so that the final absorbance of the solution was ~1.0 and the final pH was 7.0. 3.0 mL of the diluted Au NP solution was taken in a plastic disposable cuvette and its UV-vis spectrum was recorded (using a Hitachi U-2900 spectrophotometer). 50.0 mL of 0.1 mgmL^{-1} native protein solution was added to the Au NP, mixed well and left for 5 min followed by another wavelength scan. For preparing different mole fractions of the protein, definite amounts of native and denatured protein solutions were mixed together. 50.0 mL of the mixture thus obtained was added to 3.0 mL of Au NP solution as described before and the UV-vis spectrum was recorded before and after addition of the

protein. It may be mentioned here that in order to avoid sticking of the protein stabilized Au NPs to the walls of the cuvette, a new cuvette was used for recording of each spectrum. The ratio of the peak area of UV-vis spectrum of Au NP plus protein to that of Au NP only was calculated and plotted against the respective mole fraction of the protein.

5.2.5 *Calculation of the area under the UV-vis spectrum*

This was performed using the software associated with the data acquisition of the spectrophotometer. The area was calculated by selecting two wavelengths as end points in the absorption spectrum. The area under the graph (in between the selected points) was taken as the area value. For all the proteins, the extreme wavelengths were set at 445 and 650 nm. A typical view of such area is shown in the Appendix (Figure 4-2).

5.2.6 *Temperature dependent denaturation study of proteins*

Different test tubes with 1.0 mL solution of native α-amylase were taken and heated in a water bath at 60 ^{0}C. The test tubes were taken out at various time intervals and cooled quickly in a room temperature water bath, to have protein solutions denatured to different extents. 50.0 mL of each of this solution (as well as that of native solution) was added to 3.0 mL of citrate-stabilized Au NPs incubated for 5 min and the resultant UV-vis spectrum was recorded. The ratio of the peak area for citrate-stabilized Au NPs with protein to that of Au NP only were calculated by following the same method as already described before in the Experimental section. These area ratios were plotted against the time of denaturation. Untreated protein solution corresponds to 0 min of denaturation. This was done at 65 ^{0}C and 70 ^{0}C also. Similar experiments were performed for BSA (at 50 ^{0}C, 60 ^{0}C and 70 ^{0}C) and AMG (at 70 ^{0}C, 80 ^{0}C and 90 ^{0}C).

5.2.7 *Calculation of mole fraction of native protein in the solutions denatured for different time intervals (at a particular temperature)*

To calculate the exact mole fraction corresponding to each value of area/area of Au NP denoted in Figure 8 for α-amylase, first of all the observed area/area of Au NP values were normalized (by multiplying by a common factor) so that the value at time equal to 0 min is same as that corresponding to mole fraction equal to 1 in Figure 6(A). The

normalized values thus obtained (say y′) were used in the following equation to calculate the corresponding mole fractions: $y' = mx' + c$, where m is the slope and c the intercept of the linear fit in Figure 6(A). The x′ values are the required mole fraction values and were plotted against time in min (of denaturation) as shown in Figure 8. Similarly calculations were done for BSA and AMG.

5.2.8 *Sample preparation for TEM analysis*

Solutions containing citrate-stabilized Au NPs and those of Au NPs in the presence of 50.0 mL each of native, denatured and mixture of 50 : 50 native–denatured were drop cast onto Cu grids (5 min after protein addition and UV-vis analyses) and then left for air drying overnight. These grids were further analyzed by a Jeol 2100 TEM machine (operated at a maximum voltage of 200 kV).

5.2.9 *Fluorescence studies of proteins*

50.0 mL of 0.1 mg mL^{-1} native α-amylase was added to 3.0 mL of phosphate buffer, and the emission spectrum was recorded after setting the excitation wavelength at 280 nm (using a Perkin Elmer LS 55 Fluorescence Spectrometer). This was compared with that of 50.0 mL of 0.1 mg mL^{-1} native α-amylase in the presence of citrate-stabilized Au NPs (of dilution as used in regular experiments) after 5 min incubation. Similarly, fluorescence emission spectra for same amount of denatured α-amylase and a mixture of native and denatured α-amylase (50: 50) were recorded in presence and absence of citrate-stabilized Au NPs. Also, fluorescence spectra of native, denatured and mixed BSA and AMG were recorded in a similar fashion.

5.3 Results and Discussion

It is known that UV-vis extinction spectrum of citrate-stabilized Au NPs broadens in the presence of proteins such as α- amylase, BSA and AMG, when proteins are either in the native or denatured form.[27] Also, the area under the extinction curve changes linearly with the change in concentration of the protein (being either in native or denatured form) up until certain concentration of the protein. This limiting concentration varies from protein to protein and also between the native and denatured conformations of a particular protein. It is important to mention here that the total concentration of protein

that has been used here was decided in a way such that it falls within linear region of broadening of total area under the UV-vis curve *versus* concentration of the protein. Thus when 0.054 µg/mL of native α-amylase was added to the citrate-stabilized Au NP solution the UV-vis spectrum broadened significantly as shown in Figure 1A. Also, when the same amount of denatured protein was added to the Au NP solution, broadening could also be observed. However, broadening was much less when denatured protein was added in comparison to the addition of same amount of native protein. Now, when a mixture of native and denatured protein was added by systematically varying their ratio, intermediate broadening was observed. In brief, systematic broadening of Au NP UV-vis extinction spectrum was observed in the presence of various ratio of native and denatured α-amylase when the total concentration of protein was kept constant.

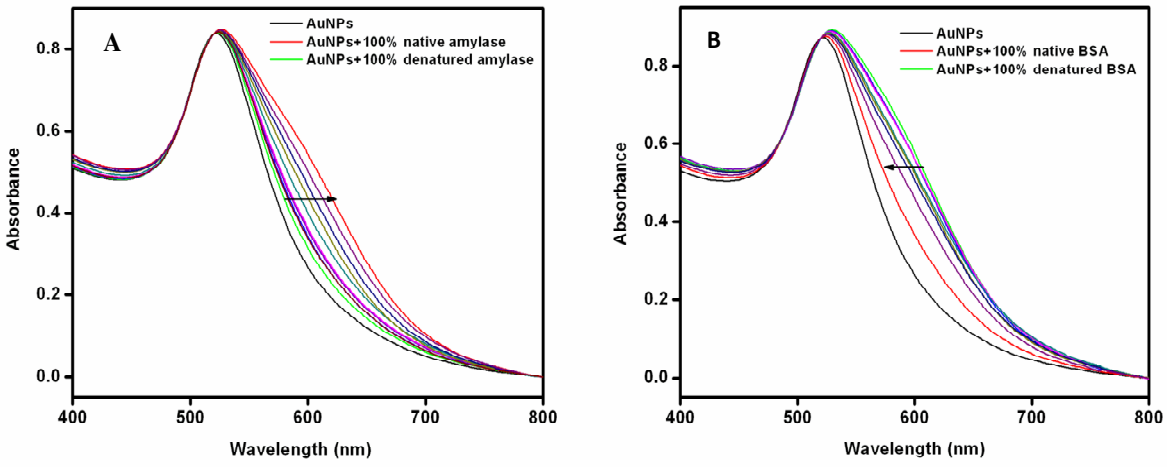

Figure 1. *UV-vis spectra of citrate-stabilized Au NPs before and after addition of protein solution with increasing mole fraction of the native form of* ***(A)*** *α-amylase and* ***(B)*** *BSA. The arrows in the figures show the increasing mole fraction of the native form.*

Similar broadening of spectrum was observed in the presence of 1.64 µg/mL native or denatured form of BSA (Figure 1B). However, here broadening was more in the presence of denatured protein than the native conformation at the same concentration. Intermediate broadening of the spectrum was observed in the presence of a mixture of native and denatured form as is clear from Figure 1B. When the experiments were carried out with 0.125 µg/mL native or denatured form of AMG the results were similar to those of BSA. The details of the results (involving AMG) are shown in Figure 2.

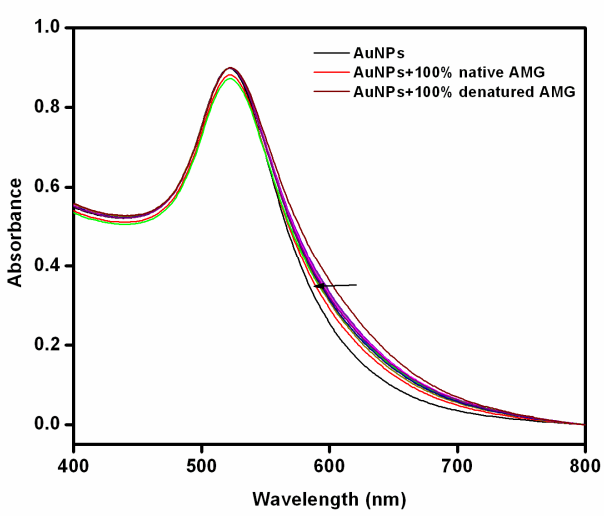

Figure 2. *UV-vis extinction spectra of citrate-stabilized Au NPs before and after addition of protein solution with increasing mole fraction of the native form of AMG. The arrows in the figures show the increasing mole fraction content of the native form.*

Essentially, broadening of the UV-vis extinction spectrum of citrate stabilized Au NPs could be observed in the presence of a mixture of native and denatured forms of a protein under study, where the variation of the ratio of the concentrations of the conformations led to discernable difference in the broadening of the spectrum. This formed the basis for finding the ratio of native and denatured conformations of a protein present in aqueous solution. Further, it is important to mention here that when similar experiments were carried out with thioglycolic acid (TGA) stabilized Au NPs, no UV-vis spectral broadening was observed in the presence of α-amylase (Figure 3), indicating specificity of interaction of protein with citrate-stabilized Au NPs.

That the change in the UV-vis extinction spectrum of citrate-stabilized Au NPs upon addition of native and denatured proteins was due to interaction of the stabilized NPs with the protein, was further substantiated by photoluminescence studies. It has been established that citrate-stabilized Au NPs quench efficiently the fluorescence from fluorophores, especially proteins.[28] In this regard, the decrease in fluorescence emission at ca. 365 nm owing to tryptophan (trp) residue in the protein acts as a marker of interaction between the citrate-stabilized Au NPs and the protein. In the present set of experiments when native, denatured or a mixture of the two forms of protein was incubated with citrate-stabilized Au NPs in buffer solutions, the fluorescence emission at

ca. 365 nm disappeared completely. The excitation wavelength was kept at 280 nm. The results for α-amylase, BSA and AMG are shown in Figure 4(A-C). As is clear from the Figures, in all cases the disappearance of the emission peak (at the total protein concentrations that were used in the UV-vis extinction studies and at the Au NP concentration that was used in each measurement) supported that indeed the proteins were attached to the citrate-stabilized Au NPs present in the medium. Also, it is important to note here that complete disappearance of the peak at 365 nm due to a mixture of native and denatured forms (0.5mole fractions) suggests that both forms of protein were completely attached to the NPs. Further, the fluorescence spectrum of native α-amylase in the presence of TGA-stabilized Au NPs was recorded to check whether the protein interacts with such Au NPs. The result is shown in the Figure 4D which demonstrated quenching of the fluorescence emission of α-amylase in presence of TGA-stabilized Au NPs. The quenching of fluorescence suggests that there is interaction between the protein molecules and the TGA-stabilized NPs. In addition, as mentioned earlier the UV-vis spectrum of TGA-stabilized NPs exhibited no discernible broadening in the presence of the protein (α-amylase).

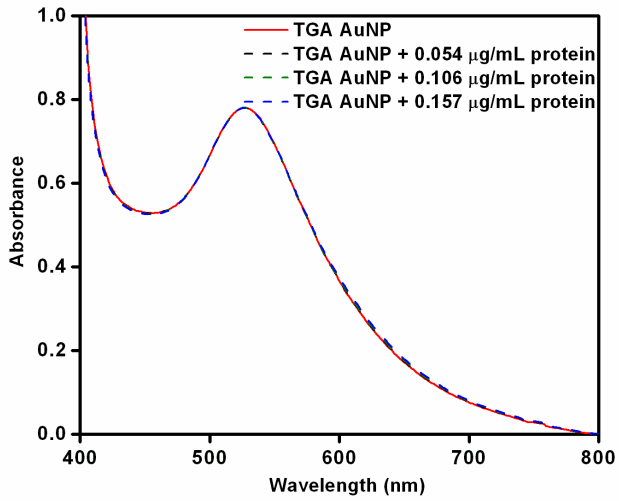

Figure 3. *UV-vis extinction spectra of TGA stabilized Au NPs before and after addition of increasing amount of native α-amylase solution.*

These mean that interaction of protein with citrate-stabilized Au NPs is different from that with TGA-stabilized Au NPs. It is plausible that citrate, being electrostatically

attached to the Au NPs, could be amenable to partial (if not complete) replacement by the protein molecules, leading to agglomeration of the NPs. On the other hand TGA, being covalently bound to Au NPs through the S–Au bond, could not be replaced, even though the protein molecules interact with the TGA-stabilized Au NPs thus showing no signs of agglomeration of the NPs. Further, a recent study by Brewer et al.[29] suggests that BSA molecules bind to the citrate-stabilized Au NPs predominantly by an electrostatic mechanism, which involves salt-bridges, for example, of the carboxylate ammonium type, between the citrate and the lysine on the protein surface and displacement of citrate by the protein molecule could not be supported by their studies.

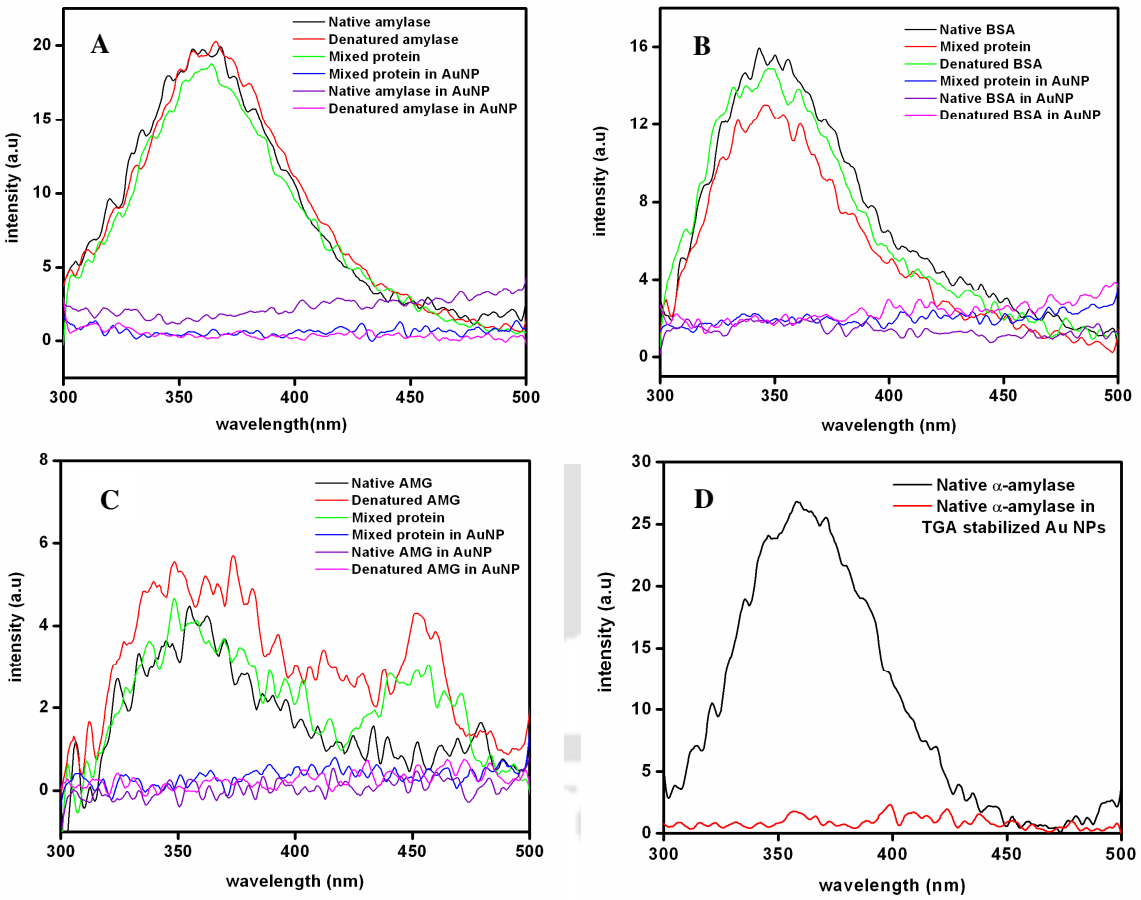

Figure 4. *Fluorescence spectra of various compositions of* ***(A)*** *α-amylase* ***(B)*** *BSA and* ***(C)*** *AMG, in the presence and absence of citrate-stabilized Au NPs.* ***(D)*** *Fluorescence spectra of native α-amylase in presence and absence of TGA-stabilized Au NPs.*

In order to further probe the interaction between the proteins and citrate-stabilized Au NPs, TEM measurements were performed with samples prepared using α-amylase. We have earlier observed that the native form of α-amylase—beyond a certain concentration—leads to substantial aggregation of citrate-stabilized Au NPs.[27] On the other hand, the denatured form of the protein does not lead to agglomeration of the NPs. Herein, TEM measurements were performed with samples evaporated on grids consisting of citrate-stabilized Au NPs only, citrate-stabilized Au NPs in the presence of native α-amylase, denatured α-amylase and a mixture of a 0.5 mole fraction of each native and denatured protein. The images are shown in Figure 5(A–D). As is evident from the Figures, the NPs in the presence of native protein exhibited maximum agglomeration (Figure 5B), whereas those in the presence of denatured α-amylase had the minimum agglomeration of NPs (Figure 5D). On the other hand, in the presence of 50% of either of native and denatured proteins (Figure 5C), the level of agglomeration was roughly in between the two.

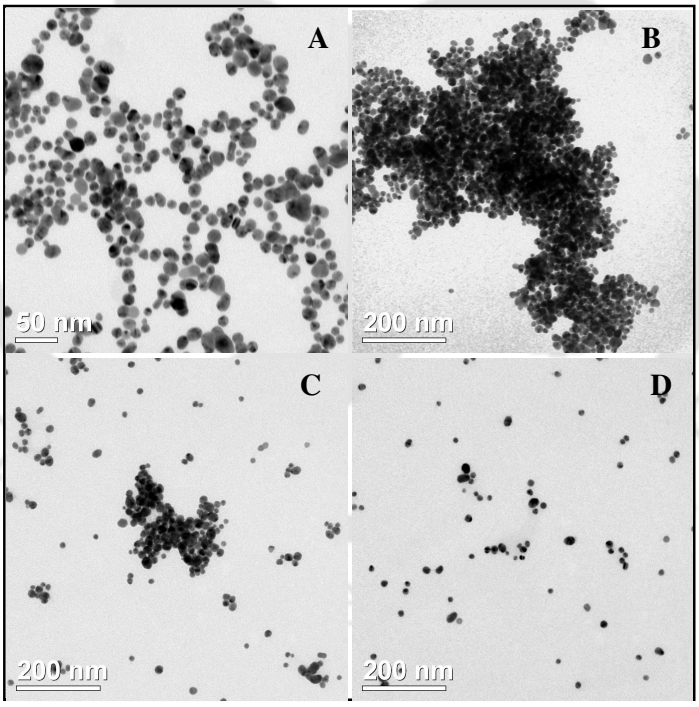

Figure 5. *Transmission electron microscopic images of* ***(A)*** *citrate-stabilized Au NPs,* ***(B)*** *citrate-stabilized Au NPs in the presence of native protein (α-amylase) only,* ***(C)*** *citrate-stabilized Au NPs in the presence of 50% native and 50% denatured protein mixture and* ***(D)*** *citrate-stabilized Au NPs in the presence of 100% denatured protein. The total concentration of protein in all the samples was the same.*

In other words, in the presence of a 0.5 mole fraction content in the mixture there was agglomeration of the NPs; however, the NPs were not substantially agglomerated like those in the presence of only native form at the same total protein concentration. There was substantial presence of unagglomerated NPs. What is interesting here is that the level of agglomeration was dependent on the conformation of the proteins, which possibly led to a differential broadening of UV-vis extinction spectrum of citrate-stabilized Au NPs. Essentially, the extent of agglomeration varied with the mole fraction of the native (or denatured) protein and this helped make the UV-vis spectral broadening a quantitative measure of the conformation content of the protein in a mixture.

The extinction of light by a colloidal Au NP solution with N particles per unit volume could be expressed as,[30]

$$A = \log_{10}\frac{I_o}{I} = \frac{NQ_{ext}l}{2.303} \qquad (1)$$

Here, I_0 and I are the intensities of incident and transmitted light, l is the path length and Q_{ext} is the extinction coefficient of a single NP. Using Mie scattering theory of small spherical metal particles, the extinction coefficient can be written as,[30]

$$Q_{ext}(\lambda) = \frac{24\pi^2 R^3 \varepsilon_m^{3/2}}{\lambda}\frac{\varepsilon''}{(\varepsilon'+2\varepsilon_m)^2+\varepsilon''^2} \qquad (2)$$

Here, R is the radius of the NP, λ is the wavelength of the light, ε_m is the dielectric function of the medium. On the other hand, ε' and ε'' are the real and imaginary parts of frequency dependent dielectric function (ε) of the NP ($\varepsilon = \varepsilon' + i\varepsilon''$). In case of the particle being coated by a layer of organic or inorganic moiety having a different dielectric constant, the extinction coefficient is then written as,[14,30]

$$Q_{ext}(\lambda) = \frac{8\pi^2 R^3 (\varepsilon_m)^{1/2}}{\lambda}\mathrm{Im}\left\{\frac{(\varepsilon_2-\varepsilon_m)(\varepsilon_1+2\varepsilon_2)+(1-g)(\varepsilon_1-\varepsilon_2)(\varepsilon_m+2\varepsilon_2)}{(\varepsilon_2+2\varepsilon_m)(\varepsilon_1+2\varepsilon_2)+(1-g)(\varepsilon_1-\varepsilon_2)(2\varepsilon_2-2\varepsilon_m)}\right\} \qquad (3)$$

Here, ε_1 and ε_2 are the complex dielectric functions of the particle core and the surface coating, whereas g is the volume fraction occupied by the surface coating. Therefore, the extinction of light would also be varying systematically provided the stabilizer constituting the surface coating of the NP is changed consistently. This could occur in two ways. Firstly, addition of protein to citrate-stabilized Au NPs could result into gradual changes in the constitution of the stabilizing layer of the NPs. At higher concentrations of the protein there could possibly be agglomeration of the protein-NP composite, thereby further changing the dielectric environment of the NP (and hence the extinction of light). Secondly, if the stabilizing layer consists of proteins in denatured or native conformation then there would be significant difference in the extinction coefficient even at the same total concentration of the protein. It has been established that there is a linear relationship between the concentration of the protein and the extinction of light due to citrate-stabilized Au NPs (in the presence of protein in either of native and denatured states).[27] Thus in the linear regime, the changes in the extinction spectrum would be additive and would linearly depend on the mole fraction of the native or the denatured form when a mixture of the two forms is present. In other words, area under the extinction spectrum (related to oscillator strength) would vary linearly with the mole fraction of the native form (or denatured form) at a fixed total protein concentration. This would be the case provided there is no associative interaction between the proteins (native and denatured conformations) stabilizing citrate-stabilized Au NPs, that would have otherwise given rise to non-linear changes. Thus in the presence of protein with two different forms, citrate-stabilized Au NPs would have extinction of light due to contributions from only citrate-stabilized Au NPs, native form of protein attached to citrate-stabilized Au NPs and denatured form of protein attached to citrate-stabilized Au NPs. Then the total area under the extinction spectrum, at fixed total Au NP and protein concentrations, could be written as follows.

$$\int A(\lambda)d\lambda = x_{NP}\int A_{NP}(\lambda)d\lambda + x_N\int A_N(\lambda)d\lambda + x_D\int A_D(\lambda)d\lambda \qquad (4)$$

Here, $A(\lambda)$ is the wavelength-dependent extinction of light by citrate-stabilized Au NPs in the presence of protein, $A_{NP}(\lambda)$ is the wavelength-dependent extinction of light by citrate-stabilized Au NPs, $A_N(\lambda)$ is the wavelength-dependent extinction of light by native protein attached to citrate-stabilized Au NPs and $A_D(\lambda)$ is the wavelength-

dependent extinction of light by completely denatured protein attached to citrate-stabilized Au NPs. Also, x_N and x_D are the mole fractions of native protein and denatured protein respectively. It is important to mention here that $x_N + x_D = 1$. Here x_{NP} is an empirical dimensionless parameter associated with the contribution of citrate-stabilized Au NPs in the overall extinction of light (in the presence of protein). In the absence of protein x_{NP}=1 and when all the NPs are stabilized by protein then x_{NP}=0. One can rewrite the equation as

$$\int A(\lambda)d\lambda = x_{NP}\int A_{NP}(\lambda)d\lambda + x_N\int A_N(\lambda)d\lambda + (1-x_N)\int A_D(\lambda)d\lambda \quad (5)$$

$$\text{Or } \int A(\lambda)d\lambda = x_{NP}\int A_{NP}(\lambda)d\lambda + \int A_D(\lambda)d\lambda + x_N\left\{\int A_N(\lambda)d\lambda - \int A_D(\lambda)d\lambda\right\} \quad (6)$$

Now, there would be variations of size of NPs and its distributions in different sets of preparations, which will be reflected in the extinction spectra. Thus the total area under the curve would vary from sample to sample. If the variation is sufficiently small then the associated changes could be accommodated by dividing both sides of the equation (6) by $\int A_{NP}(\lambda)d\lambda$. The resultant equation could be expressed as below.

$$\frac{\int A(\lambda)d\lambda}{\int A_{NP}(\lambda)d\lambda} = x_{NP} + \frac{\int A_D(\lambda)d\lambda}{\int A_{NP}(\lambda)d\lambda} + x_N\frac{\left\{\int A_N(\lambda)d\lambda - \int A_D(\lambda)d\lambda\right\}}{\int A_{NP}(\lambda)d\lambda} \quad (7)$$

The ratio of the areas in the left hand side of equation (7) will henceforth be called as the normalized area. Thus if there is no associative interaction between the native and denatured protein attached to citrate-stabilized Au NPs then the normalized area under the extinction curve ought to vary linearly with the mole fraction of the native (or denatured) content in the protein mixture. This is because at the highest concentration of either of native and denatured proteins (used here) both $\int A_N(\lambda)d\lambda$ and $\int A_D(\lambda)d\lambda$ would have constant values, in addition to $\int A_{NP}(\lambda)d\lambda$ being constant. In order to probe this, the normalized area of each of the graphs obtained after addition of different mole fractions of each protein was calculated and plotted against the mole fraction content of the native form. The results corresponding to the normalized areas under the extinction graphs of citrate-stabilized Au NPs obtained after addition of different mole fractions of α-amylase are shown in Figure 6A. The extinction curves used here correspond to those in Figure 1A. Also shown in Figure 6B is the same normalized area plots calculated from

the extinction graphs, obtained in the presence of different mole fractions of BSA, corresponding to those in Figure 1B. It is interesting to note from both the Figures that the normalized area changed linearly with the mole fraction of native (and hence denatured) form of the proteins. Similar results were obtained with AMG, as shown in Figure 7.

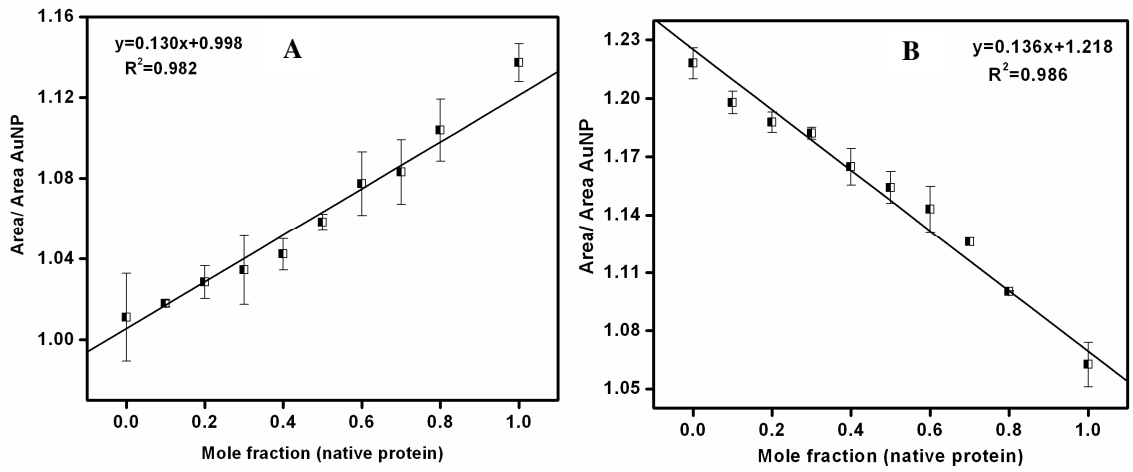

Figure 6. *Ratio of the area under the UV-vis spectrum of citrate-stabilized Au NPs in presence of α-amylase to that of citrate-stabilized Au NPs only for different composition of native:denatured protein for* ***(A)*** *α-amylase (the enzyme being denatured at 70 ^{0}C).* ***(B)*** *BSA (the enzyme being denatured at 70 ^{0}C). The data shown are the mean of three sets.*

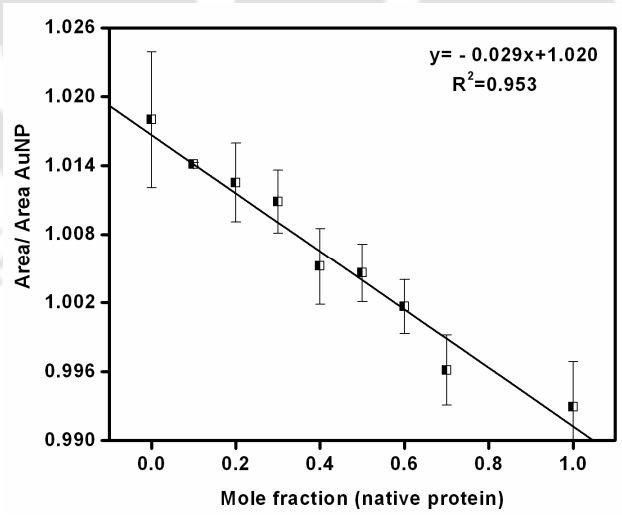

Figure 7. *Ratio of the area under the UV-vis spectrum of citrate-stabilized Au NPs in presence of AMG to that of citrate-stabilized Au NPs (only) for different composition of native:denatured AMG (the enzyme being denatured at 80 ^{0}C). The data shown are the mean of three sets.*

The linearity of the relationship between the normalized area and mole fraction content of the protein helps establish the present method of estimation of concentration of native and denatured proteins in a mixture of the two as a sound one. It also indicates that in a mixture of the native and denatured forms of a protein there is possibly no associative interaction between the two forms – at least for the proteins under investigation. However, there is an interesting and significant difference between the two—i.e. the slope of the graph in the presence of α-amylase is positive whereas that in the presence of BSA is negative. The different values of the slopes (0.131 for α-amylase and -0.137 for BSA) along with the sign demonstrate that interaction between citrate-stabilized Au NPs and protein is specific to the protein and sensitive to its conformation. The difference in the slopes could be attributed to the difference in the extent of broadening by the native and denatured states of a protein. For the case of α-amylase the broadening is greater in the presence of the native form than that in the presence of denatured form at the same concentration of the protein. Hence the slope would be positive. On the other hand, broadening is greater in the presence of denatured form of BSA in the comparison to that in the presence of native form. Hence the slope is negative.

A desirable consequence of the present method of estimation of the fractional content of the native (or denatured) form of a protein would be to be able to follow time-dependent denaturation of a protein at a particular temperature. This was pursued by first keeping several samples of the native protein solution at a designated temperature, followed by withdrawal of the samples at certain intervals of time and then quickly cooling to room temperature. A portion of the sample was then added to the citrate-stabilized Au NP solution and UV-vis spectrum of the mixture was then recorded. The results of time-dependent changes in normalized area under the Au NP extinction graphs, after addition of α-amylase to citrate-stabilized Au NPs that were kept at 60 ^{0}C, 65 ^{0}C and 70 ^{0}C respectively, are shown in Figure 8(A–C). As is clear from the Figures, the normalized areas for all the samples decreased with time and the major decrease in the normalized area occurred for samples kept for 4 min at all three temperatures. It is known from the experiments reported above that the denatured form of α-amylase broadens the extinction curve of Au NP less than that by the native form. Thus the decrease in the area under the extinction curve could be considered to be associated with the denaturation of the protein α-amylase.

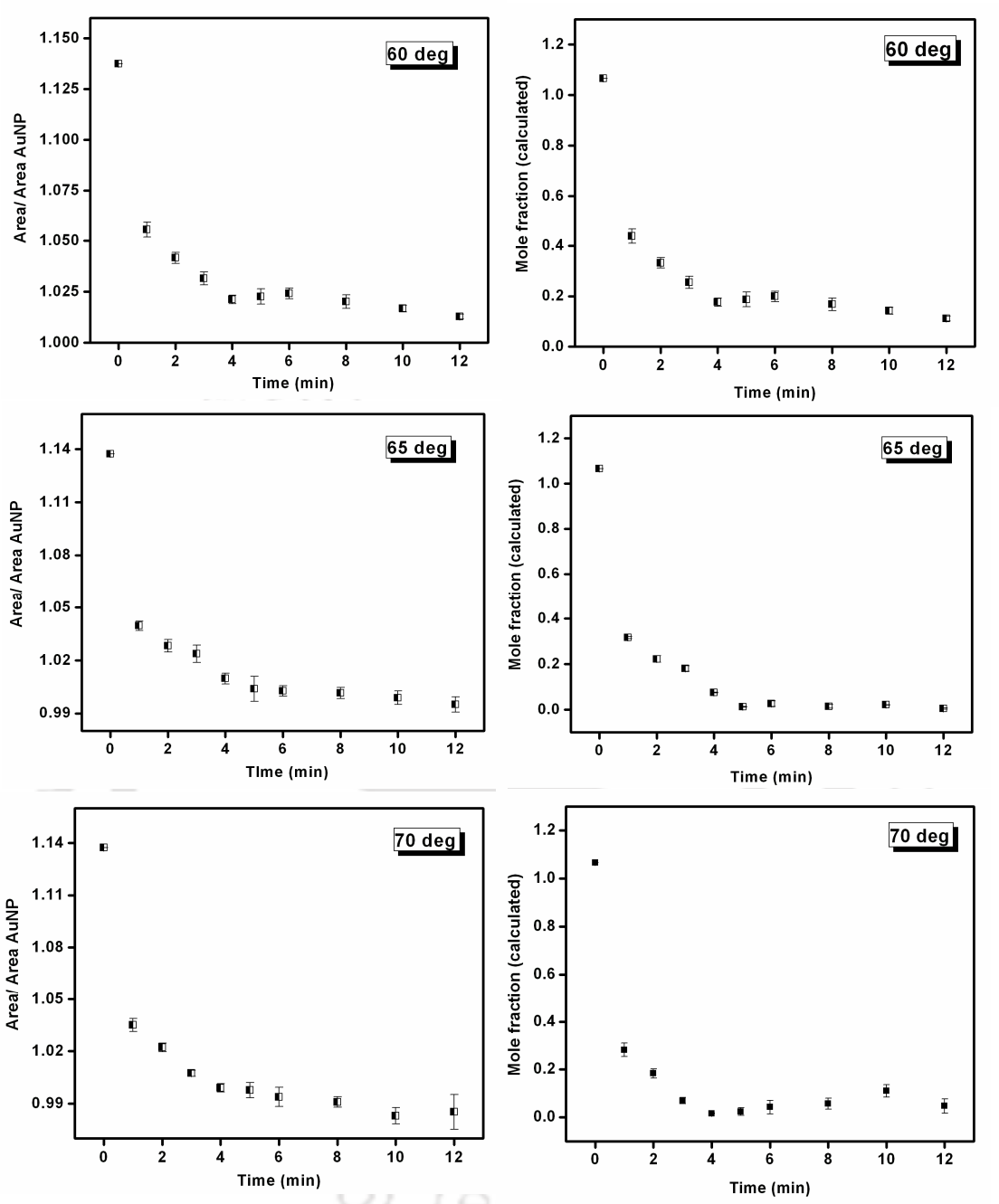

Figure 8. ***(A-C)*** *Ratio of the area of UV-vis spectrum of solution of α-amylase (0.05 mL of 0.054 μg/mL) in 3 mL citrate-stabilized Au NPs solution to that of only citrate-stabilized Au NPs plotted against the time of denaturation.* ***(D-F)*** *Time–dependent changes in the mole fraction of native protein of α-amylase denatured at different temperatures. The legend shows the temperature at which the protein* solution was *thermally heated for denaturation. The mole fractions in D-F, corresponding to area ratio of A-C, were calculated from the area of the Au NP peaks based on data in Figure 6A. The data shown are the mean of three sets.*

Hence, denaturation—if at all—was nearly complete by 4 min, when the protein was heated at the above temperatures. However, if one looks closely at the Figures one would observe that the area under the graph at saturation (after 12 min of heating) for protein treated at 60 ^{0}C was higher than those treated at 65 ^{0}C and 70 ^{0}C. For example, the normalized area for the sample treated at 60 ^{0}C was 1.01 at 12 min of heating, whereas that was 0.99 and 0.98 for the samples treated at 65 ^{0}C and 70 ^{0}C respectively. The results indicate that heating α-amylase at 60 ^{0}C for 12 min may not lead to complete denaturation of the protein. In order to have a clearer picture, the time-dependences of the normalized area under the graphs were converted into a mole fraction of the native protein content and then plotted against time. It is important to mention here that the mole fractions were calculated by using the slope in the graph in Figure 6A, in conjunction with eqn (7) and results in Figure 8(A–C). The results for the α-amylase treated at the above three temperatures are shown in Figure 8(D–F). It is interesting to observe that the protein treated at 60 ^{0}C did not denature completely, even after 12 min; with a value of mole fraction equivalent to 0.1 it appeared to have remained in the native form. On the other hand, when the protein was heated to 65 ^{0}C or 70 ^{0}C, complete denaturation occurred in about 4 min. Since the measurements were made at room temperature after being cooled from 60 ^{0}C, it is plausible that the results indicate that heating the protein at 60 ^{0}C and then cooling to room temperature may lead to partial regeneration of the original structure. On the other hand, heating α-amylase at 65 ^{0}C or higher temperatures did not lead to reversion to the original native structure of the protein. Similar observations have been made by others with respect to denaturation of BSA probed using circular dichroism spectroscopy and the primary conclusion has been that structural changes are partially reversible for BSA upon heating to 65 ^{0}C.[9] It could also be possible that the protein (α-amylase) when denatured at 60 ^{0}C, followed by cooling to room temperature, reached a conformation different from complete denaturation occurring at 70 ^{0}C and thus resulting in different area of the extinction spectrum. However, the results reported herein clearly indicate the possibility of a simple yet powerful method of quantitative estimation of structural changes that occur in the protein upon heating. The results with respect to heating of BSA at 50 ^{0}C, 60 ^{0}C and 70 ^{0}C indicated that the protein was completely denatured at 70 ^{0}C. On the other hand, partial denaturation occurred with samples heated at 50 ^{0}C and 60 ^{0}C, with the extent of denaturation higher for the sample heated at 60 ^{0}C than the same being heated at 50 ^{0}C.

The details of the results are shown in the Figure 9. The results corresponding to AMG were similar to those of BSA and are shown in the Figure 10.

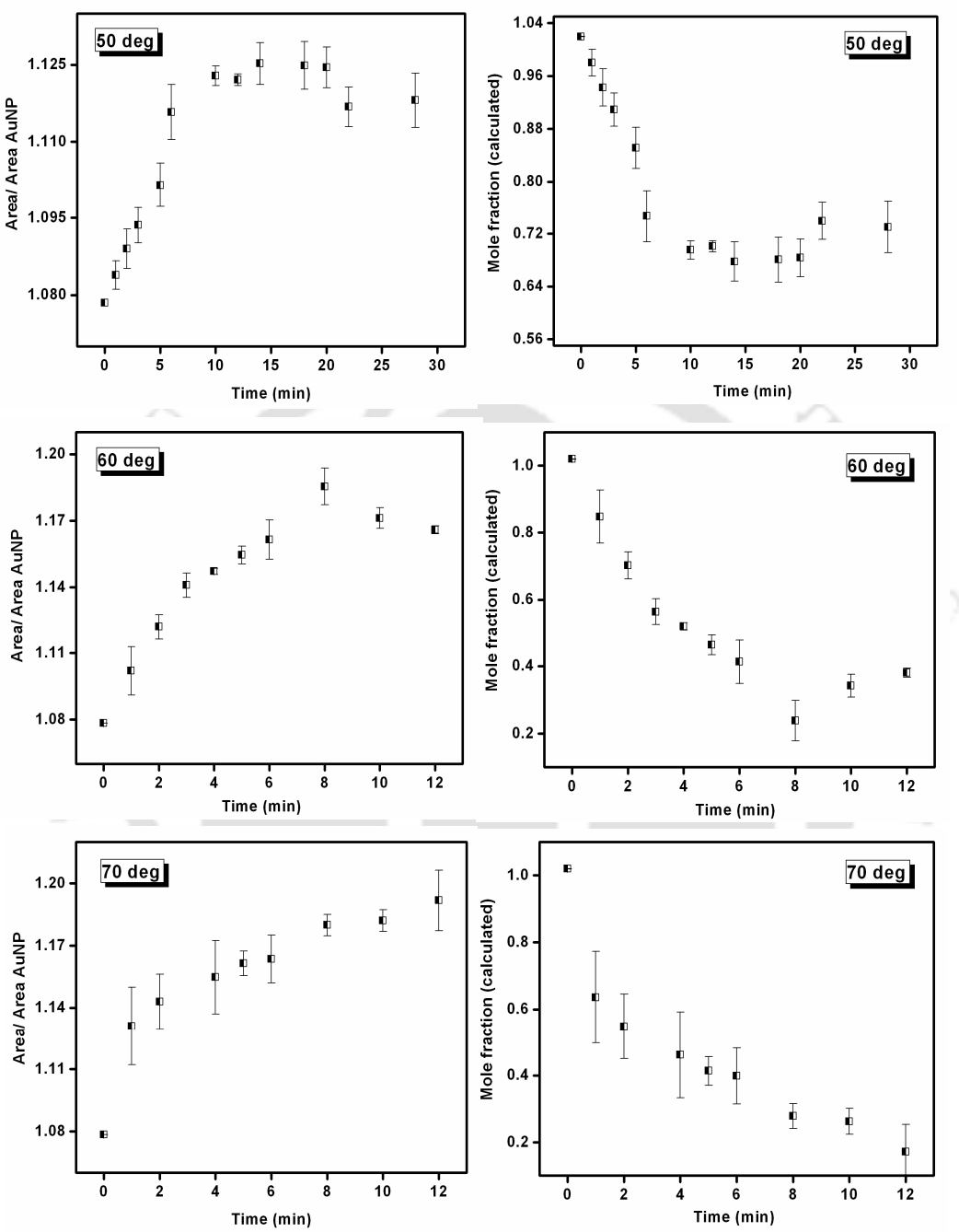

Figure 9. ***(A-C)*** *Ratio of the area of UV-vis spectrum of solution of BSA (0.05 mL of 1.64 μg/mL) in 3 mL citrate-stabilized Au NPs solution to that of only citrate-stabilized Au NPs plotted against the time for denaturation.* ***(D-F)*** *Time–dependent changes in the mole fraction of native protein of BSA denatured at different temperatures. The legends show the temperature at which the protein solution was thermally heated for denaturation. The mole fractions in D-F correspond to area ratios in A-C and were calculated from the area of the Au NP peaks based on data in Figure 6B. The data shown are the mean of three sets.*

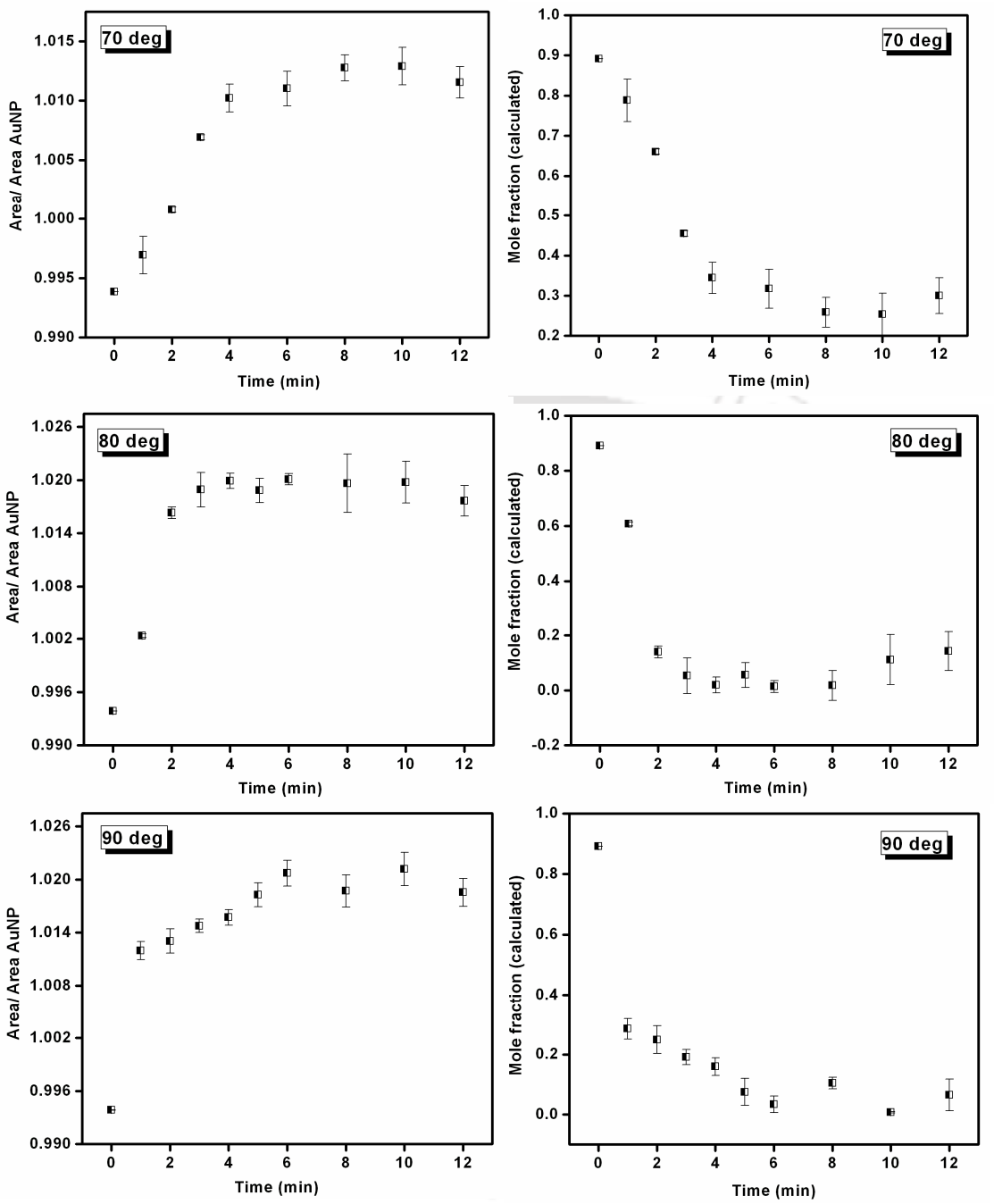

Figure 10. ***(A-C)*** *Ratio of the area of UV-vis spectrum of solution of AMG (0.05 mL of 0.125 μg/mL) in 3 mL citrate-stabilized Au NPs solution to that of only citrate-stabilized Au NPs plotted against the time of denaturation.* ***(D-F)*** *Time–dependent changes in the mole fraction of native protein of AMG denatured at different temperatures. The legend shows the temperature at which the protein solution was thermally heated for denaturation. The mole fractions in D-F correspond to area ratios in A-C and were calculated from the area of the Au NP peaks based on data in Figure 7. The data shown are the mean of three sets.*

Further, in order to obtain rate constants for denaturation of the proteins the mole fraction versus time plots were fitted to single exponentials (the data fits are shown in the Appendix, Figure 5-1 to 5-3). The rate constants for α-amylase were found to be 60.9 ± 2.79 h^{-1}, 62.40 ± 1.98 h^{-1} and 82.74 ± 9.66 h^{-1} at heating temperatures of 60 ^{0}C, 65 ^{0}C and 70 ^{0}C respectively. The results indicate that the rate of denaturation increased with temperature. On the other hand, the values of rate constants at all temperatures were an order of magnitude higher than those reported in the literature.[31] For example, denaturation of α-amylase (from *Bacillus licheniformis*) studied at 60 ^{0}C, 65 ^{0}C and 70 ^{0}C has been reported to have two rate constants with the values of the first rate constants (higher than the second ones) to be 6.2 h^{-1} 6.3 h^{-1} and 15.7 h^{-1} respectively. Similar results were obtained for studies with BSA and AMG. The results are shown in Table 1. The apparent higher values of the rate constants observed in the present experiments could be rationalized as follows. The literature studies primarily report the actual denaturation of protein as followed by activity studies, although there are some reports where experiments were performed spectroscopically in the presence of a dye molecule.

Table 1. *Rate constants for temperature-dependent denaturation of α-amylase, BSA and AMG and their comparison to literature values. All the three proteins in the present study and α-amylase in reported literature[31] were denatured at pH = 7.0; however BSA in the reported literature[32] was denatured at pH = 5.5 and AMG at pH = 4.5.[33]*

Name of the Protein	Temp. (^{o}C)	Rate constant (k, in h^{-1})		
		Present study value	Literature Value	
		k_1	k_1	k_2
α-amylase	60	60.90	6.23	0.482
	65	62.40	6.37	0.349
	70	82.74	15.66	0.666
BSA	50	10.80	-------	-------
	60	20.94	0.123	-------
	70	32.70	1.957	-------
AMG	70	20.64	0.871	-------
	80	42.78	-------	-------
	90	63.72	-------	-------

On the other hand, the present studies may indicate initial changes in conformations of the protein resulting in changes in the UV-vis spectrum of citrate-stabilized Au NPs, which is very sensitive to the conformations of the stabilizing protein.[14] In other words, initial rapid changes in conformation of a protein at an elevated temperature, which does not necessarily lead to complete loss of activity of the protein, may also contribute to the changes in the extinction, in addition to actual denaturation. Thus the increase in apparent rate constants for denaturation of the protein observed here. In short, the present method not only captures the denaturation of a protein but also possibly change in conformation which ultimately leads to thermal denaturation of a protein. Further, in order to account for the rate constants one must consider that source of protein and pH of the medium also contribute to difference in the observed rate constants of denaturation of a protein at elevated temperatures.

5.4 Summary

In brief, the method reported herein takes advantage of the changes in the UV-vis extinction spectrum of citrate-stabilized Au NPs in order to estimate the fractional content of native (or denatured) proteins in aqueous solution. The fundamental observation is that the area under the extinction curve of citrate-stabilized Au NPs broadened in the presence of the protein and the extent of broadening depended linearly on the fractional content of native or denatured form of a protein thus providing a simple method of estimation. The origin of the changes has been ascribed to the differential agglomeration of citrate-stabilized Au NPs in the presence of protein with a fractional difference in conformation. Further, the linear dependence of the area under the extinction graphs on the fractional content of the protein (in a particular conformational state) supported that there was no associative interactions between a native protein attached to citrate-stabilized-Au-NPs and a denatured protein attached to citrate-stabilized-Au-NPs. In addition, the method provided a new way of probing time-dependent denaturation of a protein at various temperatures, with the knowledge of the fractional content of the conformation. This simple yet quantitative measure of the purity of a protein is expected to find use in routine laboratory analyses at least for tests of purity, in comparison to classical tests such as those involving activity tests of a protein. Although we have reported the results of studies with three proteins, it would be

worthwhile to establish the generality of the procedure by extending the studies to involve a large number of proteins. In addition, the specificity of the interactions between the citrate-stabilized Au NPs and different proteins with specific conformations may provoke studies leading to a newer understanding of the interaction between citrate-stabilized Au NPs and proteins.

References:

1. http://www.rcsb.org
2. Lundqvist, M.; Sethson, I.; Jonsson, B. H. *Langmuir* **2004**, *20* (24), 10639.
3. Tsai, A. M.; van Zanten, J. H.; Betenbaugh, M. J. *Biotech. Bioeng*. **1998**, *59* (3), 273.
4. Wu, X.; Narsimhan, G. *Langmuir* **2008**, *24* (9), 4989.
5. Filosa, A.; Wang, Y.; Ismail, A. A.; English, A. M. *Biochemistry* **2001**, *40* (28), 8256.
6. Anderle, G.; Mendelsohn, R. *Biophys. J*. **1987**, *52*, 69.
7. Sanchez-Ruiz, J. M.; Lopez-Lacomba, J. L.; Cortijo, M.; Mateo, P. L. *Biochemistry* **1988**, *27* (5), 1648.
8. Teichroeb, J. H.; Forresta, J. A.; Jones, L. W. *Eur. Phys. J. E*. **2008,** 26, 411.
9. Takeda, K.; Wada, A.; Yamamoto, K.; Moriyama, Y.; Aoki, K. *J. Protein Chem.* **1989**, *8* (5), 653.
10. Celej, M. S.; Montich, G. G.; Fidelio, G. D. *Protein Science* **2003**, *12*, 1496.
11. Cohen, B. E.; Pralle, A.; Yao, X.; Swaminath, G.; Gandhi, C. S.; Jan, Y. N.; Kobilka, B. K.; Isacoff, E. Y.; Jan, L. Y. *PNAS* **2005**, *102* (4), 965.
12. Mannen, T.; Yamaguchi, S.; Honda, J.; Sugimoto, S.; Kitayama, A.; Nagamune, T. *Anal Biochem.* **2001**, 293, 185.
13. Chah, S.; Kumar, C. V.; Hammond, M. R.; Zare, R. N. *Anal. Chem*. **2004**, *76* (7), 2112.
14. Chah, S.; Hammond, M. R.; Zare, R. N. *Chem. Biol*. **2005**, 12, 323.
15. Teichroeb, J. H.; Forresta, J. A.; Ngai, V.; Jones, L. W. *Eur. Phys. J. E*. **2006,** *21*, 19.
16. Wang, F.; Wang, J.; Liu, X.; Dong, S. *Talanta* **2008**, 77, 628.
17. Chen, Y. M.; Yu, C. J.; Tseng, W. L. *Langmuir* **2008**, *24* (7), 3654.
18. Casanova, D.; Giaume, D.; Moreau, M.; Martin, J. L.; Gacoin, T.; Boilot, J. P.; Alexandrou, A. *J. Am. Chem. Soc*. **2007**, *129* (42), 12592.
19. Hirsch, L. R.; Jackson, J. B.; Lee, A.; Halas, N. J.; West, J. L. *Anal. Chem*. **2003**, *7* (10), 2377.
20. Soman, C. P.; Giorgio, T. D. *Langmuir* **2008**, *24* (8), 4399.
21. Mahmoud, K. A.; Hrapovic, S.; Luong, J. H. T. *ACS Nano* **2008**, *2* (5), 1051.

22. Elghanian, R.; Storhoff, J. J.; Mucic, R. C.; Letsinger, R. L.; Mirkin, C. A. *Science* **1997**, *277*, 1078.
23. Wang, J.; Liu, G.; Merkoci, A. *J. Am. Chem. Soc.* **2003**, *125*, 3214.
24. Li, H.; Rothberg, L. *PNAS* **2004,** *101* (39), 14036.
25. Park, S. J.; Taton, T. A.; Mirkin, C. A. *Science* **2002**, *295*, 1503.
26. Storhoff, J. J.; Elghanian, R.; Mucic, R. C.; Mirkin, C. A.; Letsinger, R. L. *J. Am. Chem. Soc*. **1998**, *120*, 1959.
27. Deka, J.; Paul, A.; Chattopadhyay , A. *J. Phys. Chem. C*, **2009**, *113* (17), 6936.
28. Iosin, M. ; Toderas, F. ; Baldeck, P. L. ; Astilean, S. *J. Mol. Struct.* **2009**, *924-926*, 196.
29. Brewer, S. H.; Glomm, W. R.; Johnson, M. C.; Knag, M. K.; Franzen, S. *Langmuir* **2005,** *21* (20), 9303.
30. Mulvaney, P. *Langmuir* **1996**, *12* (3), 788.
31. Violet, M.; Meunier, J. C. *Biochem. J*. **1989,** *263*, 665.
32. Lavecchia, R.; Zuorro, A. *Chem. Lett*. **2010**, *39*, 38.
33. Zanin, G. M.; De Moraes, F. F. *Appl. Biochem. Biotechnol*. **1998**, *70-72*, 383.

Chapter 6

Modulating Enzymatic Activity in the Presence of Gold Nanoparticles

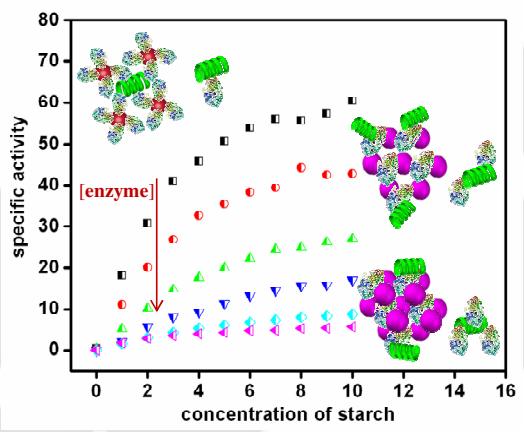

* Deka, J.; Paul, A.; Chattopadhyay, A. *Langmuir*, **2011** (*manuscript under revision*)

***Outline**:*

In chapter 2 we studied the enzymatic activity of α-amylase when covalently bound to Au NPs. After the studies on interactions (non-covalent in nature) of various proteins with citrate-stabilized gold nanoparticles (Au NPs), in chapter 4 & chapter 5, we were prompted to investigate the effect on the activity of α-amylase when it is non-covalently attached to citrate-stabilized Au NPs. Metal NPs are known to affect the biological activity of enzymes. In this chapter the effect of Au NPs on the specific activity of α-amylase has been studied. The modulation of the specific activity as a result of varying the ratio of enzyme: Au NPs has been explained on the basis of different levels of agglomeration of Au NPs and therefore on the availability of the active sites of the enzyme anchored on the Au NP surface. The results have been explained based on a model which considers the presence of enzyme bound to NP and available for enhanced catalysis, enzyme bound to NP but unavailable due to being buried inside the agglomerate and the free enzyme.

6.1 Introduction:

Interaction of metal nanoparticles (NPs) such as those of Au (and magnetic NPs) and biomolecules like proteins, peptides, RNA and DNA not only provides diagnostic tools for the identification,[1-3] assay and probe for the function of the molecule,[4,5] but also brings about changes in the activity of the biomolecule. For example, chemical or electrostatic attachment of enzymes to Au NPs may alter the catalytic properties either by increasing the affinity for enzyme-substrate formation[6-8]; enhancing its stability[6,7,9,10,11]; enhancing the rate of product formation (although significant report in this regard is still lacking)[6,7] or retention[12-14] and even some loss of activity of the enzyme.[9,10,15] Similarly, interaction with Au NPs has been found to enhance the stability of peptide[16] and DNA.[17] Understanding the mechanism of the NP induced alteration of properties of biomolecules is not only central to taking full advantages of nanoscale materials but also important in knowing the implications of manufactured nanomaterials on human health and the environment.[18] Further, enzymes constituting a bulk of biomolecules are responsible for key functions of living systems and their utility in catalytic production of medicinally important compounds provide clear opportunity to study their behavior in the presence of inorganic NPs such as those of Au. Although there are reports of NP induced changes in the properties of enzymes, paucity of literature in this regard is apparent especially with respect to clear exhibition of

significant difference in properties and understanding of the mechanisms involved. Also, it would be of significance if the enzymatic kinetics were to depend not only on the presence of Au NPs but also on their concentration ratio in the medium in such way so as to be able to modulate the kinetics. In other words, a pertinent question can be asked: would the presence of Au NPs at variable concentrations change the structure of enzyme to influence its kinetics? Addressing a part of the question would contribute towards better understanding of the fate of Au NPs if present in human body for treatment or otherwise.

Herein we report as high as 8-fold increase in the specific activity of the digestive enzyme α-amylase in the presence of citrate-stabilized Au NPs. Starch was used as the substrate for probing the enzymatic activity in the presence of Au NPs. Fluorescence spectroscopic measurements indicated attachment of the enzyme to the NPs. Also, the activity could be modulated by merely varying the enzyme: Au NP ratio. The results indicated that, for a given Au NP concentration, at low concentrations of the enzyme, the specific activity in the presence of the NPs was much higher than that due to the enzyme only. However, at higher concentrations, the activity reduced increasingly till finally reaching nearly the same as that due to pure enzyme. Further, at all concentrations the substrate-dependent activity could be fitted with Michaelis-Menten equation, with varying apparent Michaelis constant (K^a_m) and maximum velocity (V^a_{max}) for different concentration of the substrate. Interestingly, the presence of NPs rendered high activity to the enzyme even at very low concentration that is otherwise not possible in absence of the NPs. We also propose a model for explaining the observations based on Michaelis-Menten kinetics and in terms of attachment of enzyme to the NPs and subsequent agglomeration. Transmission electron microscopic (TEM) investigations indicated that while at low concentrations of the enzyme the Au NPs remained well-dispersed in the medium; however, at higher concentrations agglomeration of the NPs took place indicating the possible origin of differential activity of the enzyme.

6.2 Materials and Methods

6.2.1 *Preparation of Citrate Stabilized Au NPs*

750.0 µL of 1.7262 x 10^{-2} M $HAuCl_4$ (Sigma- Aldrich Chemical Co.) was added to 30.0 mL of MilliQ grade water and then heated to boiling. Then 126.0 mg of trisodium citrate 2-hydrate (E. Merck (India) Limited, Mumbai) was dissolved in 1.0 mL MilliQ grade water was added to the boiling solution (all at once) and refluxed for another 30 min to ensure complete reduction of $HAuCl_4$. The solution turned deep red, indicating the formation of Au NPs.

6.2.2 *Preparation of Dinitrosalicylic Acid (DNS) reagent*

The reagent consists of following two components:

Component 'A': 20.25 g of sodium potassium tartarate (Merck Specialists Private Limited, Mumbai, India) was dissolved in 60.0 mL Milli-Q grade water to which 468.0 mg of phenol (Merck Specialists Private Limited, Mumbai, India) dissolved in 9.0 mL of 10% NaOH (Merck Limited, Mumbai, India) solution was added.

Component 'B': 300.0 mg of 3,5-Dinitrosalicylic Acid (SRL, Mumbai, India) was dissolved in 60.0 mL Milli-Q grade water.

6.2.3 *Enzyme activity by DNS method*

1.0 mg/mL of α-amylase (from hog pancreas, Fluka) solution was prepared by dissolving the required amount in phosphate buffer (pH = 7.0) followed by centrifugation at 5000 rpm to remove the insoluble part. 75.0 µL of this solution was added to 24.0 mL of 2X diluted Au NPs (diluted from as-prepared solution with phosphate buffer) mixed well and left for 10 min. 2.0 mL of Au NP-amylase composite thus obtained was added to various test tubes each containing 3.0 mL of 0.00, 1.67, 3.33, 5.00, 6.67, 8.33, 10.00, 11.67, 13.33, 15.00 and 16.67 mg/mL of starch solution (Merck Specialists Private Limited, Mumbai, India; prepared in phosphate buffer of pH 7.0) respectively. The final concentration of starch in each tube was thus equal to 0.0, 1.0, 2.0, 3.0, 4.0, 5.0, 6.0, 7.0, 8.0, 9.0 and 10.0 mg/mL respectively and the enzyme concentration was 1.25 µg/mL. All of these test tubes were then incubated in water bath at 37 ^{0}C for 20 min. The reaction

mixtures were then cooled down to room temperature. 1.0 mL of the reaction mixture was taken out from each test tube to which 1.0 mL each of 'A' and 'B' components of DNS reagent were added. All of these mixtures were then incubated at 95 ^{0}C for another 10 min, followed by cooling down to room temperature. 300.0 µL of the mixture thus obtained was added to 3.0 mL of Milli-Q water and the UV-vis spectrum was recorded using a Hitachi U-2900 spectrophotometer. The absorbance at 570 nm corresponding to each tube was converted to respective maltose concentration by using the standard calibration curve obtained with maltose (Figure 6-1, Appendix). The specific activity of the enzyme was then calculated using the following formula,

Specific activity = amount of maltose produced/ (volume of 1.0 mg mL^{-1} enzyme added x 10) where the factor 10 is the time period (in min) of incubation with the DNS reagent.

Similarly the specific activities with various concentrations of starch were calculated for to 2.5 µg mL^{-1}, 5.0 µg mL^{-1}, 10.0 µg mL^{-1}, 20.0 µg mL^{-1} and 40.0 µg mL^{-1} of final enzyme concentrations.

For comparison control experiments (replacing Au NP with buffer) were carried out for each enzyme concentration.

6.2.4 *Calculation of K_m, V_{max} and k_{cat}*

For calculation of K_m and V_{max}, Lineweaver-Burk plots were plotted for each enzyme concentration. The values of K_m and V_{max} were then calculated from the slope and the intercept values. k_{cat} was calculated using the following relation:[19]

k_{cat} = µmoles of product / {µmoles of enzymes x time (in min)}

6.2.5 *To check Au NP interference with the DNS test*

Four different concentrations of maltose solution (2.50, 3.75, 5.00 and 7.50 mg/mL respectively) were prepared. To 3.0 mL of each solution, 2.0 mL of Au NP was added so that the final concentrations of maltose in the solutions were 1.50, 2.25, 3.00 and 4.50 mg/mL respectively. 1.0 mL of the mixture was taken out from each test tube to which 1.0 mL each of 'A' and 'B' components of DNS reagent were added. The mixtures were then heated to 95 ^{0}C for 10 min and then cooled down to room temperature. 0.3 mL of

the mixture thus obtained was added to 3.0 mL of Milli-Q water and the UV-vis spectrum was recorded using a Hitachi U-2900 spectrophotometer. Control experiments were performed for each of the maltose concentration (by replacing Au NPs with buffer). The absorbance at 570 nm was compared for each set (in presence and absence of Au NPs) to see the effect of Au NPs, if any (refer to Appendix, Figure 6-2).

6.2.6 *Fluorescence of α-amylase in presence of Au NPs*

12.5 µL of 1.0 mg/mL of α-amylase was added to 2.0 mL of Au NP (which made it to 2.5 µg/mL of enzyme in the final reaction mixture), mixed well and was left for 10 min. The fluorescence of Au NP both before and after addition of the enzyme was recorded using a Horiba Jobin-yvon Fluoromax-4 Spectrofluorometer, the excitation peak being set at 280 nm. Similarly fluorescence spectra were recorded for solutions containing 5.0 µg/mL, 10.0 µg/mL, 20.0 µg/mL and 40.0 µg/mL of enzyme. For control studies, fluorescence was recorded for each concentration of enzyme but in buffer instead of in the presence of Au NPs.

6.2.7 *Estimation of amount of free protein in solution*

To 6.0 mL of Au NP solution 37.5 µL of 1.0 mg/mL of α-amylase was added, mixed well and the solution was left for 10 min. The ratio of enzyme: Au NP was such that the final α-amylase concentration was equal to 2.5 µg/mL in the reaction mixture in regular experiments. Similarly four more sets were prepared with 75.0 µL, 150.0 µL, 300.0 µL and 600.0 µL of 1.0 mg/mL of α-amylase in 6.0 mL of Au NP solution corresponding to 5.0 µg/mL, 10.0 µg/mL, 20.0 µg/mL and 40.0 µg/mL of 1.0 mg/mL of α-amylase in regular experiments. The Au NP-enzyme composites thus obtained were centrifuged at 20,000 rpm in a Sigma 3-30K High Speed Cold Centrifuge for 20 min and the supernatants were collected. The supernatants were tested for the amount of protein by a simple method developed in our own laboratory using citrate-stabilized Au NPs.[20] Following this method, 0.1 mL to 0.4 mL of the supernatant solutions were added successively to 3.0 mL of Au NP solution and the UV-vis spectrum was recorded after each addition using a Hitachi U-2900 spectrophotometer. The area under the curve (from 450 nm to 650 nm range) for each spectrum was calculated using the software in the instrument itself. The ratio of the area under the graph for each spectrum to that of the

area under the graph for Au NP only were then calculated after performing proper volume corrections to take care of the dilution factor. To exactly quantify the changes in area under the graphs, a calibration curve (refer to Appendix, Figure 6-3) was prepared with the same stock of α-amylase and Au NPs used. Using the values so obtained, the total amount of protein in the 6.0 mL supernatant could thus be calculated. It must be mentioned here that in each case different dilution of the supernatant was used to obtain good results. For example, supernatants in Set 1 was used in undiluted form, Set 2 was diluted two times, Set 3 and 4 were diluted five times and Set 5 was diluted to ten times. The results obtained were finally multiplied by the required factor to get the exact value. From the concentrations of the proteins in the supernatants the concentrations of protein attached to Au NPs were obtained.

6.2.8 *Preparation of TEM samples*

12.5 µL of 1.0 mg/mL of α-amylase was added to 2.0 mL of Au NP dispersion (i.e. equivalent to 2.5 µg/mL of enzyme in final reaction mixture) and was left for 10 min. This solution was then drop cast onto Cu grid and then left for air-drying overnight. Similarly grids were prepared with 25.0 µL and 200.0 µL of α-amylase in 2.0 mL of Au NPs corresponding to 5.0 µg/mL and 40.0 µg/mL of enzyme respectively. These grids were further analyzed by a Jeol 2100 TEM machine (operated at a maximum voltage of 200 kV).

6.3 Results and Discussion

Citrate-stabilized Au NPs were synthesized using a conventional method that resulted in an average particle size of 11 $\pm$ 2 nm. The enzymatic reactions were carried out at 37 ^{0}C using starch as the substrate in pH 7.0 buffer; by first mixing the enzyme with NPs followed by subsequent transfer to the reaction medium. For kinetic studies, the product formation was followed by maltose estimation using the well-known DNS acid method,[21] details of which are available in the experimental section. Figure 1 shows specific activity versus substrate concentration plots in the presence of different concentrations of enzyme while that of Au NPs (i.e. 4.0 x 10^{12} NPs in 5.0 mL reaction mixture) was kept constant (except for the control experiment performed with enzyme only). The data in each graph represent average values of three measurements.

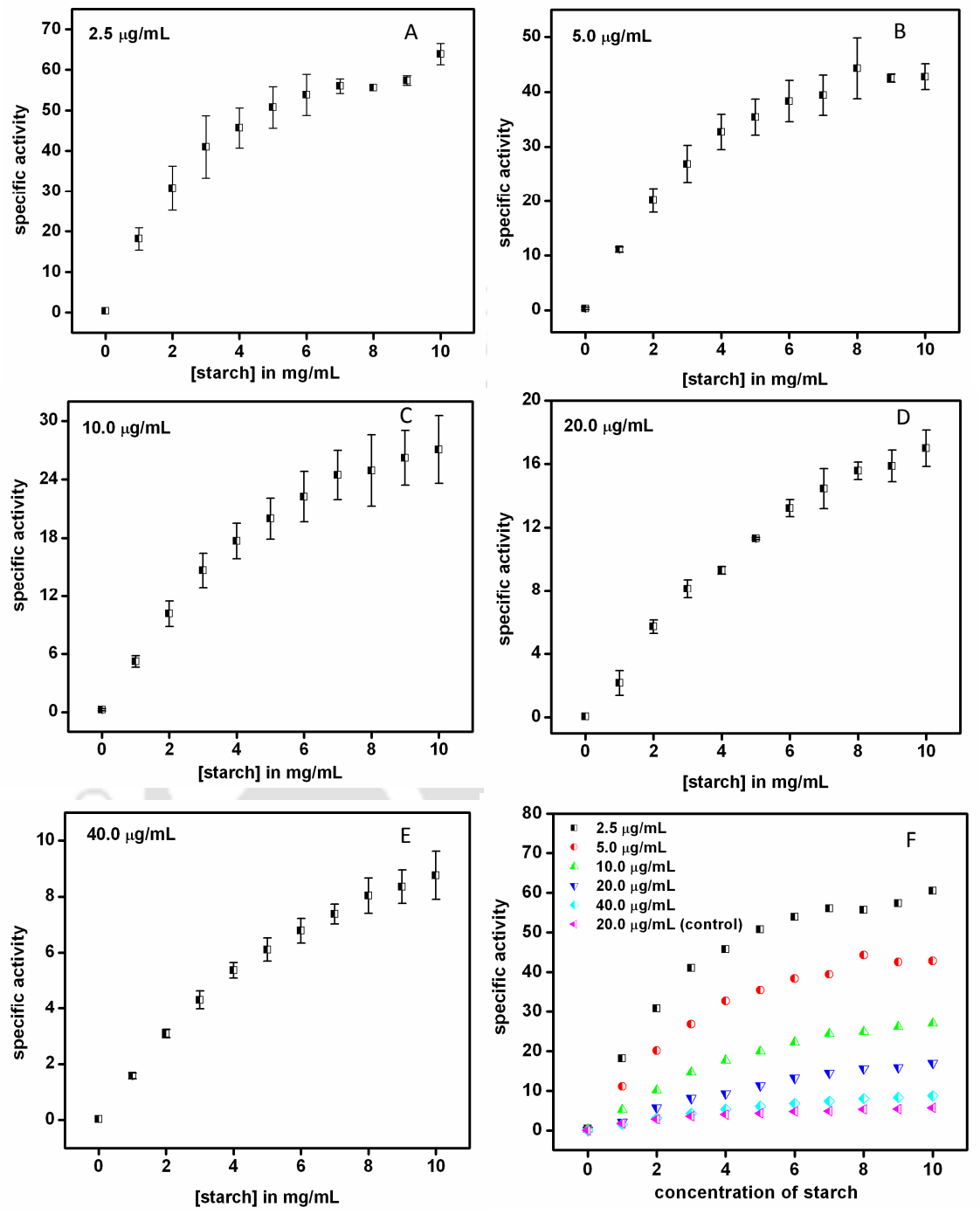

Figure 1. *Specific activity of α-amylase (in μmol mg^{-1} min^{-1}) in the presence of Au NPs. The concentration of starch is expressed in mg mL^{-1}. Graphs represent activities at enzyme concentrations indicated in the legends. The concentration of Au NPs was same for all of the above.*

A comprehensive view of the graphs combined together without the error bar is shown in Figure 1F. It is interesting to note that the results could be fitted to Michaelis-Menten equation and the calculated apparent Michaelis constant (K^a_m), rate constants for product formation (k^a_{cat}) and maximum velocity (V^a_{max}) values are included in Table 1.

Table 1. *Apparent V_{max}, K_m and k_{cat} values at the enzyme concentrations mentioned in Figure 1, calculated using Michaelis-Menten equation. The data (*) in the last row represent values corresponding to enzyme in absence of Au NPs.*

[α-amylase]/ (μg mL^{-1})	**V^a_{max} /(μmol mg^{-1} min^{-1})**	**K^a_m /(mg mL^{-1})**	**k^a_{cat} /(10^3 min^{-1})**
2.5	86.82 ± 1.81	3.66 ± 0.69	4.34 ± 0.09
5.0	72.78 ± 8.12	5.45 ± 0.52	3.64 ± 0.40
10.0	51.36 ± 4.38	9.64 ± 0.49	2.57 ± 0.46
20.0	40.60 ± 4.35	10.81± 2.29	2.03 ± 0.46
40.0	20.05 ± 1.30	11.52 ± 0.89	1.00 ± 0.15
20.0 *	11.25 ± 1.77	10.37 ± 0.64	0.56 ± 0.07

As are clear from the graphs and the table, at the lowest concentration of the enzyme (2.5 μg/mL) -where the Michaelis-Menten behavior could clearly be observed -the activity was the highest as represented by characteristic values, which were substantially different from those in absence of the NPs. For example, K^a_m value was about 0.4 time and k^a_{cat} was 8 times of that of pure enzyme indicating significant enhancement of both in substrate affinity and rate of product formation. Further, K^a_m values for higher concentrations of enzyme increased while those of k^a_{cat} and V^a_{max} decreased monotonically. The lower values of Michaelis constant (K_m) at lower enzyme concentrations indicated higher affinity towards the substrate possibly due to more favorable orientation of the enzyme structure on attaching to the Au NPs. It is important to mention here that while at the lowest concentration (2.5 μg/mL) of enzyme the specific activities were the highest, however, at the same concentration of pure enzyme the specific activities at different substrate concentrations were low and did not clearly

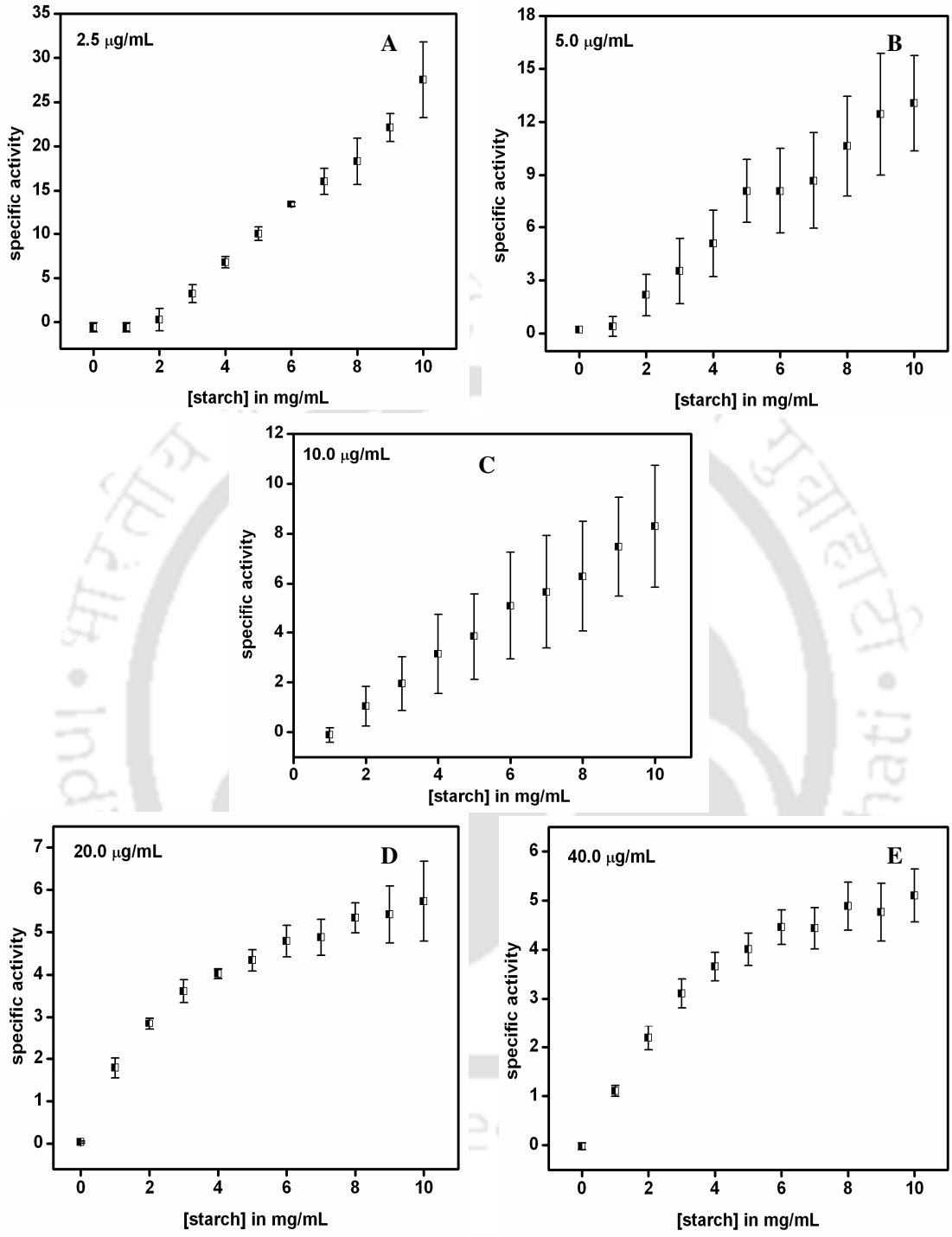

Figure 2: *Specific activity of α-amylase (μmol mg^{-1} min^{-1}) in the absence of Au NPs. Legend represents the respective concentration of enzyme at which the experiments were carried out.*

exhibit the Michaelis-Menten behavior (Figure 2). Further, experiments revealed that changing the concentration of Au NPs (other than that used herein) did not change the values of the highest activity of the enzyme, substrate affinity or rate of product formation (Figure 3 and Table 2).

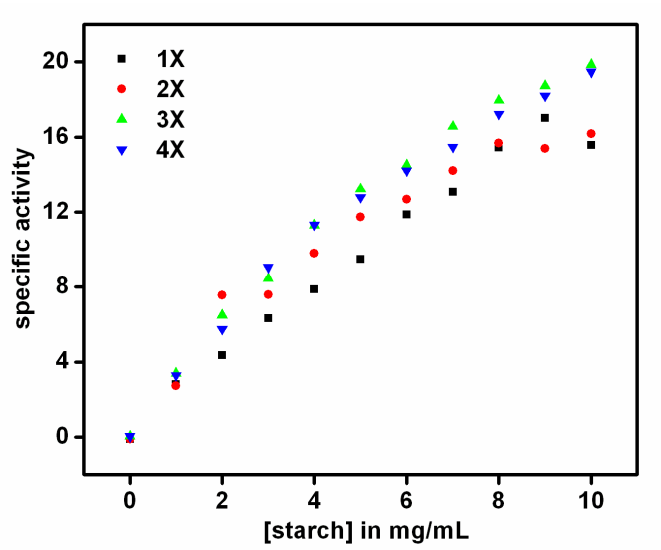

Figure 3: *The graph shows specific activity of α-amylase (20.0 μg/mL) (μmol mg^{-1} min^{-1}) in the presence of different concentrations of Au NPs. 1X refers to undiluted Au NP, 2X, 3X and 4X refers to two times, three times and four times diluted (with buffer) Au NPs respectively. The table represents the $V^a_{max,}$ K^am and k^a_{cat} values obtained for the various concentrations of Au NPs.*

Table 2: *The table represents the $V^a_{max,}$ K^a_m and k^a_{cat} values obtained for the various concentrations of Au NPs.*

Dilution of Au NP	**No. of Au NPs in the reaction mixture**	**V^a_{max}/ (μmol mg^{-1} min^{-1})**	**K^a_m / (mg mL^{-1})**	**k^a_{cat} / (10^3 min^{-1})**
1X	8.0×10^{12}	28.12	12.43	1.41
2X	4.0×10^{12}	47.21	11.60	2.36
3X	2.7×10^{12}	44.38	12.04	2.22
4X	2.0×10^{12}	44.96	12.77	2.24

TEM measurements (Figure 4 & 5) indicated that at the lowest concentration of the enzyme used, Au NPs remained isolated, while agglomeration could be observed at higher concentrations of the protein. For example, at 5.0 μg/mL of the protein the NPs were linearly assembled with occasional branching. On the other hand, at 40.0 μg/mL large agglomerated clusters could be observed. The results indicated that proteins were attached to the NPs and at their higher concentration agglomeration of the composite took place.

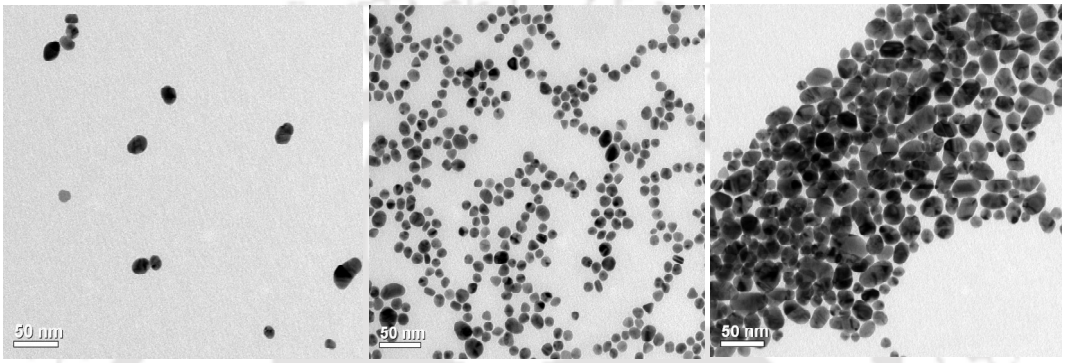

Figure 4. *TEM images of Au NPs from the media (post starch digestion) with concentrations of α-amylase being 2.5 μg/mL, 5.0 μg/mL and 40.0 μg/mL respectively (left to right).*

Fluorescence spectroscopic studies revealed that at all concentrations, the proteins were attached to the NPs (Figure 6), as evident from the decrease in the intensities. As observed earlier, presence of Au NPs leads to quenching of tryptophan fluorescence hence leading to vanishing of the fluorescence peak of α-amylase when attached to Au NPs.[20] In the present case the peak didn't vanish completely (except for the lowest concentration of the enzyme used i.e. at 2.5 μg/mL) indicating the presence of free enzyme in the medium, in addition to those attached to the NPs. The complete disappearance of fluorescence at the lowest concentration of the enzyme means possible absence of free enzyme in the medium at that concentration.

The above results could be explained in terms of attachment of the enzyme to the NPs and subsequent agglomeration at higher concentrations as represented schematically in Scheme 1. α-amylase consists of two cysteine thiol groups which are exposed to the medium and away from the active site.[14]

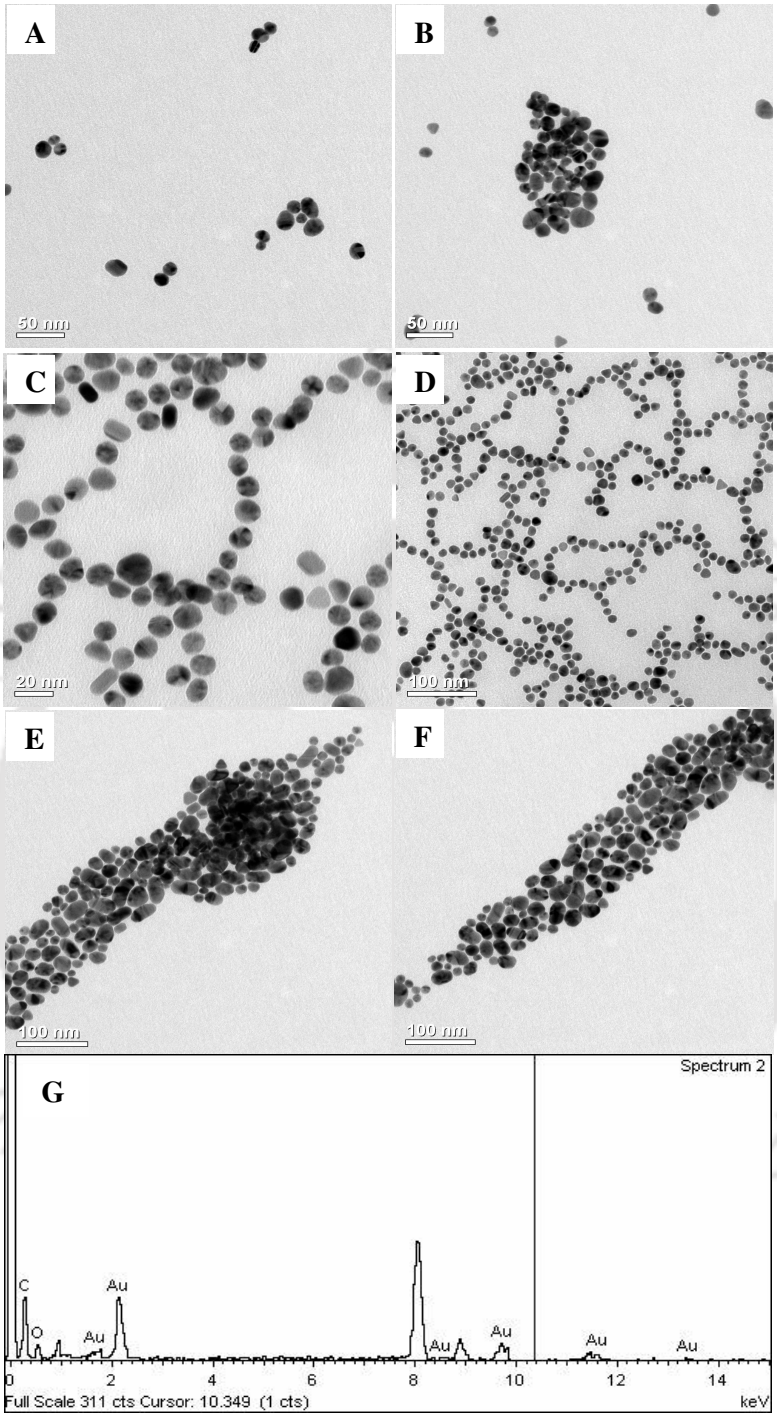

Figure 5. *Additional TEM images, showing arrangement of Au NPs in presence of* ***(A & B)*** *2.5 µg/mL,* ***(C & D)*** *5.0 µg/mL and* ***(E & F)*** *40.0 µg/mL of α-amylase in the reaction mixture post starch digestion and* ***(G)*** *EDX of one of the samples.*

Thus these groups could help the protein attach to the Au NPs efficiently with the active site still exposed to the medium and available for catalysis. At the lowest concentration, all the proteins were attached to the NPs and no agglomeration occurred. Because of their orientation and organization in the NPs they not only retain activity but the same was enhanced. For example, it has been recently reported that activity of lipase depends on its orientation on the functionalized Au NP surface, although no enhancement in activity was observed.[22]

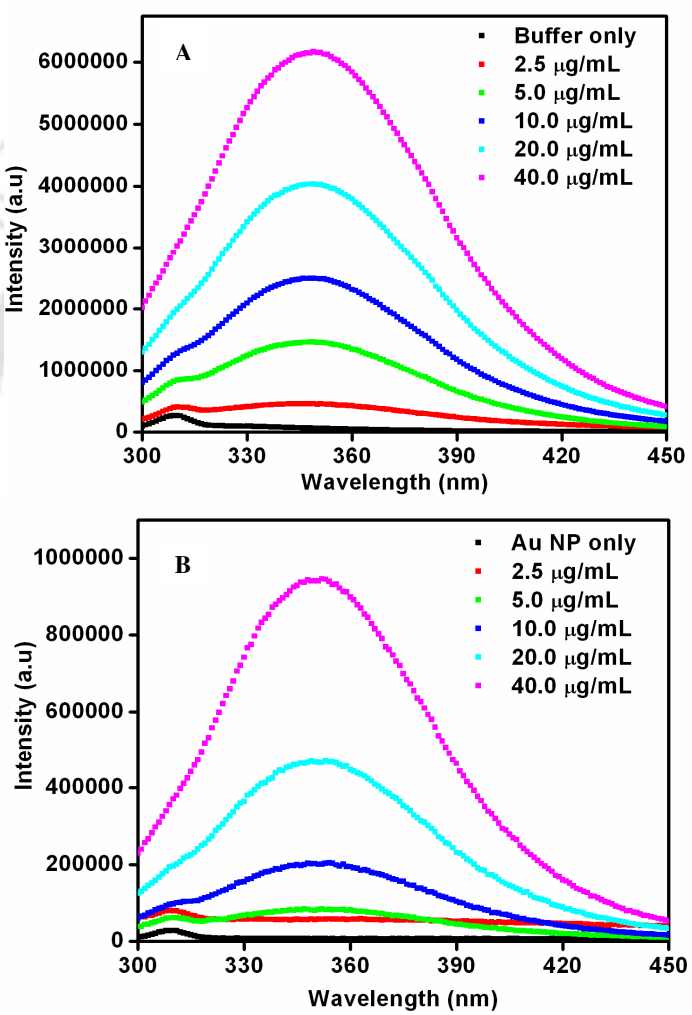

Figure 6. *Fluorescence spectra of α-amylase in* ***(A)*** *absence and* ***(B)*** *presence Au NPs. The legends show the various concentrations of the enzyme.*

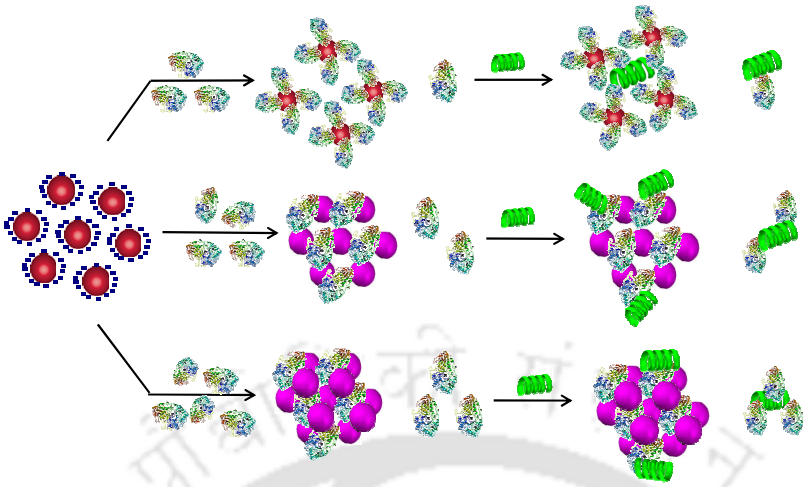

Scheme 1. *A schematic representation of possible structures present in the media consisting of citrate-stabilized Au NPs and α-amylase at different enzyme concentrations.*

At higher concentrations, agglomeration of the Au NP-enzyme mixture occurred which increased with increasing concentration. In the agglomerated structures the enzymes which remain buried inside were no more 'available' for catalysis hence the overall reaction rate decreased, although the sites which were exposed to the medium still contributed to activity. On the other hand, there may be free enzymes present in the medium which contributed to activity. Thus the overall activity is a sum of that due to enzymes attached to NPs and exposed to the medium plus that due to free enzymes. In the presence of Au NPs the catalytic activity of α-amylase could be represented by the product formation rate as in equation [1], i.e. in terms of product formation from two separate but parallel reactions – one due to active Au NP-enzyme composite and the other due to free enzyme. Thus overall specific activity could be written in terms of specific activity of the active composite (mole fraction being x) and free enzyme (mole fraction being y) and as written in equation [2], with each following Michaelis-Menten behavior.

$$\frac{dP}{dt} = (k_{cat}^{AuE}[AuES] + k_{cat}^{E}[ES]) \qquad [1]$$

$$V_{sp} = \frac{V_a^{max}[S]}{K_m^a + [S]} = x\frac{V_{AuE}^{max}[S]}{K_m^{AuE} + [S]} + y\frac{V_E^{max}[S]}{K_m^E + [S]} \qquad [2]$$

Here, k_{cat}^{AuE} and k_{cat}^{E} are the rate constants for product formation from [AuES] and [ES] complexes respectively. v_{sp} is the specific activity of the enzyme, v_a^{max} is the apparent velocity maximum, κ_m^a is the apparent Michaelis-Menten constant, v_{AuE}^{max} and v_E^{max} are the velocity maxima of the reaction for AuE and free enzyme respectively and κ_m^{AuE} and κ_m^E are the Michaelis-Menten constants for AuE and free enzyme respectively.

Here AuE represents Au NP-enzyme active composite and E represents free enzyme. Also, x and y are the mole fractions of active composite and free enzyme present in the medium respectively and thus z (1-x-y) is the fraction of enzyme attached to Au NPs which remains inactive.

Now, the inactive enzymes, although attached to the NPs but being buried inside agglomerated structures, do not contribute to product formation. In order to account for the apparent specific activity (Figure 1) in terms of specific activities of the active composite and the free enzyme (equation 2), one needs to know the values of x, y and z. This was pursued by first finding out the fraction of free enzyme. The enzyme-Au NP mixtures, with different concentrations of the enzyme, were centrifuged to precipitate and thus separate the enzyme attached with the NPs. The enzyme present in the supernatant was estimated using a method established in our laboratory.[20] The different fractions of the free enzyme present in the media thus estimated are given in Table 3. Further, it was observed that at the lowest enzyme concentration used here there was no free enzyme and no apparent agglomeration (as was observed in TEM in Figure 4 & 5). Hence specific activity at the lowest concentration was taken as the specific activity of the active Au NP-enzyme composite. Also, the specific activity of only enzyme was measured. Using these two values of specific activities and the knowledge of mole fractions of free enzyme, the observed apparent substrate-dependent specific activities at various concentrations of the enzyme as shown in the graphs in Figure 1F were fitted based on equation 2. The fitted graphs are shown in Figure 7.

Table 3. *The fraction of enzyme attached to Au NPs and active (x), free enzyme (y) and the fraction attached to NPs but inactive (z). The data (*) in the last column represent values corresponding to enzyme in absence of Au NPs.*

[α-amylase] (μg mL^{-1}) →	**2.5**	**5.0**	**10.0**	**20.0**	**40.0**	**20.0***
x	1.000	0.580	0.313	0.153	0.036	0.000
y	0.000	0.420	0.687	0.794	0.824	1.000
z	0.000	0.000	0.000	0.053	0.140	0.000

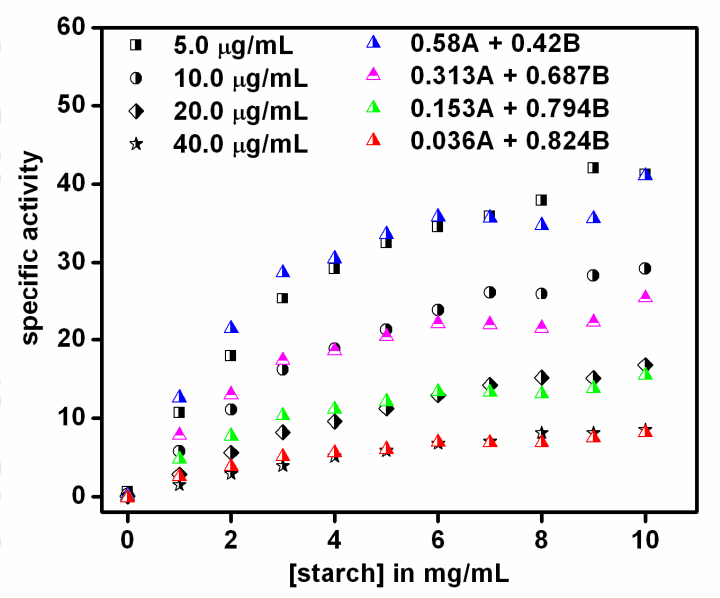

Figure 7. *Fitting of specific activity (μmol mg^{-1} min^{-1}) graphs in presence of varying enzyme concentrations in figure 1F based on equation 2. For each graph, the value of mole fraction of active enzyme (x) attached to NPs was taken to be that which generated the best fit. The mole fraction of free enzyme (y) was found from experiments described above. Here A represents specific activity of enzyme-Au NP mixture at the lowest enzyme concentration, while B is the specific activity of free enzyme.*

It must be mentioned here that in order to achieve the fitting, the mole fractions of active enzyme attached to Au NP (x) needed to be guessed and values corresponding to best fits are shown in Table 3. Obviously, the mole fractions (z) of enzyme attached to NPs but

inactive could easily be calculated, once x and y are known. The results indicated that with increasing concentrations of the enzyme the fractions of inactive (z) and free (y) enzymes increased, while that of active (x) enzyme decreased and hence the observed decrease in activity. At the highest of concentrations very little of activated enzyme remained, possibly due to large-scale agglomeration and thus the overall activity was close to that of free enzyme.

Further, in order to check the stability of the Au NP – enzyme agglomerated clusters, additional Au NPs (equivalent to one fourth of the Au NPs used for experiments) were added to the medium containing 40.0 µg/mL enzyme and Au NPs and the substrate concentration dependent specific activities were measured. The results are shown in Figure 8, which yielded the K^a_m, V^a_{max} and k^a_{cat} values equal to 11.69 mg mL^{-1}, 28.08 µmol mg^{-1} min^{-1} and 1.40 x 10^3 min^{-1} respectively, representing slight higher activity than in absence of excess NPs. Also, TEM images of the enzyme-Au NP mixture in presence of additional Au NPs are shown in Figure 9. Presence of smaller Au NP clusters was observed indicating possible formation of additional agglomerates with free enzyme that was present in the medium. This possibly contributed to small increase in activity.

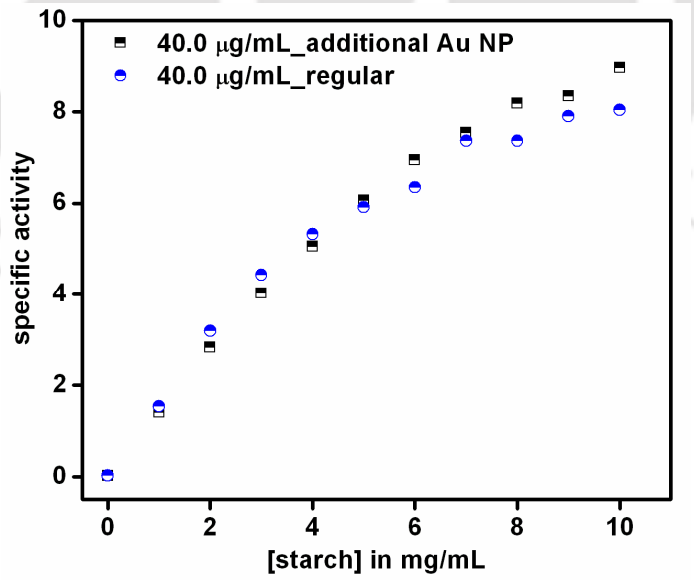

Figure 8: *Specific activity of α-amylase (40.0 µg/mL) (µmol mg^{-1} min^{-1}) in the presence of Au NPs as compared to the one with same concentration of enzyme and Au NP followed by additional Au NPs to the enzyme-Au NP composite.*

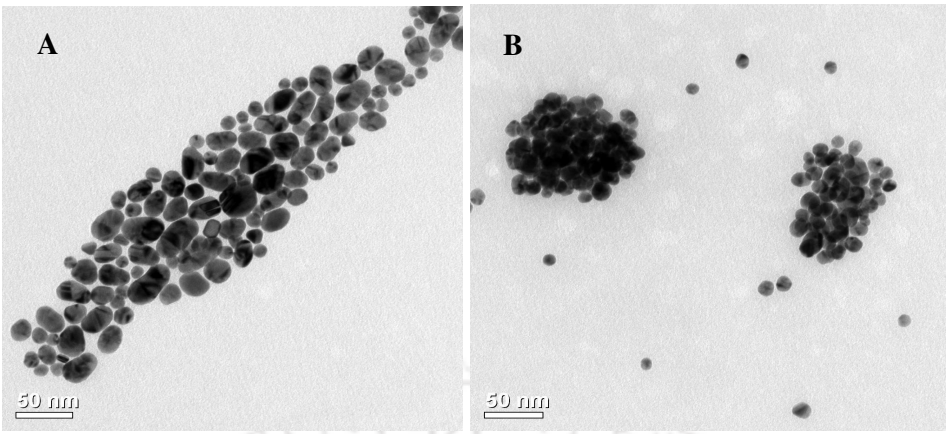

Figure 9: *TEM images of Au NPs from the media (after starch digestion) with 40.0 µg/mL of α-amylase and* ***(A)*** *regular amount of Au NPs and* ***(B)*** *additional Au NPs added to the as formed enzyme-Au NP composite.*

6.4 Summary

In brief, through a series of experiments we have been able to demonstrate that details of structures of the composite of enzyme and Au NPs, when attached to each other, are important in determining the overall activity of the enzyme. For the enzyme used here (α-amylase) the exposed thiol groups present in the structure may be responsible for the attachment to Au NPs and better orientation for enhanced reactivity. However, occurrence and the extent of aggregation at higher enzyme concentrations determined the overall activity with increasing agglomeration leading to decreased activity. It is plausible that a group of proteins attached simultaneously to a single NP, with their active sites exposed to the medium may lead to cooperative digestion of the same starch molecule and be one of the reasons behind the enhanced activity. And in the agglomerates active sites of the enzymes are not accessible to starch molecules (even in the case of retention of native structure) thereby effectively lowering the activity of the enzyme. One cannot also discount the possibility of denaturation of enzyme in the agglomerated structure and hence reduction of activity. The results presented here may provoke further studies involving interactions between NPs and biomolecules, essential in understanding the consequences of use of manufactured nanomaterials in human health and environmental systems, in addition to being useful in catalysis.

References:

1. Storhoff, J. J.; Elghanian, R.; Mucic, R. C.; Mirkin, C. A.; Letsinger, R. L. *J. Am. Chem. Soc*. **1998**, *120 (9)*, 1959.
2. Hone, D. C.; Haines, A. H.; Russell, D. A. *Langmuir* **2003**, *19*, 7141.
3. Mayer, K. M.; Lee, S.; Liao, H.; Rostro, B. C.; Fuentes, A.; Scully, P. T.; Nehl, C. L.; Hafner, J. H. *ACS Nano* **2008**, *2 (4)*, 687.
4. Wei, H.; Chen, C.; Han, B.; Wang.; E. *Anal. Chem.* **2008**, *80 (18)*, 7051.
5. Griffin, J.; Ray, P. C. *J. Phys. Chem. B* **2008**, *112 (36)*, 11198.
6. Pandey, P.; Singh, S. P.; Arya, S. K.; Gupta, V.; Datta, M.; Singh, S.; Malhotra, B. D. *Langmuir* **2007**, *23*, 3333.
7. Kouassi, G. K.; Irudayaraj, J.; McCarty, G. *Journal of Nanobiotechnology* **2005**, *3*, 1.
8. Wu, C. S.; Wu, C. T.; Yang, Y. S.; Ko, F. H. *Chem. Commun*. **2008**, *42*, 5327.
9. Dyal, A.; Loos, K.; Noto, M.; Chang, S. W.; Spagnoli, C.; Shafi, K. V. P. M.; Ulman, A.; Cowman, M.; Gross. R. A. *J. Am.Chem. Soc*. **2003**, *125*, 1684.
10. Rossi, L. M.; Quach, A. D.; Rosenzweig, Z. *Anal Bioanal Chem*. **2004**, *380*, 606.
11. Jordan, B. J.; Hong, R.; Gider, B.; Hill, J.; Emrick, T.; Rotello, V. M. *Soft Matter*, **2006**, *2*, 558.
12. Ahirwal, G. K.; Mitra, C. K. *Sensors* **2009**, *9*, 881.
13. Brennan, J. L.; Hatzakis, N. S.; Tshikhudo, T. R.; Dirvianskyte, N.; Razumas, V.; Patkar, S.; Vind, J.; Svendsen, A.; Nolte, R. J. M.; Rowan, A. E.; Brust, M. *Bioconjugate Chem*. **2006**, *17*, 1373.
14. Rangnekar, A.; Sarma, T. K.; Singh, A. K.; Deka, J.; Ramesh, A.; Chattopadhyay, A. *Langmuir* **2007**, *23 (10)*, 5700.
15. Gole, A.; Dash, C.; Ramakrishnan, V.; Sainkar, S. R.; Mandale, S. B.; Rao, M.; Sastry, M. *Langmuir* **2001**, *17*, 1674.
16. Verma, A.; Nakade, H.; Simard, J. M.; Rotello, V. M. *J. Am. Chem. Soc*. **2004**, *126*, 10806.
17. Seferos, D. S.; Prigodich, A. E.; Giljohann, D. A.; Patel, P. C.; Mirkin. C. A. *Nano Lett*. **2009**, *9 (1)*, 308.
18. Langer, R.; Tirrell, D. A. *Nature* **2004**, *428*, 487.

19. Gilbert, H. F. Basic Concepts in Biochemistry (*2nd Edition*).

20. Deka, J.; Paul, A.; Chattopadhyay, A. *J. Phys. Chem. C*. **2009**, *113 (17)*, 6936.

21. Miller.; G. L. *Anal. Chem*. **1959**, *31 (3)*, 426.

22. Brennan, J. L.; Kanaras, A. G.; Nativo, P.; Tshikhudo, T. R.; Rees, C.; Fernandez, L. C.; Dirvianskyte, N.; Razumas, V.; Skjøt, M.; Svendsen, A.; Jørgensen, C. I.; Schweins, R.; Zackrisson, M.; Nylander, T.; Brust, M.; Barauskas, J. *Langmuir* **2010**, *26 (16)*, 13590.

Chapter 7

Overview of the Thesis and Future Prospects

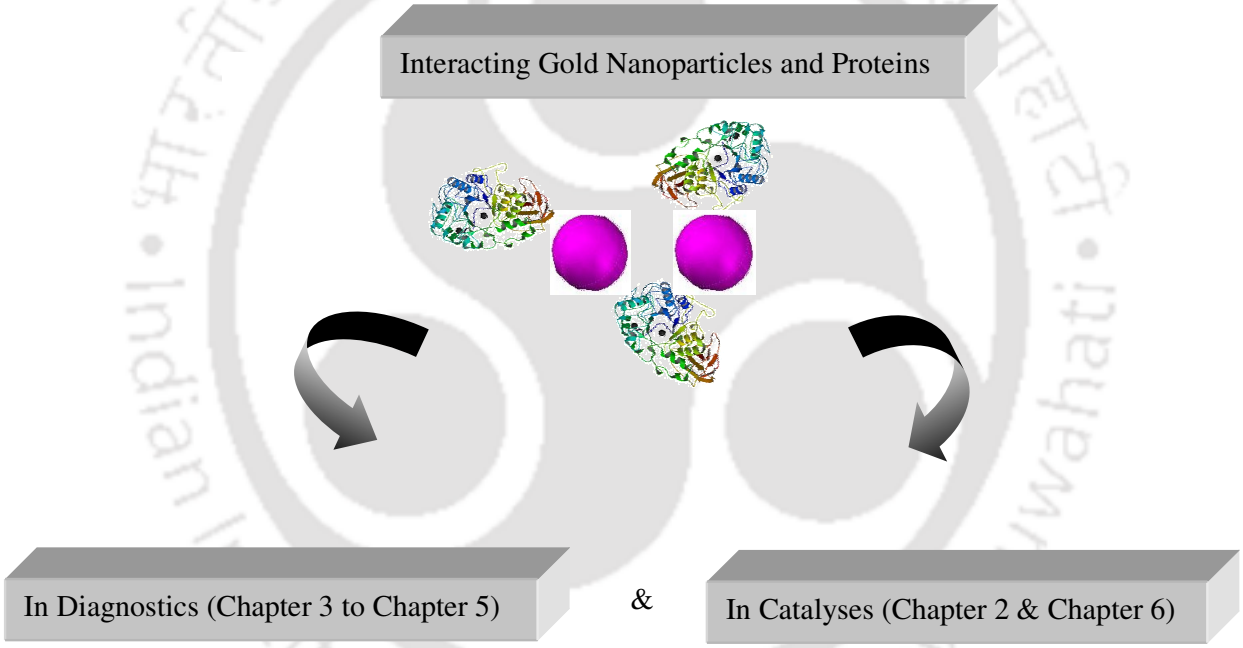

7.1 Overview of the work done

As discussed in ***Chapter 1*** (Introduction) of the thesis, the main motivation behind the work was the unique characteristic features of the Au NPs that has been extensively exploited and reported in the field of nanobiotechnology. The extraordinary ability of Au NPs to simultaneously detect and image the symptoms of a disease as well as treat it through targeted delivery to the infected cells makes the research on Au NPs even more interesting and essential. Above all, its biocompatible nature makes it an unrivaled candidate in the field of nanobiotechnology. However before the final application of any new nanomaterials in the human system, it has to undergo rigorous clinical trials and therefore a sound knowledge about various probable interactions of the specifically designed nanomaterials with biological components inside the human system would be always appreciable and relevant. Our main concern was to study the mechanisms of interactions between Au NPs and a few proteins and their outcome. We were interested in addressing a few basic questions such as: (i) what can be the mechanism of NP synthesis by an enzyme α-amylase (the synthesis of the NP by the enzyme was carried out by Abhijit *et al* and reported in BTP thesis in 2006[1])? (ii) what kind of bonds can be present in the enzyme-NP complex following NP synthesis? (iii) what can be the fate of the enzyme α-amylase, after it synthesizes Au NPs? (iv) what can be the fate of a drug vehicle comprising of starch as the carrier of Au NPs (the starch-Au NP composite was first prepared in our laboratory by Sarma *et al*[2]), when it comes in contact with α-amylase which is the digestive enzyme of starch? Such studies are relevant in the field of targeted drug delivery. In other words what kind of interactions can take place between the NPs and the enzyme when the NPs are released from the carrier? (v) what can be the effect of non-covalent interactions between citrate-stabilized Au NPs (citrate being loosely bound to the Au NPs surface) and a few proteins and how does the type of interactions vary from proteins containing free and solvent exposed thiol groups to those not containing free and exposed thiol groups? (vi) how can the presence of citrate-stabilized Au NPs affect the biological activity of the enzyme, α-amylase?

The work done for ***Chapter 2*** threw light on the mechanism of Au NP synthesis by the enzyme α-amylase and on the biological activity of the enzyme after the NP synthesis. It was revealed that the activity was still retained by the enzyme and was comparable to

equal amount of free enzyme. Its worth mentioning that such study on the mechanism of NP synthesis by a purified biomolecule was carried out for the first time.

Since we were interested in investigating the fate of a drug vehicle in presence of a reactant, we chose starch-Au NP composite (starch being the substrate of α-amylase and also being a promising candidate for drug delivery vehicle) and investigated its behavior when it came in contact with the digestive enzyme, α-amylase. As discussed in ***Chapter 3*** it was interesting to note that the starch was digested by the enzyme in a similar fashion as for free starch. Also the rate of starch digestion for the composite was same as that of free starch. The normal starch-iodine test for following the starch digestion could be performed even with the composite containing Au NPs. It was discovered that the Au NPs released from the starch-Au NP composite after the break down of the starch coating was sequestered by the enzyme, α-amylase, without any change in the size of the NPs. Even though digestion of starch was a prerequisite for the release of the NPs, the sequestration of the NPs from the composite was enzyme specific as revealed by the comparative studies with amyloglucosidase (AMG) which cleaves the 1, 6 glycosidic bonds in starch. Lower amount of the enzyme AMG was found to be associated with the NPs as compared to those of α-amylase with same amount of NPs. This indicated the preferential binding of the enzyme α-amylase with Au NPs as compared to AMG with Au NPs. This was explainable based on the studies carried out in Chapter 2, which demonstrates the role of thiol group in binding Au NP to the enzyme α-amylase. Since AMG is devoid of free thiol groups hence it is reasonable that lesser number of enzyme molecules would be attached to the NPs. Thus, the NP release can be tuned by the judicious combination of encapsulating materials and choice of appropriate enzyme. As an outcome of the study, surface plasmon resonance (SPR) of the NPs was discovered to be a tool for following starch digestion kinetics.

The beautiful organization of the Au NPs (after its sequestration from the starch-Au NP composite) by α-amylase and the differential behavior of the two enzymes towards NPs, as observed in the previous work provoked us to carry out detailed study of the interaction of different types of proteins with Au NPs. We chose citrate-stabilized Au NPs for the purpose since they are easy to prepare and the loose cover of citrate can be easily replaced by other molecules leading to association with the NPs. ***Chapter 4*** is about weak electrostatic interactions between citrate-stabilized Au NPs and a few

proteins, which gave rise to the development of a simple and sensitive method of protein estimation. The change in the SPR of citrate-stabilized Au NPs due to the presence of a specific protein was the parameter for quantifying the amount of the protein. The agglomeration of NPs in presence of protein was the driving force behind the change in the SPR signals. Also, the specificity of interaction from protein to protein as well as the two forms (native and denatured) of the same protein gave was an added advantage which allowed us to use the method to distinguish between the two conformations of the same protein.

Extending the work in Chapter 4 for a mixture of the two different conformations of a protein we were able to develop a method which can exactly estimate the conformational content (i.e the amount of native or denatured form of a protein) in a mixture, the results were reported in ***Chapter 5***. This method was also based on the weak non-covalent interactions between the proteins and NPs and on the optical properties of the citrate-stabilized Au NPs.

Chapter 4 & 5 indicated that the non-covalent interactions between the citrate-stabilized Au NPs and enzymes lead to agglomeration of the NPs. And the extent of agglomeration depended on the amount of protein. We were interested in investigating the effect of such interactions on the enzymatic activity of α-amylase. ***Chapter 6*** reports the enhancement of the specific activity of the enzyme in the presence of citrate-stabilized Au NPs. Interestingly the specific activity could be tuned by varying the enzyme: Au NP ratio. It was realized that the level of agglomeration of the NPs dependent on the enzyme: Au NP ratio was the main reason behind the change in the specific activity of the enzyme. The availability and proper orientation of the active site of the enzyme was the factor behind the enhancement (as compared to free enzyme) and modulation of its specific activity.

7.2 Future prospects

Essentially, through the works presented in the thesis we hope to have been able to establish that interactions between metal nanoparticles (NPs) such as those of Au and proteins provide important information related to synthesis of NPs by protein, following the kinetics of digestion of a composite by a protein and assays as well as about the conformation of the protein especially fractional content in a medium. In addition, that the activity of a protein could be influenced by the presence of Au NPs has been clearly

demonstrated. These results bring out new opportunities in using 'non-functionalized' Au NPs such as the citrate-stabilized ones to probe further into nature of biomolecules and their functioning in a medium. For example, a pertinent extension could be the probe of a mixture of proteins (two or more) in a medium. That would bring not only interesting results about the nature of interaction of individual proteins in the presence of a mixture but also the possibility of knowledge of the interactions among the proteins themselves, which may otherwise not be so easy to know. The linear nature of the area under the extinction (of Au NPs) curve versus concentration of protein provides enough reason to be optimistic in this regard. Another important point that remains to be probed is the nature of specific interactions between a protein and the NP especially from the point of molecular bonds. Of course the extension of the studies involving important biomolecules other than proteins is an avenue that remains to be explored. In addition, applying the knowledge and techniques developed herein in real examples involving proteins and other biomolecules for the development of diagnostics and therapeutics is a hope one can not only nurture but also see through it being carried out.

Finally, I sincerely hope that the thesis would encourage younger and aspiring scientists to pursue research not only as a career alternative but also as fulfillment of ambitions in contributing fundamental understanding in science so that future technology might benefit from the accrued knowledge. That there is plenty of room for sincere efforts in pursuing modern science, so essential for the contribution to the progress of humanity at large, must not be lost in the conundrum of competition in the quest for knowledge.

Reference:

1. Rangnekar. A. *B. Tech Project Thesis* **2006**, IITG.

2. Sarma, T. K.; Chattopadhyay A. *Langmuir* **2004**, *20(9)*, 3520-3524.

Appendix

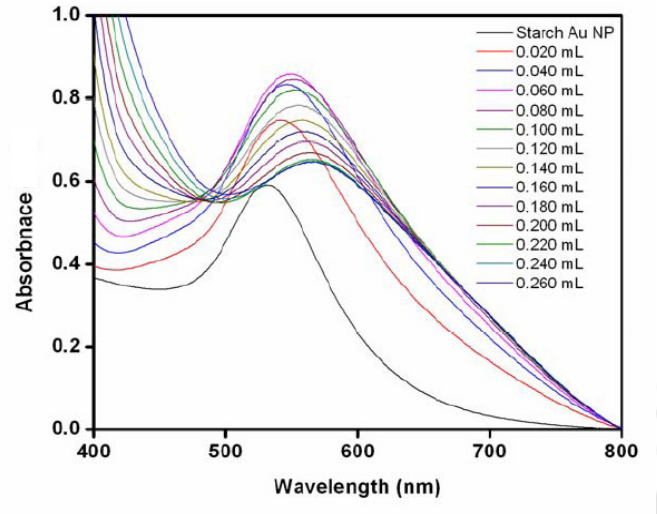

Figure 3-1. *UV-Vis spectra of starch-Au NPs (black color) and that of starch-Au NPs after iodine addition. The amount of iodine added, for each sample, is shown as legend in the graph.*

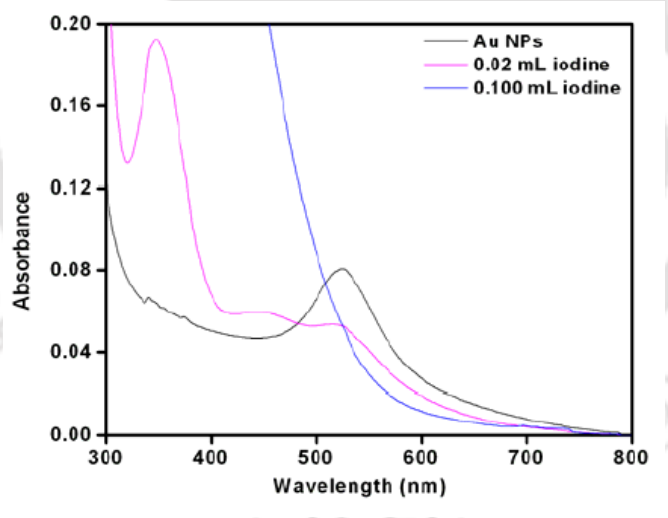

Figure 3-2. *UV-Vis spectra of Au NPs only (synthesized by H_2O_2 reduction) and Au NPs treated with different amounts of iodine. The colored graphs are due to respective amount of iodine added to the Au NP solution.*

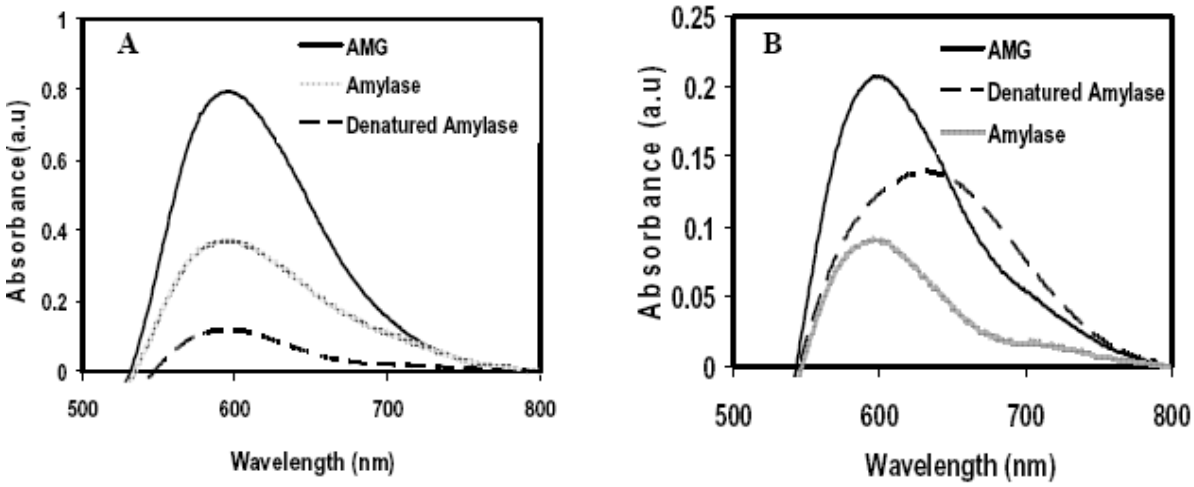

Figure 3-3. *UV-Vis spectra of Bradford test for protein estimation. The spectra in* ***(A)*** *were obtained using parent enzyme solutions and* ***(B)*** *were of respective supernatants after centrifugation of the reaction mixtures. AMG stands for amyloglucosidase.*

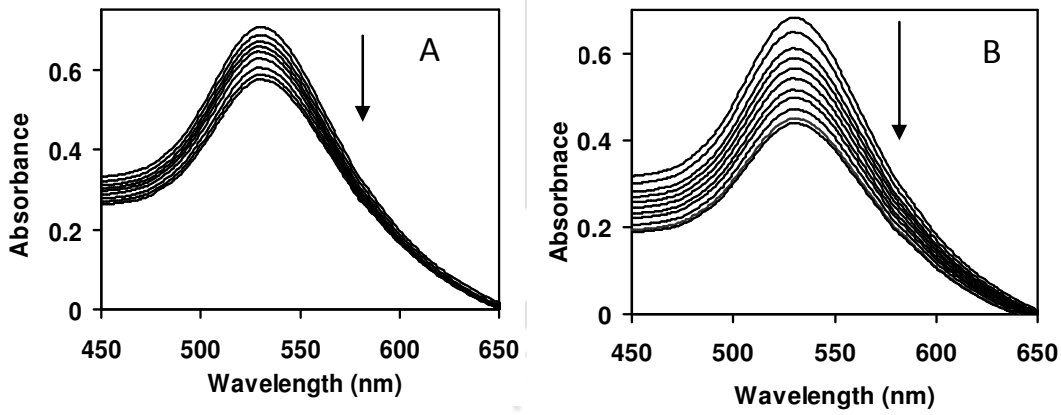

Figure 3-4. ***(A)*** *Surface plasmon resonance probe of starch-Au-NP digestion using reaction conditions stated in Figure 16 (A; set 1) in chapter 3.* ***(B)*** *Surface plasmon resonance probe of starch-Au-NP digestion using reaction conditions stated in Figure 16 (A; set 2) in chapter 3.*

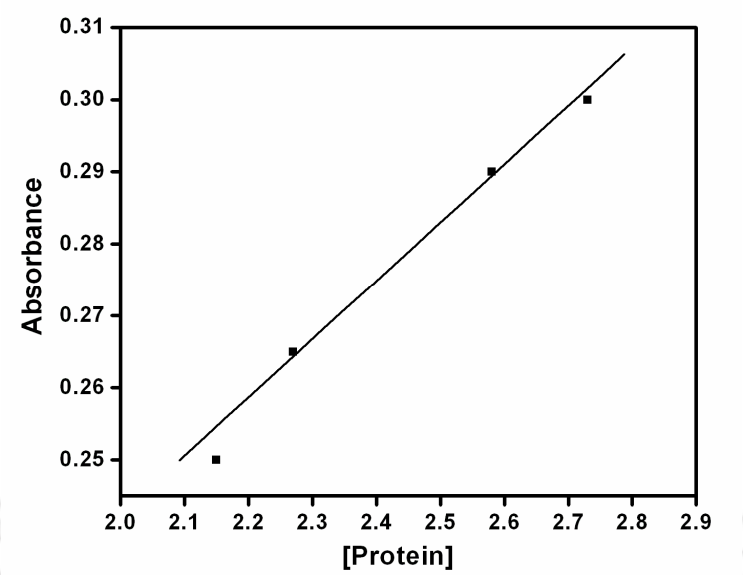

Figure 4-1. *Change in absorbance of the probe dye (λmax = 595 nm) used for Bradford test as a function of α-amylase concentration. The x-axis shows concentration of protein as determined from the calibration graph (obtained by using BSA as the standard protein) and is in terms of microgram per mL.*

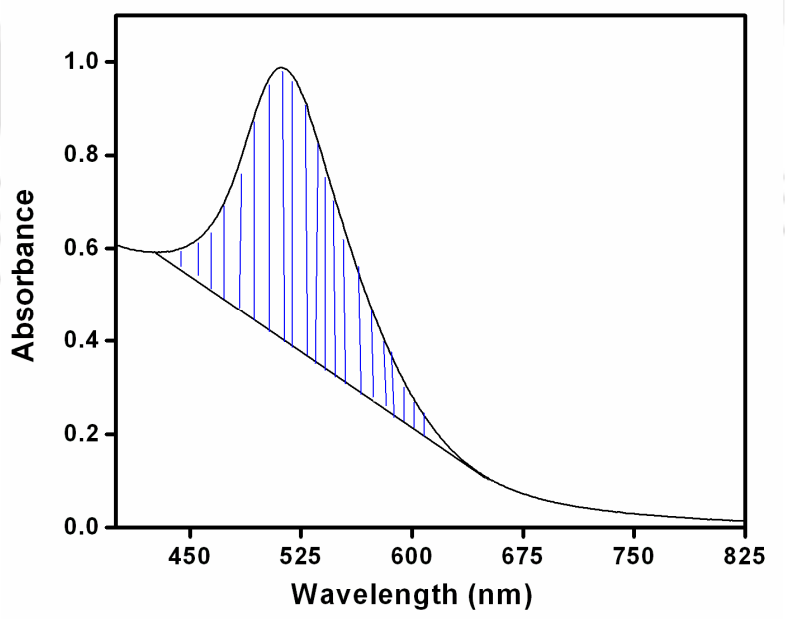

Figure 4-2. *A typical graph showing the area calculated under the curve, after selecting the wavelength region, using the software associated with the UV-vis spectrophotometer (Hitachi U-2800).*

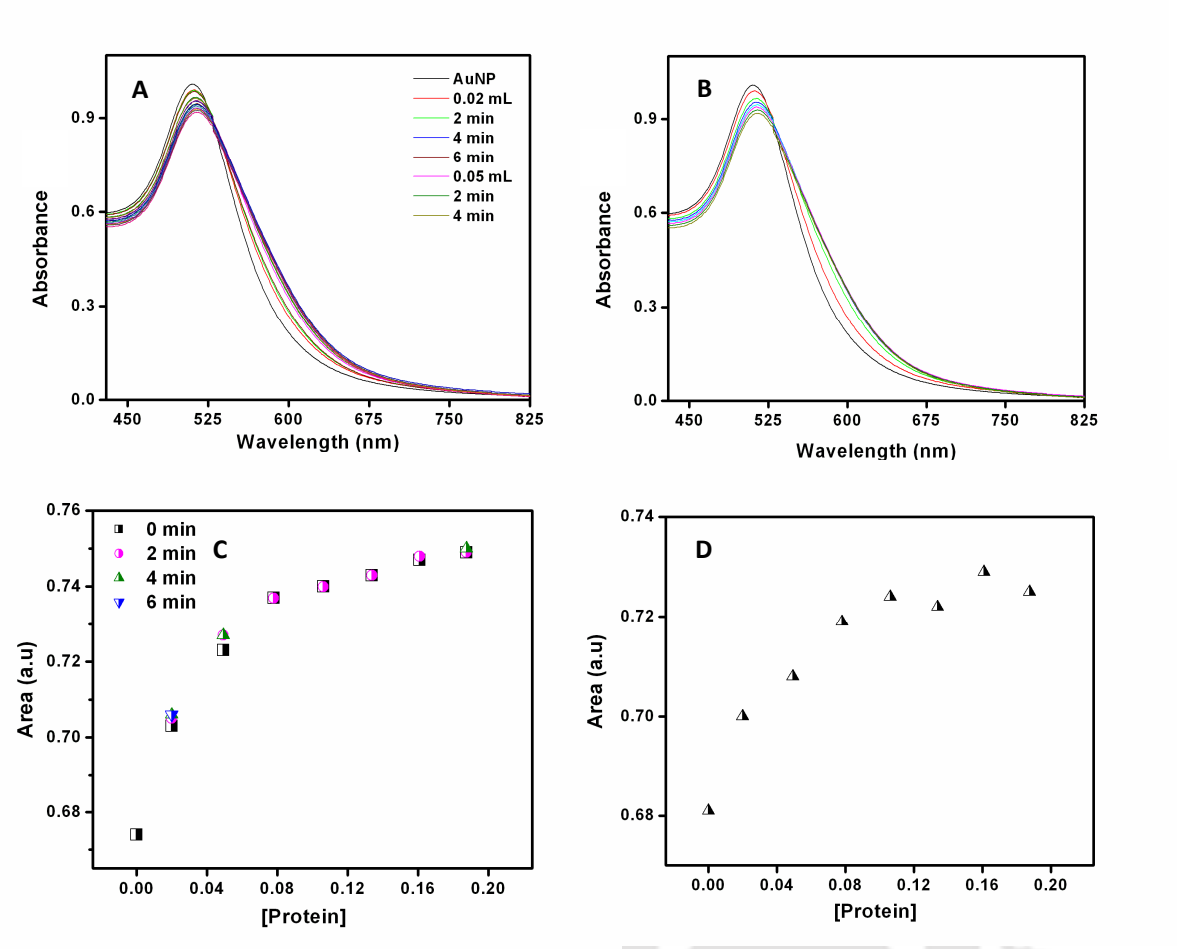

Figure 4-3. ***(A)*** *Time dependent UV-vis spectra of Au NPs on successive addition of native α-amylase (the legend shows initial time period in presence of 0.02 mL and 0.05 mL of 0.1 mg/mL α-amylase solution).* ***(B)*** *UV-vis spectra of Au NP on successive addition of native α-amylase without time lag.* ***(C)*** *Peak area versus [protein] in microgram per mL for graph in 'A' and* ***(D)*** *Peak area versus [protein] in microgram per mL for graph in 'B'. The range of final protein concentration in Au NPs solution in (A) and (B) is 0.02 µg/mL to 0.187 µg/mL.*

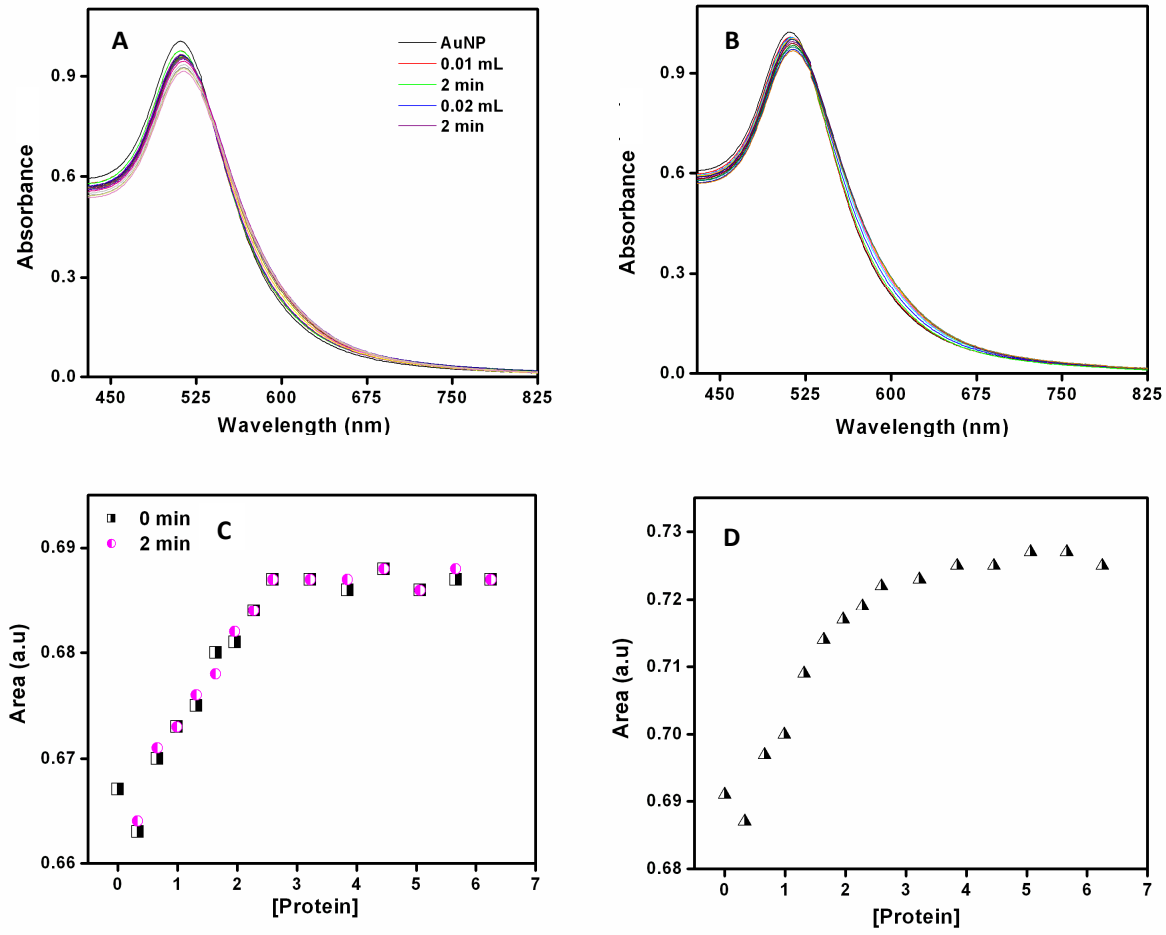

Figure 4-4. ***(A)*** *Time dependent UV-vis spectra of Au NPs on successive addition of native BSA (the legend shows initial time period in presence of 0.01 mL and 0.02 mL of 0.1 mg/mL enzyme solution).* ***(B)*** *UV-vis spectra of Au NP on successive addition of native BSA without time lag.* ***(C)*** *Peak area versus [protein] in microgram per mL for graph in 'A' and* ***(D)*** *Peak area versus [protein] in microgram per mL for graph in 'B'. The range of final protein concentration in Au NPs solution in (A) and (B) is 0.332 µg/mL to 6.25 µg/mL.*

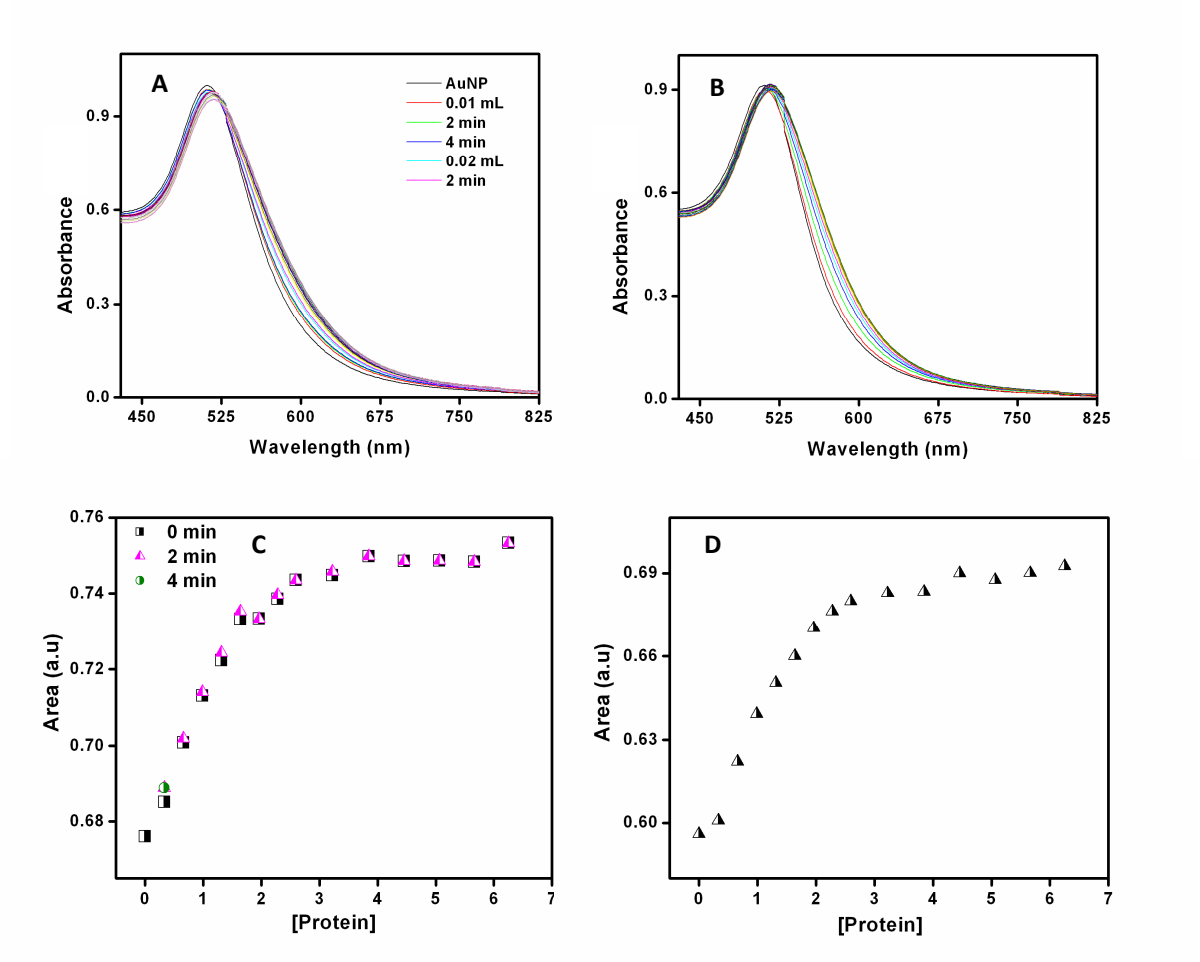

Figure 4-5. ***(A)*** *Time dependent UV-vis spectra of Au NP on successive addition of denatured BSA (the legend shows initial time period in presence of 0.01 mL and 0.02 mL of 0.1 mg/mL enzyme solution).* ***(B)*** *UV-vis spectra of Au NP on successive addition of denatured BSA without time lag.* ***(C)*** *Peak area versus [protein] in microgram per mL for graph in 'A' and* ***(D)*** *Peak area versus [protein] in microgram per mL for graph in 'B'. The range of final protein concentration in Au NPs solution in (A) and (B) is 0.332 µg/mL to 6.25 µg/mL.*

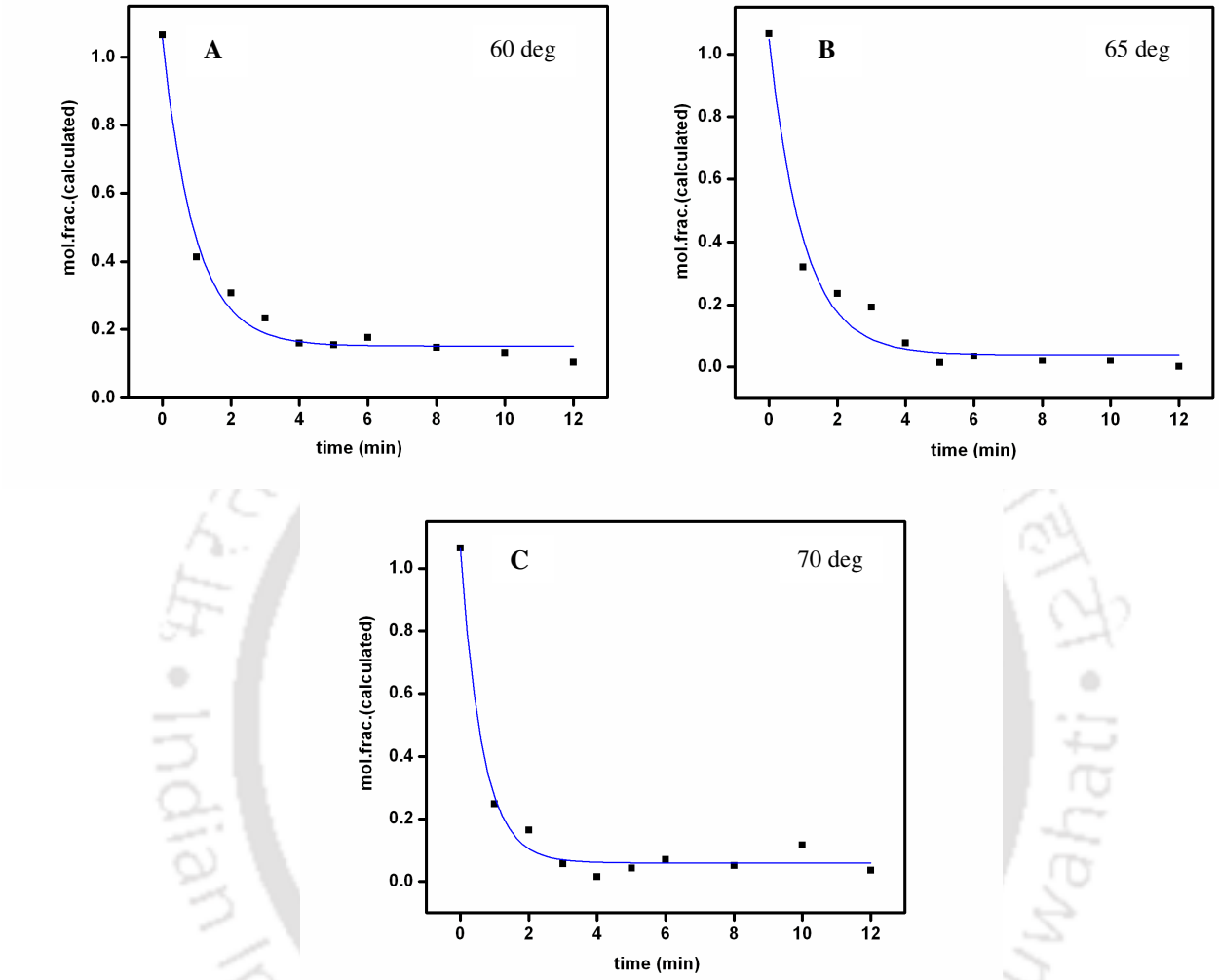

Figure 5-1. *Single exponential fits of the data obtained in the time-dependent thermal denaturation studies for α-amylase. Temperatures of denaturation are shown in the legends.*

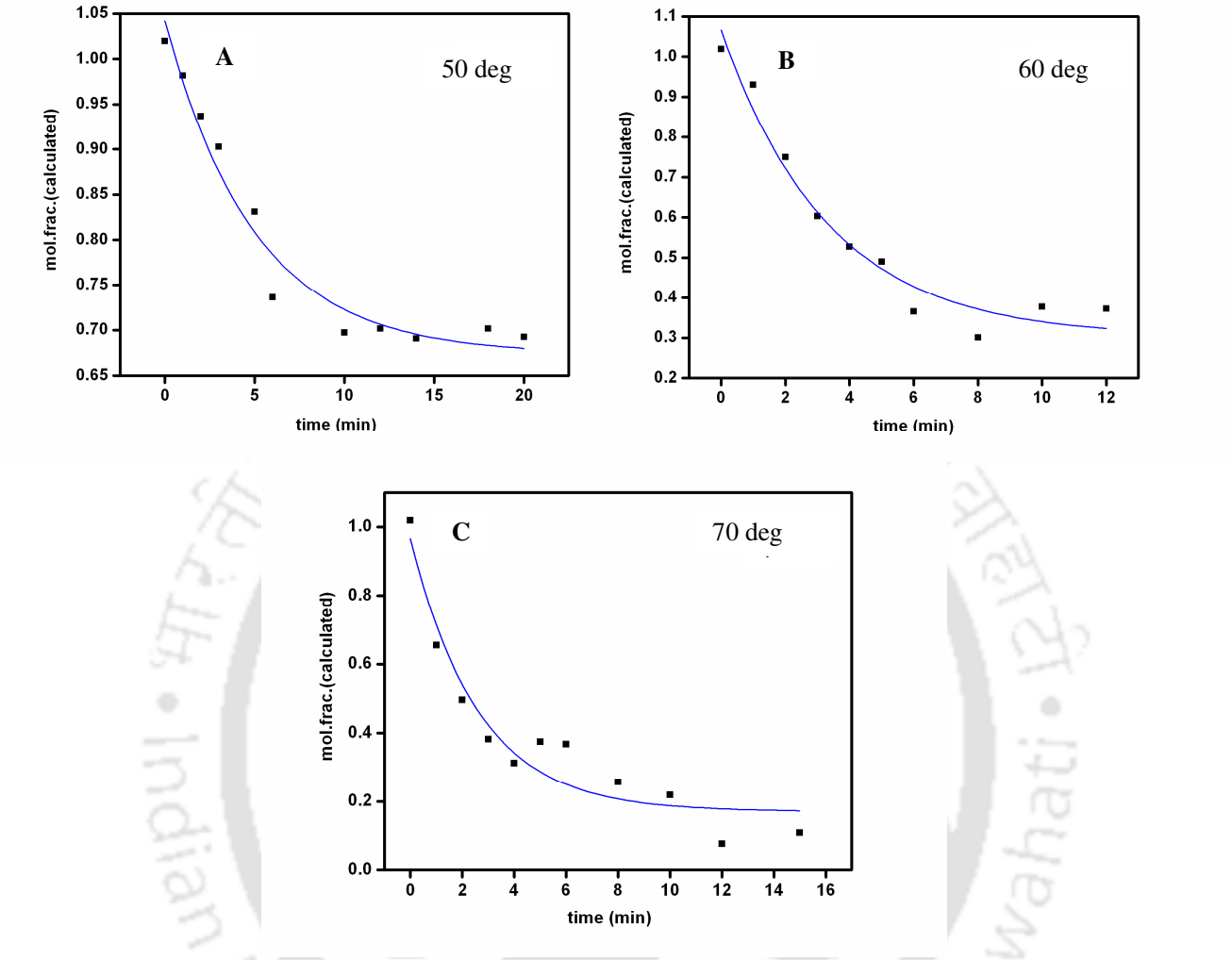

Figure 5-2. *Single exponential fits of the data obtained in the time-dependent thermal denaturation studies for BSA. Temperatures of denaturation are shown in the legends.*

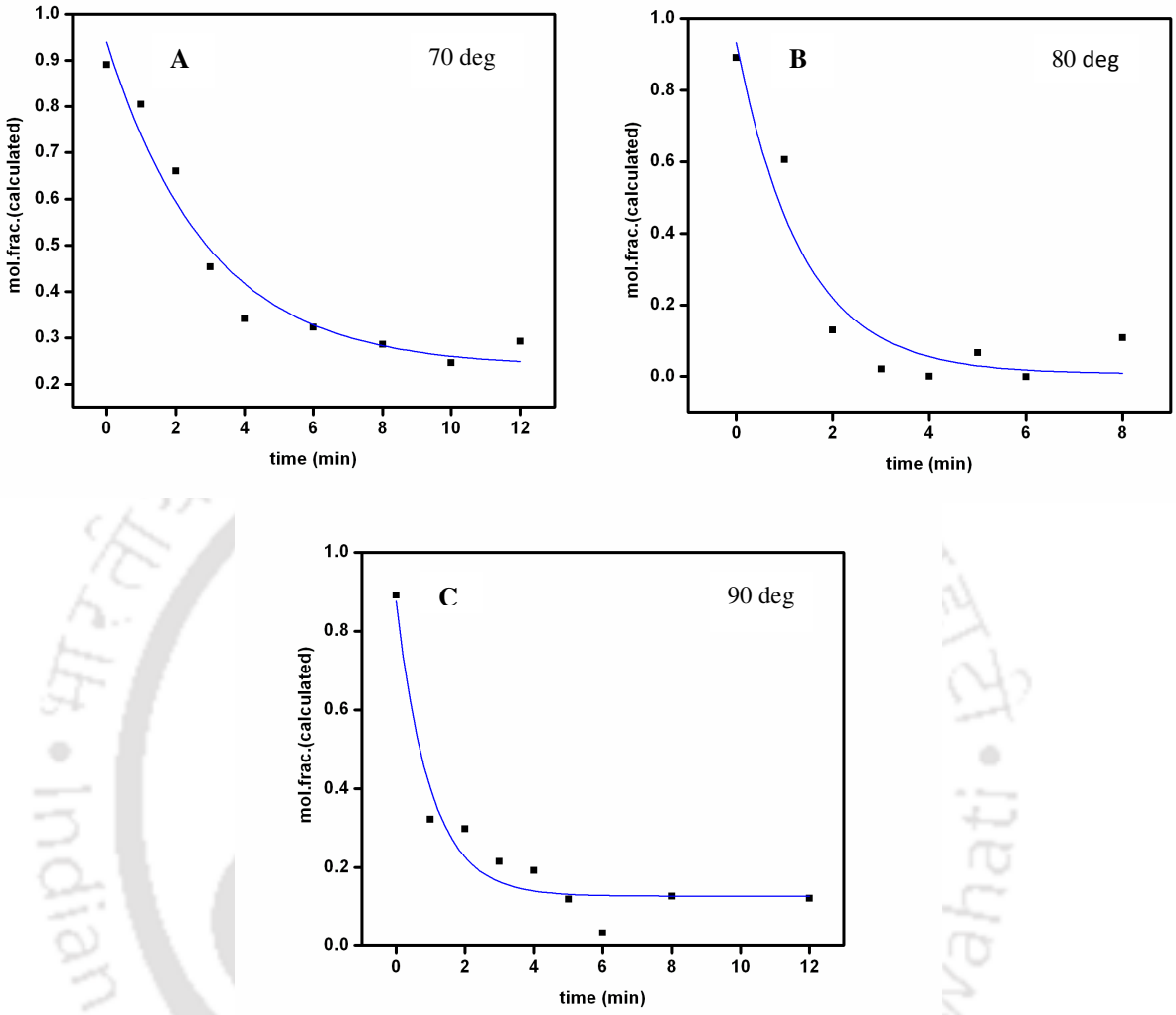

Figure 5-3. *Single exponential fits of the data obtained in the time-dependent thermal denaturation studies for AMG. Temperatures of denaturation are shown in the legends.*

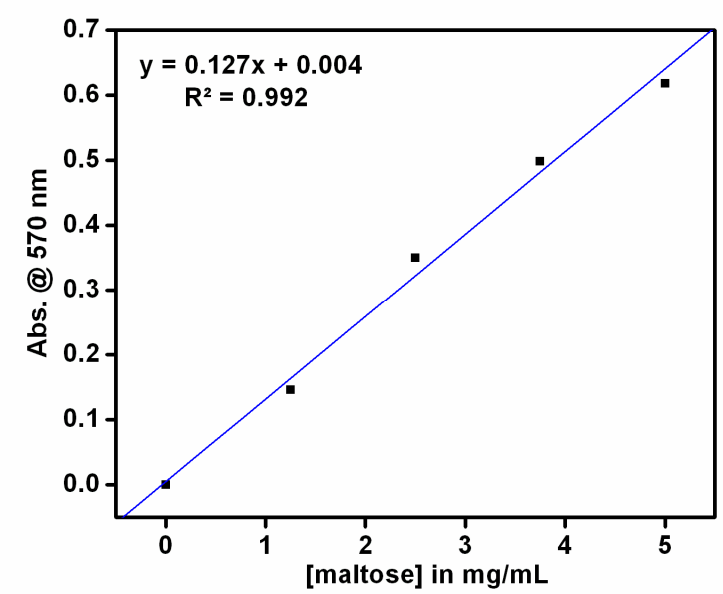

***Figure 6-1**: Calibration graph for DNS method of maltose estimation, as prepared with known concentrations of maltose. The graph shows absorbance at 570 nm of the UV-vis spectrum of the known concentration of maltose after treating with DNS.*

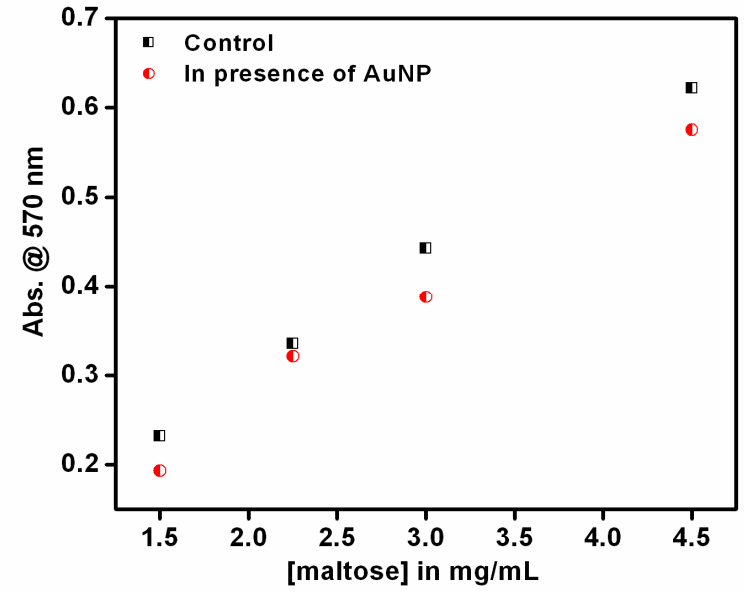

***Figure 6-2**: Control experiment performed in absence and presence of Au NP to check whether Au NP interferes with the DNS test, which was negative. The graph shows the absorbance at 570 nm of the UV-vis spectrum of product formed (maltose) after treating with DNS.*

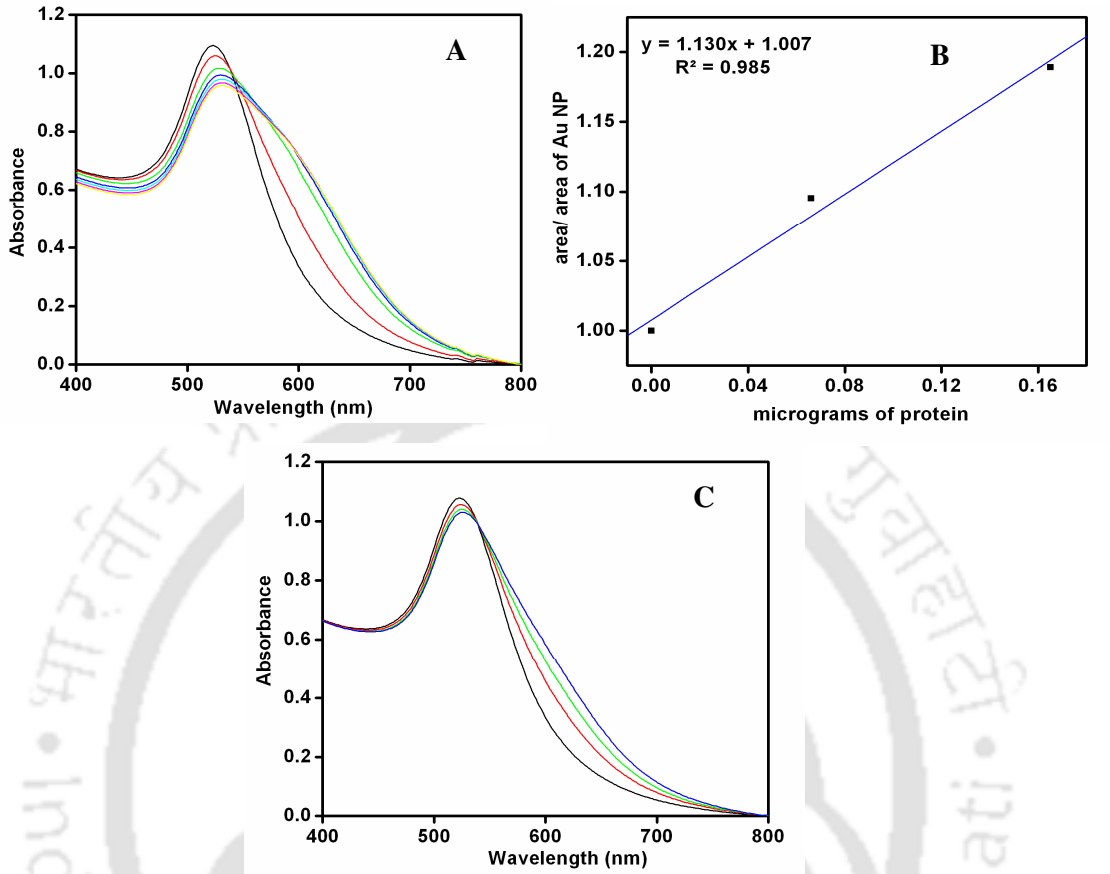

***Figure 6-3**: **(A)** UV-vis spectra of Au NPs in presence of increasing amount of α-amylase. **(B)** Calibration graph for calculating micrograms of protein as generated by plotting the ratio of area under graphs (in 'A') for Au NP in presence of definite amount of protein to that of Au NP only. **(C)** UV-vis spectra of Au NPs in presence of different amount of the supernatant (of the same solution) after separating from the Au NP bound enzyme by centrifugation. Refer to the text above for details of the process of estimation.*

Calculation of number of nanoparticles and fraction of surface atom using a spherical cluster approximation model:[1]

$$W = V \times M \times A.\,wt/\,1000 \qquad [1]$$

Where, W is the weight of the Au particles in the medium, V is the final volume of the reaction in mL, M is the molar concentration of Au^{3+} ion and A. wt is the atomic weight of Au atom.

Here an excess of citrate was used, so assumed that all of $HAuCl_4$ was converted to Au NPs.

750.0 µL of 1.7262×10^{-2} M $HAuCl_4$ was reduced. Hence the moles of $Au^{3+} = 1.295 \times 10^{-5}$.

Therefore weight of $Au^{3+} = 1.295 \times 10^{-5}$ mol $\times$ 196.97 g $mol^{-1} = 2.55 \times 10^{-3}$ g.

Since the total volume in which $HAuCl_4$ was reduced = 30.0 mL hence concentration of Au^{3+} = Au(0) = 8.5×10^{-5} g/mL.

In our experiments we had diluted Au NPs to two times, hence [Au] = 4.25×10^{-5} g/mL.

We had taken 2.0 mL of this solution and added to 3.0 mL starch solution. Hence final [Au] = 1.7×10^{-5} g/mL i.e. 8.5×10^{-5} g of Au was present in the medium (5 mL).

From the TEM results, we observed that Au NPs were spherical in shape, and we can roughly write,

$$V_{cluster} = NV_{atom} \qquad [2]$$

$$\frac{4}{3}\pi (R_{cluster})^3 = N \frac{4}{3}\pi (R_{atom})^3 \qquad [3]$$

Here, $V_{cluster}$ is the volume of a cluster (NP) and V_{atom} is the volume of an atom, $R_{cluster}$ is the radius of a cluster and R_{atom} atomic radius and N is the total number of atoms within the cluster. From eqn. 1 & 2,

$$R_{cluster} = N^{1/3} R_{atom.} \qquad [4]$$

Calculation of amount of gold nanoparticles formed (N_{NP}) when 8.5 x 10^{-5} g of Au particles were used for catalysis:

From the TEM results we know that average diameter of Au NP was 11 nm. Therefore $R_{cluster}$ = 5.5 nm. Also radius of gold atom i.e. R_{atom} = 0.137 nm. Therefore the number of gold atoms per nanoparticle was estimated using eqn. [4],

$N = (R_{cluster} / R_{atom})^3 = (5.5 / 0.137)^3 = 64703$ gold atoms per nanoparticle.

Amount of gold particles used, W = 8.5 x 10^{-5} g = 8.5 x 10^{-5} g / 196.97 g mol^{-1} = 4.315 x 10^{-7} moles.

No. of gold atoms,

$N_{atom} = 4.315 \times 10^{-7} \times 6.023 \times 10^{23} = 2.599 \times 10^{17}$

No. of nanoparticles in 8.5 x 10^{-5} g of gold particles,

$N_{NP} = N_{atom} / N = 2.599 \times 10^{17} / 64703 = 4.02 \times 10^{12}$

= 4.02 x 10^{12} nanoparticles were formed per 8.5 x 10^{-5} g of Au.

Reference:

1. Lewis, J. D.; Day, M. T.; Mac Pherson, V. J.; Pikeramenou, Z. *Chem Commun*. **2006**, 1433.

Publications and Presentations

Publications

1. Rangnekar, A.; Sarma, T. K.; Singh, A. K.; **Deka, J**.; Ramesh, A.; Chattopadhyay, A. *Langmuir* **2007**, *23*, 5700-5706.
   Retention of Enzymatic activity of α-Amylase in the Reductive Synthesis of Gold Nanoparticles.

2. **Deka, J**.; Paul, A.; Ramesh, A.; Chattopadhyay, A. *Langmuir (Letter)* **2008**, *24(18)*, 9945-9951. (Appeared in Nanowerk, and Nano Newsflash: http://www.nanowerk.com/spotlight/spotid=6959.php.)
   Probing Au Nanoparticle Uptake by Enzyme Following Digestion of Starch-Au-Nanoparticle Composite.

3. **Deka, J**.; Paul, A.; Chattopadhyay, A. *J. Phys. Chem. C*. **2009**, *113*, 6936–6947.
   Sensitive Protein Assay with Distinction of Conformations Based on Visible Absorption Changes of Citrate-Stabilized Au Nanoparticles.

4. **Deka, J**.; Paul, A.; Chattopadhyay, A. *Nanoscale (Communication)* **2010**, *2*, 1405–1412.
   Estimating Conformation Content of a Protein Using Citrate-Stabilized Gold Nanoparticles.

5. **Deka, J**.; Paul, A.; Chattopadhyay, A. *Langmuir*, **2011** (*manuscript under revision*)
   Modulating Enzymatic Activity in the Presence of Gold Nanoparticles.

Presentations

1. **Deka, J**.

   Presented a poster titled 'Synthesis and Sequestration of Au Nanoparticles by alpha-amylase' in the 10th Chemical Research Society of India (**CRSI**) National Symposium held at Indian Institute of Science, Bangalore, India, during February 1st – 3rd, 2008.

2. **Deka, J**.

   Oral presentation titled 'Gold Nanoparticles in Probing Proteins' in International Conference on Advanced Nanomaterials and Nanotechnology (**ICANN- 2009**), held at Centre for Nanotechnology, Indian Institute of Technology Guwahati, India, during December 9th – 11th, 2009.

3. **Deka, J.**

   Presented a poster titled 'Probing Proteins via Interaction with Gold Nanoparticles' in International Conference on Nanoscience and Technology 2010 (**ICONSAT 2010**), held at Indian Institute of Technology Bombay, India, during February 17th - 20th, 2010.

4. **Deka, J.**

   Presented a poster titled 'Interacting Gold Nanoparticles and Proteins in Diagnostics and Catalyses' in 3rd Asia Pacific Symposium in Radiation Chemistry (**APSRC**) 2010 and Trombay Symposium on Radiation and Photochemistry (**TSRP**) 2010, held in Lonavala, India, during September 14th-17th, 2010.